Doctoral Thesis

March, 2024

Development of a myoelectric control system for a multi-degree-of-freedom myoelectric prosthetic hand based on a long-term clinical evaluation

Supervisor

Prof. Hiroshi Yokoi

Prof. Chikako Nakayama

Prof. Kazuhiko Misawa

Joint Doctoral Program for Sustainability Research, Graduate School of Informatics and Engineering, The University of Electro-Communications, Tokyo, Japan

Yuki Kuroda

This thesis is submitted for the degree of
Doctor of Philosophy

Development of a myoelectric control system for a multi-degree-of-freedom myoelectric prosthetic hand based on a long-term clinical evaluation

Doctoral dissertation review committee

Professor	Tomonori Hashiyama
Professor	Hiroshi Yokoi
Professor	Kazuhiko Misawa
Professor	Chikako Nakayama
Professor	Shinichi Takeuchi
Associate Professor	Ryu Kato

概要

これまで障害者支援技術に関する研究が多く行われ，障害者の生活の質の向上に貢献してきた．近年では 3D プリンターなどの生産技術の発展や Internet of Things (IoT) や人工知能技術のなどの情報通信技術の発展により，これらの技術を取り入れたより高機能な障害者支援技術の研究開発が行われるようになってきた．障害者支援技術が高機能化，機能の細分化が進められていく中で，より障害者にとって有用な技術の開発の為，臨床適用による評価などを行い，障害者の実際の声を取り入れることの重要性が増してきている．

また，障害者支援技術に関する研究では，個人の障害を治療したり改善したりすることで障害を克服しようとする個人モデルに基づくアプローチを中心としてきた．障害者支援技術の研究開発がこれに該当する．さらなる障害者の生活の質向上のためには，障害を社会の障壁ととらえ社会を改善していくような社会モデルに基づいた取り組みを増やしていく必要がある．具体的には開発した技術の社会実装，障害者からの新技術へのアクセスを円滑にする，社会実装を通して社会制度の改革を促すなどが考えられる．

近年障害者を中心として障害者支援技術の研究開発を行う手法が提唱されている．研究者たちが気づきにくい実生活上の問題に対処する支援技術を提案することができるため，有用なアプローチである．しかしながら，実際には障害当事者もニーズがわからないことが多く，また技術的な知識がない場合，気づきにくい課題点も多く存在すると考えられる．また，このような手法のみを直ちに最適な開発方法としてしまえば，研究者が委縮し，障害者支援技術の研究開発が減少してしまう恐れがある．これでは障害者の機会損失につながってしまい，結局のところ障害者にとってデメリットになってしまう．よって，現在の研究開発のプロセスから大きく逸脱しない方法で障害者のニーズを多く取り入れた研究開発手法を行う必要がある．

よって本研究では，「筋電義手の開発を通して障害者支援技術・制度の問題点を明らかにし，障害者の生活の質を持続的に向上する障害者支援技術の開発方法について検討する．」ことを目的として研究を行った．筋電義手とは，筋が収縮する際に発生する電気信号である筋電位を用いて制御可能な電動義手である．

本研究では目的を達成するために，新たな開発アプローチとして長期臨床適用によるフィードバックを活用した障害者支援技術を開発するアプローチを提案した．

本研究は次の 4 つに大別される．

- 実用的な多自由度筋電義手システムの開発
- 臨床適用における機能評価と主観評価による障害者の要求解明
- 臨床適用により得られたパターン認識制御に関する課題を解決する制御手法の開発
- 安価で高機能な義手を完成用部品に登録することでユーザーのアクセシビリティを向上

第 2 章では，筋電義手の関連技術，過去の研究で調査された筋電義手に関する要求についてまとめた．これらを基にして今後の筋電義手の研究開発のためのロードマップの作成と，目標を達成するための問題設定を行った．

第 3 章では，開発した多自由度筋電義手である BIT-UEC-Hand について解説した．開発した義手は，動作をシームレスに変更可能なパターン認識制御機能を有しており，既存の商用 5 指電動義手と比較して 100-200 g ほど軽量であった．既存研究では義手の軽量化がユーザーにとって優先順位が高い要件となっており，この分野への重要な貢献であるといえる．また，開発した BIT-UEC-Hand を用いた長期臨床適用を行い，その過程でタスク評価とアンケート評価を行った．結果として，タスク評価により，遂行可能なタスク数の増加がみられることがわかったが，動作数増加に伴う制御信頼性の低下も指摘された．また，アンケート評価により多自由度筋電義手が仕事面において有効に機能する可能性が示唆された．これらの結果は，これまで盛んに研究されてきたパターン認識制御において，多様な動作が使用可能な利点とそれに伴う制御安定性の低下を支持するようなものであった．

第 4 章では，筋電位の時変性を原因とする筋電義手の制御安定性の低下に対処する手法の開発を行った．時変性に追従するためのアプローチとして学習・自己組織化・適応を挙げ，既存手法がそれぞれどのアプローチに対応するか解説を行った．その後，提案手法として，より安定的で即応性の高い手法として，この 3 つのアプローチを組み合わせた時変性追従手法を提案した．このシステムについての評価を行った結果，最適化していない場合の識別率に対して，有意に高い識別率を示すことがわかった．

第 5 章では，上肢欠損者が実現可能な動作パターン数の制限に対処するために，筋電情報のみによらず，タッチセンサから得られるハンドと把持物体の接触状態の情報に基づいて自律的に物体に適応し，物体把持を可能とする筋電義手制御手法の開発を行った．このシステムの評価を行った結果，上肢欠損児を含む 6 名の参加者の筋電信号を用いて評価を行った結果，被験者によらず物体のピックアップタスクが可能であること，従来の手法と比較して多様な物体の把持が可能であることを物理エンジンによるシミュレーションによって確認した．また，本手法を適用するための理想的なハードウェアに必要な要件についても検証された．

第 6 章では，開発した BIT-UEC-Hand の完成用部品への登録について要件を解説し，登録後の販売状況や補装具支給のプロセスから現状の問題点について考察した．特に，2 点の問題点を挙げた．1 点目は医師が支給する筋電義手の選択をするため，医師への周知が必要であることであたった．2 点目は労災保険による支給の場合「よく使いこなしていること」が要件となっており，訓練用義手の支給や，訓練用プログラムの確立が開発した義手の普及に必要となっていることを述べた．また，これまで述べた提案システムの様々な被験者への適用結果についてもまとめと考察を行った．

最後に第 7 章では，本研究により障害者の生活の質がどのように改善されたか議論した．最後に本研究の結論と今後の展望について述べた．

Abstract

Considerable research has been conducted on assistive technologies for people with disabilities, which have improved their quality of life (QOL). Recent developments in manufacturing technologies, such as 3D printers, and information and communication technologies, such as the Internet of Things (IoT) and artificial intelligence, have accelerated the development of advanced assistive technologies for persons with disabilities. As these technologies become more sophisticated and specialized, there is a growing need to conduct clinical evaluations and incorporate the actual voices of people with disabilities, hence, creating more valuable solutions for them.

In addition, most studies on assistive technologies for persons with disabilities focus on approaches based on the individual model, which aim to overcome disabilities by treating or improving the individual disabilities. To further improve the QOL of people with disabilities, it is necessary to increase efforts based on the social model, which view disability as a social barrier and seek to improve society. Specifically, a protocol considering the implementation of the developed technology in society, facilitating access to new technology for people with disabilities, and promoting the reform of social systems through social implementation is necessary.

In recent years, methods for developing assistive technologies centered on people with disabilities have been proposed. This is significant because it enables researchers without knowleges about real-life of people with disabilities to propose assistive technologies to address real-life problems they may not have been previously addressed. In reality, however, the needs of people with disabilities are often not well understood, and several issues may be difficult to identify without specialized technical knowledge. If such methods are immediately adopted as the optimal developmental methods, researchers may be discouraged, potentially leading to a decrease in research and development efforts for assistive technologies. This could lead to lost opportunities for this population, ultimately putting them at a disadvantage. Therefore, it is necessary to conduct research and develop methods that consider the diverse needs of persons with disabilities without

significantly deviating from the current research and development process.

Therefore, this study aimed to clarify the problems of assistive technologies and systems for persons with disabilities through the development of a myoelectric prosthetic hand and to investigate methods for developing assistive technologies that can sustainably improve their QOL. A myoelectric prosthetic hand (MPH) is an electric prosthetic hand that can be controlled using myoelectric potentials, which are electrical signals generated when the muscles contract.

To achieve the objectives of this study, as a new developmental approach, this study proposed a method that utilizes feedback from long-term clinical applications.

The study is presented in four main steps:

- Development of a practical multi-degree-of-freedom (DOF) MPH system.
- Elucidation of the requirements of people with disabilities through functional and subjective evaluation in clinical application of the MPH.
- Development of control methods to solve issues related to pattern recognition obtained from clinical application of the MPH.
- Improving user accessibility by registering inexpensive and highly functional MPHs as components for ready-made parts (完成用部品).

The remainder of the paper is organized as follows. In Chapter 2, the related technologies for MPHs and their requirements that have been investigated in previous studies are summarized. Based on these previous studies, a roadmap for the future research and development of MPHs was created. Finally, a problem was set up based on these requirements to achieve the study’s objective.

Chapter 3 describes a multi-DOF MPH developed by the University of Electro-Communications (UEC) and the Beijing Institute of Technology (BIT), called the “BIT-UEC-Hand.” The developed MPH has a pattern recognition control function that enables seamless change of motions and is 100—200 g lighter than the existing commercially available five-finger electric prosthetic hands. This is an essential contribution to prosthetics, as lightweight MPHs are a high-priority requirement for the users of assistive prostheses. In addition, a long-term clinical application of the BIT-UEC-Hand was conducted, and, in the process, task and questionnaire evaluations were performed, which are described in Chapter 5. Task evaluation revealed an increase in the number of tasks that could be performed. However, as the number of movements increased, the control reliability decreased. The questionnaire evaluation results showed that the multi-DOF MPH could function effectively. These results support the advantage of the availability of various motions in pattern recognition control, which has been extensively studied, and the accompanying decrease in the control stability.

A method to address the MPH's loss of control stability caused by time variation in electromyogram (EMG) signals was developed and described in Chapter 4. Learning, self-organization, and adaptation were identified as approaches for the system to follow the time variation in the EMG signals, and the approaches that corresponded to each of the existing methods were explained. A time variation tracking method combining these three approaches was then proposed, which is more stable and responsive compared with the existing method. Evaluation of the developed system showed that it achieved a significantly higher recognition rate than the nonoptimized system.

In Chapter 5, to address the limitation in the number of movement patterns that can be realized by people with upper limb deficiency, an MPH control method was developed that could autonomously adapt to an object and grasp it based on information on the contact state between the hand and grasped object obtained from a touch sensor, rather than solely on EMG information. The evaluation results of a physics engine simulation, using EMG signals from six participants, including a child with an upper limb deficiency, confirmed that the object pickup task is possible regardless of the participant; moreover, the optimized system enables the grasping of a wider variety of objects compared to conventional methods. The requirements for ideal hardware to apply the proposed method were also verified.

In Chapter 6, the requirements for the registration of the developed BIT-UEC-Hand as ready-made parts, the current problems based on the sales situation after registration, and the process of supplying the prosthetic device are discussed. In particular, two problems were noted: first, the need to inform the physicians about the MPH because they are responsible for selecting the prosthetic device to be supplied; and second, in the case of supply by an industrial accident compensation insurance, user must have a "used mastery" proficiency level with the supplied MPH. Therefore, it is necessary to provide prosthetic hands for training and establish training programs to promote the use of the developed prosthetic hands. The results of the application of the proposed system described up to this point to the various participants are also summarized and discussed.

Chapter 7 discusses the impact of this study on the improvement of the QOL of people with disabilities. Finally, the conclusions of this thesis and future prospects are discussed.

Contents

Chapter 1 Introduction

1.1 Population of people with disabilities and their protection for realizing a sustainable society

1.1.1 Population of people with disabilities

The World Health Organization (WHO) and the World Bank estimate that more than 1 billion people or approximately 15 % of the world's population (based on 2010 global population estimates) experience a significant disability. This number is increasing owing to various factors, such as an increase in the aging population(World Health Organization. and World Bank. 2011). In Japan, the Cabinet Office reported that approximately 9.65 million people or 7.6 % of the total population have some form of disability(Cabinet Office Japan 2022). This figure is considerably lower than the estimated ratios of people with disabilities by the WHO and World Bank, even considering the trend of high percentages of this population in developing countries. It is assumed that several people with disabilities are not diagnosed by a doctor or are considered to be outside the scope of Japanese statistics. In Japan, disability is classified into three categories at the time of the survey: physical, intellectual, and mental disability, with approximately 4.36 million, 1.094 million, and 4.193 million persons having physical, intellectual, and mental disabilities, respectively. This estimate shows that the number of persons with disabilities is increasing. These facts make it even more essential to provide security for the disabled in Japan.

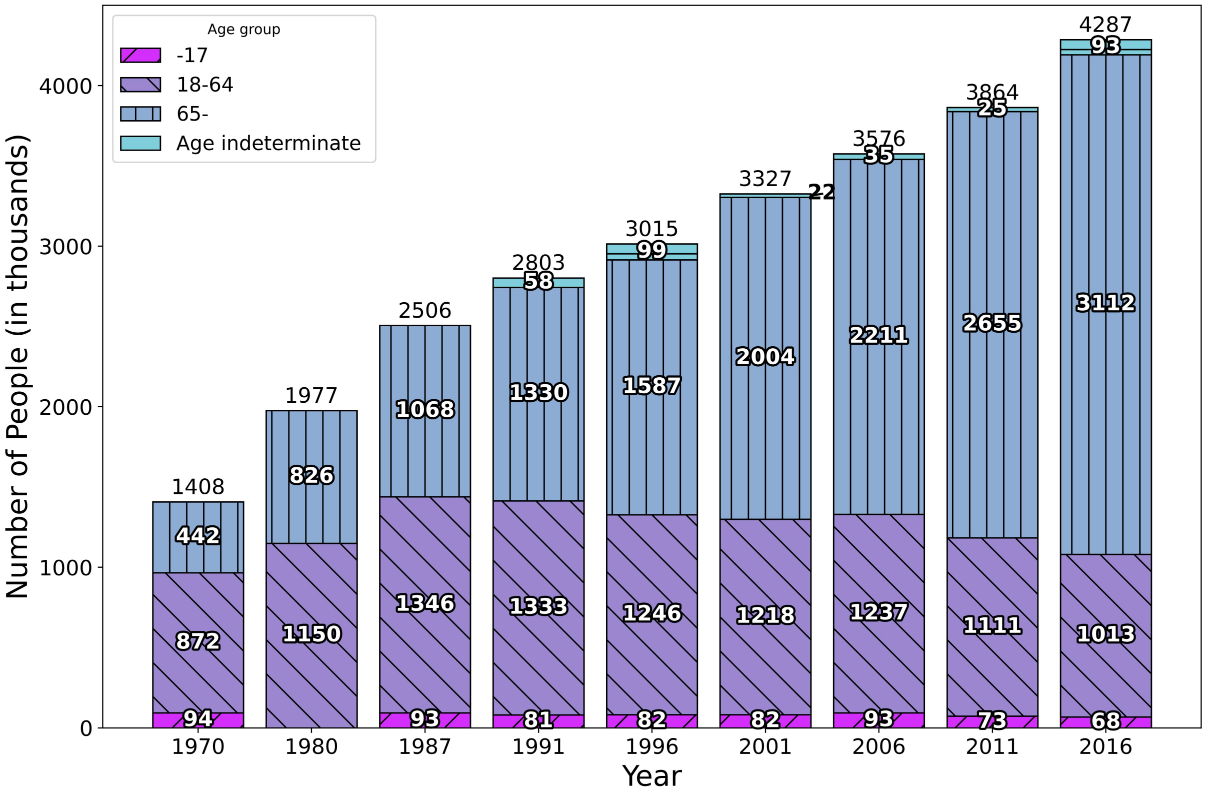

Fig.1.1: Number of persons and children with physical disabilities by age group (not institutionalized). Prepared with reference to (Cabinet Office Japan 2022).

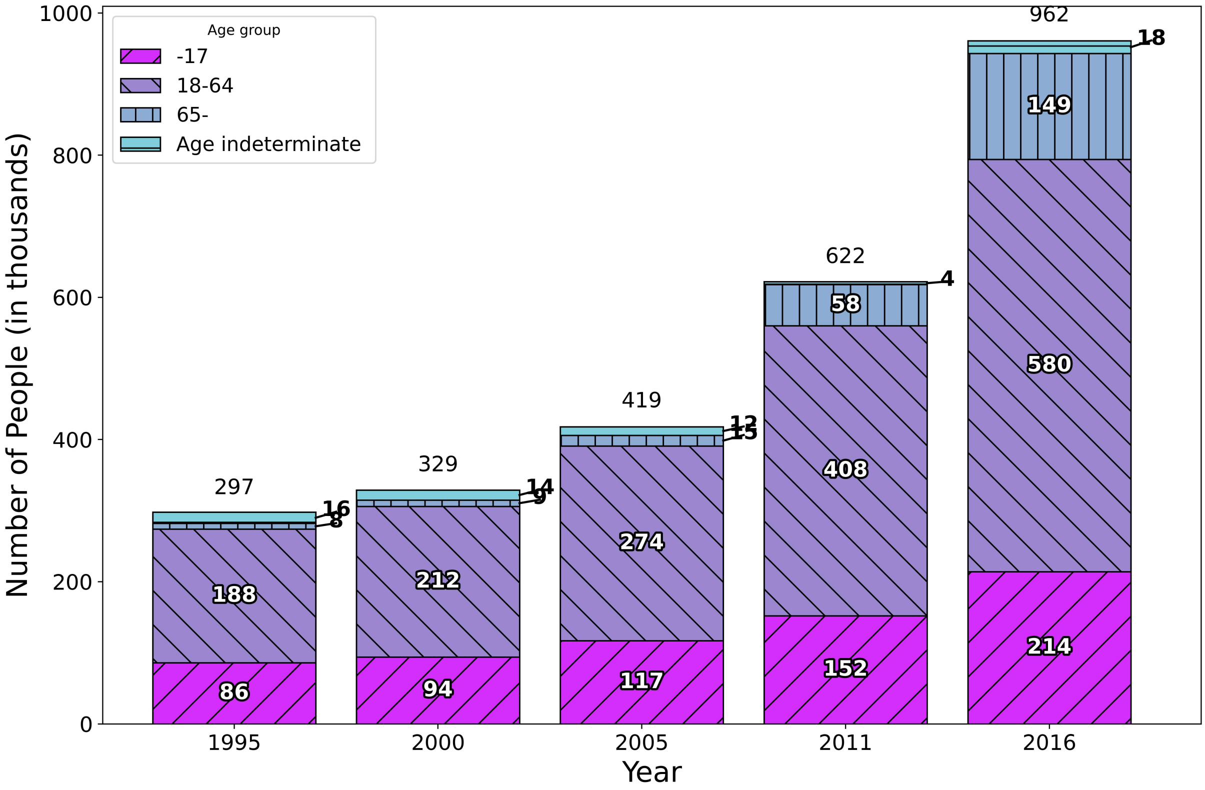

Fig.1.2: Number of persons and children with intellectual disabilities by age group (not institutionalized). Prepared with reference to (Cabinet Office Japan 2022).

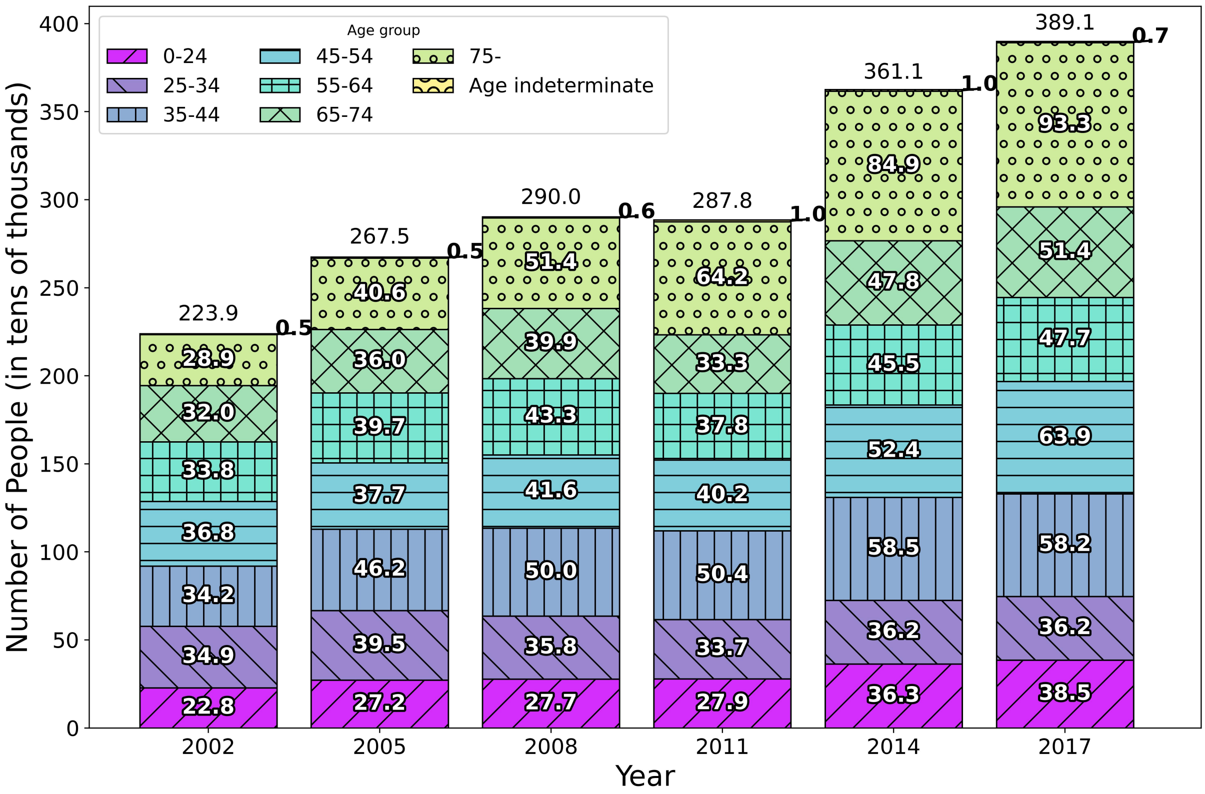

Fig.1.3: Number of persons and children with mental disabilities by age group (not institutionalized). Prepared with reference to (Cabinet Office Japan 2022).

1.1.2 Protection of people with disabilities

One of the most significant events related to discrimination against people with disabilities in the modern era is the spread of eugenics and the enactment of the law of sterilization, which was based on eugenics. In 1859, Charles Darwin's "On the Origin of Species" was published. This book argued that organisms evolve to adapt to their environment through natural selection. Since then, attempts to interpret humans and their society through Darwinian principles have begun to appear. Eugenics was one of these attempts.

Eugenics was proposed by Francis Galton, Darwin's cousin, as "a movement to improve the human race, or at least to halt its perceived decline, through selective breeding (Wikler 1999)".

There are two types of eugenics: positive eugenics, which aims to actively increase good genetic traits, and negative eugenics, which aims to suppress bad genetic traits. However, due to the challenges in achieving an increase in positive genetic traits, negative eugenics was actually practiced; a typical example of negative eugenics is sterilization (S. Yonemoto et al. 2000). Sterilization refers to the removal of reproductive capabilities through surgical procedures that involve cutting or tying the vas deferens or fallopian tubes.

Laws on sterilization were enacted in the United States, Germany, and Sweden in the first half of the 20th century. In Japan, the Eugenic Protection Act was enacted in 1948; official statistics show that approximately 855,000 sterilizations were performed under the Eugenic Protection Act until 1994, when the law was amended to the Maternal Health Act and the eugenic provisions were removed.

Such eugenic thought rapidly declined after the Nazi eugenic policies in Germany were revealed post World War II (Lombardo 2018). However, even today, the ideological foundations that served as the starting point of eugenics is still accepted in some parts of the world (Ladd-Taylor 2017).

This eugenic ideology that discriminates against people with disabilities has been rejected from scientific and ethical perspectives (Brosius and Kreitman 2000; Notake 2005; Aultman 2006; Buchanan et al. 2001), as explained in the following sections.

Necessity of protecting people with disabilities from a scientific perspective (species survival)

Brosius and Kreitman; Notake argued for the necessity of protecting people with disabilities from the perspective of species preservation. The human species survives as a collective by creating new individuals (children) to pass on genetic information. Humans produce new individuals with unique genetic information through sexual reproduction. However, this diverse genetic combination can sometimes result in individuals who are less adapted to current environmental conditions.

If such errors in the replication of genes between individuals (mutations) do not occur, adaptation to infectious diseases and new illnesses will not take place, and the species will perish. This genetic diversity is, in fact, a survival strategy for the human species.

Moreover, humans lack foresight, and environmental and social conditions can change significantly over a few generations, making future prediction impossible. For instance, certain genes considered disadvantageous in past environments have adapted over time to current conditions. In areas where malaria is endemic, a high incidence of sickle cell anemia is observed. This is because the red blood cells of individuals with sickle cell disease are resistant to malaria (Wiesenfeld 1967). Additionally, hereditary hemochromatosis, a genetic disorder causing excessive iron absorption, could have been naturally selected to compensate for iron-deficient diets, suggesting a possibility of survival (Feder et al. 1996).

Necessity of protecting people with disabilities from an ethical perspective

According to WHO, it is estimated that approximately 15 % of the world's population lives with some form of disability (World Health Organization. and World Bank. 2011). Furthermore, in many regions, there is an increase in disabilities due to the worsening of chronic health conditions such as diabetes, cardiovascular disorders, mental illnesses, cancer, and respiratory diseases. Additionally, the risk of disability increases with age. Therefore, it can be considered that everyone is at a risk of becoming disabled.

In such circumstances, how can everyone maintain happiness and quality of life? This question can be addressed by employing the Capability Approach of Sen (Sen 1999).

The Capability Approach is a theoretical framework containing two normative claims (Robeyns 2021; Robeyns 2005):

1. The freedom to achieve well-being is the most important moral value.
2. Well-being should be understood based on people's "capabilities" and the "functions" they realize.

Capabilities refer to the actions and states people can achieve by choice, such as getting married, receiving education, consuming adequate nutrition, or traveling. Notably, the term "capability" in the general sense does not merely refer to actions that an individual can achieve. Rather, it encompasses a broader meaning that includes social and environmental elements. Functions are the realized capabilities. Whether an individual can convert a range of means, such as resources and public goods, into functions, or in other words, whether they possess certain capabilities, depends largely on personal, social, and environmental conditions. These are termed as conversion factors.

Based on this theory, ensuring a diverse range of people's capabilities implies that even if someone becomes disabled, they will not lose happiness or quality of life (Toboso 2011). Therefore, the protection of people with disabilities becomes essential.

1.2 What is a disability?

Humans have evolved and acquired a variety of abilities. These include bipedal mobility that enables us to move over large obstacles, hands that can perform complex movements with tools, eyes that can distinguish various colors, and so on. However, these abilities are those considered typical or standard in an individual, and not all humans have the same capability. For example, We have all observed people in wheelchairs or those using white canes to detect obstacles in their path. Some people have acquired or congenital characteristics that make them different from the typical person, such as a lack of vision or lower extremities. These people are generally referred to as being disabled. However, the definition of the term "disability" is unclear to many. For example, people that use eyeglasses daily are not referred to as being disabled in Japan, even though they cannot perform their daily activities typically without eyeglasses. Therefore, how is a person with a disability defined?

1.2.1 Individual model and social model

Two significant disability models have been proposed: the individual (medical) model and the social model. The concepts of each model are described as follows (Ogawa and Sugino 2014)(Hori 2021):

Individual model
: The cause of the problems associated with a disability is "individual impairment". It is necessary to treat, improve, or make these individual impairments less noticeable for people with disabilities to adapt to society.

Social model
: Disability is viewed as a social barrier (disability), and society must take responsibility for its resolution. Proponents of this model believe that the assertion of rights based on the experiences of people with disabilities is a means to solve problems.

In this manner, each model differentiates between impairment and disability by defining them using different terms. The idea of distinguishing between these two terms to pursue social responsibility for a socially formed disability was developed from the Fundamental Principles of Disability published by the Union of the Physically Impaired Against Segregation in the 1970s. The Fundamental Principles of Disability define impairment and disability as follows (Union of the Physically Impaired Against Segregation 1976):

Impairment
: Lacking part of or all of a limb, or having a defective limb, organ or mechanism of the body.

Disability
: The disadvantage or restriction of activity caused by a contemporary social organization which takes no or little account of people who have physical impairments and thus excludes them from participation in the mainstream of social activities.

1.2.2 Bio-psycho-social model

The International Classification of Functioning, Disability and Health (ICF), established by the WHO in 2001, uses the "bio-psycho-social model" as a framework for understanding disability (World Health Organization 2001). The ICF considers function and disability as a dynamic interaction between the health status and contextual factors, which are both individual and environmental, as shown in Fig.1.4. In this context, disability is an umbrella term for impairment, activity limitation, and participation limitation and refers to the negative aspects of the interaction between an individual (in a state of health) and his/her contextual factors (environmental and personal factors).

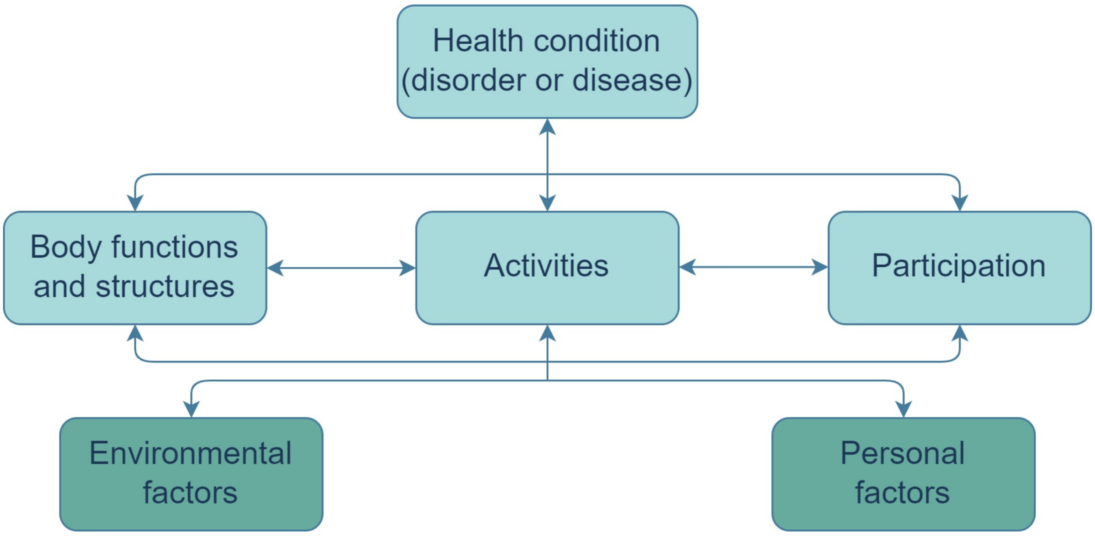

Fig.1.4: Bio-psycho-social model. Prepared with reference to (World Health Organization 2001).

However, according to Ogawa and Sugino, ICF can objectively measure the "degree of disability," but it cannot define a "person with a disability. In other words, it can measure the "type of disability," but cannot indicate to what extent a person is "disabled" and to what extent they are "not disabled." The only way to determine a "person with a disability" is for the government to define the term politically through legislation or for people with disabilities to identify themselves as "persons with disabilities" and for society to recognize this (Ogawa and Sugino 2014).

The scope of disability varies from country to country, as it depends on the environment in which the individual belongs, as described in the bio-psycho-social model. One example is Brazil, where several children are forced to drop out of school because they cannot afford reading glasses, which are widely available in many high-income countries (Mont 2007). However, as mentioned earlier, most people in Japan are not defined as being disabled simply because eyeglasses are easily accessible.

1.3 Disability and technological development

Historically, there has been a close relationship between people with disabilities and technology. Efforts have been made toward compensating for lost bodily functions owing to physical impairments through technological means. Such technologies that maintain or enhance an individual's function and autonomy are known as assistive technology.

In particular, assistive technologies are some of the most effective mediators in achieving broad development goals such as the Sustainable Development Goals (SDGs), which advocate "leaving no one behind" and cover a wide range of economic, social, and environmental development (Tebbutt et al. 2016; MacLachlan et al. 2018). For example, even with improved access to food, water, and sanitation services, people with disabilities and the elderly may need assistive technologies such as wheelchairs, hearing aids, or glasses for mobility and information access.

The hand is a crucial part of the human body, essential for interacting with the external world. Most tools that are used in daily life require hand manipulation, making them inaccessible if a person lacks hand functionality. This limitation can significantly reduce the quality of life and freedom of employment.

Engineers have long attempted to replicate hand functionality through prosthetic hands. The replicated functions and methods have evolved with changes in technology and social circumstances. While the focus used to be solely on the individual model, emphasizing complementing or restoring hand function, recent years have seen an increasing adoption of a social model approach, including the introduction of policies to improve accessibility.

Here, the prosthetic hand is used as a model case to explain the evolution of the relationship between disability and technological development, considering both the individual and social models. Additionally, this discussion considers the constitution of an appropriate method for developing assistive technologies for users, in light of these transitions.

1.3.1 Approach based on individual model: prosthetic hand

Prosthetic hands replace hand functions in people with congenital or acquired loss of hand function. Four types of prosthetic hands are available: cosmetic prosthetic hands that replace the appearance of the hand and the role of pressing an object; activity-specific prostheses that are specialized for specific tasks rather than appearance; body-powered prosthetic hands that transmit shoulder movement to the hand through a harness and enable the hand to open and close; and electric prosthetic hands that enable the hand to be driven by a motor powered by electricity delivered through a battery. The MPH is a type of electric prosthetic hand that reads and controls the user's motion intention from myoelectricity generated when the muscles contract. In recent years, MPHs have been used because they have the appearance of cosmetic prosthetic hands and can overcome the limitation of not being able to open and close at the position where the wire is slack, as is the case with body-powered prosthetic hands. In Japan, Myobock by Ottobock is the most commonly used assistive device(Tanaka 2018).

1.3.2 Approach based on social model: improving accessibility

The systems utilized to support people with disabilities have been improved in various ways. This section presents the essential support systems and treaties for people with disabilities available in Japan and other countries (Table.1.1).

Table.1.1: History of support for people with disabilities

Era	Japan	Foreign countries
1990		Americans with Disabilities Act (United States)
1993	Basic Act for Persons with Disabilities	
2006	Services and Supports for Persons with Disabilities Act	Convention on the Rights of Persons with Disabilities (CRPD) adopted(United Nations)
2012	Act on Providing Comprehensive Support for the Daily Life and Life in Society of Persons with Disabilities	
2014	Japan ratified the CRPD	

Americans with Disabilities Act (ADA)

The ADA is a civil rights act proposed in the United States, enacted in 1990, and amended in 2008. One of the significant purposes of the ADA is to guarantee employment opportunities to all people with disabilities; there are two important rules in the ADA regarding employment (Tokoro 2010):

Prohibit discrimination against people with disabilities in employment
This rule prohibits discrimination in hiring, recruitment, job training, dismissal, compensation, etc., based on disability.

Providing reasonable accommodation for people with disabilities
Employers are required to adjust the work environment. Specifically, these include the provision of ramps, sign language interpreters, Braille books, flexible working hours, and vacations.

However, evaluations of the effectiveness of the ADA in improving the employment status of people with disabilities are divided. Although the ADA came into effect in 1990, the employment rate of people with disabilities has been reported to be declining until 2000 since its enactment; this has been attributed to the excessively high costs borne by the companies to comply with the ADA act(Acemoglu and Angrist 2001). However, positive evaluations included improvements in the workplace (National Council on Disability 2007).

Convention on the Rights of Persons with Disabilities (CRPD)

The CRPD is a treaty that was adopted by the United Nations General Assembly in December 2006, based on the concept of international human rights law. It aims to ensure the dignity and security of the human rights of people with disabilities of all types (Ogawa and Sugino 2014). In Japan, it was ratified in 2014. The Convention is characterized by its clarification of the rights of people with disabilities and its practical guarantees of rights, such as reasonable accommodation, based on the social model of disabilities (Okamura 2015). The main contents of the Convention are summarized byMinistry of Foreign Affairs of Japan as follows:

General Principles
: Respect for the dignity, autonomy, and independence of people with disabilities; non-discrimination; complete and adequate participation and inclusion in society; etc.

General Obligations
: To ensure and promote the full realization of all human rights and fundamental freedoms of all people with disabilities without any discrimination based on disability, including failure to provide reasonable accommodation, etc.

Measures for the realization of the rights of people with disabilities
: The Convention stipulates the measures to be taken by the state parties concerning the right to liberty, such as the freedom of body, prohibition of torture, and freedom of expression, and social rights, such as education and labor. The realization of social rights is allowed to be achieved progressively.

Framework for implementation of the Convention
: Establishment of a national framework for implementation and monitoring of the Convention. Consideration of reports from each state party in the committee on the rights of people with disabilities.

Japan has developed domestic laws in preparation for the ratification of the Convention. Specifically, the Basic Act for Persons with Disabilities was amended in 2011, the Act for Eliminating Discrimination against Persons with Disabilities was enacted, and the Act to Facilitate the Employment of Persons with Disabilities was amended in 2013.

Basic Act for Persons with Disabilities (BAPD)

The BAPD is a law that established basic principles regarding measures to support the independence and social participation of people with disabilities. It was enacted in 1993 as an amendment to the Basic Act for Countermeasures Concerning Mentally and Physically Handicapped Persons, which was originally enacted in 1970. In the 2011 amendment, the definition of "person with disabilities" (Article 2, Item 1) was changed from "a person who, because of a disability, is continuously and substantially restricted in daily life or social life" to "a person with a disability who is in a state of facing substantial limitations in their continuous daily life or social life because of a disability or a social barrier". The Annual Report on Government Measures for Persons with Disabilities (Summary) 2012 (Cabinet Office Japan 2012) explained that the definition was revised "based on the so-called 'social model,' which states that the limitations people with disabilities face are not solely because of functional disabilities but arise from the various barriers in society" (Okamura 2015).

Services and Supports for Persons with Disabilities Act (SSPDA)

The SSPDA is a law enacted in 2005 that established administrative procedures and cost-sharing for providing medical care and services for people with disabilities. It is based on the concept of "service as a right," in which service users select the services they need and pay a fee to purchase them from service providers (Ogawa and Sugino 2014). This law was enacted as part of the "Social Welfare Basic Structural Reform," which changed the administrative procedures from a safeguarding system to a contract system and the fees from a tax system to a social insurance system. This change addressed the situation where the rights and autonomy of recipients were not guaranteed under the previous system. The reorganization of the service system and strengthening of employment support and community life support were epoch-making features of this act (Kitagawa 2018).

Kitagawa summarized the six aspects that have changed with the enactment of the SSPDA from (Hiraoka et al. 2011; Sato and Ozawa 2013) as follows (Kitagawa 2018):

1. People with mental disabilities who were not included in the support system were also included, and a centralized service provision system was established that transcends the types of disabilities.
2. The centralized service provision system by the municipalities was established, and the services were divided into "Payment for Services and Supports for Persons with Disabilities" (mandatory budgetary measure), which was provided uniformly throughout the country, and "Community Life Support Program" (mandatory budgetary measure), which was provided according to local conditions and budgets. In addition, local governments are obliged to formulate welfare plans for people with disabilities to develop the infrastructure of the service system.
3. The employment support function was fundamentally strengthened by introducing a new category of support for people with disabilities who wish to work at home or in public companies based on individualized support plans and by introducing a new category of employment transition support business.
4. From the viewpoint that people with disabilities themselves become members of the system and support the costs together, "fair burden" or "fair benefit sharing" according to actual expenses, such as food and service usage fees are required. The primary purpose of introducing the "fair burden" was to reduce the use of services by people with disabilities and to reduce the burden on the national treasury (Sugimoto 2008).
5. Transparency and clarification of the service use decision mechanism were made. The government introduced six levels of disability classification uniformly throughout the country and set 106 survey items for all people with disabilities who use services; it certified their disability level based on the primary and secondary judgment of the municipal examination board. The types of services to be provided and usage fees were determined.
6. The government's financial responsibility has been clarified by making it obligatory

for the government to bear the costs.

As mentioned above, this law has been evaluated by some as an attempt to curb social security costs owing to the tightening of state finances (Okamura 2015). In particular, increasing the benefit-sharing burden of services has provoked strong opposition from persons with disabilities (Nakagawa and Nitta 2015). This is because people with disabilities are forced to use multiple services and long-term residential care services, and, yet, their income level is low in comparison, increasing their burden.

Act on Providing Comprehensive Support for the Daily Life and Life in Society of Persons with Disabilities (APCSDLLSPD)

The APCSDLLSPD is a law that was amended from the SSPDA in 2012. The background of the revision stems from lawsuits filed at various places in Japan claiming that the "copayment" system violates the Constitution, infringing on equality under the law, the right to life, and the right to the pursuit of happiness. In the written agreement reached to settle the lawsuits (Ministry of Health and Welfare 2010), the then Democratic Party of the Japan government decided to abolish the SSPDA and implement new comprehensive welfare legislation.

In terms of content, the objectives and fundamental principles included in the BAPD were also incorporated into this law. The basic principle of the law is that support for daily and social life based on the law shall be provided comprehensively and systematically to ensure opportunities for social participation, coexistence in the community, and the removal of social barriers to realize a symbiotic society. Major changes include the addition of intractable diseases, etc., to the scope of disability to fill the "gap in the system" and the revision of the "disability level classification" to determine the payment of independence support benefits, such as long-term care benefits to the "disability support classification" that comprehensively indicates the standard level of support needed according to various disability characteristics and other physical and mental conditions (Okamura 2015). In addition, the 2010 amendment to the user-fee system for welfare service benefits changed to the principle of "ability to pay."

Assistive medical devices (AMD) payment system in Japan

In Japan, the AMD payment system was established based on the APCSDLLSPD. The AMD payment system provides a part of the cost required for the purchase or repair of prosthetic devices. The term "AMD" is defined in Article 5-23 as "artificial limbs, braces, wheelchairs, and other devices specified by the Minister of Health, Labour and Welfare (MHLW) as those complementing or replacing the physical functions of persons or children with disabilities which are intended for continuous use over long periods, or otherwise, as those devices conforming to the standards prescribed by Order of the MHLW." Here, "prescribed by Order of the MHLW" is defined in the "Standards for the Categories of AMD and the Calculation of the Amount of Cost Required for Purchase or Repair" (Notification No. 528 of the MHLW, September 29, 2006). The applicable categories are: 1. prosthetic limbs (shell and skeletal prosthesis), 2. orthoses, 3. sitting position support devices, 4. safety bobbins for blind persons, 5. artificial eyes, 6. eyeglasses (corrective glasses, light-shielding glasses, low vision glasses and contact lenses), 7. hearing aids, 8. wheelchairs, 9. motorized wheelchairs, 10. sitting chairs, 11. standing holding devices, 12. walkers, 13. head holding devices, 14. defecation aids, 15. walking aids, and 16. communication devices for persons with severe disabilities. Prosthetic limbs, orthotic devices, and sit-to-stand devices are manufactured by combining "manufacturing element prices" and "ready-made parts (完成用部品)" according to the basic manufacturing methods specified for each of these devices. Other outlines are summarized in Table.1.2 concerning (Ministry of Health and Welfare n.d.[b]).

Table.1.2: Overview of AMD payment system

<table>
<tr><td colspan="2">Target</td><td>People with disabilities, children with disabilities, patients with intractable diseases, etc., requiring AMD *Patients with intractable diseases, etc., are limited to those diseases specified in the public notice.</td></tr>
<tr><td colspan="2">Implementing entity</td><td>municipality</td></tr>
<tr><td colspan="2">Application method</td><td>People with disabilities or guardians of children with disabilities apply to the mayor of the municipality and receive AMD expenses according to the decision of the mayor based on the judgment or opinion of the rehabilitation consultation office for persons with disabilities, etc.</td></tr>
<tr><td rowspan="2">Cost burden</td><td>public expenditure</td><td>The AMD fee is defined as the number of expenses required for the purchase, etc., of AMD (standard amount) minus the user's contribution (10 % in principle), and the following ratio bears this AMD fee: Burden ratio（Country: 50/100, Prefecture: 25/100, City: 25/100）</td></tr>
<tr><td>User-charge</td><td>In principle, a fixed rate of 10% is charged. The maximum monthly contribution is set according to the household income as follows:
(Income bracket and maximum monthly contribution)<table><tr><td>Welfare</td><td>Persons belonging to households on welfare</td><td>0 Yen</td></tr><tr><td>Low-income</td><td>Municipal tax-exempt households</td><td>0 Yen</td></tr><tr><td>General</td><td>Municipal taxable households</td><td>37,200 Yen</td></tr></table>*However, if either the person with disabilities or a household member has an income over a certain income level (the tax payment of the person with disabilities or the household member who pays the largest municipal inhabitant tax per income is 460,000 Yen or more), the AMD allowance will not be provided.
*There are measures to prevent the transition to welfare.</td></tr>
<tr><td colspan="2">Budget amount</td><td>The budgeted amount is calculated by considering past results (average unit price and average number of grant decisions).</td></tr>
</table>

1.3.3 What is appropriate assistive technology development and research for users?

As previously explained, assistive technologies, including prosthetic hands, have contributed to enhancing the quality of life for users through technological advancements and the corresponding expansion of social systems to improve accessibility. However, the rapid development of information and communication technologies and manufacturing techniques such as 3D printing has led to a lag in the establishment of social security systems, resulting in insufficient diffusion of these technologies.

For example, MPHs, commercialized in the 1960s, are assistive technologies that have been slow to disseminate in Japan. A 2001 survey showed that the penetration rate of MPH was in the range 25—40 % in the United States and was 70 % in Germany, whereas the rate was 2.3 % in Japan (Kawamura et al. 2001). Furthermore, according to a 2011 survey of ready-made parts in Japan, the number of MPH prescriptions was 5 (2.3 %) out of 219 new prescriptions for prosthetic hands (Kajimoto 2013). At that time, the provision was based on the SSPDA act; however, even after taking this statistic into account, the number of new prescriptions for MPH was small.

This subsection summarizes research that review the kind of assistive technology development and research that should be pursued to improve this situation.

Research Gap in Assistive Technology

The Global Research, Innovation, and Education on Assistive Technology (GREAT) Summit, organized by WHO' s Global Cooperation on Assistive Technology (GATE), discussed global priority research topics for GATE to ensure access to high-quality, affordable assistive products worldwide (Smith et al. 2018; MacLachlan et al. 2018). Building on this summit, MacLachlan et al. organized thoughts on how to unravel and understand the practical gap between the need for appropriate assistive devices, their provision, and their use (MacLachlan et al. 2018). The principles for accessing assistive devices are described as follows (MacLachlan et al. 2018; World Health Organization 2022):

Awareness Potential users and healthcare/welfare professionals must be aware of the potential for assistive technology to mitigate or overcome many disabilities.

Availability There must be a sufficient quantity of products and services to meet the needs of those requiring them, and they must be provided near the users' residences.

Affordability Products and services must be affordable for users, and economic barriers must be identified and addressed.

Accessibility Services, facilities, and information should be easy to access and fair for everyone, regardless of the personal background or attributes.

Adaptability Products and services must be adaptable to individual needs and responsive to changes in people' s needs and goals over time.

Acceptability The product and service design and provision must consider efficiency, reliability, simplicity, safety, and aesthetics. Users should be able to choose and control their use of products and services, which must be appropriate for their age, gender, and cultural elements.

Quality Products must meet standards for strength, durability, performance, safety, and comfort. Guidelines, including staff training requirements, must be met, and users should be involved in assessing the quality of products and services.

These principles can be used to identify the strengths and weaknesses of the current assistive technology system and develop strategies to reduce access barriers.

For instance, in the development of assistive technologies for dementia, although the quantity and diversity of technologies are rapidly expanding, there still are structural challenges to their adoption as assistive devices. These include inadequate clinical validation and a lack of focus on the needs of potential users (MacLachlan et al. 2018). These principles highlight the necessity of user involvement, particularly in the aspects of "adaptability" and "quality".

The lack of user involvement in many assistive devices is also pointed out by Smith et al. However, they also note that not all potential consumers can envision using a product until they try it in a natural environment (Smith et al. 2018).

Crip technoscience manifesto

Shew criticizes technoableism, the idea that technological development is the only way to solve the problems of people with disabilities. Shew argues that the design of technology and artificial intelligence to address disability issues is often led by people not deeply involved in the disability community. The author viewed this as being problematic to technology design based only on what is imagined as problems of the disabled and elderly and introduced Crip technoscience (Hamraie and Fritsch 2019) as a framework for considering appropriate technology for people with disabilities (Shew 2020). Crip technoscience aims at technopolitics (the design and use of technology to realize political objectives) that people with disabilities and the disability community themselves build. Crip technoscience consists of four main principles (Hamraie and Fritsch 2019), described below by quoting key sections from the original text.

1. Crip technoscience centers the work of disabled people as knowers and makers

   Unlike typical approaches to disability that objectify disabled people and situate expertise in medical professionals and non-disabled designers or engineers, crip technoscience posits that disabled people are active participants in the design of everyday life.
2. Crip technoscience is committed to access as friction

   As Kelly Fritsch explains, ... , the etymology of the word "access" reveals two frictional meanings: access as "an opportunity enabling contact," as well as "a kind of attack" (Fritsch, O'connor, and Thompson 2016). Taking access as a kind of attack reveals access-making as a site of political friction and contestation. While historically central to the fights for disability access, crip technoscience is nevertheless committed to pushing beyond liberal and assimilation-based approaches to accessibility, which emphasize inclusion in mainstream society, to pursue access as friction, particularly paying attention to access-making as disabled peoples' acts of non-compliance and protest.
3. Crip technoscience is committed to interdependence as political technology

   As Alison Kafer (2013) demonstrates, the imagination of disability in feminist technoscience is often limited to either eugenicist ideals of a disability-free future or to "depoliticized" ideals of the cyborg hybrid body (Kafer 2013)(p. 8–10); disability is either a "master trope of human disqualification" (Snyder and Mitchell 2006)(p. 125) or a "seamless" integration of body and machine (Kafer 2013)(p. 105). ... If, as Kafer argues, disabled people have often uneasy or "ambivalent relationship[s] to technology" (Kafer 2013)(p. 119), our practices of interdependence, access intimacy, and collective access can be understood as alternative political technologies: "disabled people," she writes, "[are not] cyborgs because of our bodies (e.g., our use of prosthetics, ventilators, or attendants), but because of our political practices" (p. 120). Crip technoscience offers interdependence as a central analytic for disability–technology relations, recognizing that in the disability culture, community, and knower–maker practices, interdependence acts as a political technology for materializing better worlds.

4. Crip technoscience is committed to disability justice

   Crip technoscience emphasizes that disabled people are not mere consumers of, or objects for, assimilationist technologies, but instead have agential, politicized, and transformative relationships to technoscience.

As a specific example of Crip technoscience, C. Kim and W. Kim described Mission Arm Japan (MAJ), established in 2014 and introduced in Ito's book, *The Remembering Body* (Ito 2019). MAJ provides planning, proposal, and development support to companies specializing in prosthetic limbs and products for people with disabilities. Natsuko Kurasawa is a right shoulder amputee who suffered from phantom pain and the sensation of having a right arm even after amputation. Kurasawa discovered through a proposal by Minatsu Takekoshi, who joined MAJ as a designer and researcher, that a 3D printer could relieve phantom pain by creating a shoulder pad that fits snugly to the body. The two then lived together while experimenting with different types of padding. Through Kurasawa's case study, Ito highlighted the importance of disabled people making their own needs tangible. Technology "for the people with disabilities" developed by engineers for non-disabled people is often out of sync with the needs of people with disabilities. However, Takekoshi stated that people with disabilities often do not know what their needs are. This is why Crip technoscience, in which through communal living, disabled people become the center of knowledge production with the cooperation of technologists, is important.

Research Gap in Prosthetic Hand Research and Development

As presented in Section 1.3.3 and 1.3.3, it has been pointed out that various gaps exist as common issues for assistive devices for people with disabilities.

Similar gaps have been identified in the development of prosthetic hands. Kawamura conducted a survey among 427 individuals with upper limb amputations to evaluate their desires for prosthetic hands. The results revealed that despite a small number of MPH users at the time, a majority of amputees expressed a desire to use them (KAWAMURA et al. 1999). Although this study dates back to 1999, a 2011 survey in Japan indicated that out of 219 new prescriptions for prosthetic hands, only 5 (2.3 %) were for the MPH (Kajimoto 2013). This suggests that the gap between the needs of upper limb amputees and the supply of MPHs likely persists.

The limited availability of MPHs for actual users remains a significant problem. A Google Scholar search for a "multi degree of freedom myoelectric prosthetic hand" yielded 11,800 results (as of December 23, 2023). However, as will be described in more detail in Section 2.3.1, as of December 2023, the only commercially available multi-DOF MPHs in Japan, excluding those developed in this study, are Ottobock's Bebionic and Ossur's i-limb. This disparity between desire to use and supply indicates that the social implementation of such research is considerably limited. Evidently, the approach to disability in research has been predominantly based on an individual model, focusing on treating or improving individual disabilities. However, to further enhance the quality of life for people with disabilities, it is necessary to increase efforts based on a social model, such as improving accessibility to high-functioning prosthetic hands through social implementation.

The fact that most research is conducted in laboratories and lacks sufficient clinical studies is another reason for the slow social implementation (Geethanjali 2016). As mentioned in Section 1.3.3, this lack of clinical research is a common issue for other assistive devices. As pointed out in Sections 1.3.3 and 1.3.3, it is necessary to develop user-friendly assistive devices by incorporating user feedback through clinical research.

The mismatch between users and technology is a problem not limited to assistive devices. However, for assistive devices, where the user base and market are small, incorporating user feedback becomes even more critical (Choi 2015). Particularly, as noted in Section 1.3.3, technologies designed ”for disabled people” by non-disabled engineers often miss the needs of the disabled. Often, the disabled themselves may not fully understand their needs (Ito 2019). Therefore, having disabled users try out assistive devices under expert guidance to analyze problems and identify improvements may be effective.

Moreover, disability cases vary even within the same type, and the corresponding assistive devices differ accordingly. Improving accessibility for a diverse user base remains a challenge. For example, there has been little research on prosthetic hands for children compared to adults. This is due to stricter constraints such as weight and the area available for placing sensors on residual limbs in children (Nakao et al. 2022), rendering it challenging to apply the same systems as those of adults. Technically overcoming such limitations in coverage will also improve accessibility.

1.4 Research Objective

Considerable research has been conducted on assistive technologies for people with disabilities, which have improved the quality of life (QOL) of people with disabilities. Recent developments in manufacturing technologies, such as 3D printers, and information and communication technologies, such as the Internet of Things (IoT) and artificial intelligence, have accelerated the research and development of more sophisticated assistive technologies for persons with disabilities that incorporate these technologies. As assistive technologies for people with disabilities become more sophisticated and their functions more segmented, it is becoming increasingly important to conduct clinical evaluations and incorporate the actual voices of people with disabilities to develop more valuable technologies for them.

In addition, most studies on assistive technologies for persons with disabilities have focused on approaches based on the individual model described in Section 1.3, which aims to overcome disabilities by treating or improving individual disabilities. Research and development of assistive technologies for people with disabilities falls into this category. To further improve the QOL of people with disabilities, it is necessary to increase efforts based on the social model, which views disability as a social barrier and seeks to improve society. Specifically, a protocol considering the implementation of the developed technology in society, facilitating access to new technology for people with disabilities, and promoting the reform of social systems through social implementation is necessary.

In recent years, methods for the research and development of assistive technologies centered on people with disabilities have been proposed (Hamraie and Fritsch 2019). This is valuable because it allows researchers to propose assistive technologies to address real-life problems they may not know. In reality, however, as mentioned in (Ito 2019), the needs of people with disabilities are often unknown, and several issues are difficult to identify without technical knowledge. In addition, if such methods are immediately adopted as the optimal developmental method, researchers may be discouraged, and the research and development of assistive technology for persons with disabilities may decrease. This would lead to lost opportunities for this population, which would ultimately be a disadvantage. Therefore, it is necessary to conduct research and develop methods that incorporate many of the needs of persons with disabilities in a manner that does not deviate significantly from the current research and development process.

The objective of this study is as follows:

To clarify the problems of assistive technologies and systems for persons with disabilities through the actual development of a myoelectric prosthetic hand and to investigate methods for developing assistive technologies that can sustainably improve their QOL.

1.5 Structure of this paper

In this chapter, the situation of people with disabilities and the need for the protection of people with disabilities, the concept of disability, recent changes in thinking about disability, and the relationship between disability and technology are described. Subsequently, the support system as well as the research and diffusion status of assistive technology for persons with disabilities are summarized using the prosthetic hand as a model case. The purpose of this study is clarified.

In Chapter 2, a roadmap of this research field is first developed to clarify the position of this research. The related technologies for MPHs and the requirements for MPHs that have been investigated in previous studies are then summarized. Finally, a problem is set up based on these requirements to achieve the study' s objective.

In Chapter 3, the BIT-UEC-Hand, a multi-DOF MPH that I developed, is described. Subsequently, a long-term clinical application and assessment of the BIT-UEC-Hand, and, in the process, task and questionnaire evaluations, are conducted and described.

A method to improve the control stability of the MPH to solve the problems observed during long-term clinical application was developed, which is described in Chapter 4. Learning, self-organization, and adaptation were identified as approaches to follow the time variation in EMG signals, and the approaches that corresponded to each of the existing methods were explained. This study then proposed a time variation tracking method by combining these three approaches, which is more responsive than the existing method.

In Chapter 5, to address the limitation in the number of movement patterns that can be realized by people with upper limb deficiency, an MPH control method was developed that could autonomously adapt to an object and grasp it based on information on the contact state between the hand and grasped object obtained from a touch sensor, rather than solely on EMG information. The purpose of this chapter is to verify the effectiveness of this approach and pre-emptively test the hidden design requirements of multi-DOF prosthetic hands through physical simulations. This will establish guidelines for the technical development of hardware based on the proposed method in this study.

In Chapter 6, the requirements for the registration of the developed BIT-UEC-Hand as ready-made parts, the current problems based on the sales situation after registration, and the process of supplying prosthetic devices are described. Additionally, a summary and discussion is presented on the results of the application of the proposed system that have been described thus far to various participants.

Chapter 7 discusses how this study improved the QOL of people with disabilities. Finally, the conclusions of this thesis and future prospects are discussed.

The structure of this paper is illustrated in Fig.1.5.

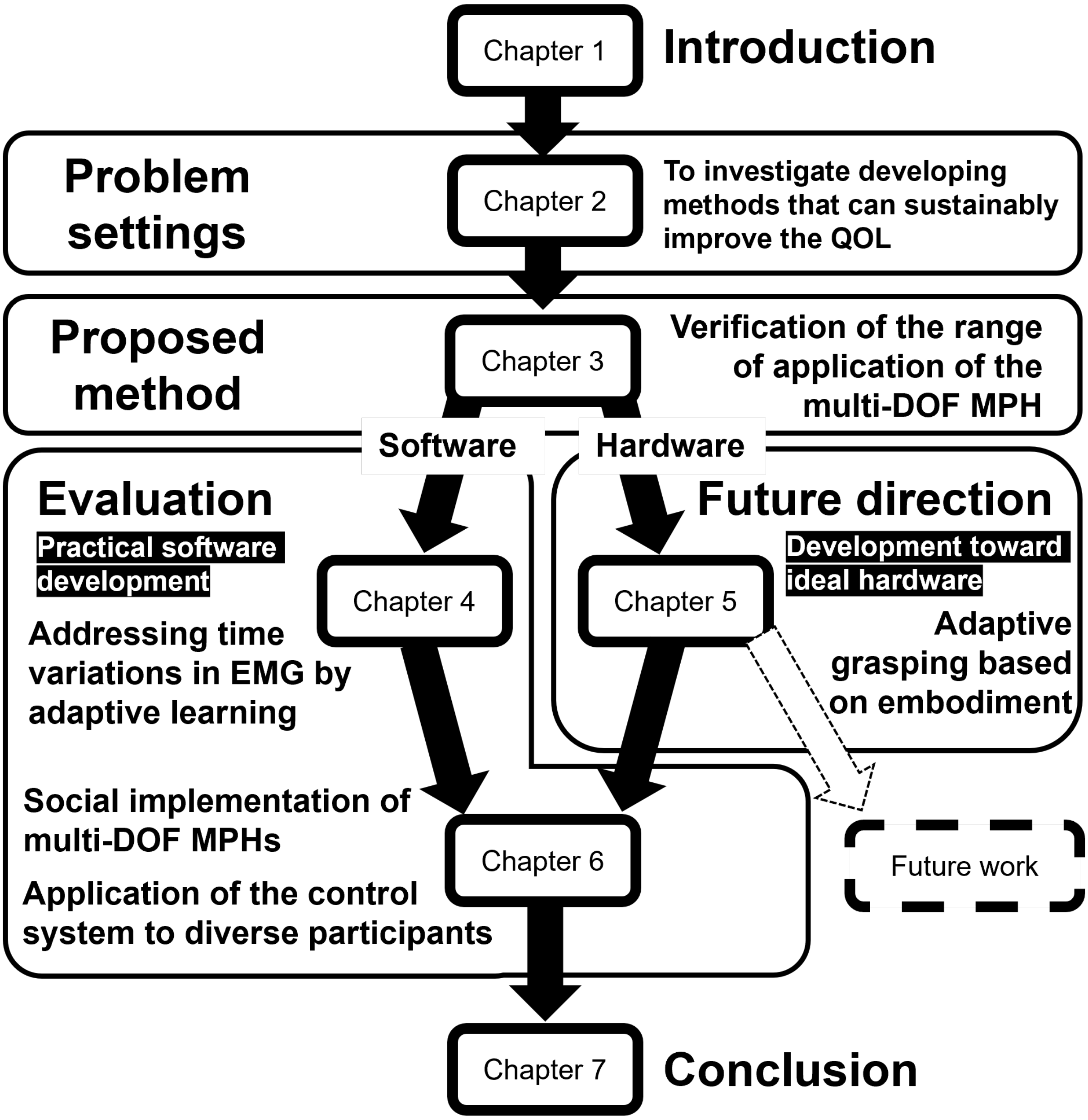

Fig.1.5: Structure of this paper.

Chapter 2 Problem setting: Myoelectric prosthetic hand and functions to be realized

2.1 Introduction

This chapter summarizes the related technologies for MPHs and the requirements for MPHs that have been evaluated in previous studies. Based on these requirements, a problem to achieve the study' s objective is set up.

Section 2.2 describes the general system configuration and control methods for MPHs.

In Section 2.5, the position of this study in MPH research is clarified using a roadmap.

Section 2.3 describes and compares previous studies on electric hands, focusing on commercial MPHs.

Section 2.4 classifies the control methods of MPHs into six categories and describes the existing control methods.

In Section 2.6, the requirements for the long-term clinical application of the multi-DOF MPH are clarified based on previous related studies.

Section 2.7, summarizes the studies investigating the users' requirements for MPHs and clarifies the requirements that should be considered when developing a prosthetic hand.

Section 2.8, describes the functional requirements for the implementation of a multi-DOF MPH.

In Section 2.9, the functional requirements of the MPH control system are described. Specifically, the section discusses the issue of the time variation of myoelectric signals and the limitation of the number of recognizable motions.

Section 2.10 describes the practical requirements for an MPH control system.

Finally, Section 2.11 describes the problem setting of this study.

2.2 Myoelectric Prosthetic Hand

An MPH is an electric prosthetic hand that can be controlled using myoelectric potentials, which are electrical signals generated when the muscles contract. Because myoelectric prostheses use biological signals as the control input, they are believed to be more intuitive than body-powered prosthetic hands.

2.2.1 System configurations

MPHs consist primarily of an electric hand, controller, EMG sensor, battery, and socket. Depending on the required function, a cosmetic glove may be used in addition to the electric hand.

Electric Hand
: The electric hand replaces the function of the human hand and primarily aims to replace the grasping function and appearance.

Controller
: The controller is the brain of the MPH system that controls the electric hand and measures myoelectricity. The controller may be mounted on the electric hand or on the socket independent of the electric hand.

EMG Sensor
: EMG sensors are used to measure the myoelectric potential generated when muscles contract. They consist of an electrode that touches the skin and an amplifier that amplifies the weak myoelectric potential read by the electrode and filters out the noise. Ag/AgCl electrodes are primarily used as electrodes; however, in recent years, sensors using conductive silicone, which can measure EMG signal robustly, have also become commercially available (Togo, Yuta, et al. 2019).

Battery
: The battery is a component that supplies electricity to the MPH system. Nickel-cadmium and lithium-ion batteries are commonly used. However, in recent years, with the development of battery technology, lithium polymer batteries that can

output large currents have also been used.

Sockets

The socket is a component that connects the residual limb to the MPH system. It consists of an inner socket that fits into the residual limb and support that holds the load of the MPH and protects the inner components from the outer environment.

Cosmetic Glove

Cosmetic gloves are used to cover the electric hand. They are primarily used for aesthetic purposes and improve the friction of contact points. Vinyl chloride and silicone are the predominantly used materials. In recent years, gloves made of more flexible elastomers have been developed to reduce the load on the joint drive of electric prosthetic hands.

2.2.2 Control method

The MPH is used by attaching the socket to the user's residual limb.

The control of MPHs generally consists of three processes: "EMG measurement," which measures EMG signals; "motion intention estimation," which determines what the user intends to do from the measured EMG; and "motion generation," which determines explicitly the control amount of the actuator based on the determined motion intention. The "motion intention estimation" method includes proportional control, in which the voltage input to the motor is proportional to the strength of the EMG (Bottomley, Wilson, and Nightingale 1963), and pattern recognition, in which the user's motion intention is estimated from the EMG using machine learning and the motion is reproduced by the MPH (Jiang et al. 2014; Hiroshi Yokoi et al. 2009).

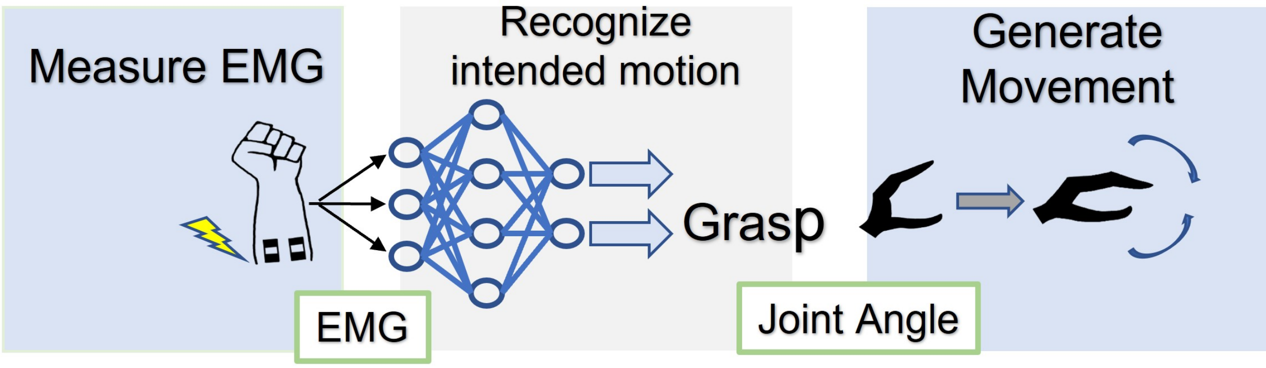

Fig.2.1: Control method of the MPH

2.3 Previous studies: Electric hand

Several electric hands have been developed for use as MPHs. This section summarizes the features of electric hands that are already available in the market. Electric hands developed until 2013 are outlined in detail in (Belter et al. 2013). The summary is based on the research by Belter et al. with the addition of latest information.

2.3.1 Commercial MPH

Table.2.1 lists the MPHs sold to date. The registration statuses and prices of the ready-made parts required to use the AMD supply system in Japan are also summarized. The weight of the hands that need gloves is also included, as gloves affect the weight of the hand during use.

Table.2.1: Characteristics of commercial prosthetic hands.

Hand name	Developer	Weight (gw)	Overall Size (mm)	Number of Joints	Degrees of Freedom	Number of Actuators	Actuation Method	Joint Coupling Method	Adaptive Grip	Registration to ready-made parts	Price (yen)
Myobock (8E38)	Ottobock	350–500	149, 152 or 154 height	2	1	1	DC motor	Fixed pinch	No	Yes	517,500-1,212,500
Bebionic	Ottobock	495–539	190–200 long, 84–92 wide, 50 thick	11	6	5	DC Motor-Lead Screw	Linkage spanning MCP to PIP	Yes	Yes	2,314,000
Michelangelo	Ottobock	–420		6	2	2		Cam design with links to all fingers	No	Yes	2,919,000
i-limb	Ossur	450–615	180–182 long, 80–75 wide, 35–41 thick	11	6	5	DC Motor-Worm Gear	Tendon linking MCP to PIP	Yes	Yes	2,445,800
UEC-e Hand	Society for the Promotion of Myoelectric Hand	130		2	2	2	Servo motor		No	Yes	86,500

Myobock

Myobock (Ottoobock Japan n.d.; Ottobock n.d.[a]; Ottobock n.d.[b]) (Fig.2.2) was the world's first commercially available MPH; it was released in 1965. Four types of devices are available depending on the opening/closing speed and control method. The opening/closing speed control method, also known as the proportional control, controls the opening and closing speed of the hand in proportion to the magnitude of the EMG. The ON–OFF control method opens and closes the hand when the EMG value exceeds a threshold. Table2.2 presents the differences between the four types of hands. The MPHs provided to unilateral upper limb amputees at public expense in Japan are typically Myobocks (Tanaka 2018).

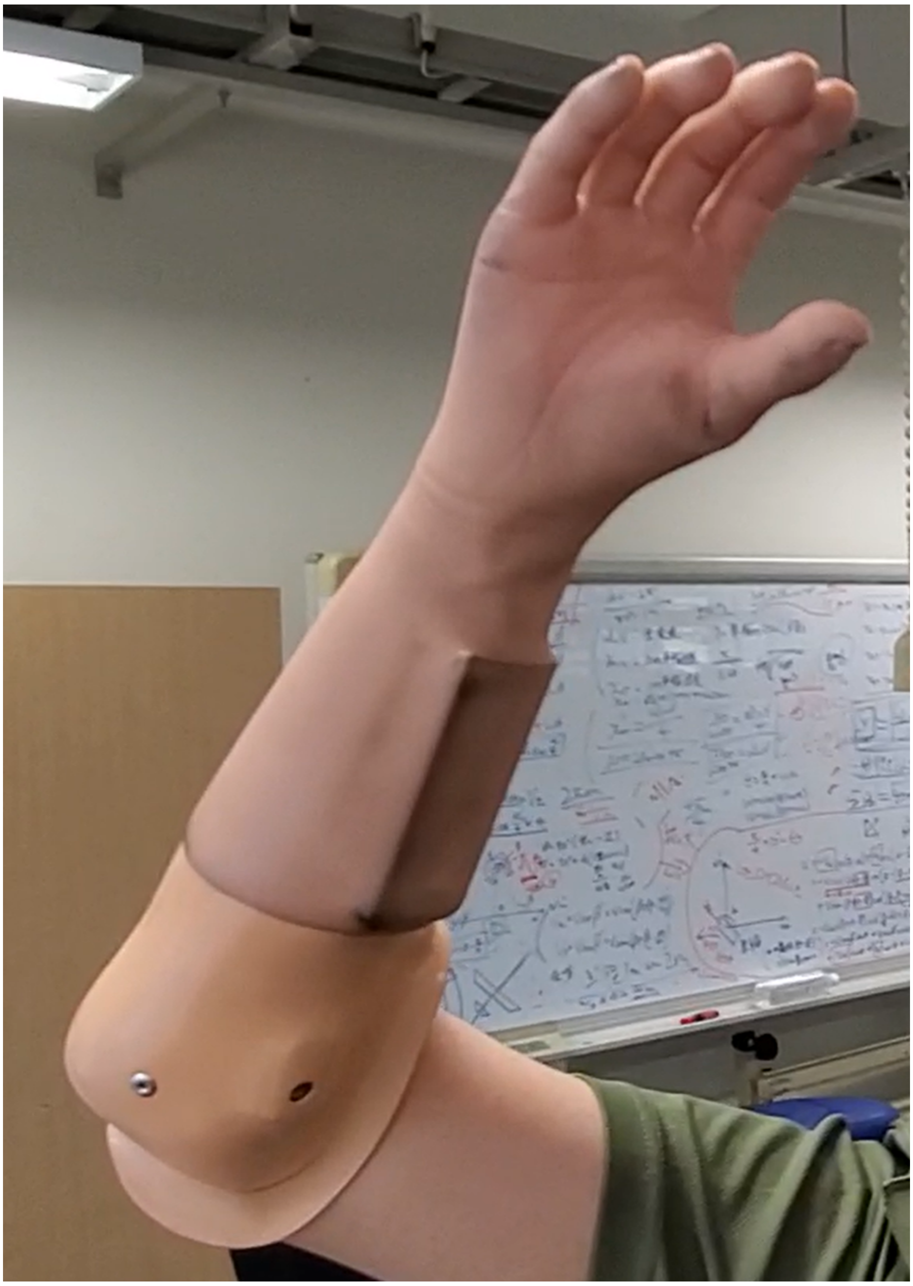

Fig.2.2: Myobock

Table.2.2: Types of Myobock

	SensorHand Speed	VariPlus Speed	DMC plus	Digital Twin
Characteristics	There is a sensor at the tip of the thumb that detects slippage of the grasped object and increases the grasping force up to 1.5 times.	The world's most popular system.	The opening/closing speed is slower than that of other models.	Constant opening/closing speed and gripping force. ON-OFF control is used for those who have difficulty in producing strong EMG signals and for those who can place EMG sensors at only one place.
Control Method	Proportional control	Proportional control	Proportional control	ON-OFF control
Grip force (N)	0–100	0–100	0–90	90
Open/Close Speed (mm/s)	15–300	15–300	15–130	110

Bebionic

The Bebionic hand is a type of MPH developed by Steeper. Ownership of the hand was transferred to Ottobock in 2017 (Steeper 2017). It is capable of producing 14 different motions. Switching between lateral and opposing thumb positions is performed passively (The Association for Technical Aids n.d.[a]). The characteristic feature of this device is that the space between the fingers can be narrowed during the gripping motion, which enables the user to hold thin objects between the fingers (Ottobock 2022).

Michelangelo

This MPH was developed by Ottobock, with separate actuators for the four fingers and thumb, which can switch between opposing and lateral positions by changing the position of the thumb. The wrist is flexible, and compensatory movements can be reduced (Ottobock 2018).

i-Limb

The i-Limb is an electric prosthetic hand originally developed by Tocuh Bionics in the UK. Ossur in Iceland has now acquired it. Several types of prosthetic hands are currently available, including i-Limb Quantum, i-Limb Ultra, and i-Limb Access; i-Limb Quantum and i-Limb Ultra are registered as ready-made parts in Japan and can be purchased through the AMD payment system (The Association for Technical Aids n.d.[b]; The Association for Technical Aids n.d.[c]). The i-Limb Quantum enables the user to select 36 patterns of hand movements. The control method utilized is proportional control, in which EMG sensors are attached to the extensor and flexor muscles of the forearm, and each electrode controls the opening and closing movements. The controlled movements can be switched in the following four ways (Össur 2018; Pacific Supply Co. n.d.):

Motion change by the built-in acceleration sensor
: The acceleration sensor mounted inside the hand can change the motion by moving the hand back and forth and left and right.

Motion change triggered by the EMG
: Motion can be changed by detecting simultaneous contractions of the flexor and extensor muscles, double impulses (consecutive muscle contractions at short intervals), and triple impulses.

Motion change by a smartphone application
: Movement can be changed using a smartphone application.

Motion change by a chip device
: Motion can be changed using a coin-shaped device called a "Grip Chip;" the motion change can be performed by placing the hand close to the Grip Chip or by double-tapping on the Grip Chip.

Universal electromyographic control electric (UEC-e) hand

The UEC-e hand is a type of MPH developed by Hoshigawa et al. at UEC (Hoshigawa et al. 2015). It is equipped with two servo motors and can move the carpometacarpal (CM) joint of the thumb and metacarpophalangeal (MP) joints of the four fingers. Moreover, it can grasp a 500-g plastic bottle despite being light in weight, weighing approximately 130 g. Pattern recognition control using an artificial neural network (ANN) is used as the control method, and the user's EMG pattern is learned by the ANN before use to enable quicker control (Kato, Yokoi, and Arai 2006). In addition, a flexible conductive silicone sensor is used as the EMG sensor, which can reduce the load on the skin compared with conventional hard Ag/AgCl electrodes (Togo, Yuta, et al. 2019). This MPH was registered as a ready-made part in 2018 (Togo, Hiroshi Yokoi, et al. 2020).

2.3.2 MPH in this study

This section presents the existing MPHs. As a commercial MPH, a multi-DOF MPH has already been registered as a ready-made part and is available for purchase using public funds. However, when an MPH is provided at public expense, it is the Myobock that is often offered because previous studies reported that 90 % of the activities of daily living (ADL) can be performed with only one non-disabled hand (Glynn et al. 1986)and the Myobock is inexpensive compared with other MPHs (Tanaka 2018). Furthermore, as explained in Section 1.3.2, the basic principle of the APCSDLLSPD is to "ensure opportunities for social participation, coexistence in the community, and removal of social barriers". Hence, it is not considered that people with disabilities can acquire physical functions similar to those of non-disabled persons. This is believed to be one of the reasons for the current situation regarding the use of assistive technology. Therefore, this study aimed to provide a multi-DOF MPH at a price range close to that of Myobock as one of the options for people with disabilities.

2.4 Previous studies: Control method

This section describes the existing control methods for MPHs. Yamanoi classified the control methods for MPHs into six major categories (Yamanoi 2019), as presented in Table2.3. Here, the control methods with a red background are primarily used for single-DOF MPHs and those with a blue background are primarily used for multi-DOF MPHs.

Table.2.3: Control method and control target

	Non-learning	Learning
Discrete	Threshold	Pattern recognition
Continuous	Single regression	Multiple regression
Discrete+Continuous	Switching control	Combination

As a factor for classifying the control methods for MPHs, the methods can be classified based on whether the control target is a discrete quantity, a continuous quantity, or a combination of the two. In the case of a discrete quantity, motion intention estimation and motion generation are independent of each other among the three steps of MPH control described in Section 2.2.2, and the motion corresponding to the estimated motion intention must be programmed manually. In the case of a continuous quantity, the control quantity of the actuator is also determined by EMG.

Two types of factors separate the control methods of MPHs: non-learning and learning. Non-learning methods focus on the presence or absence of EMG expression and perform ON–OFF control. In contrast, proportional control methods focus on amplitude intensity information and adjust the opening and closing speed of the hand accordingly. These methods have the advantage of being less susceptible to noise because they use simple EMG information. Nonetheless, they can only use limited information, and their feasible operations are few.

Consequently, they are often used to control single-DOF MPHs that can control only two motions: opening and closing of the hand. In the case of ON–OFF control for hand opening and closing, this method requires information only on the activity of one of the muscles. The proportional control requires information only on the activity of the flexor and extensor muscles. This means that if the sensors are placed in positions on the socket corresponding to the flexor and extensor muscles, the prosthetic hand can be used immediately after it is attached. Most commercially available MPHs use non-learning control methods.

In contrast, learning-type control methods use machine learning to model and control the relationship between EMG and motions using features extracted from the EMG as input. As the number of parameters to be adjusted is large when classifying and controlling motions with several DOF, such as those of a normal hand, machine learning is used to perform these operations automatically. Therefore, it can be applied to the control of multi-DOF MPHs. As with the non-training type control methods, the input of learning-type control methods can be time-domain features such as the EMG amplitude intensity information, frequency-domain features such as the power spectra, or a combination of both. This method utilizes more detailed EMG information and can realize more motions than the non-learning type method. However, the user must manipulate several types of muscle contraction patterns to take advantage of this learning method owing to the need for detailed EMG information.

Each control method is described in detail below.

2.4.1 Threshold-type • Single regression–type

Threshold–type control methods include ON–OFF control, in which the hand opens and closes when the EMG exceeds a certain threshold value. Single regression-type control methods have proportional control, in which voltage is input to the motor in proportion to the amplitude intensity of the EMG (Bottomley, Wilson, and Nightingale 1963). According to the evaluation of the proportional control method by the MPH users surveyed by Sears and Shaperman, the proportional control method received a higher evaluation than the digital control method, in which the voltage applied to the motor changes on and off (Sears and Shaperman 1991).

Ottobock's Myobock, one of the most commonly used MPHs, uses two EMG sensors, one each for the "open" and "close" switches. The control method depends on the hand option, with the ON–OFF and proportional controls being selectable.

2.4.2 Switching control type

The switching control type realizes multi-DOF motion by switching the grasping pattern of the MPH with a switch or triggering motion. The control itself is based on the ON–OFF and proportional controls. However, intuitiveness is reduced because a button must be pressed each time the motion is switched.

In the Bebionic hand by Ottobock, 14 different grasping patterns are realized by combining proportional control and switches (Ottobock US n.d.).

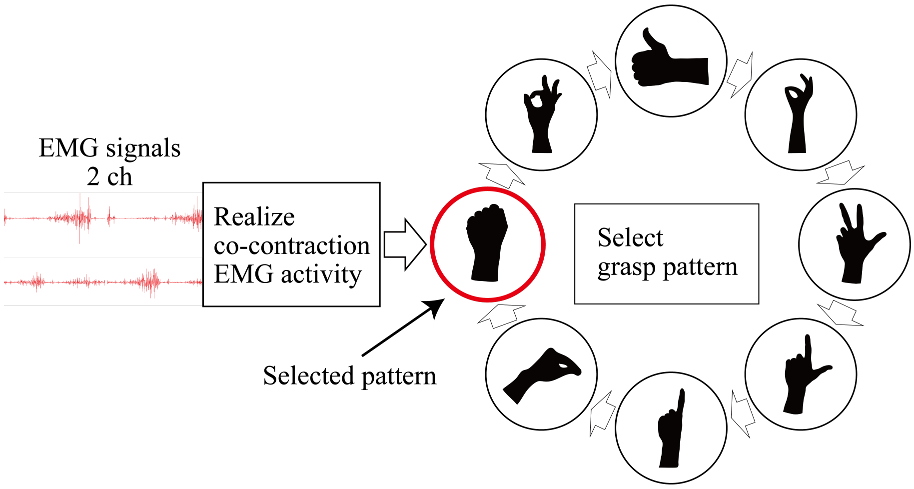

Fig.2.3: Diagram of switching type control. The case of using co-contraction for switching is shown. Prepared with reference to (Yang et al. 2019).

2.4.3 Pattern recognition type

MPH control methods based on pattern recognition generally use supervised learning, a type of machine learning, in which EMG and hand motions are sampled in advance and learned based on these signals to estimate hand motions from EMG. In this method, features are extracted by obtaining integral EMG from the EMG input by calculating the integral value or obtaining frequency components through the fast Fourier transform (FFT), which are then input to a classifier unit trained in advance to estimate hand motions. Neural networks (NNs) (Jiang et al. 2014; Hiroshi Yokoi et al. 2009), the support vector machine, linear discriminant analysis (Atzori et al. 2015), and other methods are used for discrimination.

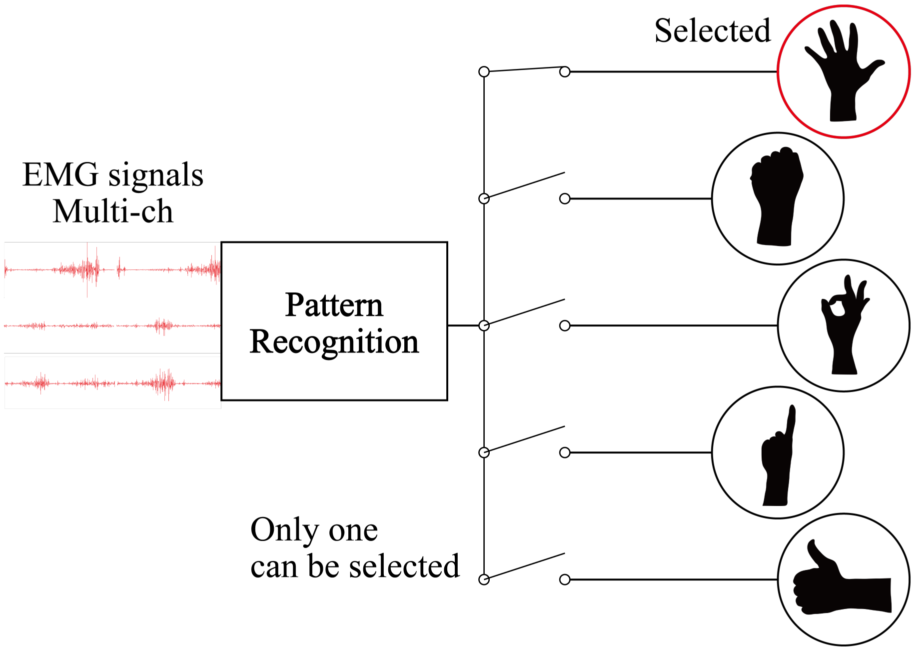

Fig.2.4: Diagram of Pattern recognition control. Prepared with reference to (Yang et al. 2019).

2.4.4 Multiple regression type

In the multiple regression-type control method, NNs and so on are used to acquire the force and joint angle data at the time of movement from force sensors and strain gauges and learn the relationship with the myoelectric potentials at that time to realize motion.

Nielsen et al. used a multilayer perceptron (also known as NN) to regress and control the three-DOFs of the wrist using five-channel EMG sensors (Nielsen et al. 2009). The multilayer perceptron uses force sensors to measure the force generated when the three-DOFs of the wrist are moved as well as the EMG signals; subsequently, these data are used to learn the multilayer perceptron.

Hioki et al. outputted the target joint angles using the NN, which enabled pinch motion with the thumb and index finger, wrist rotation, and hand opening using four-channel EMG sensors (Hioki et al. 2011). The learning method is based on combining EMG measurements during the three motions.

2.4.5 Combination type

The combination-type method combines pattern recognition and regression.

Tsuji et al. proposed a new MPH control method that considers the basic motions that constitute five-finger motions as muscle synergies and enable the control of various five-finger complex motions by combining muscle synergies (Tsuji et al. 2003; Furui et al. 2019). Using this method, they realized 10 motions (five basic movements and five compound motions) by pre-learning five motions of flexion of each finger (the ring finger and little finger are flexed simultaneously) and grip as basic motions using eight-channel EMG sensors. The prosthetic hand uses an encoder to detect the grasping of an object and switches for proportional control to generate a grasping force according to the muscle contraction level calculated from the EMG.

2.4.6 Summary of the control method and control target

This section presents the six classified MPH control methods and existing research related to these methods. The review demonstrates that most commercially available MPHs employ ON–OFF, proportional, or switching controls between these and grasping patterns using switches. Although the multiple regression type and the combination type have been realized at the research stage, no long-term clinical studies have been conducted, and these methods are not practical at this stage. On the contrary, the pattern recognition type has been used in clinical studies in recent years (Franzke et al. 2019; Simon, Turner, et al. 2019; Resnik et al. 2018), and previous studies have reported that MPHs with the pattern recognition-type control tend to use more variety of motions than those with the conventional switching-type control (Simon, Turner, et al. 2019). Therefore, this study uses the pattern recognition-type control, which is expected to have more practical use in multi-DOF MPHs.

2.5 Position of this study in MPH research

Before describing the problem setting in detail, the position of this study in context to related research is clarified. For this purpose, Fig.2.6 shows a roadmap for MPH research. The roadmap is divided into social impact, development method, hardware, and software, in descending order of influence. Each element influences each other; however, the upper elements have a greater influence on the lower elements. The items addressed in this study are circled in red, and their influence on the other elements is indicated by arrows. The problems to be solved in this study are also indicated by red squares.

Additionally, the explanation of the relationships between the elements of the roadmap and their respective frames is illustrated in Fig.2.5. When the frames are diagonally adjacent to each other, it indicates that these elements coexist in the same period. The distinction between the dashed and solid lines is particularly important. These represent the stages of implementation for the items addressed in this research, with dashed lines indicating elements that are implemented only in a research environment, and solid lines representing elements that have reached a stage where they can be used in everyday life.

With these considerations in mind, each item is described in chronological order.

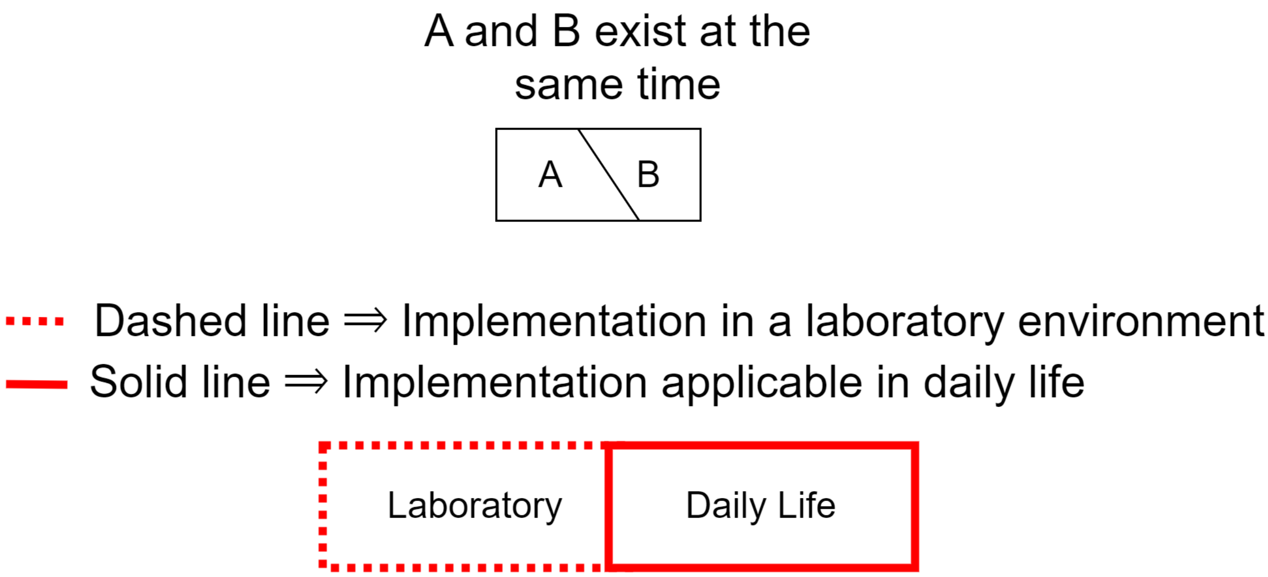

Fig.2.5: Explanation of the differences in relationships based on the types of frames in the roadmap.

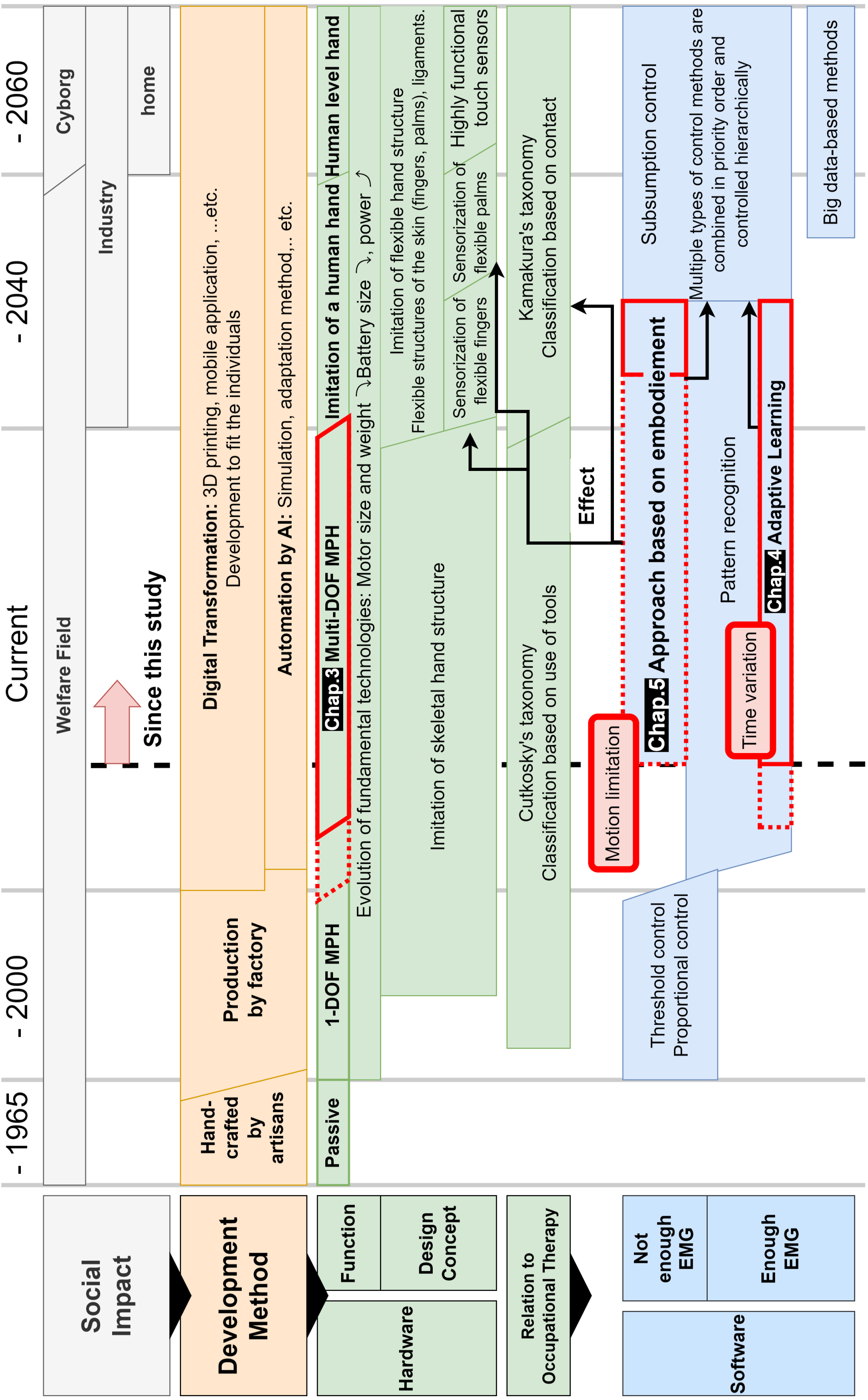

Fig.2.6: MPH's technology roadmap.

2.5.1 Prosthetic hand until approximately 1965

The earliest description of a prosthetic hand is that of an ornamental forearm prosthesis around 330 B.C., and an iron forearm prosthesis with a passive mechanism around 219–201 B.C (Takahashi 2011). The fact that prosthetic hands were produced as early as they were indicate that hands have been important to humans since ancient times.

The oldest extant iron prosthetic hands include the Florenz prosthetic hand and the Getz von Berlichingen prosthetic hand, which are believed to have been made in the late 15th century. These prosthetic hands were made by arm smiths and watchmakers.

2.5.2 Prosthetic hand until approximately 2000

Since the commercialization of the single-DOF myoelectric prosthetic hand in 1965, this type of single-DOF prosthetic hand has been in common use to this day. The control is either threshold control, in which the prosthetic hand moves when the myoelectric potential exceeds a certain value, or proportional control, in which the grasping force and speed of the prosthetic hand change in proportion to the magnitude of the myoelectric potential.

In this case, the hand, controller, battery, and other components of the prosthetic hand are manufactured at a factory. The prosthetist then makes a socket that matches the shape of the user's residual limb, and the prosthetic hand is assembled into this socket to complete the prosthetic hand.

2.5.3 Modern prosthetic hand

Today, advances in battery and motor technology have made it possible to reduce the size and weight of drive units, bringing multi-DOF MPHs to a level where they can be used in everyday life. These hands are now being sold and used commercially.

In addition, the manufacturing and control methods of machines have changed considerably owing to advances in digital technology (Digital transformation (DX)) and artificial intelligence technology.

Regarding hardware, there are examples of low-cost MPHs manufactured using 3D printers (Togo, Hiroshi Yokoi, et al. 2020), one of the DX technologies. Unlimited Tomorrow sells MPHs using 3D scanning and 3D printers (Tomorrow n.d.). The company uses a 3D scanner to scan the residual limb at each home and then uses a 3D printer to create a socket based on the data. This enables the production of MPHs without the need for a prosthetist.

This study also attempts to produce a low-cost multi-DOF MPH using a 3D printer and to commercialize it.

Regarding software, machine learning, a type of artificial intelligence, is used to make effective use of the multi-DOF MPH. In particular, pattern recognition that uses machine learning to learn and map the relationship between the motion of an operation target and the pattern of myoelectric potentials, and then predicts the motion from the newly input myoelectric potentials is applied. This method enables the user to use a large number of motions as long as the user can separate the muscle contraction patterns, and is suitable for controlling a multi-DOF MPH. This method has reached a stage where it can be used in daily life and has already been implemented and sold in some prosthetic hands (Togo, Hiroshi Yokoi, et al. 2020). However, these methods have the following problems.

Problem1
: EMG have the characteristics of instability and time-variation.

Problem2
: The number of separable muscle contraction patterns is limited.

In this study, each of these issues is addressed by the following methods.

1.Adaptive learning
: A method that adapts to and follows time variation in EMG

2.Approach based on embodiment
: A method that enables autonomous adaptive grasping of objects based not only on myoelectric information but also on information about the state of contact between

the hand and grasped object obtained from the touch sensor.

As shown in Fig.2.6, there are examples of adaptive learning implemented in a laboratory environment. However, all these are intended for use with devices such as PCs that are difficult to carry, and none are at a stage where they can be used in daily life.

The embodiment-based approach is a new concept not previously proposed as a control method for MPHs, as shown in Fig.2.6.

These methods will be fundamental in MPH research in the modern era and beyond. The reasons for this are explained in the next subsection.

2.5.4 Prosthetic hand after modern times

The prosthetic hand, which only improves the degree of freedom, acquires dexterity by imitating the flexible structure of the human hand (Fig.2.7). The approach based on embodiment (Fig.2.8) enables skillful control by combining an MPH with this flexible structure. This approach is described in Chapter 5 of this paper. When controlling a prosthetic hand by effectively utilizing the flexible structure, the flexible structure inevitably involves contact with an object. The embodiment-based approach autonomously adapts to the object based on the information about the contact state between the hand and grasped object obtained from the touch sensor, and thus enables adaptive grasping of the object by utilizing information that becomes richer as the number of flexible structures that have touch sensors increases. So far, this concept has not been proposed in the control of MPHs, and the embodiment-based approach development results discussed in Chapter 5 of this thesis will be a guide for future multi-DOF MPH research and development.

To effectively utilize an embodiment-based approach, it is crucial to have a hand that imitates the flexible structure of the human hand and fingers and palms that can maintain this flexibility while acquiring contact information. This is because the human hand uses its flexible structure to limit control space, thereby achieving stable control (V. K. Nanayakkara et al. 2017) and efficiently collecting contact information (Heller, Rogers, and Perry 1990; Voisin, Benoit, and Chapman 2002). The embodiment-based approach described in Chapter 5 of this thesis will emphasize the importance of these developments. Specifically, the hand's flexible structure will facilitate interaction between the hand and objects, restrict the control space, and utilize it for kinesthetic control, leading to dexterous hand control. However, until now, no research in MPHs has connected these structures with intelligence. An embodiment-based approach on the hand's physicality enables more efficient learning, leading to dexterous control; this research contributes significantly to understanding the mechanisms of grasp stabilization enabled by these hand structures.

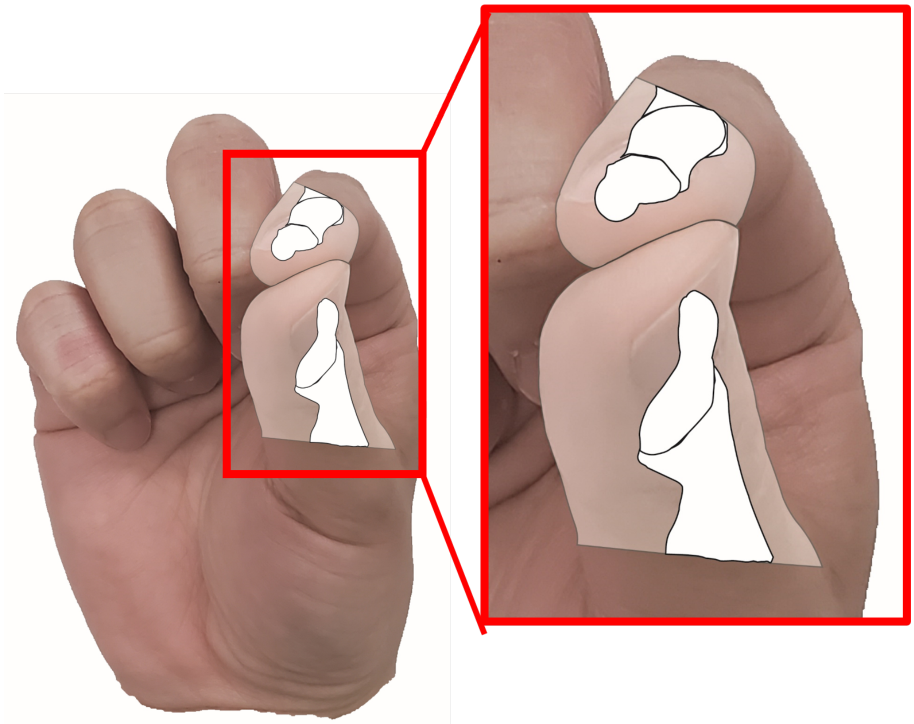

Fig.2.7: Flexible structure of the hand. The softness of the fingertips allows them to deform around the object being grasped, increasing the contact area, and stabilizing the grip. The hand also contains various other flexible structures such as tendons and ligaments.

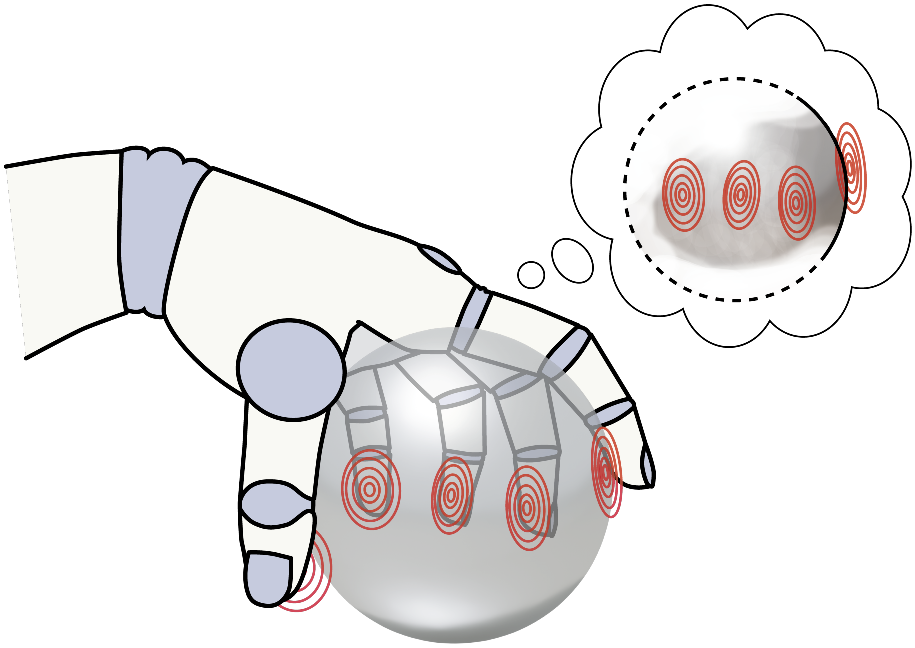

Fig.2.8: Embodiment-based approach. The hand's movement adapts to the shape of the object being grasped, based on the contact state between the hand and object obtained from touch sensors.

Regarding software, the parallel processing performance is expected to improve due to the technological innovation of mobile devices with DX. In this case, research is expected to progress in the direction of combining multiple control methods as a more stable method of controlling MPHs. Here, the subsumption architecture by Brooks will serve as a reference. Subsumption architecture enables robots to combine prioritized actions in parallel and operate hierarchically, creating an autonomous control system that is flexible with respect to its environment (Brooks 1986). Here, this system is applied to a control system for MPHs and the control method is called subsumption control. By combining adaptive learning, pattern recognition control, and an embodiment-based approach, an MPH control system that can control more stable and skillful motion can be created.

If MPHs acquire functions equivalent to those of human hands in the above manner, they can be used not only for welfare purposes, but also as end-effectors of autonomous labor in industry and the home. In addition, as MPHs approach the functions of the human hand, the fusion of man and machine will be accelerated (cyborg).

2.6 Requirements: Requirements for long-term clinical application of multi-DOF MPHs

Few studies have been conducted on the long-term clinical application of multi-degree-of-freedom myoelectric prosthetic hands. In particular, there are even fewer studies on the long-term clinical application of myoelectric prosthetic arms with pattern recognition control, which have recently been put to practical use. There have been studies on the long-term application of a high-performance MPH including the long-term application of a five-finger MPH with a commercial pattern recognition function (Coapt COMPLETE CONTROL) for more than eight weeks (Simon, Turner, et al. 2019) and a six-month application of Michelangelo, a commercially available MPH (Luchetti et al. 2015). Simon, Turner, et al. applied multi-DOF MPHs to four individuals with upper limb deficiencies over a period of eight weeks. They found that users tended to use a greater variety of motions through pattern recognition. Studies that evaluated high-functioning MPHs by interviewing the stakeholders have also been reported. Franzke et al. interviewed experienced MPH users and therapists (Franzke et al. 2019) and reported that pattern recognition was evaluated as being intuitive but unreliable for everyday use and that the users required extensive training. L. J. Hargrove et al. compared pattern recognition control with conventional direct control, which includes conventional threshold control and proportional control, in patients undergoing targeted muscle reinnervation (TMR) surgery. TMR is a surgical procedure in which the residual nerve in the amputated limb is surgically transferred to the residual muscle nerve and reinnervated to enable efficient control of the MPH(Todd A Kuiken et al. 2007). Participants used the pattern recognition control at home for six to eight weeks. The results showed that seven out of eight participants preferred the pattern recognition control(L. J. Hargrove et al. 2017).

These studies are summarized in Table.2.4.

According to Table.2.4, the duration of clinical application varied, but most of the studies were conducted for more than two months. Therefore, this study aims to achieve clinical application for more than two months.

In addition, the evaluation method is often a combination of not only task evaluation but also subjective evaluation using questionnaires. Therefore, in this study, a combination of these evaluation methods is used.

Although the number of participants in previous studies has been four or more, it is difficult to secure participants in Japan, where the use of myoelectric prosthetic hands is low. Therefore, the goal is to conduct long-term clinical application to at least two participants.

When evaluating a multi-DOF MPH, it is desirable to be able to evaluate it with a greater number of patterns than when controlling a single-DOF MPH. Therefore, in this study, at least four motions have to be included in the upper limb function evaluation test in addition to the motions possible with a single-DOF MPH, i.e., resting, grasping, and opening.

Table.2.4: Summary of studies on long-term clinical application of multi-DOF MPHs

Reference	Type of Prosthesis	Pattern Recognition	Duration	Number of Participants	Evaluation Method	Findings
(Simon, Turner, et al. 2019)	i-limb Ultra Revolution Hand	Coapt COMPLETE CONTROL system	8 weeks	4	Pattern recognition	Users tend to use a wider variety of movements
(Luchetti et al. 2015)	Michelangelo	-	6 months (3 months:functional assessment, 6 months: psycho-social assessment)	6	Functional assessment (task and questionnaire) and psycho-social assessment (interview and questionnaire)	Three months later, manual dexterity improved.
(Franzke et al. 2019)	Michelangelo	Pattern recognition system provided by Ottobock Healthcare Products	Used several times between 1 and 2 years	15 prosthesis users (Four of these users had experience with pattern recognition)	Semi-structured interviews with prosthesis users and therapists	Pattern recognition allows intuitive use but lacks reliability and needs significant training.
(L. J. Hargrove et al. 2017)	1 DOF hand	(Todd A. Kuiken et al. 2016)	6-8 weeks	8	Task assessment, Time-of-use statistics from control system and subject's report	Subjects after TMR surgery preferred pattern recognition over DC.

2.7 Requirements: Users' Requirements for MPH

2.7.1 Engdahl et al.'s study

Engdahl et al. used a Likert scale to survey 149 upper limb deficient individuals regarding their interest in each skill level of MPH (Engdahl et al. 2015). Two questionnaires were administered: one in which each skill level was independent and another in which the skill levels were cumulatively added as the questions progressed. The results of these questionnaires are presented in Tables.2.5 and 2.6, respectively.

In Table.2.5, wrist rotation, simple grasping movements, and various types of grasping movements received the highest ratings, whereas in Table.2.6, slow opening and closing movements received the highest ratings. According to Cipriani, Controzzi, and Carrozza, grip, precision, and lateral grasping account for 35%, 30%, and 20%, respectively, of the minimum ADL required by a person (Cipriani, Controzzi, and Carrozza 2010). The study by Cipriani, Controzzi, and Carrozza and the results of this survey indicate that the emphasis is on the user's demand for the prosthetic hand to enable ADLs. However, in Table.2.5, various types of grasping movements are also rated among the highest technology levels. Table.2.6 lists the tasks requiring advanced motor control (writing with a pen or typing)that are also rated highly at 68%. This indicates a high need for MPHs that enable advanced hand control.

Table.2.5: Probability of favorable responses for individual technology levels. Prepared with reference to (Engdahl et al. 2015).

Performance level	Positive responses (%)
1. Open and close your hand slowly	72
2. Open and close your hand, and also rotate your wrist	74
3. Move to any location in your workspace and perform a simple grasp	74
4. Move to any location in your workspace and perform one of several types of grasps, in which you can control the force used	74
5. Perform fine tasks like writing with a pen or typing	51
6. Perform fine tasks and have touch sensation in the missing limb	40

Table.2.6: Probability of favorable responses on the cumulative level of technology. Prepared with reference to (Engdahl et al. 2015).

Performance level	Positive responses (%)
1. Open and close your hand slowly	78
2. Do all the above AND rotate your wrist	71
3. Do all the above AND move to any location in your workspace and perform a simple grasp	77
4. Do all the above AND perform several types of grasps, in which you can control the force used	75
5. Do all the above AND perform tasks that require fine motor control (such as writing with a pen or typing)	68
6. Do all the above AND have touch sensation in the missing limb	59

2.7.2 Cordella et al.'s study

Cordella et al. reviewed the literature investigating the needs of previous upper extremity prosthetic users (Biddiss and Chau 2007; Kyberd and Hill 2011; Jang et al. 2011; Pylatiuk, Schulz, and Döderlein 2007; Ostlie et al. 2012; Bouffard et al. 2012; Luchetti et al. 2015) and summarized the requirements to be met by the prosthetic devices (Cordella et al. 2016). Here, this study summarized the essential requirements from Cordella et al.'s review, focusing on those related to MPHs.

Kyberd and Hill investigated the hours of daily use of MPHs and found that, in a survey of 42 individuals, 40% used MPHs for 12 h or more and 43% used them for 8–12 h. A survey of 2- to 5-year-old children showed an average of 5.8 h of use per day (Egermann, Kasten, and Thomsen 2009). The results of sPylatiuk, Schulz, and Döderlein's study are presented in Table.2.7. The duration of use tended to be long in these studies, which may be related to the fact that the studies were conducted to evaluate the needs of people who use prosthetic hands (Kyberd and Hill 2011).

Table.2.7: Time of prosthesis usage at work and while performing recreation activities (%)(Pylatiuk, Schulz, and Döderlein 2007)

	Time of prosthesis usage	females	males	children
At work / school	$\geq$ 8h	83	86	14
	4–6 h	17	14	14
	0–4 h	0	0	72
During recreation	$\geq$ 8h	67	67	12
	4–6 h	0	6	0
	0–4 h	33	27	88

In addition, Biddiss and Chau and Kyberd and Hill summarized the priorities for the design and features of MPHs. The results of these two studies are presented in Table.2.8. From Table.2.8, it can be observed that the weight of the prosthetic hand is an essential factor. This is a severe problem in the study by Pylatiuk, Schulz, and Döderlein, in which 77 % of the respondents reported that their prosthetic hand was too heavy. In particular, as summarized in Table refTable:CommercialMPH, multi-DOF MPHs require several motors to be mounted inside the hand and tend to be heavier than low-DOF types. Therefore, developing a lightweight multi-DOF MPH is essential in improving user convenience.

Considering that the weight of a human hand is approximately 400 gw, there are several multi-DOF MPHs that weigh 400–500 gw, as reported in (Kaye and Konz 1986) and Table.2.1, which appear to be comparably heavy. However, humans reduce the load by distributing this weight to the upper limb through the muscles, fascia, tendons, and bones, among others (Liu et al. 2022; Sun, Cao, and Song 2020; Lessard et al. 2016). When an MPH is attached to a person with an upper limb defect, the MPH and the residual limb are entirely independent; therefore, the loads of the MPH and grasping object are applied to the residual limb. Hence, the MPH needs to be as light as possible.

Reliability is also mentioned, and improving the reliability of electrodes and batteries is also highly important.

Table.2.8: Survey results on the priority of features to be developed for MPH

(Biddiss and Chau 2007)	(Kyberd, Wartenberg, et al. 2007)
Weight	1) Ability to move separately the fingers and thumb
Glove durability	2) Ability to prevent object slipping
Cost	3) Adaptability of grip strength
Sensory feedback	4) Increase the wrist Range of Motion(RoM)
skills/dexterity	5) Increase movement speed
Heat	6) More natural appearance (size, color, and surface materials)
Appearance	7) Control of temperature/transpiration
Reliability	8) Reliable precision
Independently moving fingers	9) Less weight
Fit	10) Reduction of noise
Wrist movement/control	11) Increase sensory feedback

2.8 Requirements: Design requirements for a multi-DOF MPH

2.8.1 Implementation requirements

In this section, we will describe the implementation requirements that have to be considered when applying MPHs. As described in Section 2.2.1, an MPH consists of an electric hand, controller, EMG sensor, battery, and socket. When in use, the electric hand is connected to the end of the socket; the controller, EMG sensor, and battery are built inside the socket. In some MPHs at the research stage, the controller, battery, and sensor were mounted and installed outside the socket (Kato, Yokoi, and Arai 2006). In the case of wire-driven or pneumatic actuator-type multi-DOF MPHs (Seki et al. 2013; Seki et al. 2014; Ryu Kato and Hiroshi Yokoi 2009; Ryu Kato 2008; G. Gu et al. 2021), the motor and pump module may be mounted in a pouch for portability.

In the laboratory, short-term experiments can be conducted in such a state; however, in actual home use, such systems can easily break down owing to the generation of shocks during use. As reported by Bhaskaranand, Bhat, and Acharya, repeated failures were cited as the primary reason for discontinuing the use of prosthetic hands. Therefore, it is essential to manage shock generation during MPH use. In other words, it is crucial to protect the controller, which is prone to failure, and the cables that connect the electric hand, EMG sensor, and battery from shocks by placing them inside the socket. To achieve this, the controller must be miniaturized to the point where it can be built into the socket. Similarly, the battery must be sufficiently small to be built into the socket or not protrude from the socket. The shock resistance of the electric hand itself is also essential.

For the controller, if the user has a long residual limb, the controller should be mounted close to the wrist of the socket. Therefore, this study refers to the statistics of the wrist width of the Japanese as the size that can be mounted in the socket (Kouchi 2012). According to Kouchi, the average wrist width of the Japanese is 55.5 mm, and the minimum is 45.8 mm. Even if the controller is mounted in the center of the socket, the width or depth of the controller should be smaller than this because the height of the controller is basically smaller than the width or depth of the socket. Therefore, the size of the controller should be less than 40 $\times$ 40 $\times$ 20 mm to enable a larger margin than the minimum wrist width of 45.8 mm.

The battery should be designed for the long-term use of the myoelectric prosthetic hand, as described in Section2.7.2. However, since there is a trade-off between the usable time and battery weight, the longer the usable time, the heavier should the battery be. Moreover, the battery must be replaceable.

2.9 Requirements: Functional requirements for MPH control systems

2.9.1 Addressing time-variation in EMG

Typically, EMG is used to control electric prosthetic hands. Although there are studies on controlling MPHs using muscle bulges or brain waves, these have not yet reached practical application. Currently, EMG is the most practical source of control signals; it has been used for many years and its usefulness has been verified.

During the use of an MPH, physiological and psychological factors can alter the myoelectricity during the performance of any given movement. Sensinger, B. A. Lock, and Todd A. Kuiken has specifically mentioned the causes of such changes: electrode conductivity changes (perspiration and humidity), electrophysiological changes (muscle fatigue, atrophy, or hypertrophy), spatial (displacement) changes (electrode movement on the skin or soft tissue fluid fluctuations), user changes (cognitive intent variations or contraction intensity changes), and other potential factors (Sensinger, B. A. Lock, and Todd A. Kuiken 2009).

Pattern recognition control uses supervised learning, a type of machine learning, in which myoelectric signals and hand motions are sampled in advance and learned from them to estimate hand motions from myoelectric signals. The purpose of pattern recognition is to map a newly input EMG pattern to one of the hand motions. The concepts to be recognized by pattern recognition, such as hand motions, are referred to as classes. When "grasp" is set as one of the classes, for example, it is called a label. A pair of myoelectric signals (data) and hand motions (labels) is called teacher data. The operation of the associating data and labels is called labeling.

Fig.2.9 illustrates the concept of pattern recognition control. In pattern recognition control, myoelectric potentials are basically converted into a feature vector that represents the characteristics of the data by FFT or other means. The space formed by these feature vectors is called the feature space. In the feature space, clusters with similar features are formed; these are called clusters. In pattern recognition, feature vectors are classified by drawing boundaries that divide these clusters. Hand movement corresponding to the new EMG data can be estimated depending on the side of the decision boundary that the new input comes from. The patterns around the decision boundary are similar; hence, they may contain erroneous motions. Therefore, the area around the decision boundary is sometimes treated as unrecognizable, otherwise called a reject area.

As shown in the lower part of Fig.2.9, because EMG signals vary interpersonally, the position of the training data for the same movement differs. By creating individual training data for each person in advance, pattern recognition control can create a classifier tailored to each individual, thus enabling it to accommodate personal differences.

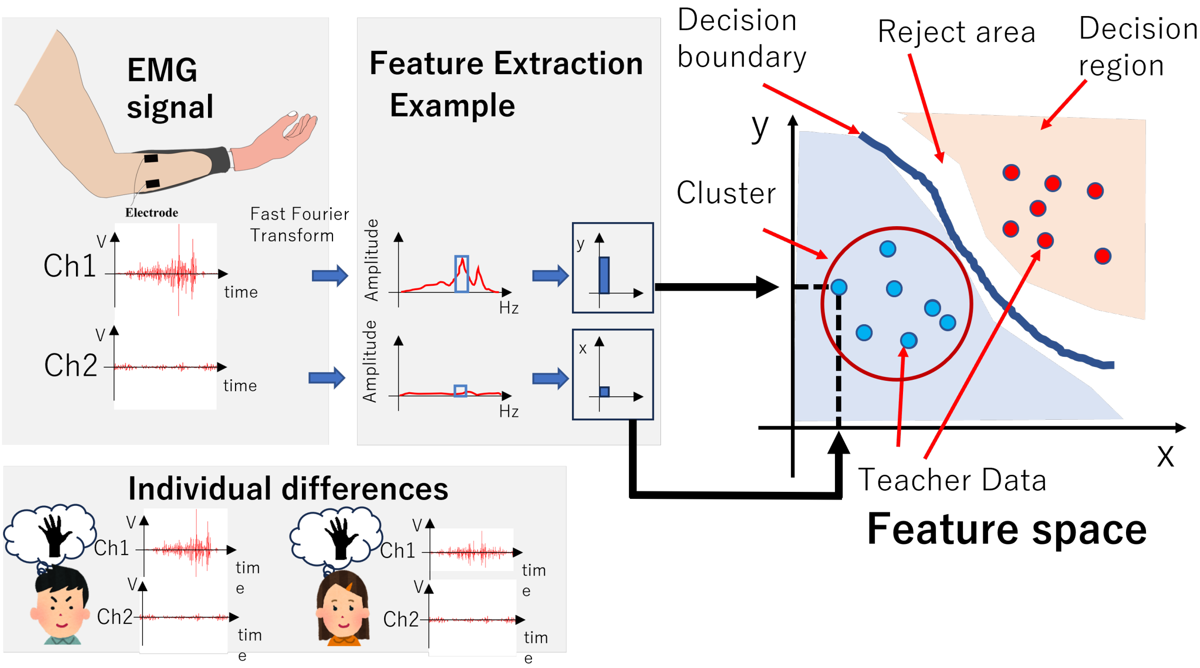

Fig.2.9: Explanation of pattern recognition control method.

In pattern recognition control, recognition depends on the teacher data obtained in advance. If this is the case, the correspondence between myoelectric patterns and motions can change owing to the time variation of the myoelectric potentials, resulting in malfunctions.

Therefore, for a stable MPH control system, it is necessary to deal with this time variation.

Q. Huang et al. referred to such a method of online updating of classifiers following time-varying changes adaptive learning and classified it into supervised adaptation and unsupervised adaptation, depending on whether the learning method requires labeled samples to relearn the prediction model or not (Q. Huang et al. 2017). Supervised adaptation is also called online learning in some studies (Nishikawa et al. 2000). There are also methods that combine supervised and unsupervised adaptation, which are referred to as semi-supervised adaptation in this study. Supervised adaptation can achieve high recognition accuracy, but it requires a complicated learning process in which labeled samples are repeatedly acquired. Unsupervised adaptation is easier to use because it does not require retraining; however, there is a risk that the recognition accuracy will be degraded (Sensinger, B. A. Lock, and Todd A. Kuiken 2009).

Studies that address the time variation of EMG are discussed in more detail in Chapter 4.

2.9.2 Limitation of the number of recognizable motions

Pattern recognition control is expected to be of practical use in multi-DOF MPHs; however, problems exist due to its characteristic of realizing various motions using different muscle contraction patterns.

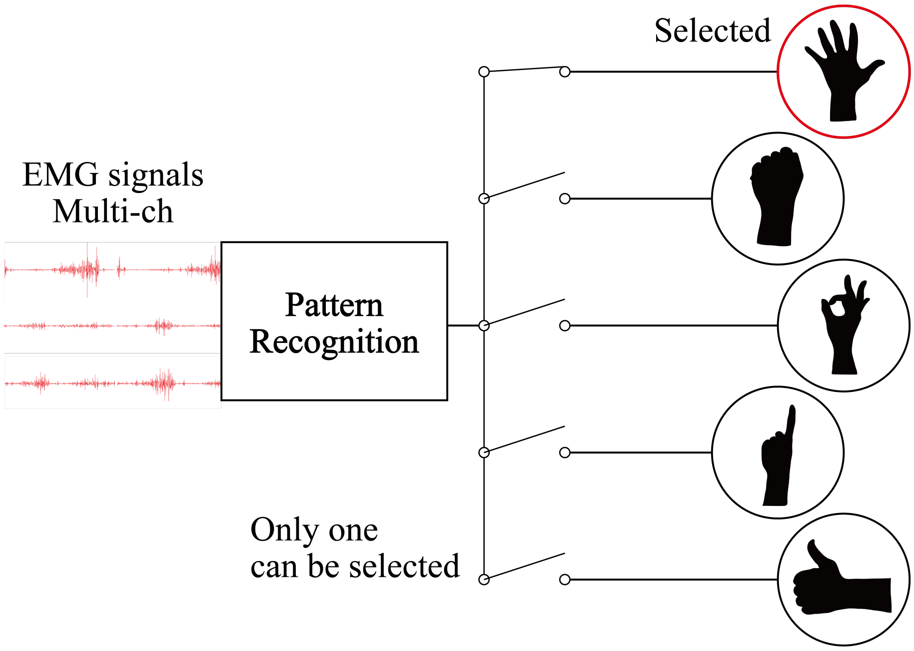

Fig.2.10: Conceptual diagram of pattern recognition control. The complexity of the user's operation increases with the number of movements. Prepared with reference to (Yang et al. 2019).

In pattern recognition control, the operator changes the muscle contraction pattern and intensity of muscle contraction to achieve multiple movements. In this case, there is a one-to-one correspondence between the myoelectric patterns and hand movements. In other words, as the number of degrees of freedom to control increases, the muscle control required of the operator becomes more complex and difficult to control. In particular, because humans unconsciously perform grasping that is adaptive to the shape of the object to be grasped, operability is reduced when the user chooses to do this.

Fig.2.11 summarizes the grasping motions of a sphere in the grasp classification by Cutkosky. Even with variations in only the sphere size, there are several types of grasping actions, highlighting the difficulty in selecting the appropriate grasping motion while controlling a prosthetic hand.

If adaptive grasping of objects becomes possible, users will not need to select specific grasping motions. This will enable movement patterns to be allocated to other functions besides object grasping, hence, improving operability.

Fig.2.11: Grasping types for sphere from Cutkosky 's taxonomy (Cutkosky 1989).

Therefore, this research sets the requirement to handle 20 different types of objects or directional variations, as the upper extremity functional test (Carroll 1965), a functional assessment method for hemiplegic patients; moreover, it uses 17 items for evaluation. Directional variations are included because, as indicated in Cutkosky's taxonomy, the grasping method changes with direction. Additionally, the capability to perform multiple hand movements is desirable, hence a requirement of five or more movements is set.

2.10 Requirements: Practical requirements for MPH control systems

2.10.1 Hardware restrictions

Most of the studies dealing with time variation use an offline evaluation method in which the recognition rate is calculated and evaluated based on the myoelectric data measured in advance. Even in the case of online evaluations that assess the recognition rate while actually using an MPH or EMG recognition system, the system is configured using a PC (personal computer), and no adaptive learning system has been found with a portable device that can be used in a practical environment.

Adaptive learning in a practical environment requires the use of a different thread or a different computer than the one used in the main process to learn improved teacher data without interrupting or delaying the main process, EMG classification, during the learning process. Considering this, the following five configurations are possible for a system that can be used in a practical environment.

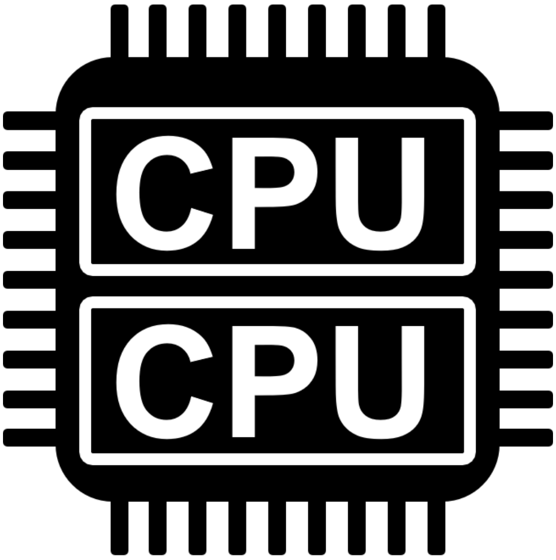

(a) Edge computing (multicore microcontroller)

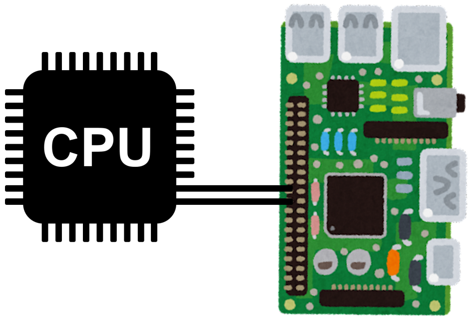

(b) Distributed computing (microcontroller + single board computer)

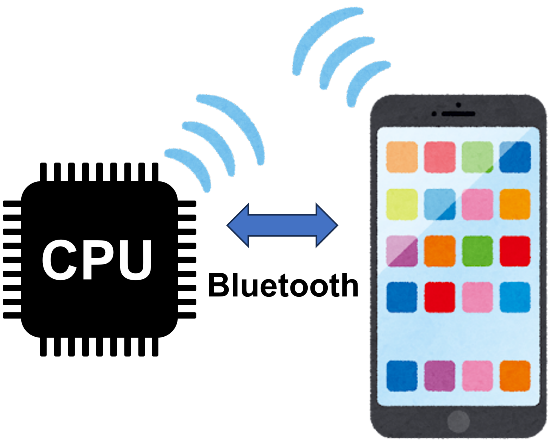

(c) Mobile edge computing (microcontroller + mobile device)

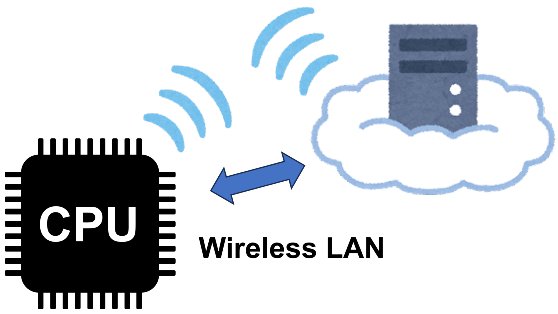

(d) Cloud computing (microcontroller + cloud server)

Fig.2.12: Conceptual diagram of the system configuration for adaptive learning.

1.Edge computing

This method uses a multi-core microcontroller. Because adaptive learning is possible with a single microcontroller, the controller can be minimized. The method also reduces power consumption. However, the processing performance is inferior to that of single-board computers, tablets, smartphones, and cloud servers.

2.Distributed computing

This method combines a microcontroller for real-time processing such as EMG sampling and motor control, and a microcontroller or single-board computer with high processing power for machine learning processing. However, there are disadvantages such as a larger controller size and higher power consumption.

3.Mobile edge computing(Mao et al. 2017)

This method replaces machine learning processing by connecting a tablet or smartphone via Bluetooth or wireless LAN to a microcontroller for real-time processing such as EMG sampling and motor control. The recent advances in the functionality of tablets and smartphones have made it possible to achieve processing capabilities similar to those of PCs. One of the disadvantages is that the communication situation may become unstable depending on the environment.

4.Cloud computing

This is a method in which a microcontroller is connected to the internet for real-time processing such as EMG sampling and motor control, and a cloud server replaces the machine learning process. One of the disadvantages is that the real-time performance may be degraded depending on the distance from the server.

Table.2.9: Comparison of system configurations for adaptive learning

Item	Edge Computing	Distributed Computing	Mobile Edge Computing	Cloud Computing
Configuration	Multicore microcontroller	Two microcontrollers or A microcontroller and a single-board computer	Microcontroller + Tablets or smartphones	Microcontroller + Cloud server
Processing Power	✓ Limited processing capability	✓✓ Superior to multicore microcontrollers. Some are equipped with GPUs.	✓✓✓ Recent flagship models can have processing powers equivalent to PCs.	✓✓✓✓ High processing capability.
Power Consumption	✓✓✓✓ Most have low power consumption.	✓ The higher the processing power, the more the power consumption.	✓✓✓ Consumes power for communication.	✓✓✓ Consumes power for communication.
Size	✓✓✓ May be slightly larger due to the number of cores.	✓ Tends to be larger as processing power increases.	✓✓✓✓ Compact as it offloads computational processes externally.	✓✓✓✓ Compact as it offloads computational processes externally.
Real-time Capability	✓✓✓✓ High real-time performance due to the combination of microcontrollers.	✓✓✓ Real-time performance decreases when using a single-board computer.	✓✓ Delay occurs due to communication.	✓ Delay increases with longer communication distances.
Communication Stability	✓✓✓✓ Stable as it is connected on the circuit.	✓✓✓✓ Stable as it is connected on the circuit.	✓✓ Can be unstable depending on the environment.	✓ Can be unstable depending on the environment. Worse than mobile edge computing as it requires internet connection.

The most important factor is to place the controller inside the socket; hence, miniaturization of the controller is of paramount importance. Therefore, distributed computing methods are not suitable for this system because they increase the size of the device as the processing performance is increased.

Edge computing methods offer high performance in terms of power consumption, size, real-time performance, and communication stability. However, the processing performance of microcontrollers including those with high performance is limited compared to other devices.

The cloud computing approach has the major advantage of high computational performance; however, its long communication distance makes it inferior in terms of real-time performance. A major disadvantage is that it cannot be used without an internet connection. Even today, internet access is unstable in some rural areas, and communication tends to be unstable in places where the signal is weak, such as underground regions. Moreover, when many people use the internet simultaneously during a large-scale event, the connection becomes unstable.

Mobile edge computing methods have two major advantages: mobile devices such as tablets and smartphones have become as powerful as PCs in recent years, and they do not require additional devices for high-performance computation processing to be added to the microcontroller, making them small in size. In addition, the user does not need to carry more devices, because mobile device applications are often used to provide the labeling required for supervised learning. However, there is a disadvantage in that information such as the EMG must be exchanged between the microcontroller and the mobile device via communication, resulting in a communication delay. Bluetooth and wireless LAN are communication methods between the microcontroller and mobile device; however, these methods may cause unstable connections in some environments, such as crowds. Therefore, the mobile edge computing method is expected to operate in such a way that when the control of the myoelectric prosthetic hand becomes unstable, the device is connected to the mobile device for a short period of time (several minutes) to perform adaptive learning, and then the learned parameters are sent to the microcontroller to reflect the learning results. In this case, because there is a possibility that teacher data may be stored in the microcontroller, the method must improve the discrimination stability while limiting the amount of teacher data. The advantage of this method is that, except during adaptive learning, the myoelectric prosthetic hand can be controlled by the microcontroller, thus solving the real-time problem.

Therefore, this study adopts the mobile edge computing method.

2.10.2 Usage restrictions

When using an adaptive learning system for MPHs in a practical environment, various restrictions need to be considered. This section describes these restrictions.

Restrictions due to manual labeling

When controlling MPHs by pattern recognition, the labeling of the teacher data is mainly done by the user or an assistant using an external device such as a tablet. Yamanoi et al. highlighted the limitations in this process (Yamanoi et al. 2021). According to Yamanoi et al., the general control flow of an MPH hand is as follows.

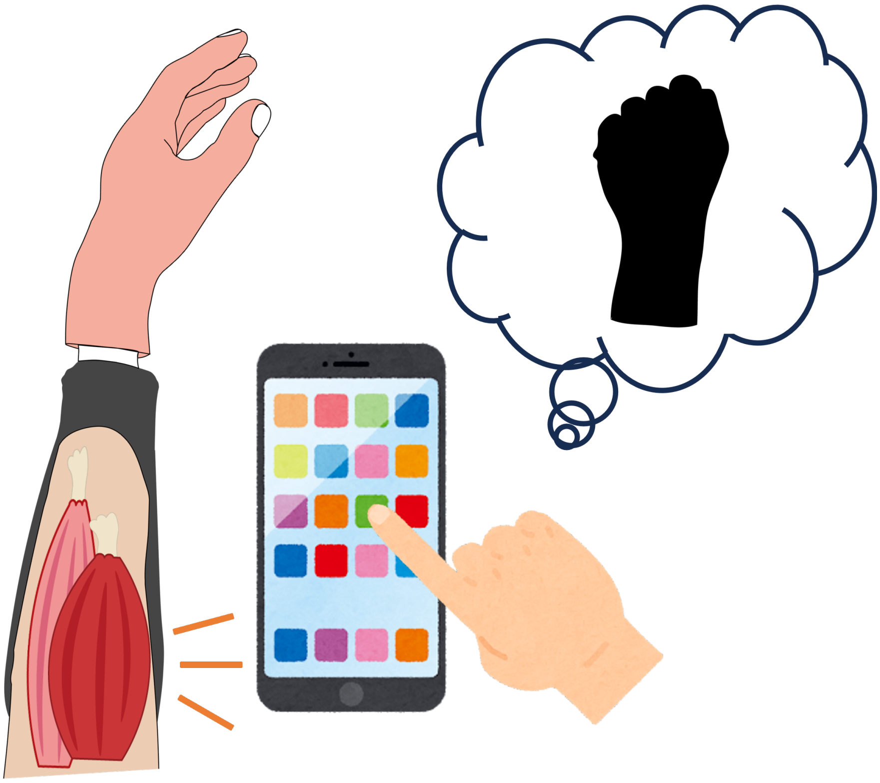

Fig.2.13: Labeling process. The user must press a button corresponding to the desired movement when performing specific muscle activities, thus labeling the signal.

1. The subject wears the myoelectric hand.
2. The subject demonstrates a specific muscle activity, and the signals are stored with a label for the corresponding posture.
3. Steps 1–2 are repeated for every pattern that needs to be learned.
4. After all the necessary data are stored, the classifier learns from these input data.
5. After learning, the classifier is able to classify the current muscle activity using the learned parameters and control the robot hand based on the classification results.

Yamanoi et al. pointed out the problem of labeling in step 2, where, unlike general pattern recognition such as image processing, the correctness of the labels of the training data is unknown in the case of myoelectric prosthetic hands. Furthermore, because the training data are manually collected by humans, similar movements are labeled with different movements, making classification difficult. In the case of infants who have difficulties communicating with others, it is difficult to apply pattern recognition control methods because of the difficulty of labeling. This problem was addressed in a study in which pattern recognition control methods were applied to infants; the results showed that similar supervised data were measured for different actions, indicating the need for methods that do not depend on human ability to label the movements (Hiyoshi et al. 2018).

In contrast, supervised and semi-supervised adaptation require labeling of new input data by the user. As mentioned earlier, labeling human ability is required, although it is a useful method that can improve and stabilize the discrimination accuracy if the labeling human ability is high. There are methods such as those proposed in Ryu Kato's research that control the addition of newly labeled teacher data based on the degree of competition for the training data (Ryu Kato 2008); however, if the human labeler's ability is low, there is a risk that effective teacher data will not be obtained.

Therefore, unsupervised adaptation is preferable because it can improve the classifier's performance regardless of the ability of the human labeler.

Restrictions by user proficiency level

Ryu Kato mentioned that there is a correlation between the proficiency level and the motion recognition rate. They also noted that the distribution of feature vectors output by the user becomes larger when the user's proficiency level is low (Ryu Kato 2008).

Yamanoi et al.; Ryu Kato mentioned that mathematically ideal teacher data would have low within-class variance, high between-class variance, and boundary data eliminated (Yamanoi et al. 2021; Ryu Kato 2008) as shown in Fig.2.14. However, as Simon, B. A. Lock, and Stubblefield's study pointed out changes in the muscle contraction force (Simon, B. A. Lock, and Stubblefield 2012), which increase intra-class variance, are a major cause of poor recognition; hence, it would be difficult to control a myoelectric prosthetic hand using such ideal teacher data without a high degree of proficiency.

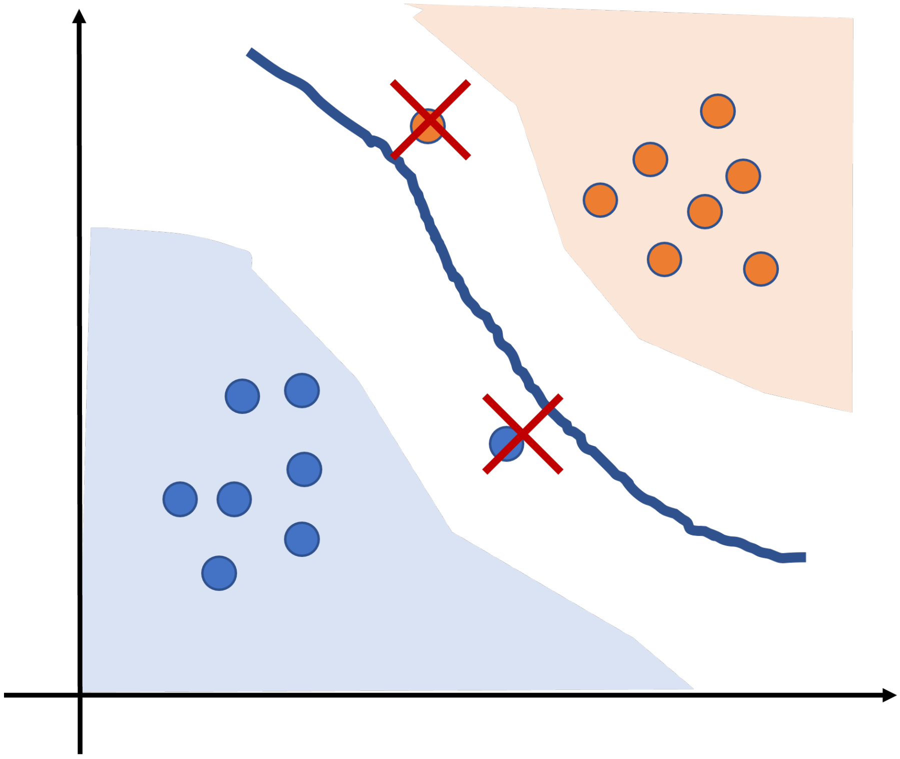

Fig.2.14: Ideal teacher data. The blue and red areas represent the regions identified by pattern recognition for each respective movement.

Although it is possible to change the adaptive learning method applied according to the level of proficiency, the user's usability may change or the system configuration of the myoelectric prosthetic hand may need to be changed. In such cases, changing the adaptive learning method is a significant burden for the user.

Therefore, it is necessary to develop an adaptive learning method that can improve the recognition rate regardless of the user's proficiency level.

2.10.3 Recognition rate to be achieved

Definition of recognition rate

The recognition rate is one of the most widely used and important indicators of the stability of MPH control. It is generally defined as the percentage of time or number of data that are correctly identified out of the data acquired for evaluation. Although the number of data does not change even if the recognition rate is calculated based on time for devices with high real-time performance such as microcontrollers, in this study, the evaluation is based on the number of data because myoelectric recognition is performed using mobile devices such as tablets and smart phones.

When N^y_{all} evaluation data of a motion y to be evaluated are measured, $N^y_{correct}$ is the "number of pieces identified as y" and N^y_{error} is the "number of pieces not identified as y". In this case, the motion identification rate of R^y (%) for motion y is obtained using the following equation:

$$R^y = \frac{N^y_{correct}}{N_{all}} \tag{2.10-1}$$

$$N^y_{all} = N^y_{correct} + N^y_{error} \tag{2.10-2}$$

Here, the calculation method of the recognition rate in the case of an unrecognizable area in pattern recognition is considered. Additionally, the following two calculation methods are considered:

If unrecognizable is considered as an incorrect answer N^y_{error}
In this case, the evaluation is relatively severe. When controlling the MPH, the evaluation may be far from the actual operability because the control of the MPH hand is often not performed when the identification is impossible.

If unrecognizable is regarded as the correct answer $N^y_{correct}$
The recognition rate becomes comparatively high. As mentioned earlier, when controlling a myoelectric prosthetic hand, control is often not performed when identification is not possible; hence, this method reflects the actual operability. However, when the percentage of unrecognizable is high, the change of operation may be delayed owing to the mixture of unrecognizable; in such cases, caution is paramount.

The evaluation used in the experiments in this study is specifiedA.

Recognition rate enables stable control

A recognition rate that enables stable control has not been found in any study that provides a particularly well-founded value, as described in the study by B. Lock, Englehart, and Hudgins. However, some previous studies have set 85 % as the threshold for a stably controllable recognition rate (Ryu Kato 2008; Yamanoi 2019). Recently, however, Kasuya, Ryu Kato, and Hiroshi Yokoi developed a recognition stabilizing filter, which could improve the recognition rate by determining the final recognition motion by majority voting based on the frequency of recognitions (Kasuya, Ryu Kato, and Hiroshi Yokoi 2015). Considering the use of the recognition stabilization filter, the stable control of MPHs is achievable even with a relatively low threshold value for recognition rates calculated before applying the filter.

Therefore, in this study, the recognition rate that enables stable control is set to 80 %.

2.11 Summary of problem settings

This study used the MPH as a model case with the following objective:

To clarify the problems of assistive technologies and systems for persons with disabilities through the actual development of a myoelectric prosthetic hand and to investigate methods for developing assistive technologies that can sustainably improve their QOL.

In Japan, for a user to receive an MPH under the public support system, it must be registered as a ready-made part. However, as mentioned in Section 2.3, there are no inexpensive and highly functional multi-DOF MPHs in the market. The current APCSDLLSPD does not focus on people with disabilities acquiring functions similar to those of non-disabled people; it tends to provide MPHs only with the minimum necessary functions. However, this limits the freedom of choice of occupation, and it is difficult to state that sufficient guarantees are provided. Therefore, providing users with access to highly functional MPHs as an option would help eliminate the obstacles of the current support system in Japan.

In addition, recently, methods for research and development of assistive technologies centered on people with disabilities have been proposed (Hamraie and Fritsch 2019). This is valuable because it allows researchers to propose assistive technologies to address real-life problems they may not know. In reality, however, as mentioned in (Ito 2019), the needs of people with disabilities are often unknown, and several issues are difficult to recognize without technical knowledge. In addition, if such methods are immediately adopted as the optimal developmental methods, researchers may be discouraged, and the research and development of assistive technology for persons with disabilities may decrease. This would lead to lost opportunities for this population, which would ultimately be a disadvantage. Therefore, it is necessary to conduct research and develop methods that incorporate many of the needs of persons with disabilities in a manner that does not deviate significantly from the current research and development process. Therefore, as a new developmental approach, this study proposed an approach to develop assistive technology for people with disabilities that utilizes feedback from long-term clinical applications.

Specifically, the following four approaches were used to achieve the objectives of this study:

- Development of a practical multi-degree-of-freedom (DOF) MPH system.
- Elucidation of the requirements of people with disabilities through functional and subjective evaluation in clinical application.
- Development of control methods to solve the issues related to pattern recognition revealed by clinical application.
- Improving user accessibility by registering inexpensive and highly functional MPHs as components for ready-made parts (完成用部品).

The problem set by the users’ requests and implementation requirements described thus far are summarized in Table.2.10 and Table.2.11.

Table.2.10: Summary of problem setting regarding engineering requirements

<table>
<tr><td colspan="4">Condition</td><td>Achievement Goal</td></tr>
<tr><td rowspan="9">Development of a practical MPH</td><td colspan="2" rowspan="3">Hand</td><td>DOF</td><td>Independent drive of 5 fingers</td></tr>
<tr><td>Strength</td><td>Handle external forces</td></tr>
<tr><td>Weight</td><td>Below 350 g</td></tr>
<tr><td colspan="2">Controller</td><td>Size</td><td>Below 40 × 40 × 20 mm</td></tr>
<tr><td rowspan="2">Sensor</td><td>Number of Channels</td><td>3</td><td rowspan="5">People with upper limb deficiencies can distinguish more than four motions in the task evaluation</td></tr>
<tr><td>Electrodes</td><td>Hybrid electrodes</td></tr>
<tr><td rowspan="2">Software</td><td>Control method</td><td>Pattern recognition</td></tr>
<tr><td>Teaching method</td><td>Tablet application</td></tr>
<tr><td colspan="3"></td></tr>
<tr><td rowspan="9">Addressing the challenges of pattern recognition control</td><td colspan="2" rowspan="7">Control stability</td><td>Method</td><td>Adaptation to time-variability</td></tr>
<tr><td>Adaptation method</td><td>Unsupervised adaptation</td></tr>
<tr><td>Adaptation requirement</td><td>Adapt regardless of proficiency, improve recognition rate or number of stable motion</td></tr>
<tr><td>Recognition Rate of stable control</td><td>Above 80%</td></tr>
<tr><td>Adaptation time</td><td>2-5 minutes</td></tr>
<tr><td>Number of training data</td><td>50</td></tr>
<tr><td>Portability</td><td>Portable (MPH + smartphone or tablet)</td></tr>
<tr><td colspan="2" rowspan="2">Realization of adaptive grasping adapted to the shape of the object</td><td>The number of objects or directions to adapt</td><td>20</td></tr>
<tr><td>Number of grasping motions realized by adaptive grasping</td><td>5</td></tr>
</table>

Table.2.11: Summary of problem settings regarding rehabilitation and social implementation

Condition		Achievement goal
Evaluation through Long-term clinical application	Evaluation period	More than 2 months
	Number of participants	2 people
	Evaluation method	Task evaluation and questionnaire evaluation
Improving user accessibility	Method	Registering the Multi-DOF MPH as ready-made parts
	Price	Comparable to the widely shared Myobock in Japan

2.12 Conclusion

This chapter summarized the related technologies for MPHs and the requirements for MPHs that have been investigated in previous studies. Subsequently, based on these requirements, a problem was set to achieve the study' s objective.

Section 2.2 described the general system configuration and control methods for MPHs.

In Section 2.5, the position of this study in MPH research was clarified using a roadmap.

Section 2.3 compared and described previous studies on electric hands, focusing on commercial MPHs.

Section 2.4 classified the control methods for MPHs into six categories and the existing control methods.

In Section 2.6, the requirements for the long-term clinical application of the multi-DOF MPH were clarified based on previous related studies.

Section 2.7 summarized the studies investigating users' requirements for MPHs and clarified the requirements that should be considered when developing a prosthetic hand.

Section 2.8 described the functional requirements for the implementation of a multi-DOF MPH.

In Section 2.9, the functional requirements of the MPH control system were described. Specifically, the section discussed the issue of time variation of myoelectric signals and the limitation of the number of recognizable motions.

Section 2.10 described the practical requirements for an MPH control system.

Section 2.11 described the problem setting for this study.

Chapter 3 Development and long-term clinical application of multi-DOF myoelectric prosthetic hand

3.1 Introduction

In this chapter, the five-finger, multi-DOF MPH (BIT-UEC-Hand) equipped with a pattern recognition function that I developed is described. This prosthetic hand is lightweight and has a mechanism to release external forces onto the fingers, preventing damage and ensuring safe use. It is also equipped with an EMG sensor for robust measurement and a recognition stabilization filter to cope with the limitations in computer performance.

The BIT-UEC-hand consists of a hand, controller, EMG sensor, battery, and socket. The hand was developed in a joint research project conducted at UEC and BIT. The BIT-hand developed in the collaborative research is equipped with a controller developed in the Yokoi Laboratory of the UEC called the "BIT-UEC-hand." Fig.3.1 shows the main functions of the BIT-UEC-hand.

Fig.3.1: Overview of the BIT-UEC-hand

Several commercial multi-DOF MPHs have been sold in recent years, and some people use these devices daily. However, examples of the usage of multi-DOF MPHs by the actual users are limited and their characteristics and problems faced during use have not been fully identified. Developing a highly functional MPH and improving its performance based on user feedback is the key to enhancing user convenience. Feedback, especially in the long-term application of MPHs, is the most important variable for revealing hidden problems in the clinical environment. This chapter identifies the characteristics and issues of a multi-DOF MPH controlled by pattern recognition through a long-term clinical application and clarifies the functions that are highly necessary for the users.

Section 3.2 describes the developed hardware of the BIT-UEC-Hand.

Section 3.3 describes the developed software for the BIT-UEC-Hand.

Section 3.4 describes the method for the long-term clinical application of the multi-DOF MPH in this study.

Finally, Section 3.5 presents the results and discusses the long-term clinical application experiment conducted in this study.

3.2 Hardware

3.2.1 Five-finger-driven electric prosthetic hand

The hand is predominantly made of nylon, with aluminum alloy at some joints and rubber at each fingertip. The weight of the hand is approximately 330 gw, which is 100-200 gw lighter than the existing commercially available five-finger electric prosthetic hands. This is expected to reduce the load on the user. This device consists of 11 joints. The active DOFs are one for each finger (thumb: CM joint and other fingers: MP joint, for five DOFs), whereas the MP joint of the thumb can be adjusted in three steps, as passive DOFs, and the wrist can rotate by 360 degrees. A linear motor (thumb: LAS10-23D and other fingers: LA10-21D; Beijing Inspire Robots Technology Co., Ltd.) was used as the actuator, and the maximum pinch force of the fingertips was approximately 12 N. Fingers other than the thumb have a mechanism to release external forces. Therefore, they can cope with impacts from the dorsal side of the fingers, which is expected in daily life owing to the lack of somatosensory and body possession senses, thus providing a high degree of safety.

(a) Palmar

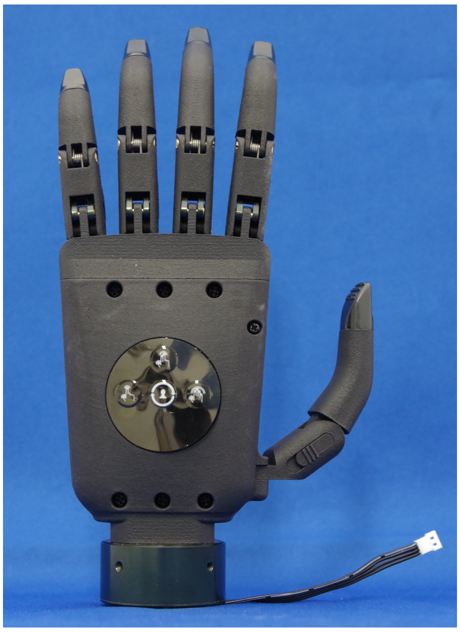

(b) Dorsal

Fig.3.2: BIT-UEC-Hand

3.2.2 Controller

As the controller is built into the socket, it is compact and lightweight, with dimensions of 35 × 35 × 14 mm, excluding the connector and a weight of 28 g. The lower part is equipped with a microcontroller 200-MHz SH72546R (Renesas Electronics Corporation), which has a calculation speed sufficient for real-time EMG signal analysis, and the upper part is equipped with a connector for connecting the sensor and the motor as well as a Bluetooth module (RN42-I/RM, Microchip Technology Inc.) used for communication with the tablet.

Fig.3.3: Controller of the BIT-UEC-Hand

3.2.3 EMG sensor

The EMG sensor comprises an electrode component that contacts the skin and a sensor amplifier component that amplifies minute myoelectric potentials. The electrode component is made of conductive silicone, which enables a more stable myoelectric signal measurement against external forces compared with the dry electrodes generally used in commercial MPHs. For further details, please refer to (Togo, Yuta, et al. 2019). A 50-Hz notch filter and a 50-Hz high-pass filter were built into the sensor amplifier component to mitigate the 50-Hz electromagnetic noise caused by commercial power sources in eastern Japan.

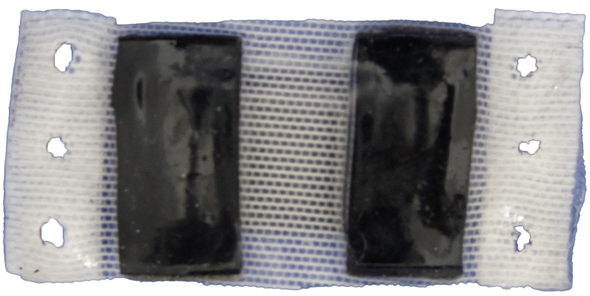

Fig.3.4: Sensor of the BIT-UEC-Hand

3.2.4 Battery

The battery used is a high-power lithium polymer that can drive multiple motors. Even when the hand constantly runs, it can be used for approximately 2.5 h. In addition, the cartridge system allows for an immediate battery replacement if the battery runs out.

Fig.3.5: Battery of the BIT-UEC-Hand

3.3 Software

3.3.1 EMG classification system

The hand component of the MPH is controlled by recognizing the user' s intention to move through pattern recognition based on the EMG of the user' s forearm. An overview of the control is shown in Fig.3.6. In addition to this system, a motor switch is mounted on the socket wrist that allows the hand movement to be fixed manually to address the reliability problem of pattern recognition control, as presented by Franzke et al. (Franzke et al. 2019).

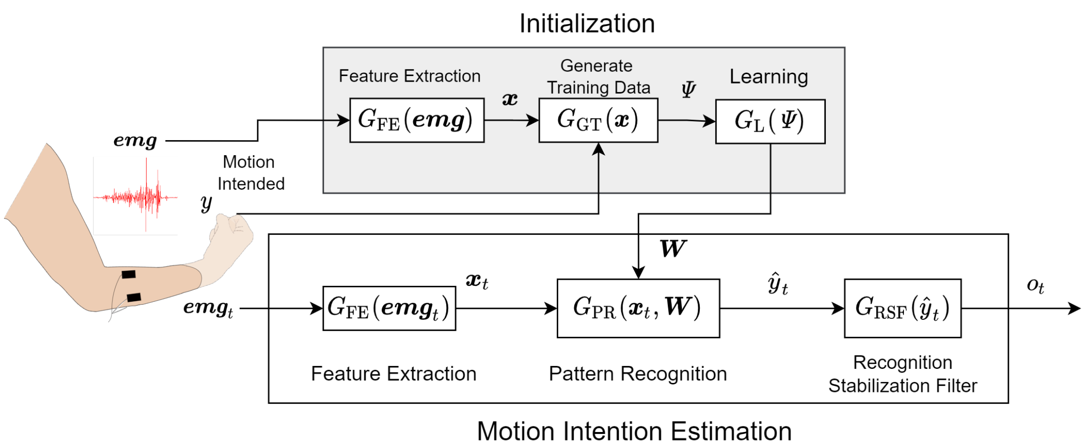

Fig.3.6: Classification of EMG signals

The system consists of two processes: initialization and motion intention estimation. First, the motion intention estimation is described. EMG signals $\boldsymbol{emg}_t$ measured by the EMG sensor at time t are converted into a feature value $\boldsymbol{x}_t$, which is in a data format that facilitates the discrimination of motion intention by the feature extraction function G_{FE}. The pattern recognition function G_{PR} then outputs $\hat{y}_t$, which is the predicted value of the motion intention. In this case, $\hat{y}_t$ is selected from the set of motion intentions Y learned at initialization. The $\hat{y}_t$ is input into the recognition stabilizing filter G_{RSF}, which outputs the motion intention o_t. The recognition stabilization filter refers to time-series data of the estimated motion patterns stored in a ring buffer for a certain period. It determines the output based on the proportion of estimated motion patterns in the time series(Kasuya, Ryu Kato, and Hiroshi Yokoi 2015). Assuming that the ring buffer stores the past N outputs, the ring buffer set B_t at time t is $B_t = (\hat{y}_{t-N}, \hat{y}_{t-N+1}, ..., \hat{y}_t, \hat{y}_t)$. In this case, the recognition stabilization filter G_{RSF} performs the following process:

$$B_t \bigcup \hat{y}_t \rightarrow B_t \tag{3.3-1}$$

$$B_t \setminus \hat{y}_{t-(N+1)} \rightarrow B_t \tag{3.3-2}$$

$$o_t = \arg\max_{i \in Y} f_i(B_t) \tag{3.3-3}$$

where f_i in (3.3-3) is a function that calculates the number of class i in the buffer.

Next, initialization is described. After EMG $\boldsymbol{emg}$ is measured, it is converted into feature $\boldsymbol{x}$ by the feature extraction function G_{FE} as in the case of motion intention estimation. At this time, the motion intention y when EMG $\boldsymbol{emg}$ is generated is measured simultaneously . y is measured by pressing a button on the tablet application that indicates the motion intention, which triggers the measurement of the EMG. Subsequently, teacher data $\psi = (\boldsymbol{x}, y)$ are generated by the teacher data generation function G_{GT}. The teacher data are buffered by G_{GT}, and after obtaining a certain number of teacher data, a set of teacher data Ψ is obtained. Using G_{Ψ}, the relationship between the EMG and motion intention is statistically learned by the learning function G_{L}, and the parameter $\boldsymbol{W}$ of the pattern recognition function G_{PR} is derived.

The specific configurations for each function employed In this study are detailed in Table 3.1.

3.3.2 Android application

An Android application, SignalViewer, was used to record the motion intention y shown in Fig.3.6. SignalViewer is an Android application developed by Qt, a cross-platform application framework. It can visualize EMG signals, display feature values, and acquire teacher data by connecting to a controller via Bluetooth communication.

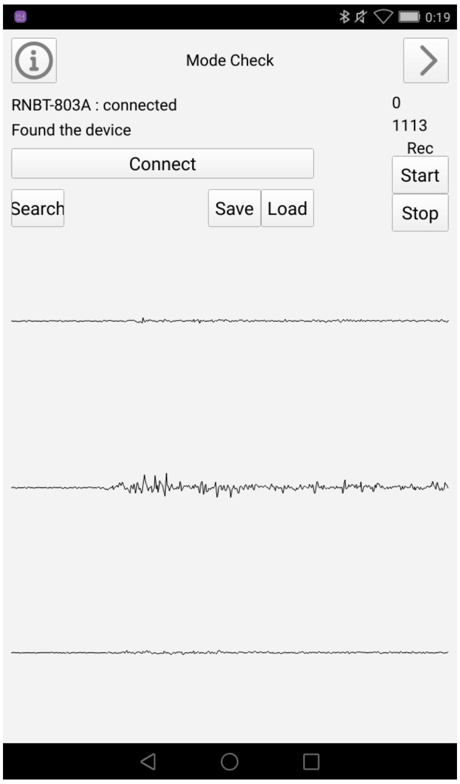

(a) ModeCheck

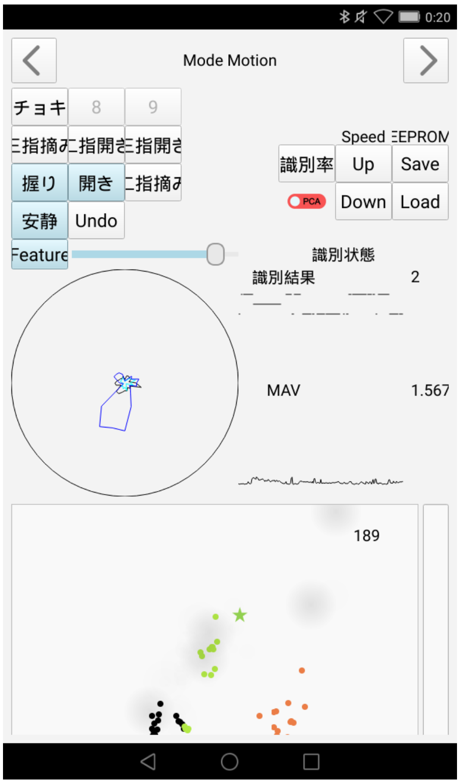

(b) ModeMotion

Fig.3.7: SignalViewer display screen. (a) ModeCheck enables connection to Bluetooth and display of raw EMG signals. (b) ModeMotion enables the acquisition of teacher data, confirmation of identification results, and display feature values using a radar chart.

Table.3.1: Experimental conditions.

Measurement	
Sampling frequency (Hz)	2000
Quantization bit rate (bit)	12
Filter (hardware)	· 50 Hz notch filter · 1—to-1000-Hz bandpass filter
Filter (software)	50-Hz high pass filter
Potential range (V)	-2.5 to 2.5
Feature Extraction Function: G_{FE}	
Method	Fast Fourier Transform (FFT)
Period (ms)	10
Number of samples	256
Overlapping samples	236
Window function	Hann window
Extracted frequencies (Hz)	23.4375, 46.875, 70.3125, 93.75, 140.625, 187.5, 250.0, 312.5
Smoothing (points)	5
Pattern Recognition Function: G_{PR}	
Method	ANN
Number of input layer neurons	$D = 24$
Number of hidden layer neurons	32
Number of output layer neurons	8
Activation function	Sigmoid
Learning Function: G_{L}	
Method	Gradient descent
Learning rate	0.01

3.4 Long-term clinical evaluation of people with upper limb deficiency using the BIT-UEC-Hand

A clinical evaluation of the BIT-UEC-hand was conducted with the cooperation of two participants having an acquired upper limb deficiency over a period of approximately three months. Participant A was a male in his 40s, a user of a two-DOF MPH with pattern recognition control who had been using the device for more than 10 years at the time of the study. The participant underwent a short amputation of the right forearm. Participant B was a male in his 30s, a user of a single-DOF MPH with proportional control who had been using it for approximately five months. The participant underwent a short amputation of the left forearm. The purpose and content of the experiment were fully explained to the participants in advance, and their consent to participate was obtained. This experiment was conducted with approval from the UEC ethics committee.

The evaluation methods included task and questionnaire evaluation. The evaluation schedule for each participant is shown in Fig.3.8. The number of days for each evaluation was counted from day 0 when the BIT-UEC-hand was confirmed to be used without any problems and when each participant began to use the MPH at home. Notably, each evaluation facility was different owing to the differences in participants' residence, etc., and the evaluation tests differed depending on the facilities maintained at the evaluation facility.

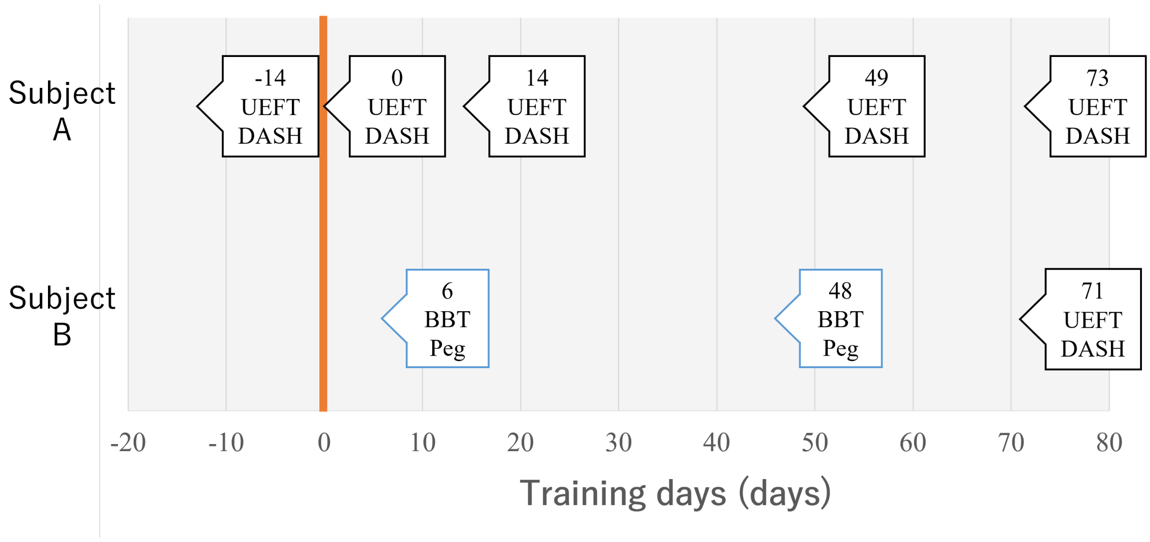

Fig.3.8: Experiment schedule

3.4.1 Task evaluation

Task evaluation is one of the most widely used evaluation methods for assessing the performance of MPHs. Representative evaluation methods include the Southampton hand assessment procedure (SHAP)(Light, Chappell, and Kyberd 2002), bocks and block test (BBT)(Mathiowetz et al. 1985; Platz et al. 2005), and the action research arm test (Yozbatiran, Der-Yeghiaian, and Cramer 2008). However, these methods depend on the task execution time, making it difficult to evaluate multi-DOF MPHs, which require time to drive the hand, or in the early stages of training. The assessment of capacity for myoelectric control (ACMC)(Hermansson, Fisher, et al. 2005; Hermansson, Bodin, and Eliasson 2006) is a method that does not depend on the task performance time. The ACMC scores are based on 30 items related to gripping, holding, releasing, and bimanual coordination in daily activities, not on specific tasks. Therefore, conducting the test is difficult without specialized knowledge. Hence, the upper extremity function test (UEFT)(Carroll 1965) was used in the present study to evaluate the upper limb function in a defined task without temporal evaluation. In addition, the BBT and large peg pull test were used to evaluate the time required to perform supplementary tasks. In the task evaluation, the participant selected the movement patterns that were stable and controllable from the following: resting, full-finger grip, open, two-finger pinch, and three-finger pinch. Therefore, the number of movements used depended on the stability of control on that day.

Upper extremity function test

The UEFT is an upper extremity functional assessment method for patients with hemiplegia (Carroll 1965). It is suitable for the assessment of arm mobility in addition to the evaluation of the hand. The results of a 32-item task to handle 17 objects shown in Fig.3.9 are evaluated. The UEFT evaluates tasks based on the following four levels: 3 points: the task is completed successfully; 2 points: the task is completed but slowly or very clumsily; 1 point: the task is partially completed; and 0 points: no part of the task can be completed. In this study, however, some of the evaluation and task performance methods were modified such that a person could perform the task using an MPH.

In the pinch evaluation, only one movement is evaluated for each item. When pinching is performed using multiple fingers, each finger is separately assessed (e.g., if the task is successfully completed with a three-finger pinch, 3 points are given for each item pinched with the index finger and the thumb and for each item pinched with the thumb and middle finger). As the BIT-UEC-Hand currently uses only the index finger and thumb for a two-finger pinch, the evaluation items for using different fingers for a two-finger pinch are not preferable. Therefore, this evaluation provides higher points to cases in which a pinch with more contact points is possible.

Small balls and washers, such as marbles and iron balls, were originally removed from a saucer or a protruding nail; however, in this experiment, they were placed on the palm of the participant' s healthy hand or on a desk. In this case, the maximum score was set to 2. The test should be conducted in a sitting position; however, owing to the limited range of motion of the MPH, the test was conducted in a standing position when necessary. In this experiment, clothes iron was substituted with a dumbbell of a similar mass owing to availability issues.

Fig.3.9: Items for UEFT

Bocks and block test (BBT)

The BBT is a measure of manual dexterity (Mathiowetz et al. 1985; Platz et al. 2005). The test consists of placing a wooden block of 2.5 cm per side in one of two adjacent boxes, carrying the block one at a time for 1 min, and evaluating the number of pieces moved. Fig.3.10 shows the BBT in action.

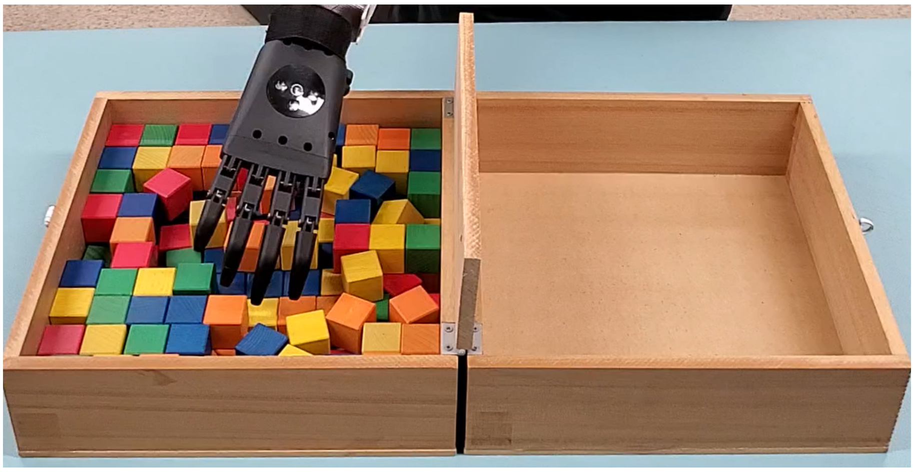

Fig.3.10: Bocks and block test

Large peg pull test (Peg)

The peg test is used for evaluating manual dexterity (Tiffin and Asher 1948). Usually, the number of cylindrical pegs that can be inserted into a board with holes in a certain time is evaluated. However, in this study, a pull-out test was conducted instead of the insertion test, which requires the coordinated action of a normal hand; this was because only the skill of the MPH control needed to be measured. The number of pegs that could be pulled out in 1 min was recorded. Fig.3.11 shows the peg test in action.

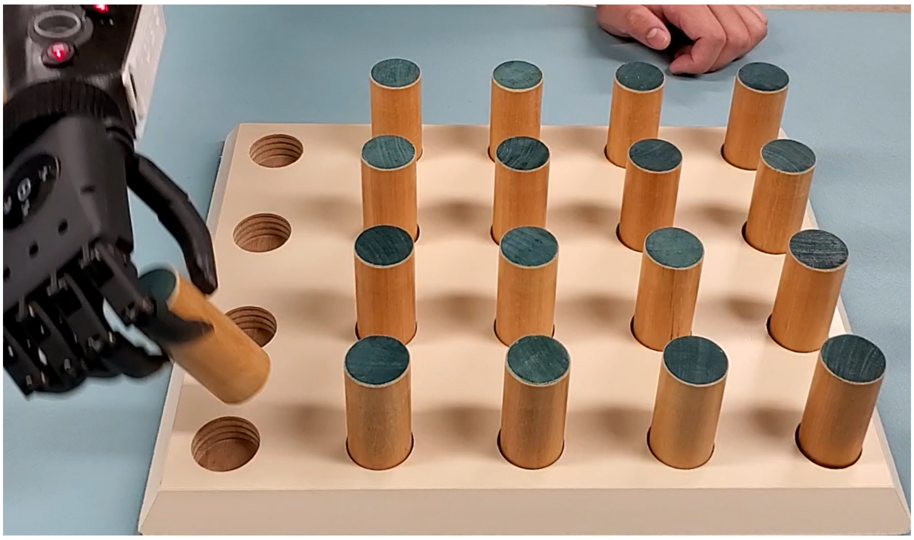

Fig.3.11: Large peg pull test

3.4.2 Questionnaire evaluation

Disability of the arm, shoulder, and hand (DASH)

The DASH is a self-assessment instrument that evaluates the degree of disability in people with disabilities in their upper limb function in daily life (Hudak et al. 1996). The Japanese version of DASH, that is, DASH-JSSH (Imaeda et al. 2005), was used in this study. The questionnaire consisted of two choice items: Disability/Symptoms (DASH-DS) and Work (DASH-W); and Sports/Music (DASH-SM). Each question is evaluated on a 5-point scale, with higher scores indicating greater disability. The respondents were asked to answer questions about their symptoms during the last week and imagine how well they could perform the activities they did not actually perform. In this study, the participants were instructed to give answers about their condition when using the BIT-UEC-Hand, and the questionnaire was evaluated.

Additional questionnaire

After the clinical experiment, an additional questionnaire regarding the control of the multi-DOF MPH was administered. The questionnaire items are listed in Table.3.2.

Table.3.2: Additional questionnaires

Questions (options)
From how many or more motions, including resting motions, does it become difficult to use the device in daily life?
Frequency of relearning (1: relearn every time; 2: relearn frequently; 3: rarely relearn; and 4: never relearn)
Burden of relearning (1: Not at all burdensome [no problem as it is]; 5: Quite burdensome [difficult to continue using])

3.5 Results and Discussion

3.5.1 Task evaluation

A graph summarizing the results of the UEFT is presented in Fig.3.12, and a graph summarizing the actions that are feasible in any trial in the UEFT is presented in Fig.3.13. Feasibility is defined as a score of 2 or 3 on the UEFT. Participant A already had a high score from the second trial, indicating that he could become proficient with the multi-DOF MPH in a short period, even before the start of home training. In the third trial, which was the first time the participant was evaluated with the four-motion control, a slight decrease in the score was observed compared with that in the previous trial. In the fourth trial, the participant achieved a higher score than that in the third trial.

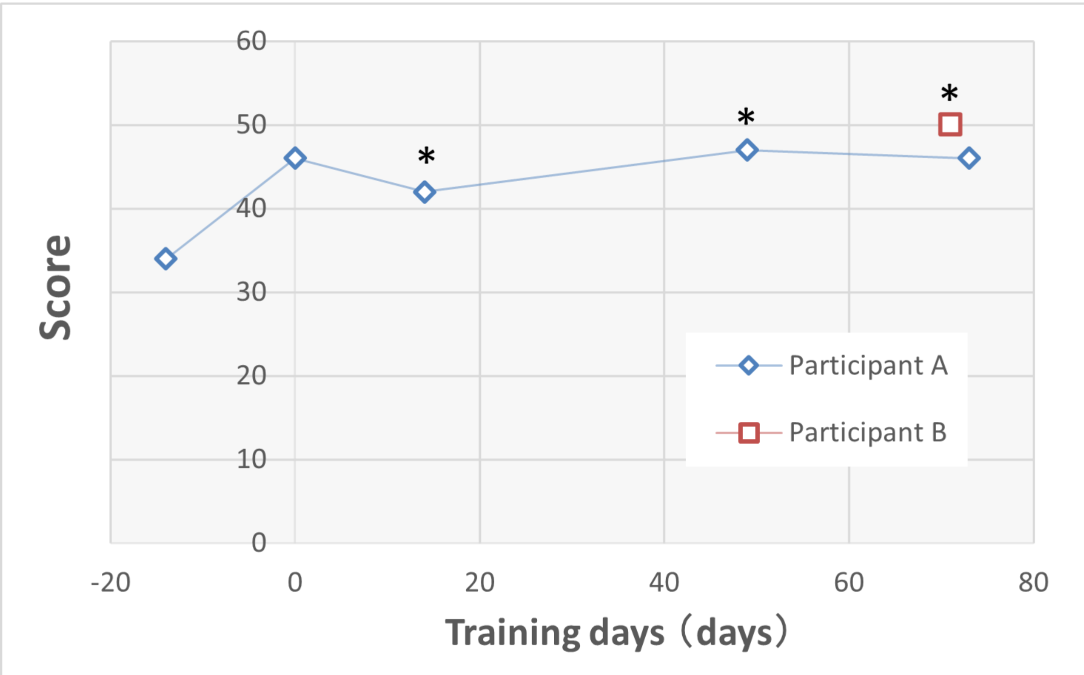

Fig.3.12: UEFT results. Notably, the number of motions used was different for each test. Four motions were evaluated when * was on the pointer; otherwise, three motion controls were used. Day 0 is the day on which the use of the MPH was started in each home.

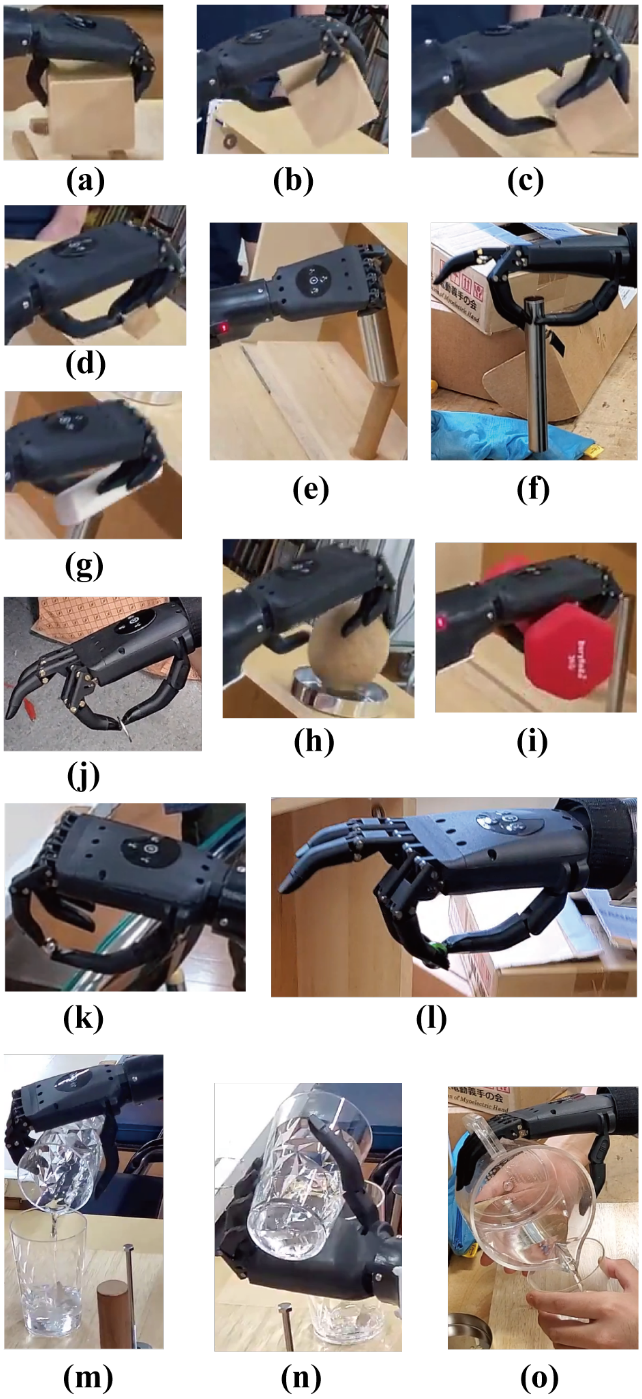

Fig.3.13: Tasks that could be performed with UEFT. This table summarizes the actions that resulted in two or three points that were determined to be feasible by the UEFT. (a)Wooden cube [9 cm], (b)wooden cube [7 cm], (c)wooden cube [5 cm], (d)wooden cube [2.5 cm],I)large iron pipe [ϕ 38 mm], (f)small iron pipe [ϕ 19 mm], (g)slate [2.5 $\times$ 1.2 $\times$ 11 cm], (h)sooden ball [7.5 cm], (i)dumbbell [3 kg, ϕ 28 mm], (j)steel washer [ϕ 78 mm $\times$ 2 mm], (k)glass marble [ϕ 17 mm], (l)metal sphere [ϕ 11 mm], pour water from glass into glass, (m)pronation, (n)supination, and (o) pour water from pitcher into glass.

Graphs summarizing the BBT and peg test results are presented in Figure3.14 and Figure3.15, respectively.

Although these results are for reference only because the scores were obtained from a single trial, the fact that the score decreased more for four movements than for three in both tests suggests that multiple-pattern control may have a negative impact on the speed and control accuracy. This result appears to support the reliability issue of pattern recognition in everyday movements reported by (Franzke et al. 2019).

On the contrary, participant B, a user of an MPH with proportional control, performed the evaluation task using the three-motion control from the early stages of training. After 80 days, he surpassed the UEFT score of participant A, a user of an MPH with pattern recognition control, contradicting previous studies, which indicated that extensive training was necessary. This result may be attributed to the fact that participant B effectively utilized the motor switches mounted on the MPH system used in this study to fix the hand motion during the experimental process; this may have provided some support for the reliability of the control.

In addition, the UEFT results showed that participants tended to score higher when identifying the four movements. Because the UEFT does not have a time limit, it is believed that even when the control reliability or task execution speed is low, the score is not affected, and the number of tasks that can be executed can be increased by searching for the most appropriate action.

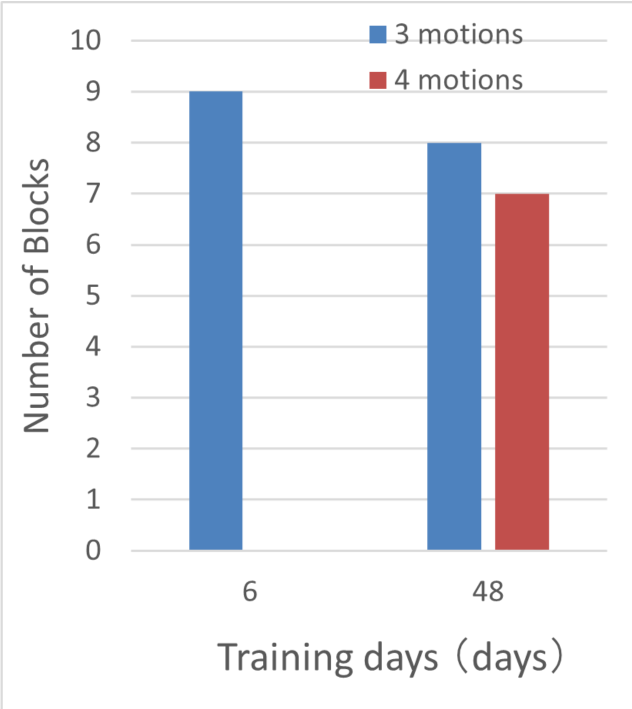

Fig.3.14: BBT results

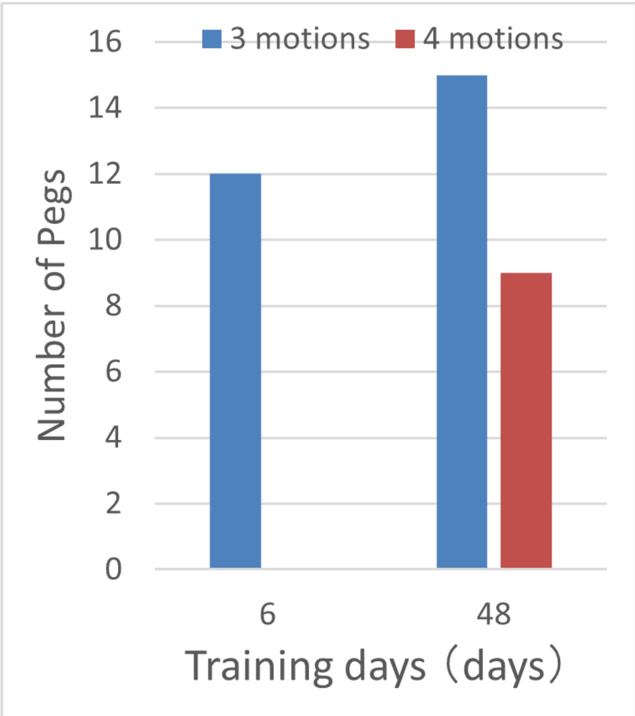

Fig.3.15: Peg test results

3.5.2 Questionnaire evaluation

The DASH results are shown in Figure3.16; the results of the additional questionnaire are presented in Table3.3. A higher DASH score indicates a higher degree of disability.

The DASH results showed no significant improvement in the degree of disability in daily life. This may be because both participants in this study were single-handed amputees and could perform most of their daily activities using their normal hand side (Glynn et al. 1986). However, there was a significant improvement in the degree of disability related to work. These results suggest that improvements in the capability to perform tasks with myoelectric prosthetic hands may contribute more significantly to reducing disability in work environments than in the ADL. Therefore, it is necessary to review recent research trends that often focus on the realization of ADL in the study of MPHs.

In addition, the performance of the MPH may significantly impact the choice of occupation. The public payment system in Japan often provides a single-DOF MPH, namely, Myobock (Ottobock) (Tanaka 2018); however, based on the results of this study, it may be needed to actively offer a more functional multi-DOF MPH to ensure equal occupational choices. Participant A currently utilizes the BIT-UEC-Hand in the workplace (Fig.3.17), indicating its effectiveness.

The results of the additional questionnaire also revealed the limitations of the current pattern recognition control. The number of usable motions was 4 or 5, including the resting motions. Even if the number of sensors utilized is three channels, several studies reported that more than 10 movements could be realized with a high discrimination rate (Ryu Kato 2008). The performance difference between the laboratory and clinical environments was remarkable. These findings support those reported in previous studies, which indicated that the identification rate is not proportional to the actual usability of the control system (L. Hargrove et al. 2007; B. Lock, Englehart, and Hudgins 2005).

Regarding relearning, both participants answered that they needed to relearn frequently. However, participant A, who had been a user of the pattern recognition-controlled MPH before the experiment, did not consider relearning as a significant burden, indicating individual differences in recognition. Participant B, however, felt that relearning was relatively burdensome. Therefore, it is essential to develop methods that reduce the burden of relearning to eliminate the barriers of pattern recognition control.

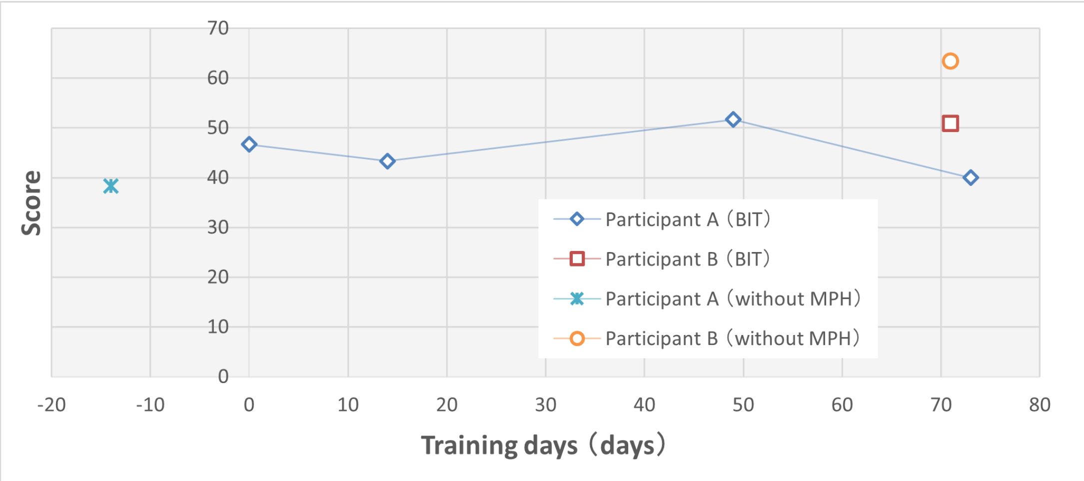

(a) disability/symptom

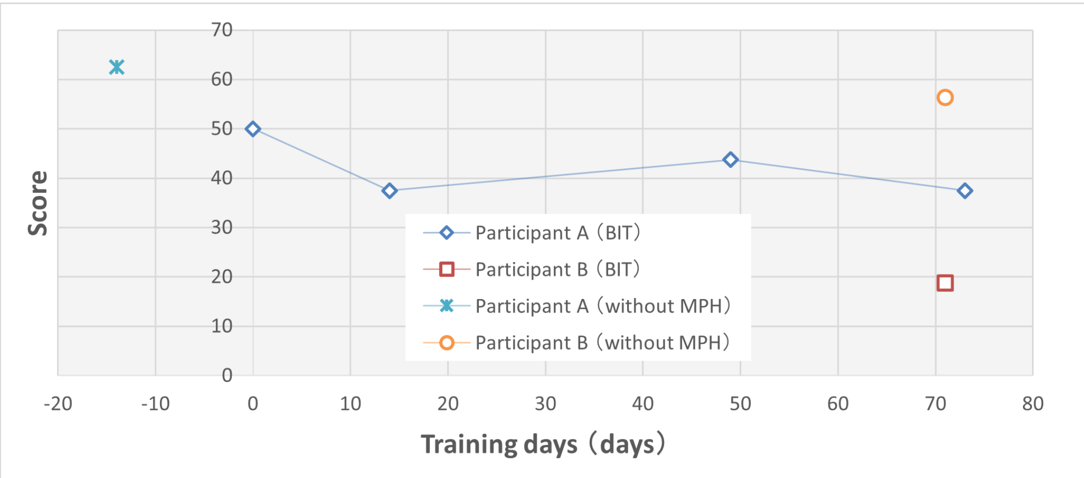

(b) work

Fig.3.16: Results of the questionnaire regarding the degree of disability. A higher value indicates a higher degree of disability

Table.3.3: Results of additional questionnaires

Questions (options)	Participant	
	A	B
From how many or more motions, including resting motions, does it become difficult to use the device in daily life?	4	5
Frequency of relearning (1: relearn every time; 2: relearn frequently; 3: rarely relearn; and 4: never relearn)	2	2
Burden of relearning (1: Not at all burdensome [no problem as it is]; and 5: Quite burdensome [difficult to continue using])	1	3

(a) Participant A harvesting a shiitake mushroom using the unaffected side by holding down the mushroom bed with the BIT-UEC-hand

(b) Participant A holding and carrying a case containing shiitake mushrooms using both hands

(c) Participant A grabs dried mushrooms using the BIT-UEC-hand and places them in a bag

Fig.3.17: Participant A working with the BIT-UEC-hand

3.6 Conclusion

This chapter described the five-finger, multi-DOF MPH (BIT-UEC-hand) equipped with a pattern recognition function that I developed. In addition, the chapter identified the characteristics and issues of a multi-DOF MPH controlled by pattern recognition through a long-term clinical application and clarified the functions that were more necessary for users.

Section 3.2 described the developed hardware of the BIT-UEC-hand.

Section 3.3 described the developed software of the BIT-UEC-hand.

Section 3.4 described the method of long-term clinical application of the multi-DOF MPH in this study.

Section 3.5 described the results and discussion on the long-term clinical application conducted in this study.

Chapter 4 Learning system that tracks the time variation of the EMG

4.1 Introduction

In this chapter, a method is developed and evaluated to address the reduction in the control stability of MPHs caused by time variations in the EMG.

Section 4.2 describes the time-variation of the EMG, which is the cause of the instability of recognition. Referring to previous studies, the time variability of the EMG was classified into three types based on the speed of change.

Section 4.3 describes conventional methods for managing time variation in the EMG signals. Learning, self-organization, and adaptation are listed as approaches to manage time variation, and the approach to apply to each conventional method is discussed.

Section 4.4 describes the method that tracks the time variation in the EMG developed in this study, which is based on the frequency of the data input.

In Section 4.5, the results and discussion of an experiment involving non-disabled participants for a wide range of time variations are described.

In Section 4.6, the results and discussion of an experiment involving a person with upper limb deficiencies for a wide range of time variations are described.

In Section 4.7, the results and discussion of an experiment involving non-disabled participants for a narrow range of time variations are described.

4.2 Problem: Time-variation in EMG

As described in Section 2.9.1, during the use of an MPH, physiological and psychological factors can alter the myoelectricity during the performance of any given movement. Sensinger, B. A. Lock, and Todd A. Kuiken specifically mentioned the causes of such changes: electrode conductivity changes (perspiration and humidity), electrophysiological changes (muscle fatigue, atrophy, or hypertrophy), spatial (displacement) changes (electrode movement on the skin or soft tissue fluid fluctuations), user changes (cognitive intent variations or contraction intensity changes), and other potential factors (Sensinger, B. A. Lock, and Todd A. Kuiken 2009).

This phenomenon in which the probability distribution of the target data changes over time is referred to as "concept drift." Concept drift can be classified into two types, virtual concept drift and real concept drift, based on its effect on the decision boundary, which is the boundary between the classes in pattern recognition (Gama et al. 2014; Krawczyk and Cano 2018). The former does not affect the decision boundary (posterior probability) but only affects the conditional probability density functions. The latter involves the decision boundary (posterior probability).

The objective of this study is to establish a learning system that adapts to such temporal variations in the EMG signals.

4.2.1 Classification by speed of change

In addition, Krawczyk and Cano classified concept drift into five categories based on the severity and speed of changes (Krawczyk and Cano 2018) as shown in Figure 4.1. The data flow is classified into five categories as shown in Fig.5.1. Here, the data flow is represented as a sequence of states $S = (s_1, s_2, ..., s_n)$. In this case, a state is a subsequence generated according to a certain distribution, and state $S + i$ is generated by distribution D_i. Therefore, in the case of a steady data flow, $D_j = D_{j+i}$ when $s_j \rightarrow s_{j+i}$. Sudden concept drift is characterized by s_j being rapidly replaced by s_{j+1} and $D_j \neq D_{j+1}$. Gradual concept drift is considered to be a phase in which the rate of change is slow and the state is in transition, and s_{j+1} is generated by a change in the ratio of D_j and $D_j + 1$ as well as mixing. In incremental concept drift, the rate of change is more gradual, and the change in D_j and $D_j + 1$ is not statistically significant. Recurring concept drift is characterized by the reappearance of the state of the k previous iterations as $D_{j+1} = D_{j-k}$. Finally, outliers (blips) are randomly generated, have no meaningful information, and should be ignored. In real-world data, these five categories are not clearly distinguishable but have mixed characteristics.

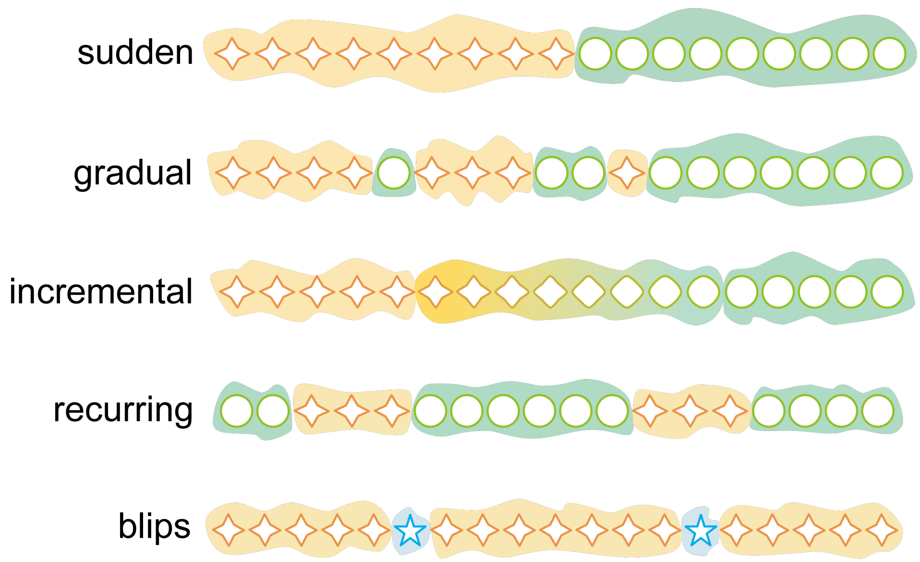

Fig.4.1: Classification of the concept drift based on the severity and speed of change. Prepared with reference to (Krawczyk and Cano 2018)

Based on Krawczyk and Cano's idea, it could be possible to classify the time variation in the EMG based on the speed of change. Therefore, the time variations in the EMG are classified into fast (instantaneous), medium (seconds to minutes), and slow (hours) changes, referring to previous studies on changes in the EMG. In light of Krawczyk and Cano' s classification, each of these changes can have characteristics similar to those of sudden, gradual, and incremental concept drifts. These time variations in the EMG and the studies that addressed them are listed in the Table.4.1 below.

Table.4.1: Concept drift in EMG and the studies that addressed it

Speed of change	fast (instantaneous)	medium (seconds to minutes)	slow (hours)
Types and characteristics of change	•Electrode misalignment •Arm posture change •Teacher data measurement error(Hiyoshi et al. 2018) •Electrode' s spatial (displacement) changes(Sensinger, B. A. Lock, and Todd A. Kuiken 2009)	Most common causes of poor control (Simon, B. A. Lock, and Stubblefield 2012) •Level change during dynamic muscle contraction •User changes (cognitive intent variations or contraction intensity changes)(Parajuli et al. 2019)	•Electrode conductivity changes (perspiration, humidity) •muscle fatigue(Cifrek et al. 2009)(Sadoyama, Miyano, and Higashi 1981) •Changes in skin impedance
Studies addressed	•[Learning + Adaptation] Adding new teacher data and modification of teacher data based on simple reaction time (NISHIKAWA et al. 2001) •[Learning + Self-organization] Connect SOM to output layer of ANN(H.-P. Huang et al. n.d.) •[Learning + Adaptation] Data update based on distance between representative particles and input data(Y. Gu et al. 2018)	•[Learning] Improvement of feature(Al-Timemy et al. 2016)	•[Learning + adaptation] Adding new teacher data, modification of teacher data based on simple reaction time and managing teacher data modification by the degree of competition in the feature space (Kato, Yokoi, and Arai 2006; Ryu Kato 2008) •[Learning + Adaptation] Evaluation of teacher data based on output results(TSUJI et al. 1993) •[Learning + Adaptation] Data update based on distance between representative particles and input data(Y. Gu et al. 2018)(Q. Huang et al. 2017)

4.2.2 Classification by range of change in feature space

In the case of EMG pattern recognition, in addition to classification based on the speed of the time-variation change, classification can also be based on the range of change in the feature space. The changes in the feature space during fast and slow changes have been described in (Ryu Kato 2008) and (NISHIKAWA et al. 2001). In a study by NISHIKAWA et al. that analyzed changes in the feature space with electrode movement, it was noted that for some movements, after electrode movement, there was no teacher data in the same position as before the movement, or another cluster moved into an area where a cluster of another movement previously existed. It is stated that there were cases where there was no teacher data at the location that overlapped before the move or another cluster moved into an area where there was previously a cluster of another behavior. However, most of the clusters overlapped with the clusters that existed before the electrode movement. This means that the change in the probability distribution of the EMG potentials is small. In a study by Ryu Kato, which analyzed changes in the feature space of the teacher data with long-term use of an MPH, outliers due to either motion teaching errors or signal noise were observed in the early stages. In the early stages, there was an overlap between clusters of teacher data and a large intra-cluster variance; however, as the user became more proficient, there was less overlap between clusters and the intra-cluster variance decreased. The fact that similar characteristics were observed in the early and late changes, and that the same adaptation method was used by Y. Gu et al. for both the fast and slow changes (Y. Gu et al. 2018), suggests that the changes in the feature space are characterized by similar characteristics.

This study measured the gap in the feature space between the time of teacher data measurement and actual use (recognition rate measurement), which is one of the fast changes and is shown in Fig.4.2. As in the analysis of Ryu Kato; NISHIKAWA et al., overlapping of clusters and overlapping of evaluation data (evaluation) of one class on teacher data (teacher) of another class are observed.

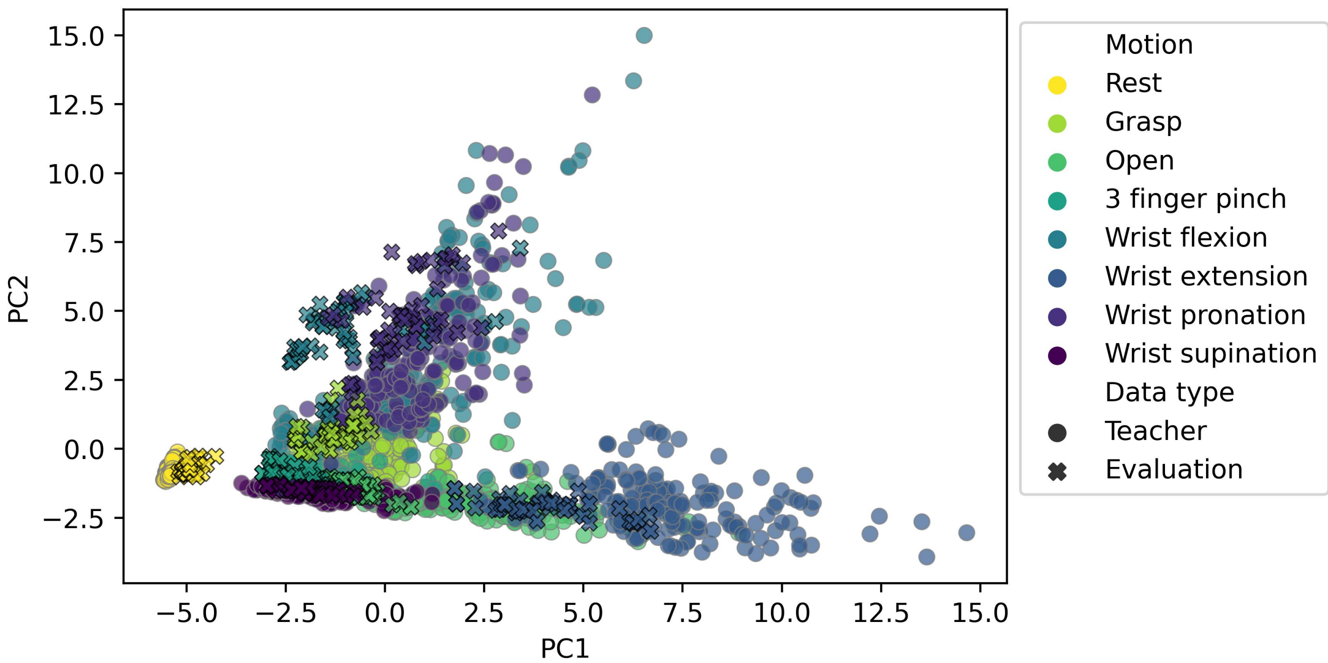

Fig.4.2: Changes in feature space due to fast time variation (teacher data measurement error)

As presented in Table.4.1, there are currently no analyses of changes in the feature space due to medium time variation, because there are few studies that have addressed this issue. Therefore, this study measured the EMG of the person with an upper limb deficiency during three movements (resting, grasping, and opening) by changing the muscle contraction force at regular intervals. This is shown in Fig.4.3. Compared to the distance between the teacher and evaluation data in Fig.4.2, difference in the muscle contraction force causes a significant change in the feature space.

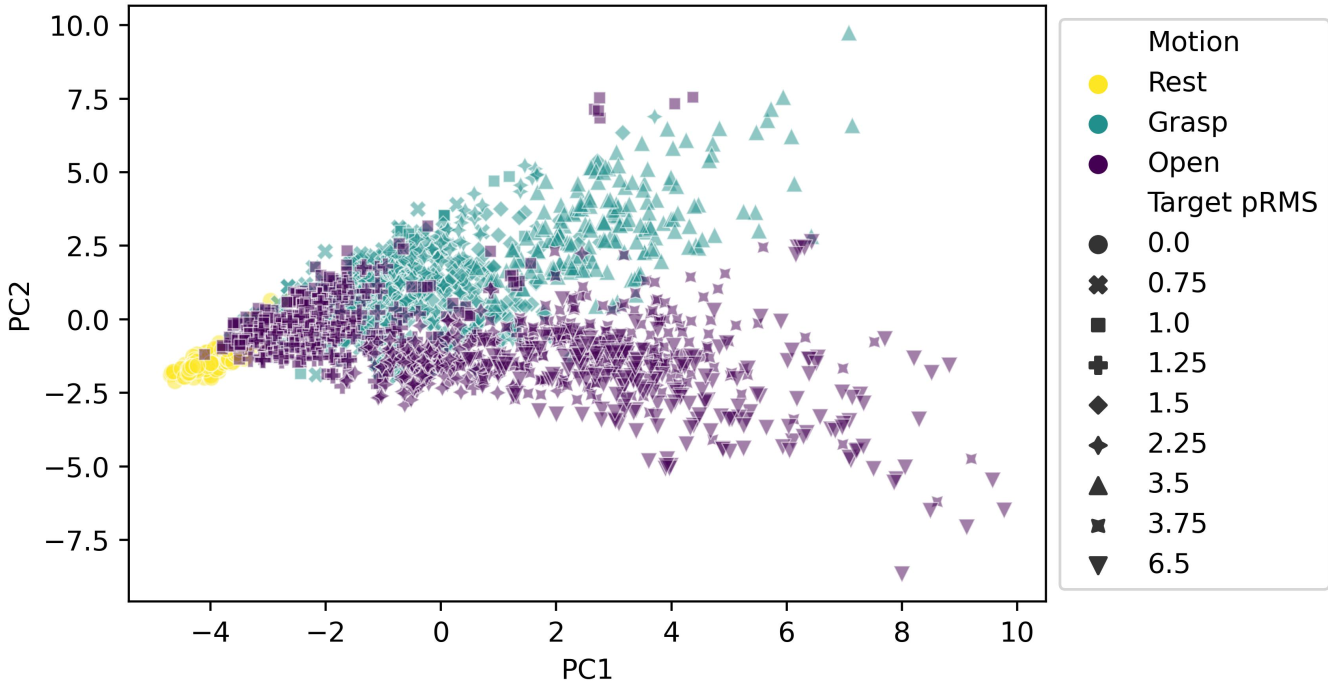

Fig.4.3: Changes in feature space due to medium changes (changes in muscle contraction force)

Based on the above, the changes in the feature space due to the time variation of the EMG were classified into two types. Fig.4.4b illustrates the difference of the change in the feature space by the time variation of the EMG.

Narrow range variation

Fast and slow changes are applicable. Most of the clusters overlap with the clusters before the change, except in the case of outliers such as noise. In other words, the change in the probability distribution of the data is small.

Wide range variation

A medium change is applicable. A large change in the feature space causes a large change in the position from the cluster before the change or a large variance. In other words, the change in the probability distribution of the data is large.

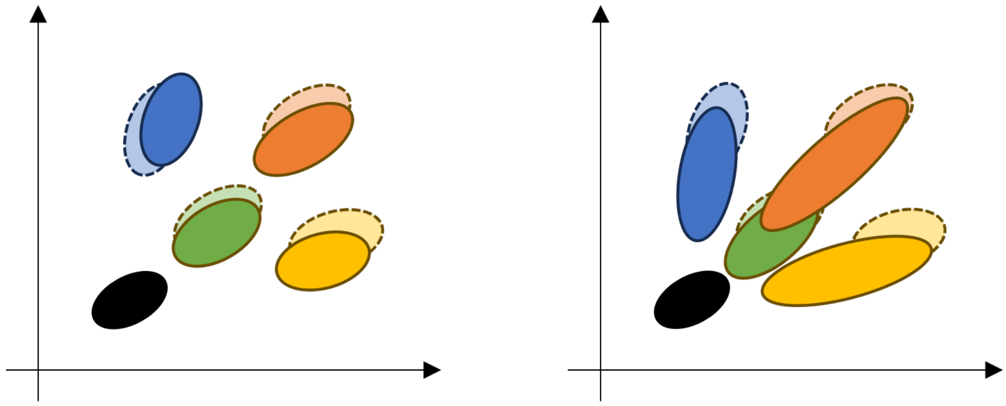

(a) Narrow Range Variation **(b)** Wide Range Variation

Fig.4.4: Difference of the change in the feature space by the time variation of EMG signals. The light-colored clusters are those before the change. Darker clusters are those after the change.

Particular attention should be paid to wide range changes. In the case of wide range changes, large changes in the position of data in the feature space tend to result in clusters overlapping each other. Specifically, there is a risk that clusters that had different probability distributions before the change are recognized as the same cluster after the change. For example, if differences in the overall magnitude of the features were the main discriminative factor rather than differences in the individual components of the features, these discriminative abilities may be lost when attempting to adapt to differences in the muscle contraction force. Fig.4.5 shows the feature space of the teacher data with the dimensionality reduced to two dimensions when such a discriminative tendency was actually observed during control of an MPH by a person with an upper limb deficiency. The muscle contraction force is zero for the resting movement. The rest, grasp, and open movements are aligned side by side at the position where the second principal component (PC2) is 0 on the coordinates. Therefore, it can be considered that these three movements are recognized mainly by the difference in the first principal component (PC1).The muscle contraction force is zero in the resting movement, and PC1 can be considered to be a component close to the muscle contraction force.

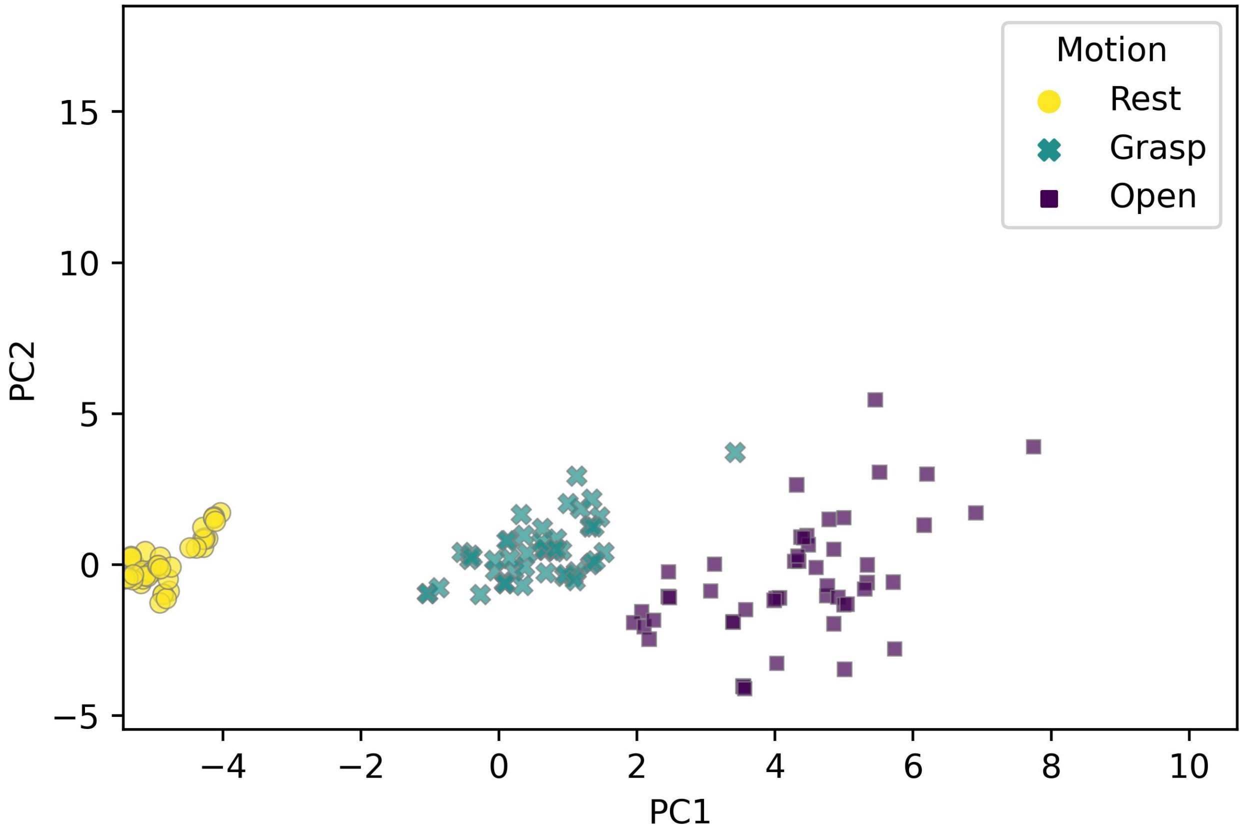

Fig.4.5: Cluster placement when differences in the overall feature magnitude are the primary discriminant, rather than differences in the individual components of the feature

To address this problem, it is necessary to adopt approaches such as changing the muscle contraction patterns, modifying the feature values, or increasing the number of sensors. This allows the formation of a feature space that can effectively deal with time variation without overlapping clusters, even when the muscle contraction forces are different.

4.3 Conventional methods for managing time variations in EMG

As presented in Table.4.1, various time variations in the EMG have been noted over the years, and studies have been conducted to address these issues using the following three approaches:

Learning
: Objects (teacher) to be learned are needed for evaluation.

Self-organization (spontaneous formation of complex systems from simple elements)
: Need relationships between data (e.g., the similarity of myoelectric signals) for evaluation.

Adaptation
: Only the outcome of whether data are selected is needed for evaluation, and only chosen data exist.

These approaches, either alone or combined, are used to manage the time variation. As Section 2.9.1 described, Q. Huang et al. referred to such a method of online updating of classifiers following time-varying changes as adaptive learning and classified it as supervised and unsupervised adaptation, depending on whether the learning method required labeled samples to relearn the prediction model or not (Q. Huang et al. 2017). Supervised adaptation is also referred to as online learning in some studies (Nishikawa et al. 2000). There are also methods that combine supervised and unsupervised adaptation, which this study refers to as semi-supervised adaptation. Supervised adaptation can achieve a high recognition accuracy, but requires a complicated learning process in which labeled samples are repeatedly acquired. Unsupervised adaptation is easier to use because it does not require retraining; however, there is a risk that the recognition accuracy will be degraded (Sensinger, B. A. Lock, and Todd A. Kuiken 2009).

The following is an explanation provided by the previous studies presented in Table.4.1:

H.-P. Huang et al. addressed time degeneration owing to the reallocation of EMG sensors by reducing the dimensionality by combining self-organizing maps (SOMs) in the input layer of the ANN. This approach is a mixture of learning by ANNs and the self-organization of the SOM (H.-P. Huang et al. n.d.).

Y. Gu et al. and Q. Huang et al. used data updates based on the distance between representative particles (RPs) and input data to update the teacher data in adaptive learning. RPs are down-sampled from the teacher data to maintain the distribution characteristics of the feature space; they are added, deleted, or replaced based on the distance between the RPs and input data. Thus, this can be considered a mixed learning and adaptation approach. Y. Gu et al. used this approach to address the time variation after sensor re-fitting and 9 h of wear(Y. Gu et al. 2018), whereas Q. Huang et al. addressed the time variation at 12 h and 30 min of wear(Q. Huang et al. 2017).

Al-Timemy et al. addressed the variability of the muscle contraction force by improving the feature values (Al-Timemy et al. 2016). Therefore, this approach can be considered a learning approach because it improves the learning process.

Ryu Kato proposed a method for updating teacher data in adaptive learning based on simple reaction time (Kato, Yokoi, and Arai 2006; Ryu Kato 2008). Simple reaction time is the time the person takes to respond to a stimulus. Previous studies reported that the average simple reaction time of human beings is 0.22 s (Laming 1968). In the process of deleting teacher data, if the identification of a sequence of actions requires a longer time than the simple reaction time, the evaluation value of teacher data similar to the input data is rewarded; however, if the identification of a sequence of actions requires a shorter time than the simple reaction time, it is punished. If the evaluation value of the teacher data falls below a certain value, the teacher data is deleted. In the generation of teacher data, when a single action and unrecognizable action occur within a simple reaction time, the input data at the time of the unrecognizable action that is most similar to the teacher data is generated as the new teacher data for that action. This facilitates the consideration of a method that combines learning and adaptation. Ryu Kato managed the updating of training data by defining a degree of competition based on the ratio of the classes of teacher data to which the representative vectors generated by the SOM belong; however, because this did not directly use self-organization to generate, delete, or modify data, it is not regarded as equivalent to an approach that uses self-organization.

Similarly, TSUJI et al. used a method for updating teacher data in adaptive learning that evaluates the teacher data based on the output results and updates the data based on the evaluation values (TSUJI et al. 1993). The findings suggested that this method is also a combination of learning and adaptation.

Despite the different studies described above, only a few studies have addressed medium changes, such as changes in the muscle contraction force (Al-Timemy et al. 2016). Simon, B. A. Lock, and Stubblefield noted that when discrimination becomes unstable during MPH use, the user will perform stronger muscle contractions to regain control. Trying too hard or changing the manner in which the muscle contracts are claimed to be the two most common causes of poor discrimination (Simon, B. A. Lock, and Stubblefield 2012). Ryu Kato, developed a recognition method for slow changes mainly from muscle fatigue, and confirmed the problem of reproducibility of movements such as changes in the muscle contraction force in amputees as pointed out by Simon, B. A. Lock, and Stubblefield; however, he evaluated the developed method after improving the reproducibility problem by training amputees for approximately one month, which was outside the scope of the application of the developed method. The method is not applicable to the development method. In addition, the method assumes re-labeling of movements and does not address drastic changes in the feature space owing to the physical misalignment of the sensor or unintended movement noise. Therefore, Ryu Kato emphasizes on the importance of developing a methodology to adapt to such changes. In light of the above, responding to medium changes is essential to address the instability problem in pattern recognition.

The Al-Timemy et al. study on medium change response has been compared against other features and was found to be improved. However, a comparison of the discrimination performance of the discriminators trained on one type of muscle contraction against two different types of muscle contractions showed a discrimination error of more than 30 % for all participants, which was not at a practical level (Al-Timemy et al. 2016).

4.4 Proposed Method: Method based on the frequency of the input patterns

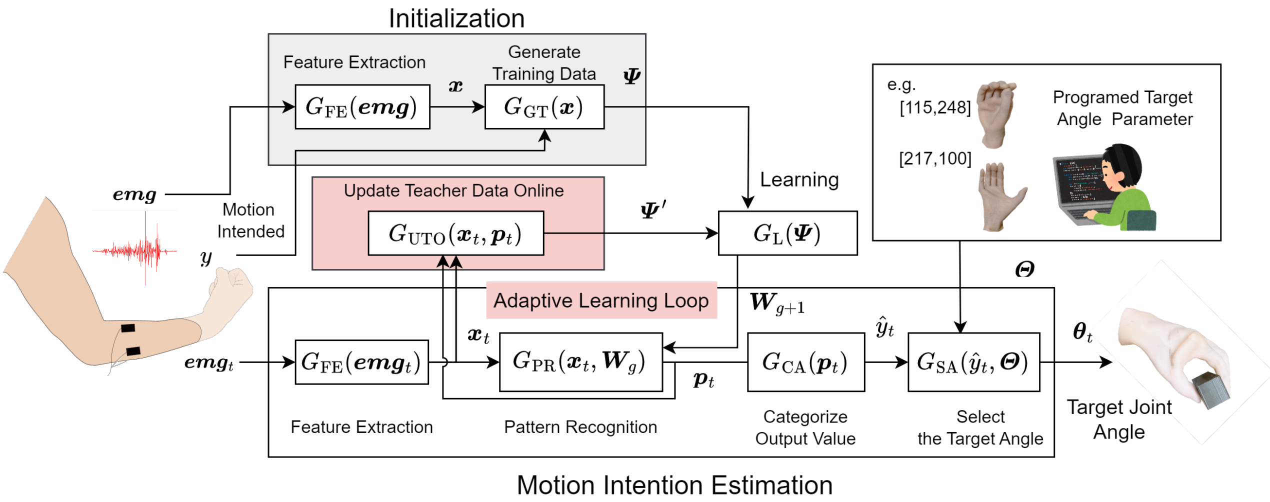

Fig.4.6: Diagram of the adaptive learning method. Here, $\boldsymbol{emg}_t$ is the electromyogram (EMG) signal measured at time t; $\boldsymbol{x}_t$ and $\boldsymbol{\Psi}$ denote the feature vector and teacher dataset, respectively; $\boldsymbol{W}_g$ is a parameter of the pattern recognition function G_{PR}; g is the number of times the parameter has been updated; $\boldsymbol{p}_t$ represents the probability of the feature vector being classified into each motion; $\boldsymbol{y}$ and $\hat{y}_t$ denote the labels of the motion; $\boldsymbol{\theta}_t$ is the vector of the target angles; and $\boldsymbol{\Theta}$ is the array of the predefined target angles.

This study proposed a method that uses learning, self-organization, and adaptation, which are the existing approaches to adapt to time variation conditions, to achieve a method that is more accurate, responsive, and stable than the existing methods. Moreover, adaptive learning is used to update the teacher data based on new input data. This is combined with self-organization, which updates the teacher data to be closer to the input data, and adaptation, which deletes or generates teacher data based on the evaluation values associated with the teacher data.

The proposed method comprised two main processes: (A) motion intention estimation and (B) adaptive learning; the latter had a sub-process involving (C) the process of updating teacher data online. Fig. 4.6 presents a diagram of the adaptive learning method. After initialization, the vector of the EMG signals $\boldsymbol{emg}_t$ was measured and converted into the feature vector $\boldsymbol{x}_t$. In process A, $\boldsymbol{x}_t$ was calculated, and the target joint angle vector $\boldsymbol{\theta}_t$ was the output. The hand was controlled according to $\boldsymbol{\theta}_t$. Subsequently, process B was performed on $\boldsymbol{x}_t$, during which $\boldsymbol{x}_t$ and $\boldsymbol{p}_t$ which is the result vector of G_{PR}, were sent to C , and G_{UTO} updated the teacher data. Process B, which was exclusive of sub-process C, was performed on the updated teacher data $\boldsymbol{\Psi}'$. Following the implementation of process B, the updated parameter array $\boldsymbol{W}_{g+1}$ was sent to G_{PR} by calculating $\boldsymbol{\Psi}'$ in G_{L}. The primary purpose of this study was to develop G_{GTO} and make G_{PR} adapt to the changes in the EMG. The details are explained below.

4.4.1 Motion intention estimation

The process of motion intention estimation is composed of four processes: (a) feature extraction, (b) pattern recognition, (c) categorization of the output value, and (d) selection of the target angle. At time t, $\boldsymbol{emg}_t$ was measured, where $\boldsymbol{emg}_t$ represents the vector of the EMG signals. $\boldsymbol{emg}_t$ was a ring buffer that stored past T_{emg} signals, with the EMG signal at time t being the latest. G_{FE} transformed $\boldsymbol{emg}_t$ to $\boldsymbol{x}_t$, a D-dimensional feature vector. In the pattern recognition process, G_{PR}, which had the parameter $\boldsymbol{W}_g$, outputted $\boldsymbol{p}_t = (p_1, p_2, ..., p_{|Y|})$. Subsequently, $\sum_{k=1}^{|Y|} p_k = 1$. $Y = \{n \in \mathbb{N}\}$ was a set of motion labels to be predefined as the MPH motions, such as grasping and opening. g denotes the updated time $\boldsymbol{W}$, and $\hat{y}_t \in Y$ represents the intended motion generated from $\boldsymbol{p}_t$ by G_{CA} as follows:

$$G_{\mathrm{CA}}(\boldsymbol{p}_t) = \begin{cases} \arg\max\limits_{k}\{p_1, ..., p_k, ..., p_{|Y|}\}. & \text{if } p_{\hat{y}_t} \geq \rho \\ \emptyset. & \text{otherwise} \end{cases} \tag{4.4-1}$$

$\emptyset$ is an empty set that was considered indistinguishable in this study. By introducing this concept, a more stable control could be achieved. ρ represents the thresholds for determining whether $\boldsymbol{x}_t$ is indistinguishable. Finally, G_{SA} selected the target joint angle vector $\boldsymbol{\theta}_t$ that corresponded to $\hat{y}_t$, and $\boldsymbol{\theta}_t$ was sent to the MPH.

Prior to the motion intention estimation, initialization is required. For initialization,

$\boldsymbol{W}_g$ was generated by the learning function G_{L}. In general, supervised learning is used in pattern recognition methods, which is a method of learning input and output relationships based on the examples of input and output pairs called "teacher data." These data, which are prepared in advance, comprise the pairs of the i-th input feature data vector $\boldsymbol{x}^i$ and the intended motion y. G_{GT} summarizes the measured pairs of teacher data and outputs a set of teacher data $\boldsymbol{\Psi}$, which was sent to G_{L}. Here, the teacher data Ψ^{y_k} were represented by $(\boldsymbol{x}^i, y_k)$, where y_k is the k-th motion label in Y. The set of the teacher data of motion y_k $\boldsymbol{\Psi}^{y_k}$ and the set of all teacher data $\boldsymbol{\Psi}$ are expressed as follows:

$$\boldsymbol{\Psi} = \bigcup_{k=1}^{|Y|} \boldsymbol{\Psi}^{y_k} = \bigcup_{k=1}^{|Y|} \{\, \Psi_1^{y_k},\, \Psi_2^{y_k},\, \cdots,\, \Psi_{|\boldsymbol{\Psi}^{y_k}|}^{y_k} \}. \tag{4.4-2}$$

The motion intention can be estimated after learning.

4.4.2 Adaptive learning

In the adaptive learning method, the parameter of the pattern recognition function $\boldsymbol{W}$ was updated sequentially, as shown in the center of Fig. 4.6. When G_{UTO} received the feature vector $\boldsymbol{x}_t$, G_{UTO} updated the set of teacher data. After repeating this process T_{UTO} times, G_{UTO} sent the updated set of teacher data $\boldsymbol{\Psi}'$ to G_{L}. Let the number of times taken for updating the teacher data T_{UTO} times be denoted as τ_{UTO}. G_{L} learns from the teacher data and generates new parameters $\boldsymbol{W}_{g+1}$. The time taken for this learning is referred to as τ_{L}. A flowchart extracted from the entire process of adaptive learning in Fig.4.6 is shown in Fig.4.7.

The amount of time of the interval for adaptive learning depends on both τ_{UTO} and τ_{L}. Generally, the learning process G_{L} occurs in a separate thread concurrently with the identification process. Therefore, the interval for adaptive learning is as follows:

When $\tau_{\mathrm{UTO}} > \tau_{\mathrm{L}}$

Initially: $\tau_{\mathrm{UTO}} + \tau_{\mathrm{L}}$

Otherwise: τ_{UTO}

When $\tau_{\mathrm{UTO}} \leq \tau_{\mathrm{L}}$

Initially: $\tau_{\mathrm{UTO}} + \tau_{\mathrm{L}}$

Otherwise: τ_{L}

However, typically $\tau_{\mathrm{UTO}} \leq \tau_{\mathrm{L}}$, hence the interval for adaptive learning can be considered to be determined by the learning time τ_{L}. Therefore, in adaptive learning, parameters are updated every τ_{L} time.

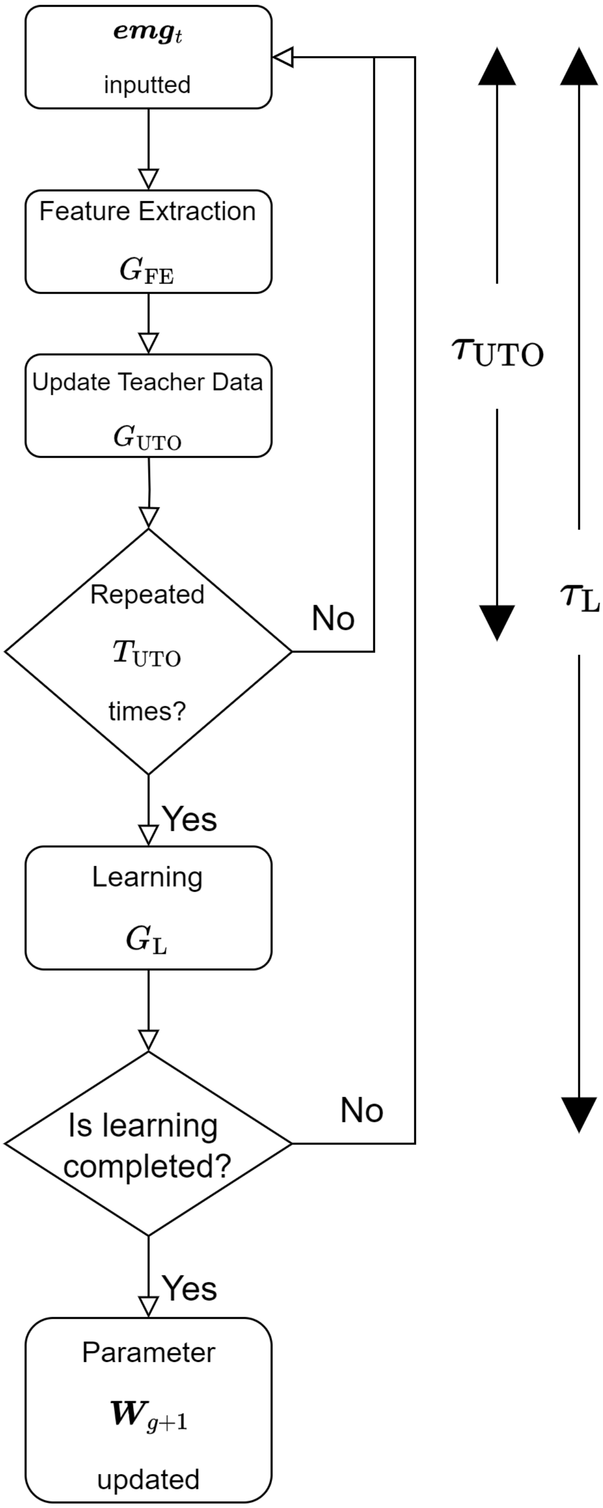

Fig.4.7: Flowchart extracted only for the adaptive learning process.

4.4.3 Updating teacher data online: Continuous clustered competitive learning

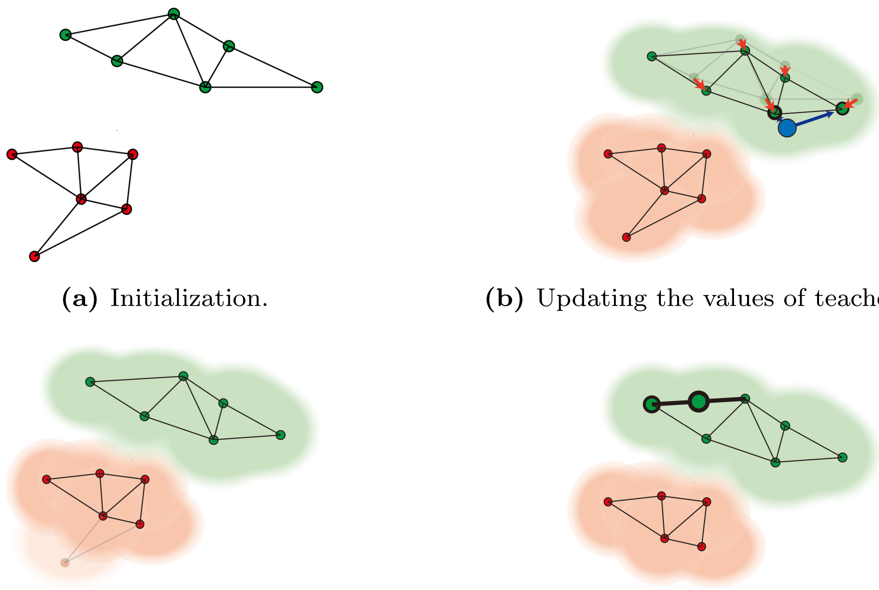

(a) Initialization. **(b)** Updating the values of teacher data.

(c) Deleting teacher data. **(d)** Inserting teacher data.

Fig.4.8: Process of continuous clustered competitive learning. Dots represent nodes, and lines represent edges. Different colors represent different motions, and the blue dot in (b) is the input data. The large green dot in (d) is the inserted node. Colored areas represent decision boundaries.

The process of updating the teacher data online (G_{UTO}) comprises five processes: 1) initialization, 2) noise filtering, 3) updating the values of teacher data, 4) deleting teacher data, and 5) inserting teacher data. Fig. 4.8 shows the schematic of these processes.

This study referred to the growing neural gas (GNG) (Fritzke 1995), a type of unsupervised neural network, to modify the teacher data based on the frequency of the input patterns. GNG successively adds and removes nodes and connectivity (edges) based on the distance between the input data and nodes. It can also perform vector quantization, which refers to approximating a set of vectors with a relatively small number of vectors. In this study, the teacher data vector was considered a node. GNG uses competitive learning (CL) (Rumelhart and Zipser 1985), a type of learning method based on Hebbian learning, where the neuron closest to the input data becomes the winner and is updated to be closer to the input data. The method includes self-organization, which updates the teacher data to be closer to the input data, and adaptation, which removes or generates teacher data based on the evaluation values associated with the teacher data, but does not include learning.

Because the EMG depends on muscle contraction patterns, simply combining learning in such a way that competitive learning is adapted to the entire data set and used as the teacher data may result in an overlap in other clusters depending on the pattern of muscle contraction for a given movement. Additionally, the proposed method is realized through interaction between humans and the adaptive system. In this case, in addition to the system adaptation, humans also inevitably model the system and adapt to it, which is referred to as a mutual adaptation system (Natsuki and Yamada 2006). In such a scenario, adaptation on the human side and system side might interfere with each other, potentially disrupting the system and hindering successful adaptation. To prevent this, the design of the interaction between humans and the adaptive system needs to be guided in a non-destructive direction.

One method to realize such a design is bootstrapping (Natsuki and Yamada 2006). This involves using newly acquired abilities to advance to the next stage of learning. Bootstrapping is known to be used in the cognitive development of infants. Morton and Johnson argued that newborns are born with some information about the facial structure, which they called CONSPEC. The system for learning visual features of the same species was named CONLERN. It has been revealed that newborns tend to follow face-like figures because of CONSPEC right after birth. This implies that CONSPEC provides the necessary information for CONLERN to learn visual features at the center of the visual field, forming a bootstrapping system (Morton and Johnson 1991; Natsuki and Yamada 2006).

In the proposed method, combining bootstrapping with competitive learning aims to limit the speed of human adaptation, maintaining a stable mutual adaptation system. The limitation of the cluster movement when combining bootstrapping with competitive learning, or in other words, the restriction of human adaptation direction, is shown in Fig.4.9. The decision region depends on the degree of competition in the feature space; however, because it is formed with some leeway around the cluster (as shown on the left of

Fig.4.9), users can freely move the cluster within this range. However, to make significant adaptations that move outside the decision region, it is necessary to gradually repeat the adaptations and move the cluster. This restricts the speed of cluster movement.

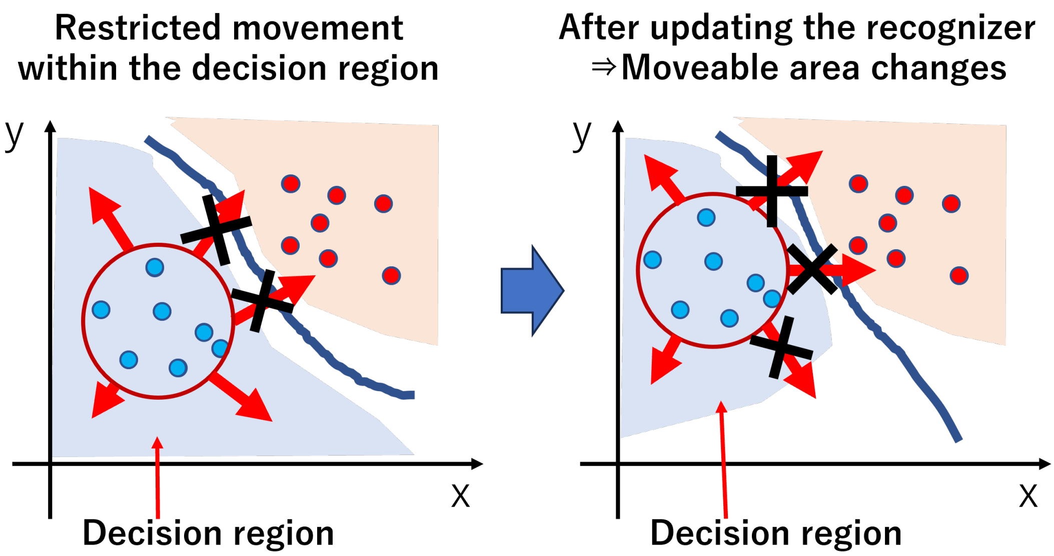

Fig.4.9: Illustration showing cluster movement restriction when combining competitive learning with bootstrapping. Movement is restricted within the decision region formed by the classifier. As competitive learning moves the cluster based on input data, the decision region changes after classifier updates, altering the area where movement is possible. The decision region is determined by the degree of competition in the feature space, and is formed with some leeway around the cluster, allowing users to freely move the cluster within this range. However, to make significant adaptations that move outside the decision region, gradual repeated adaptations are necessary to move the cluster. This restricts the speed of cluster movement.

By combining competitive learning with bootstrapping, continuous splitting of clusters and vector quantization are enabled, thus the proposed adaptive learning method is referred to as Continuous Clustered Competitive Learning (CCCL). CCCL conducts CL in parallel within each decision region updated by previous adaptive learning for each motion. The details of this method are as follows:

$\boldsymbol{A}$, which is the set of nodes, and $\boldsymbol{A}_{y_k}$, which is the set of nodes of motion y_k, are represented as follows:

$$\boldsymbol{A} = \bigcup_{k=1}^{|Y|} \boldsymbol{A}_{y_k} = \{A_1, A_2, ..., A_i, ..., A_{|A|}\} \tag{4.4-3}$$

$A_i = (\boldsymbol{w}_i, y_k, E_i)$ is referred to as node i, which is the i-th created element of A. $\boldsymbol{w}_i \in \mathbb{R}^D$ is the position of the node, and E_i is the accumulated error used as an indicator for inserting new nodes. If the accumulated error is large, it is determined that a node must be inserted.

$\boldsymbol{B}$, that is, the set of edges, and $\boldsymbol{B}_{y_k}$, that is, the set of edges of motion y_k, are represented as follows:

$$B = \bigcup_{k=1}^{|Y|} B_{y_k} = \{..., B_{i,j}, ...\} \tag{4.4-4}$$

Here, $B_{i,j} = B_{j,i} = (a_{i,j}, e_{i,j})$ is the edge between node i (A_i) and node j (A_j); $a_{i,j}$ is the age of the edge, which is used to remove unnecessary edges in regions with plasticity; and $e_{i,j}$ is the evaluation value of an edge, which is used to remove edges that have become redundant owing to time variation.

Each of the five processes is described below.

Initialization

The networks were initialized using $\boldsymbol{\Psi}^{y_k}$, the set of teacher data of motion y_k generated by G_{GT}. The teacher data were input to G_{UTO} in the order of measurement. When the i-th teacher data $\Psi^{y_k} = (\boldsymbol{x}^i, y_k)$ were input, node i $A_i = (\boldsymbol{w}_i, y_k, E_i)$ was created. Subsequently, $\boldsymbol{w}_i$ and E_i were initialized as $\boldsymbol{w}_i = \boldsymbol{x}^i$ and $E_i = 0$, and A_i was added to set A_{y_k} as follows:

$$\boldsymbol{A}_{y_k} \bigcup A_i \rightarrow \boldsymbol{A}_{y_k} \tag{4.4-5}$$

Because $\boldsymbol{A}_{y_k} \in \boldsymbol{A}$, A_i was added to $\boldsymbol{A}$. Each time an A_i was created, an edge was created as follows:

$$\begin{cases} \boldsymbol{B}_{y_k} \bigcup B_{1,2} \rightarrow \boldsymbol{B}_{y_k} & \text{if } |B_{y_k}| = 2 \\ \boldsymbol{B}_{y_k} \bigcup \{B_{s_1^{y_k}, s_2^{y_k}}, B_{s_1^{y_k}, i}, B_{s_2^{y_k}, i}\} \rightarrow \boldsymbol{B}_{y_k} & \text{if } |B_{y_k}| > 2 \end{cases} \tag{4.4-6}$$

$$B_{s_1^{y_k}, s_2^{y_k}} = B_{s_1^{y_k}, i} = B_{s_2^{y_k}, i} = (1, 1) \tag{4.4-7}$$

Here, $s_1^{y_k}$ and $s_2^{y_k}$ are the nearest and second-nearest nodes to A_i in $\boldsymbol{A}_{y_k}$, which were denoted as follows when A_i was created:

$$s_1^{y_k} = \underset{j \in \boldsymbol{A}_{y_k}}{\arg\min} ||\boldsymbol{w}_i - \boldsymbol{w}_j|| \tag{4.4-8}$$

$$s_2^{y_k} = \underset{j \in \boldsymbol{A}_{y_k} \backslash \{s_1^{y_k}\}}{\arg\min} ||\boldsymbol{w}_i - \boldsymbol{w}_j|| \tag{4.4-9}$$

Learning: Noise filtering based on bootstrapping

Following initialization, the input feature vector $\boldsymbol{x}_t$ and pattern recognition results $\boldsymbol{p}_t$ were sent to G_{UTO} from G_{FE} and G_{PR}. To prevent noise, the input based on $\boldsymbol{p}_t$, which is the probability of the vector being classified into each motion, was filtered. The minimum probability $\boldsymbol{\rho}_{\min} = \{\rho^1, ..., \rho^{y_k}, ..., \rho^{|Y|}\}$ was set to filter the noise. This ensures that the cluster movement is restricted within the decision region formed by the pattern recognition function G_{PR} learned from the teacher data $\boldsymbol{\Psi}$ updated by the previous adaptive learning. The nearest node s_1 and the second-nearest node s_2 to $\boldsymbol{x}_t$ in $\boldsymbol{A}$ were denoted as follows:

$$s_1 = \underset{j \in \boldsymbol{A}}{\arg\min} ||\boldsymbol{x}_t - \boldsymbol{w}_j|| \tag{4.4-10}$$

$$s_2 = \underset{j \in \boldsymbol{A} \backslash \{s_1\}}{\arg\min} ||\boldsymbol{x}_t - \boldsymbol{w}_j|| \tag{4.4-11}$$

If $p_{y_k} < \rho_{y_k} \quad (y_k \in A_{s_1})$ was true, it returned to the beginning of 4.4.3. If it was false, it was inferred that the input was not noise and all $e_{i,j}$ were increased as follows:

$$e_{i,j} \leftarrow e_{i,j} + 1. \quad \forall e_{i,j} \in \boldsymbol{B} \tag{4.4-12}$$

If $y_h \neq y_l \quad (y_h \in A_{s_1}, y_l \in A_{s_2})$ was true, it was assumed that the input was on the decision boundary between motions y_h and y_l and returned to the beginning of 4.4.3.

Self-Organization: Updating teacher data values

The parameters of the edges that were bound to node s_1 were updated as follows:

$$a_{s_1,j} \leftarrow a_{s_1,j} + 1. \quad \forall j \in N_{s_1} \tag{4.4-13}$$
$$e_{s_1,j} \leftarrow 0. \quad \forall j \in N_{s_1} \tag{4.4-14}$$

The set of order numbers of the direct neighbors of node i was represented as $N_i \in \mathbb{N}$ such that N_{s_1} was the set of the direct neighbors of node s_1. Furthermore, the squared error between the input data $\boldsymbol{x}_t$ and node s_1 was added to the accumulated error E_{s_1} of node s_1.

$$E_{s_1} \leftarrow E_{s_1} + ||\boldsymbol{x}_t - \boldsymbol{w}_{s_1}|| \tag{4.4-15}$$

Similarly, the position of node s_1 and the nodes that were connected to node s_1 were updated. Subsequently, η_1 and η_2 ($\eta_1 > \eta_2$) were used as the learning coefficients.

$$w_{s_1} \leftarrow w_{s_1} + \eta_1 \cdot (\boldsymbol{x}_t - \boldsymbol{w}_{s_1}), \tag{4.4-16}$$
$$w_j \leftarrow w_j + \eta_2 \cdot (v - w_j). \quad \forall j \in N_{s_1} \tag{4.4-17}$$

If there was an edge between s_1 and s_2, the edge's age was reset to 0. If there was no edge, a new edge was created.

$$\begin{cases} a_{s_1,s_2} \rightarrow 0 & \text{if } B_{s_1,s_2} \in \boldsymbol{B} \\ \boldsymbol{B} \bigcup B_{s_1,s_2} \rightarrow \boldsymbol{B} & \text{if } B_{s_1,s_2} \notin \boldsymbol{B} \end{cases} \tag{4.4-18}$$

Adaptation 1: Deleting teacher data

The edges that were older than the predefined threshold $a_{\max}$ or the edges whose evaluation value exceeded the threshold $\boldsymbol{e}_{\max} = \{e^1_{max}, ..., e^i_{max}, ..., e^{|Y|}_{max}\}$ were deleted. In addition, if the number of edges in each motion was below the minimum value $g_{\min}$, no edge was deleted.

$$\begin{aligned} &\boldsymbol{B} \setminus B_{i,j} \rightarrow \boldsymbol{B} \\ &\text{if } a_{i,j} > a_{max}, \text{ where } a_{i,j} \in B_{i,j} \quad \forall B_{i,j} \in \boldsymbol{B}. \end{aligned} \tag{4.4-19}$$

Consequently, if a node unrelated to other nodes appeared, it was deleted. If the number of nodes in each motion was less than the minimum value $n_{\min}$, no node was deleted.

$$\begin{aligned} &\boldsymbol{A} \setminus A_i \rightarrow \boldsymbol{A} \\ &\text{if } N_i = \emptyset \wedge |\boldsymbol{A}_{y_k}| > n_{\min} \text{ where } y_k \in A_i \quad \forall A_i \in \boldsymbol{A} \end{aligned} \tag{4.4-20}$$

Adaptation 2: Insertion of teacher data

Operations (a) and (b) were performed for each of the λ data inputs. For the other input times, only (b) was performed.

(a) The following operations were performed for each of the λ data inputs. Let A_q be the node with the largest accumulated error. The longest edge was selected among the edges connected to the node with the largest accumulated error A_q. Let A_f be the node that binds to this edge. A node r was inserted to bisect the edge. If the number of nodes in each class exceeded the maximum value $n_{\max}$, no nodes were added and process B commenced.

$$\begin{aligned} &\boldsymbol{A} \bigcup A_r = \{w_r, y_k, E_r\} \rightarrow \boldsymbol{A} \\ &w_r = 0.5 \cdot (w_q + w_f),\ y_k \in A_r,\ E_r = 0. \end{aligned} \tag{4.4-21}$$

$$\text{where } E_q = \max\{E_j, E_j \in \boldsymbol{B}\}, f = \arg\max_{j \in N_q}\{||w_q - w_j||\}. \tag{4.4-22}$$

Subsequently, the edge between nodes q and f was deleted, and new edges $B_{q,r}$ and $B_{r,f}$ were created.

$$\boldsymbol{B} \setminus B_{q,f} \rightarrow \boldsymbol{B} \tag{4.4-23}$$

$$\boldsymbol{B} \bigcup \{B_{q,r}, B_{r,f}\} \rightarrow \boldsymbol{B} \tag{4.4-24}$$

The accumulated errors, E_q and E_f, were updated, and E_r was initialized as follows:

$$E_q \leftarrow E_q - \alpha E_q \tag{4.4-25}$$

$$E_f \leftarrow E_f - \alpha E_f \tag{4.4-26}$$

$$E_r = E_q \tag{4.4-27}$$

Process B commenced.

(b) Finally, all the accumulated errors of the node were reduced as follows.

$$E_i \leftarrow \beta E_i (\forall i \in A) \tag{4.4-28}$$

A return was made to the beginning of 4.4.3.

4.4.4 Shadow System: Development of a learning parameter transfer system between mobile devices and microcontrollers

As described in Section 2.10.1, a mobile edge computing approach was employed to realize adaptive learning in a real environment. In this study, this system is referred to as the Shadow System because it substitutes the computational process of pattern recognition with a background computer (shadow). Fig.4.10 shows the difference between the two operation methods.

Fig.4.10a shows the operation method during adaptive learning. The microcontroller does not perform pattern recognition during adaptive learning, and the processing related to pattern recognition is performed by the mobile device instead. The mobile device processes the feature vector $\boldsymbol{x}_t$ received from the microcontroller via Bluetooth communication, and finally transfers the recognition result $\hat{y}_t$ to the microcontroller via Bluetooth communication. On the mobile device, the main thread generates teacher data (G_{GT}), estimates the motion intention (G_{PR}, G_{CA}), and updates the teacher data (G_{UTO}), whereas another thread performs classifier training (G_{L}), which requires time for processing.

The operation method after adaptive learning is shown in Fig.4.10b. After the adaptive learning is completed, the parameters $\boldsymbol{W}_g$ of the pattern recognition function G_{PR} are transferred from the mobile device to the pattern recognition function G_{PR} on the microcontroller via Bluetooth communication. It should be noted that the pattern recognition function G_{PR} must be the same for the mobile device and microcontroller to ensure parameter compatibility. After transferring the parameters, the microcontroller alone can control the myoelectric prosthetic hand using the parameters after adaptive learning.

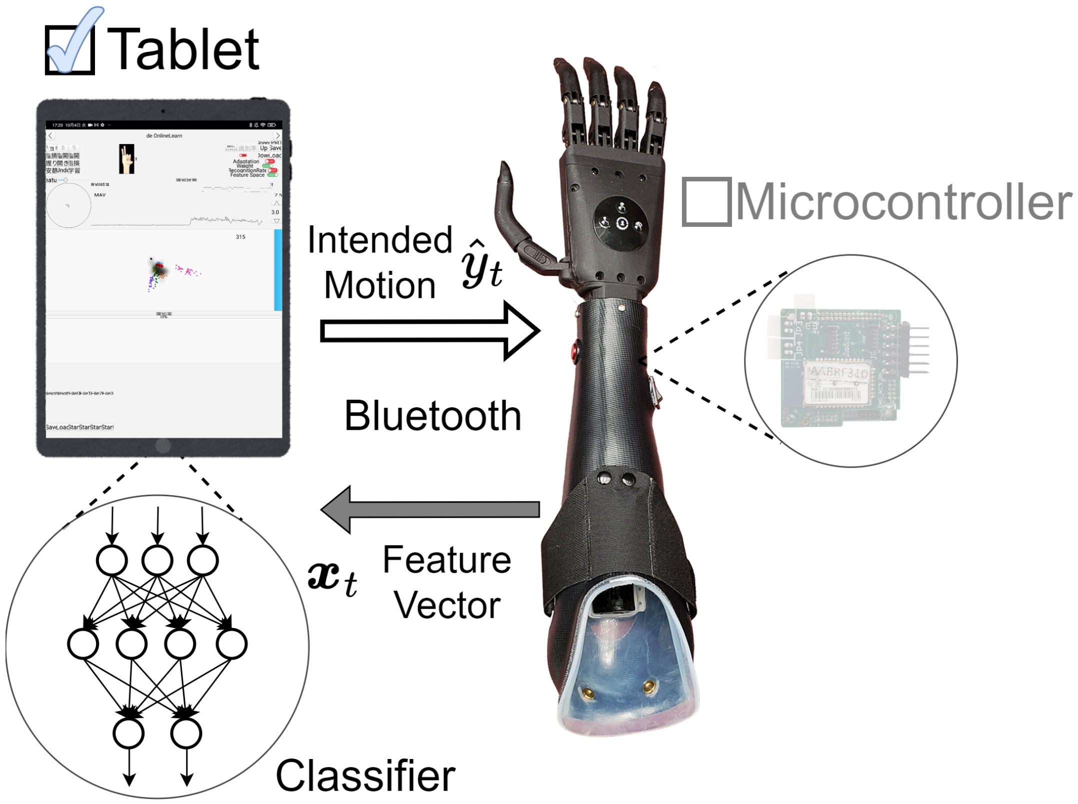

(a) System operation during adaptive learning

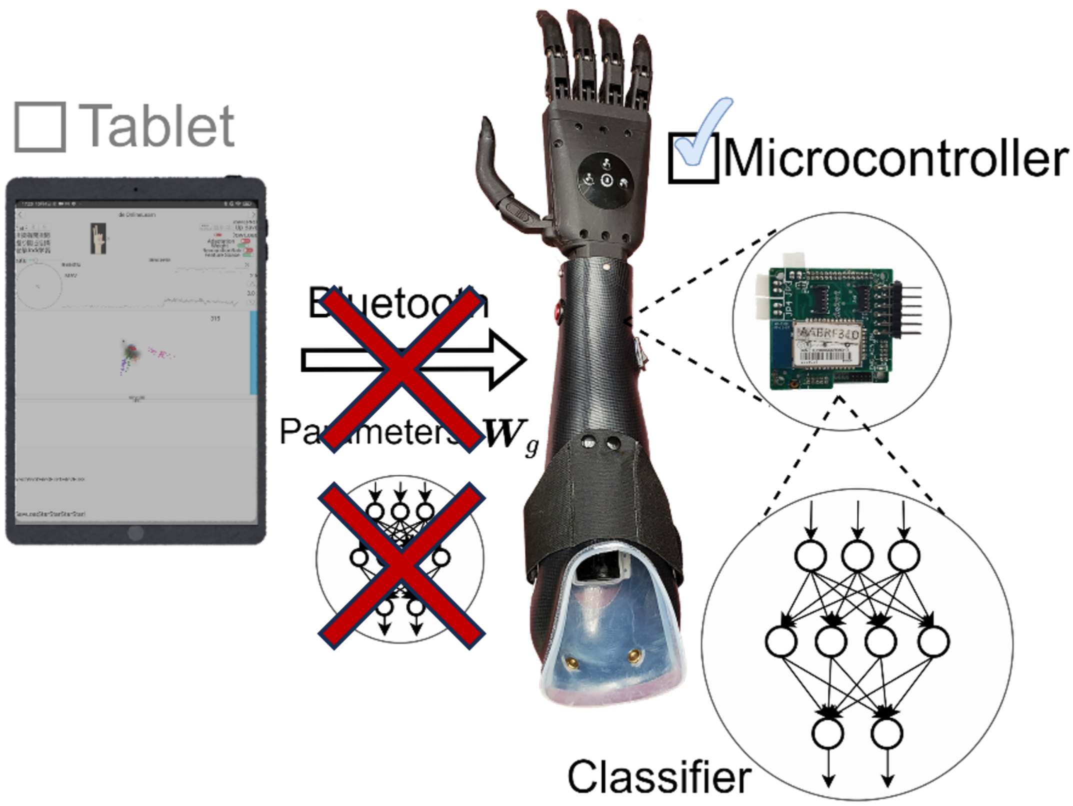

(b) System operation after adaptive learning

Fig.4.10: Operation method of the shadow system

A chart diagram showing the details of this system process is shown in Fig.4.11.

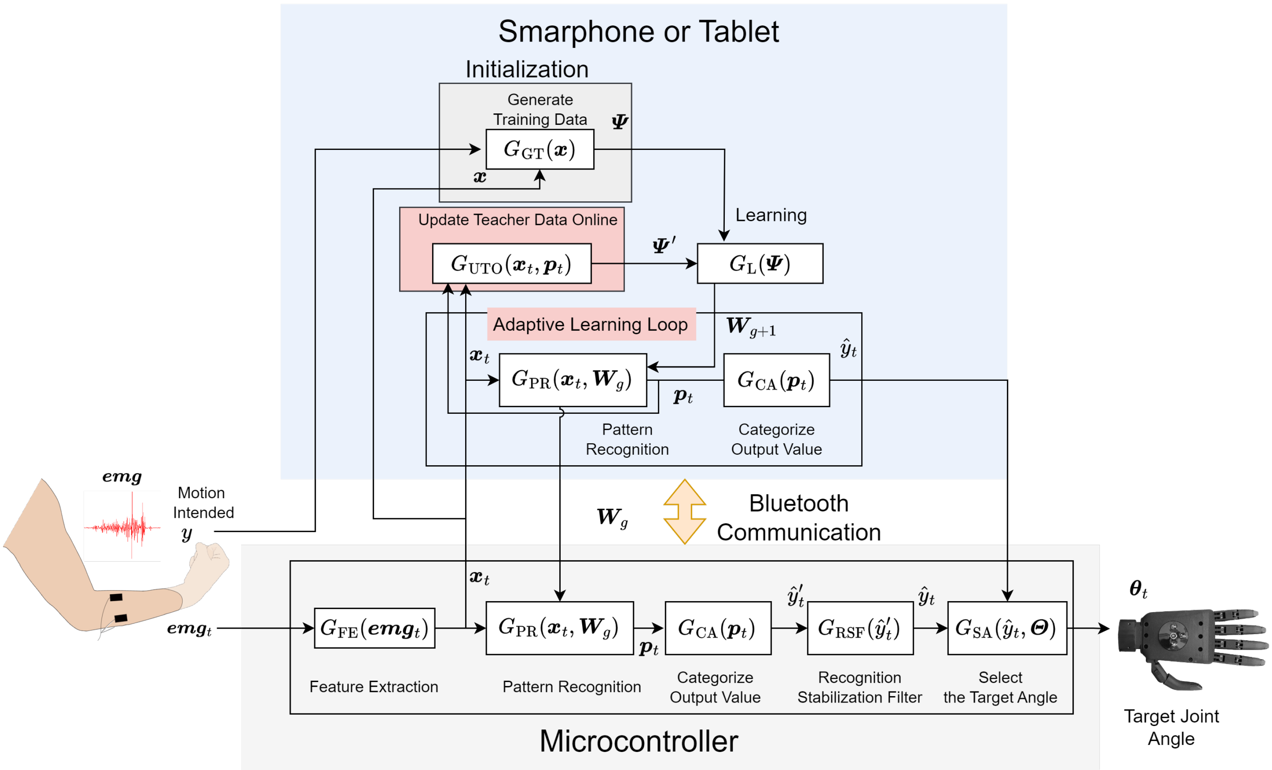

Fig.4.11: Details of shadow system. Each process corresponds to Fig.4.6.

4.5 Experiment1-1: Adaptation to wide range time variation by non-disabled participants

To verify the effectiveness of the proposed method for a wide range of time variation, a recognition experiment was conducted with non-disabled participants. The participants were instructed to perform three movements, namely resting, grasping, and opening, and the MPH control system in this study identified the motion intention. In this experiment, the number of discriminative motions was limited to three to avoid the situation described in Section 4.2.2, where the difference in the overall size of the features becomes a major discriminative factor and cannot be adapted to a wide range of time-varying conditions. Before conducting these experiments, the performance with artificial data was verified. These results are shown in Appendix A.

This study focused on evaluating the adaptability of the differences in the muscle contraction force between the supervised data measurement and actual use. Specifically, the study investigated whether the discriminator would adapt to and control a task that was subsequently performed using a weaker muscle contraction force if it was trained using a force greater than the muscle contraction force during normal use.

First, the teacher data was measured using a strong muscle contraction force to verify the model' s adaptability for differences in the muscle contraction force. Subsequently, the participants were instructed to repeat the task of opening and closing the MPH for 10 min. They were instructed to perform the task with as little force as possible. The recognition rates were then measured three times for various muscle contraction forces: before the task, after the 5-min task, and after the next 5-min task. The experimental conditions are explained in detail in the following subsections.

4.5.1 Experimental conditions

Table.4.2: Experimental Condition of the Experiment1-1.

Measurement	
Sampling frequency (Hz)	2000
Quantization bit rate (bit)	12
Filter (Hardware)	· 50 Hz notch filter · Bandpass filter with a 1–1000 Hz bandwidth
Filter (Software)	50-Hz High pass filter
Potential range (V)	-2.5 to 2.5
Feature Extraction	
Period (ms)	10
Number of samples	256
Overlapping samples	236
Window function	Hann window
Extracted Frequency (Hz)	23.4375, 46.875, 70.3125, 93.75, 140.625, 187.5, 250.0, 312.5
Smoothing (points)	5
Bluetooth Communication	
Sending Period (ms)	20
Processing when sending accumulated feature vectors	Averaging
Motion Intention Estimation	
Method	Artificial Neural Networks (ANN)
Number of Neurons (input layer)	$D = 24$
Number of Neurons (hidden layer)	40
Number of Neurons (output layer)	3
Activate function	Sigmoid (hidden layer) Softmax (output layer)
Experiment	
Measurement motion	Rest, Grasp, Open (Fig.4.12)
Target $pMAV$ for teacher data (V)	0.6
Target $pMAV$ for recognition rate (V)	0.6, 0.5, 0.4, 0.35, 0.3, 0.275, 0.25, 0.225
Sampling points per measurement	20
Sampling times for recognition rate	3
Devices	
Microcomputer	SH72544R, Renesas Electronics Corporation
EMG sensor	Hybrid Electrode (Togo, Yuta, et al. 2019)
Smartphone	ROG Phone 3, ASUS

The experimental conditions are described in this subsection. The parameters of the CCCL were as follows: $a_{max} = 8$, $e_{max} = (3000, 3000, 3000)$, $\boldsymbol{\rho}_{\min} = (0.9, 0.6, 0.6)$, $\eta_1 = 0.006$, $\eta_2 = 0.00006$, $\lambda = 5$, $\alpha = 0.5$, $\beta = 0.95$, $n_{\max} = 50$, $n_{\min} = 20$, $g_{\min} = 100$, and $T_{\mathrm{UTO}} = 100$.

The other parameters used in the experiment are listed in Table 4.2. The experiment was conducted on four participants (A–D) with approval from the ethics committee of UEC (permit No.10006(5)).

The $pMAV$ (the pseudo-mean absolute value) was calculated to quantify the strength of the user's muscle contraction. The MAV provides information on the strength of muscle contraction. In this experiment, $\boldsymbol{emg}_t$ was transformed to $\boldsymbol{x}_t = (x_1, x_2, ..., x_i, ..., x_D)$ by G_{FE} through an FFT to extract the frequency component. Each channel's frequency component was extracted into eight dimensions for a total of 24 dimensions. Because only $\boldsymbol{x}_t$ was sent to the tablet owing to the limited communication speed, the pMAV was used as an approximation of the MAV. The pMAV was calculated as follows:

$$pMAV = \sqrt{\frac{\sum_{i=1}^{D}\{x_i\}}{n_{ch}}} \tag{4.5-1}$$

D represents the dimensions of the feature vector and n_{ch} represents the number of EMG sensors. In this experiment, D was 24 and n_{ch} was 3. Because the frequency range of myoelectricity was 5–500 Hz, and the moving average of the five neighboring points of each frequency component to be extracted was considered, the pMAV could be considered an approximation of MAV in this experiment.

The specific details of the experimental procedure are as follows:

1. Sample the teacher data for each motion. Grasping and opening motions are measured at 0.6 V.
2. Train the classifier by the teacher data.
3. Measure the evaluation data at rest and at 0.6, 0.5, 0.4, 0.35, 0.3, 0.275, 0.25, 0.225 V for the grasping and opening motions. At this time, participants sample

evaluation data while viewing the recognition results through hand movements, just as they do during actual operation.

4. Perform adaptive learning for 5 min. The participants repeat the resting, grasping, and opening movements so that their movement intentions match the actual movement of the prosthetic hand.
5. Measure the evaluation data of the rest, grasping and opening motions at 0.6, 0.5, 0.4, 0.35, 0.3, 0.275, 0.25, and 0.225 V. At this time, participants sample the evaluation data without viewing the recognition results, unlike they do during actual operation. Recognition is performed using the parameters updated by adaptive learning.
6. Perform adaptive learning for another 5 min. Participants repeat the resting, grasping, and opening motions so that their intended motions match the actual movements of the MPH.
7. Measure the evaluation data of the rest, grasping, and opening motions at 0.6, 0.5, 0.4, 0.35, 0.3, 0.275, 0.25, and 0.225 V. At this time, participants sample the evaluation data without viewing the recognition results, unlike they do during actual operation. Recognition is performed using the parameters updated by the adaptive learning.

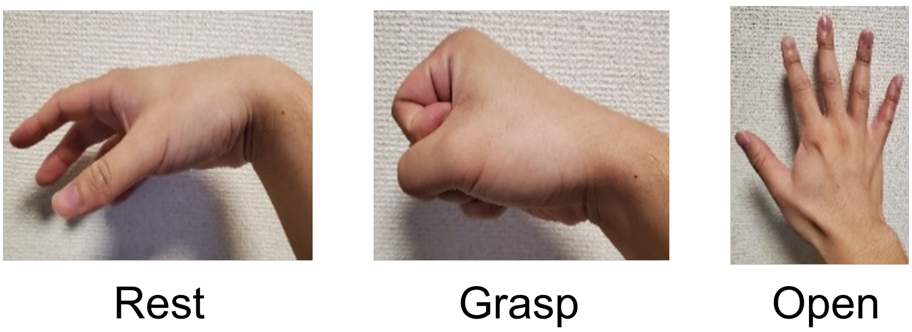

Fig.4.12: Motions evaluated in Experiment1-1.

4.5.2 Results

The averages of the recognition rates of the four participants are shown in Fig.4.13, Fig.4.13, and Fig.4.13, and changes in the teacher data of participant C are shown in Fig. 4.16. ”original” is the result of recognizing the evaluation data using the initial teacher data, and ”optimized” is the result of recognizing the evaluation data using the teacher data optimized by the proposed method. Notably, the evaluation data were measured while observing the movement of the MPH controlled by the classifier optimized by the proposed method. In this experiment, the recognition rate was calculated by assuming that the unrecognizable action was an incorrect answer.

A paired t-test was conducted to compare the mean values of the recognition rates for the same pMAV value. Consequently, for the grasping motion, the proposed method's recognition rate (optimized) was significantly larger when the target pMAVs were 0.3 and 0.35 after the 5-min task and when the target pMAV was 0.3 after the 10-min task. Furthermore, it had significantly larger recognition rates for the opening movement when the target pMAVs were 0.3 and 0.25 after the 5-min task and when the target pMAVs were 0.3, 0.275, 0.25, and 0.225 after the 10-min task.

The update interval τ_{L} was approximately 28.6 s on average.

The changes in participant C's teacher data are shown in Fig. 4.16. The yellow circles in the figure represent the teacher data in the rest mode. The EMG signals of the rest mode were the lowest compared with those of the motions measured. Fig. 4.16 shows that the clusters of grasping and opening motions became closer to the resting mode over time.

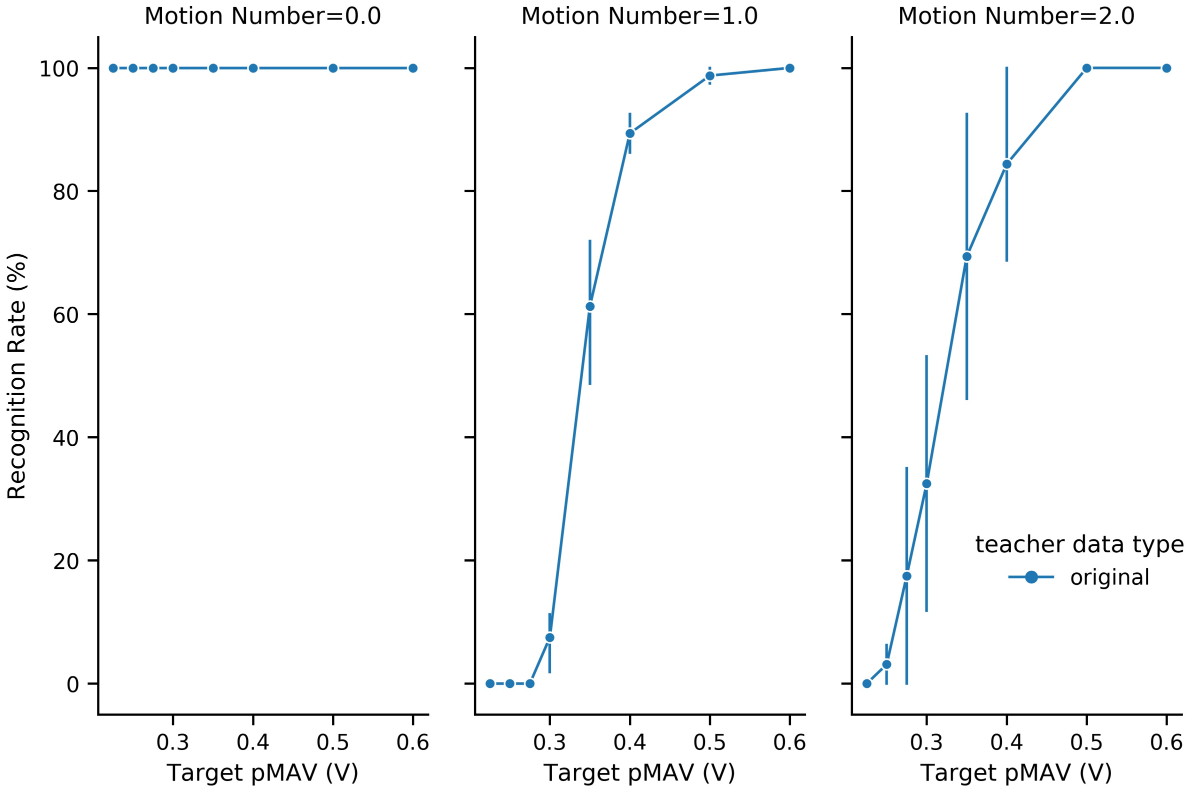

Fig.4.13: Averages of the four participants' recognition rates at 0 min. Rest: = 0; grasp motion = 1; and open motion = 2. In the resting mode, the muscles are not contracted. This indicates that the target pMAV shown on the horizontal axis is the recognition rate measured at times when the grasping and opening movements are measured at that target pMAV.

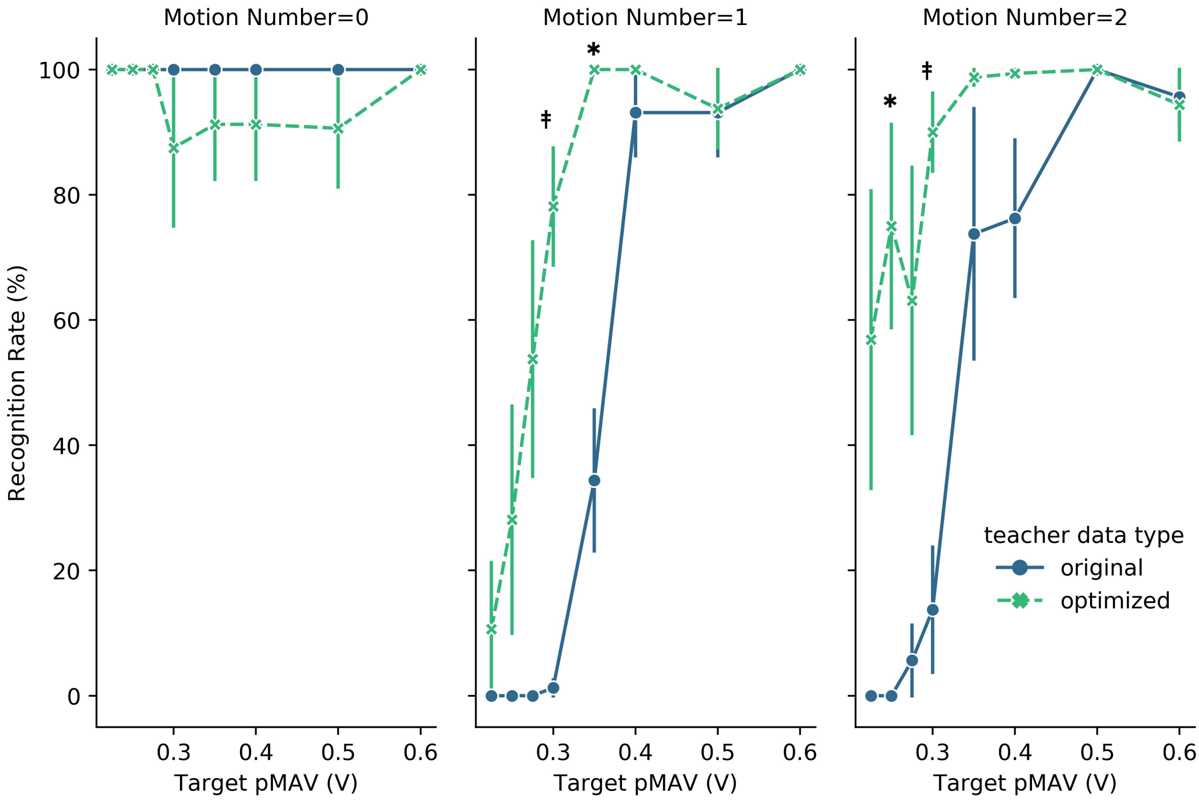

Fig.4.14: Averages of the four participants' recognition rates after 5 min task. Rest: = 0; grasp motion = 1; and open motion = 2. The paired t-test is used to compare the mean values of the recognition rates for the same pMAV values: $*$: $p < 0.05$, † : $p < 0.01$, and ‡ : $p < 0.005$. In the resting mode, the muscles are not contracted. This indicates that the target pMAV shown on the horizontal axis is the recognition rate measured at times when the grasping and opening movements are measured at that target pMAV.

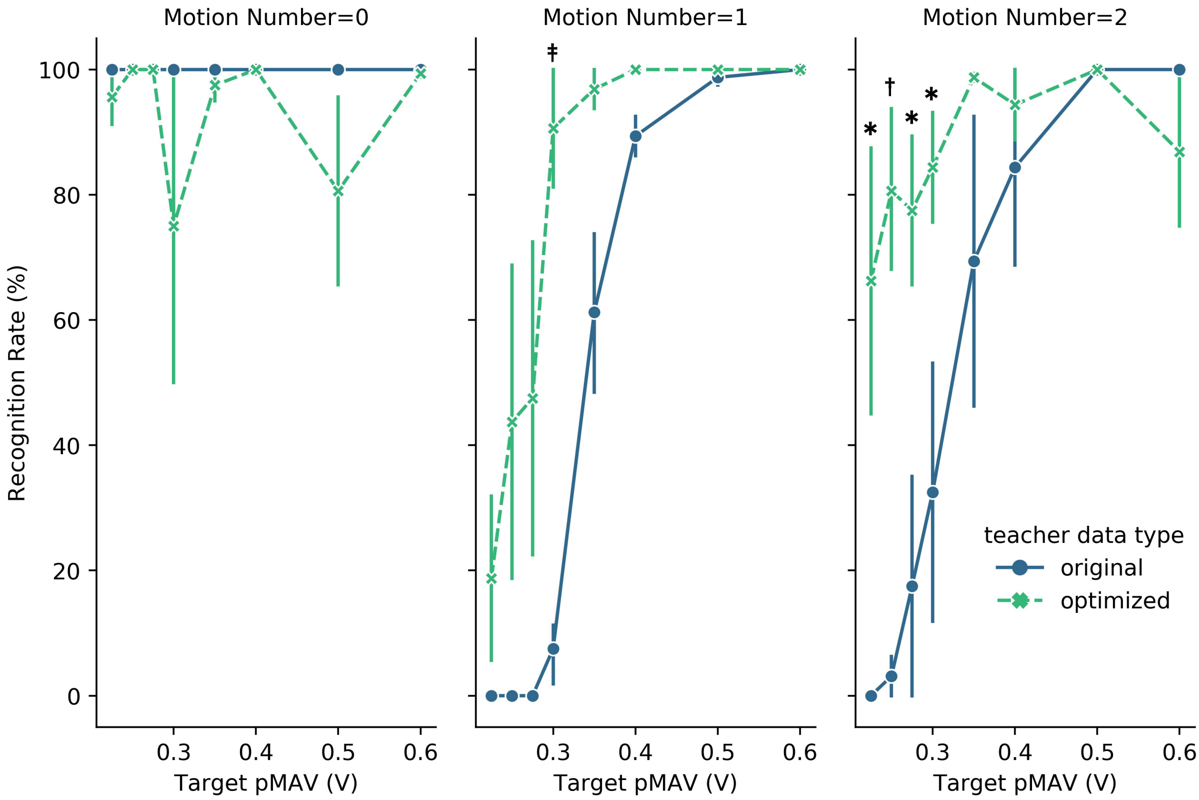

Fig.4.15: Averages of the four participants' recognition rates after 10 min task. Rest: = 0; grasp motion = 1; and open motion = 2. The paired t-test is used to compare the mean values of the recognition rates for the same pMAV values: $*$: $p < 0.05$, † : $p < 0.01$, and ‡ : $p < 0.005$. In the resting mode, the muscles are not contracted. This indicates that the target pMAV shown on the horizontal axis is the recognition rate measured at times when the grasping and opening movements are measured at that target pMAV.

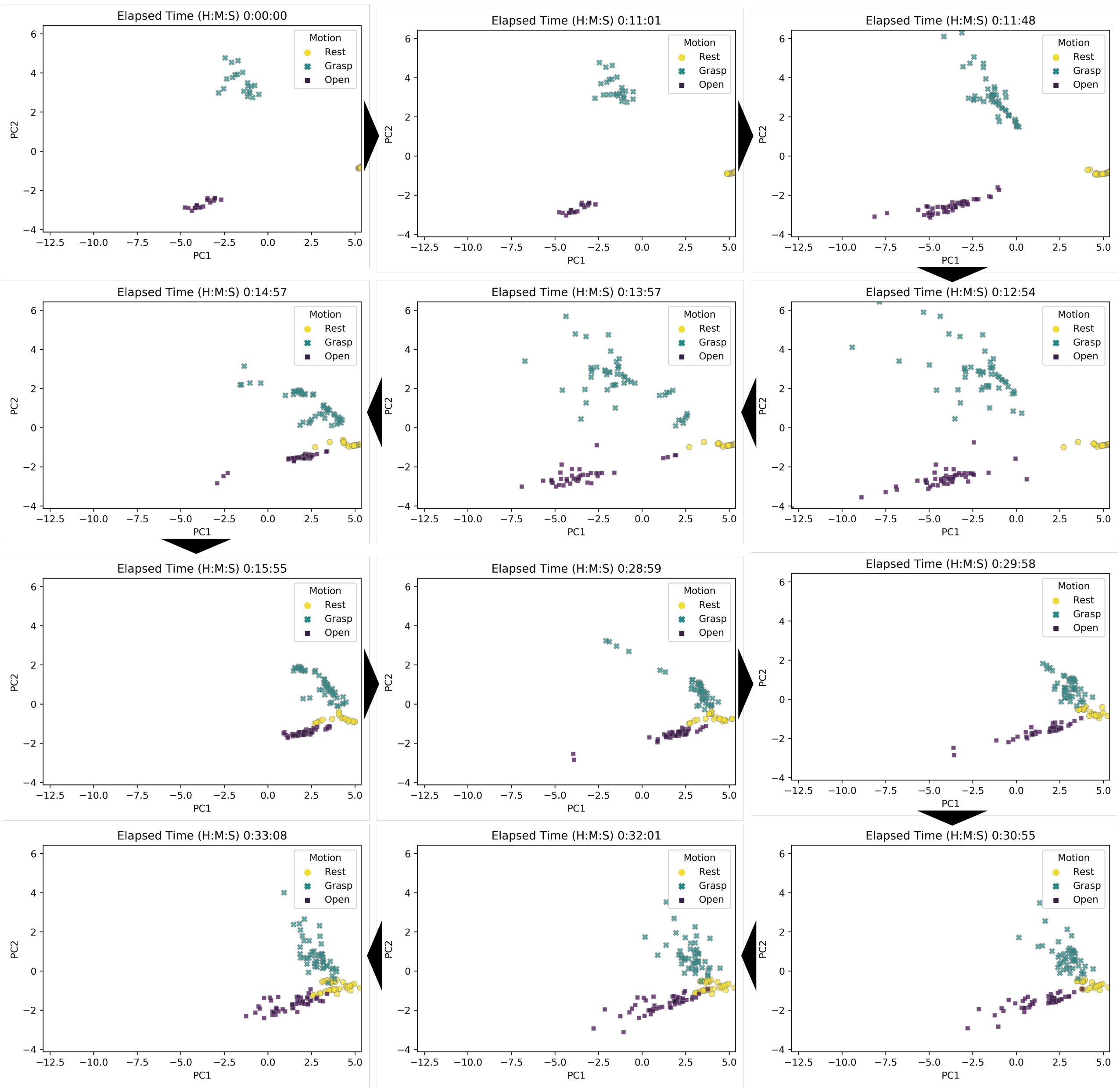

Fig.4.16: Changes in participant C's teacher data. The 24-dimensional space of the teacher data is dimensionally reduced to two dimensions through principal component analysis (PCA). The PCA is learned from the initial teacher data. The time elapsed since the first learning is indicated at the top of each figure. When the elapsed time is 0:11:01, the first measurement of the recognition rate is completed, and the first task commences while updating the teacher data. The teacher data at 0:15:55 are used for the second measurement of the recognition rate. When the elapsed time is 0:28:59, the second measurement of the recognition rate is complete, and the second task commences while updating the teacher data. The teacher data at 0:33:08 are used for the third measurement of the recognition rate.

4.5.3 Discussion

Adaptation to various muscle contraction forces

This study found that the proposed adaptive learning method enables recognition even when the muscle contraction force is lower than that at the time of the teacher data measurement. In particular, when the target pMAV was less than 0.30, the recognition was almost impossible without adaptive learning, but with adaptive learning, the recognition rate was approximately 80 %, which could make the MPH stable.

Limitations of the proposed method

Following optimization, the recognition rate improved in most cases during grasping and opening. In contrast, the recognition rate decreased in some cases in the resting mode. As shown in Figure 4.16, as the discrimination becomes possible with smaller muscle contraction forces, the teacher data for the resting mode and grasping/opening motion became closer. Simultaneously, the range of actions that could be recognized as the resting mode was narrowed. The recognition rate was measured without the feedback of the recognized motion; thus, the participant reproduced the motion, suggesting rest as it occurred before optimization, which may have caused the misidentification. These results suggest a trade-off between maneuverability at small muscle contraction forces and the range of the resting mode. It is necessary to verify the impact of optimization on the application using the feedback of recognized motions under actual conditions.

4.6 Experiment1-2:Adaptation to wide range time variation by a participant with upper limb deficiency

To verify the effectiveness of the proposed method for a wide range of time variations, a recognition experiment was conducted involving a person with an upper limb deficiency. As in Section 4.5, this study tested whether the proposed method can adapt and control three motions (resting, grasping, and opening) with different muscle contraction forces from those used in the teacher data measurement by measuring the recognition rate.

4.6.1 Experimental conditions

Table.4.3: Experimental Conditions of the Experiment1-2.

Measurement	
Sampling frequency (Hz)	2000
Quantization bit rate (bit)	12
Filter (Hardware)	· 50 Hz notch filter · Bandpass filter with a 1–1000 Hz bandwidth
Filter (Software)	50-Hz High pass filter
Potential range (V)	-2.5 to 2.5
Feature Extraction	
Period (ms)	10
Number of samples	256
Overlapping samples	236
Window function	Hann window
Extracted Frequency (Hz)	23.4375, 46.875, 70.3125, 93.75, 140.625, 187.5, 250.0, 312.5
Smoothing (points)	5
Bluetooth Communication	
Sending Period (ms)	20
Processing when sending accumulated feature vectors	Averaging
Motion Intention Estimation	
Method	Artificial Neural Networks (ANN)
Number of Neurons (input layer)	$D = 24$
Number of Neurons (hidden layer)	32
Number of Neurons (output layer)	3
Activate function	Sigmoid (hidden layer) Softmax (output layer)
Experiment	
Measurement motion	Rest, Grasp, Open (Fig.4.17)
Target $pRMS$ for teacher data (V): Grasp	1.5
Target $pRMS$ for teacher data (V): Open	2.25
Target $pRMS$ for recognition rate (V): Grasp	3.5, 2.25, 1.5, 1.0, 0.75
Target $pRMS$ for recognition rate (V): Open	6.5, 3.75, 2.25, 1.25, 1.0
Sampling points per measurement	20
Sampling times for recognition rate	9 (3 measurements per motion)
Devices	
Microcomputer	SH72546R, Renesas Electronics Corporation
EMG sensor	Dry Electrode (Togo, Yuta, et al. 2019)
Tablet	Xiaomi Pad 5, Xiaomi

The experimental conditions are described in this subsection. The parameters of the CCCL were the same as section.4.5 as follows: $a_{max} = 8$, $e_{max} = (3000, 3000, 3000)$, $\boldsymbol{\rho}_{\min} = (0.9, 0.6, 0.6)$, $\eta_1 = 0.006$, $\eta_2 = 0.00006$, $\lambda = 5$, $\alpha = 0.5$, $\beta = 0.95$, $n_{\max} = 50$, $n_{\min} = 20$, $g_{\min} = 100$, $T_{\mathrm{UTO}} = 100$. The other parameters used in the experiment are listed in Table 4.3. The experiment was conducted on a person with upper limb deficiencies with approval from the UEC ethics committee (permit No.10006(5)).

It should be noted here with caution that the index of the muscle contraction force is different from that of Section 4.5. The $pRMS$ (pseudo-Root Mean Square) was calculated to quantify the strength of the user's muscle contraction. The Root Mean Square (RMS) also provides information on the strength of the muscle contraction. In this experiment, $\boldsymbol{emg}_t$ was transformed to $\boldsymbol{x}_t = (x_1, x_2, ..., x_i, ..., x_D)$ by G_{FE} through an FFT to extract the frequency component. Each channel's frequency component was extracted into eight dimensions for a total of 24 dimensions. Let D be the number of dimensions of the feature vectors, D_{ch} be the number of dimensions of each channel, and n_{ch} be the number of myoelectric sensors. Thus, $D = 24$, $D_{ch} = 8$, and $n_{ch} = 3$ here. Because only $\boldsymbol{x}_t$ was sent to the tablet owing to the limited communication speed, the pRMS was used as an approximation of the RMS. The pRMS was calculated as follows:

Let $pRMS_k$ denote the pRMS of channel k. Then,

$$pRMS_k = \sqrt{\frac{\sum_{i=1+D_{ch}(k-1)}^{D_{ch}k} x_i^2}{D_{ch}}} \tag{4.6-1}$$

From this, the $pRMS$ is calculated as follows:

$$pRMS = \sqrt{\sum_{k=1}^{n_{ch}} pRMS_k^2} \tag{4.6-2}$$

In the case of persons with an upper limb deficiency, the magnitude of the EMG potentials may vary significantly depending on the movement. To take this into account, this study calculated the pRMS at maximal contraction in advance and determined the magnitude of the muscle contraction force to be evaluated based on the pRMS for each movement. The muscle contraction at this time was referred to as the maximal voluntary contraction (MVC), and was set as 100%MVC. As in the evaluation of the recognition rate, three sets of 20 data were sampled three times for each movement, repeated three times for each movement, for a total of 180 features. The average of the pRMS at this time was set as 100%MVC.

Using this 100%MVC as a reference, the pRMS value at which the participant set the target value of muscle contraction was determined as in Section 4.5 during the evaluation. There were five pRMS values to be evaluated: 180%MVC, 100%MVC, 50%MVC, 20%MVC, and 10%MVC. The specific pRMS values are listed in Table.4.3. The reason why the target value is above 100 µMVC is that this value is the average of the pRMS over a certain time period and is therefore calculated at a considerably lower value than the target value.

Unlike in Section 4.5, the magnitude of the muscle contraction during the teacher data measurement was set to 50%MVC instead of the maximum value. The reason for this is that the preliminary experiments confirmed that when the participant maximized the muscle contraction force, the difference in the overall magnitude of the features described in Section 4.2.2 becomes a major factor in the recognition between the grasping and opening movements, making it impossible to adapt to a wide range of time variations. Fifty%MVC is a muscle contraction force close to the participant's self-reported muscle contraction force during normal use. Unlike Section 4.5, rest was not measured at each change in the muscle contraction force, but rather nine times at the beginning of each measurement process to calculate the recognition rate.

The detailed experimental procedure is as follows:

1. The teacher data for each motion are sampled. The grasping and opening motions are measured with a 50% MVC.
2. The classifier is trained by the sampled teacher data.
3. Measure the evaluation data of the resting state, and the grasp and open motions at 180%MVC, 100%MVC, 50%MVC, 20%MVC, 10%MVC. At this time, participants sample the evaluation data while viewing the recognition results by the hand movements as they would during actual operation.
4. Five minutes of adaptive learning is conducted. Participants repeat the resting,

grasping, and opening movements so that their intended movements match the actual movements of the MPH.

5. The evaluation data of the resting state, and the grasp and open motions at 180%MVC, 100%MVC, 50%MVC, 20%MVC, 10%MVC are measured. At this time, participants sample the evaluation data while viewing the recognition results by the hand movements as they would during actual operation. This recognition is performed using the parameters updated by adaptive learning.
6. Another five minutes of adaptive learning is conducted. Participants repeat the resting, grasping, and opening movements so that their intended movements match the actual movements of the MPH.
7. The evaluation data of the resting state, and the grasp and open motions at 180%MVC, 100%MVC, 50%MVC, 20%MVC, 10%MVC are measured. At this time, participants sample the evaluation data while viewing the recognition results by the hand movements as they would during actual operation. This recognition is performed using the parameters updated by adaptive learning.

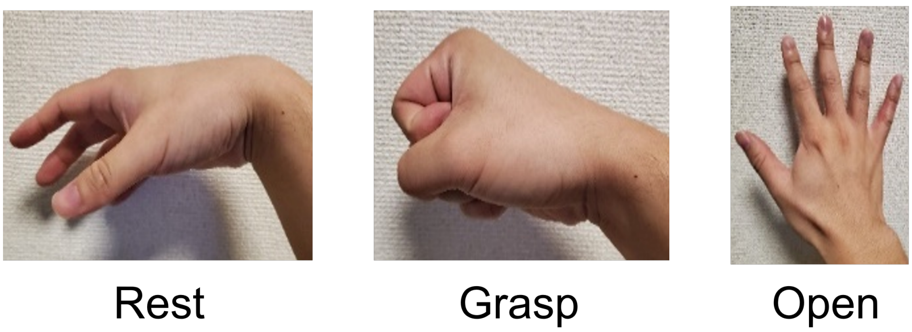

Fig.4.17: Motions evaluated in Experiment1-2.

4.6.2 Results

The results of Experiment 1-2 are shown in Fig.4.18. "original" is the result of recognizing the evaluation data using the initial teacher data, and "optimized" is the result of recognizing the evaluation data using the teacher data optimized by the proposed method. It should be noted that the evaluation data were measured while observing the movement of the MPH controlled by the classifier optimized by the proposed method. In this experiment, the recognition rate was calculated by assuming that the unrecognizable action was an incorrect answer.

The update interval τ_{L} was approximately 20.4 s on average.

As shown in Fig.4.18a, the recognition rate of the grasping motion was low and the motion was unstable in the initial teacher data. However, the recognition rate improved over a wide range of muscle contraction forces by adaptive learning, as shown in Fig.4.18b and Fig.4.18c. The changes in the participant's teacher data are shown in Fig. 4.19.

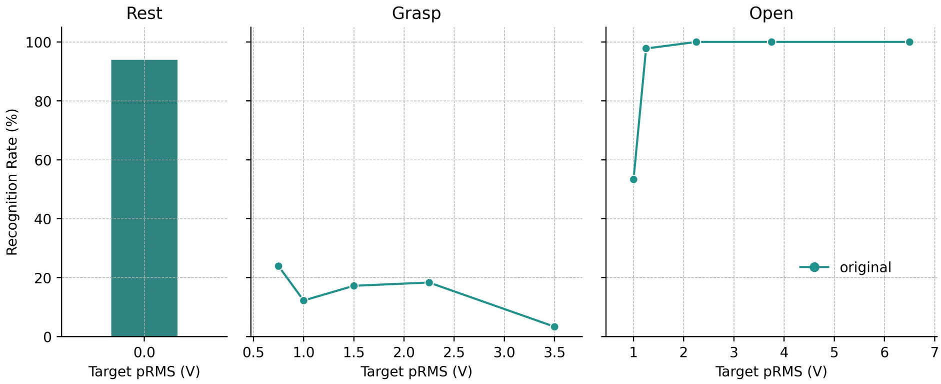

(a) Recognition rates before adaptive learning.

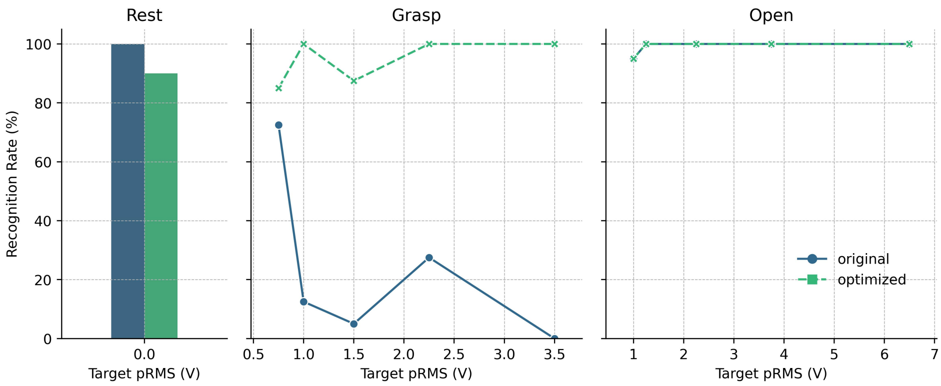

(b) Recognition rates after 5 min task.

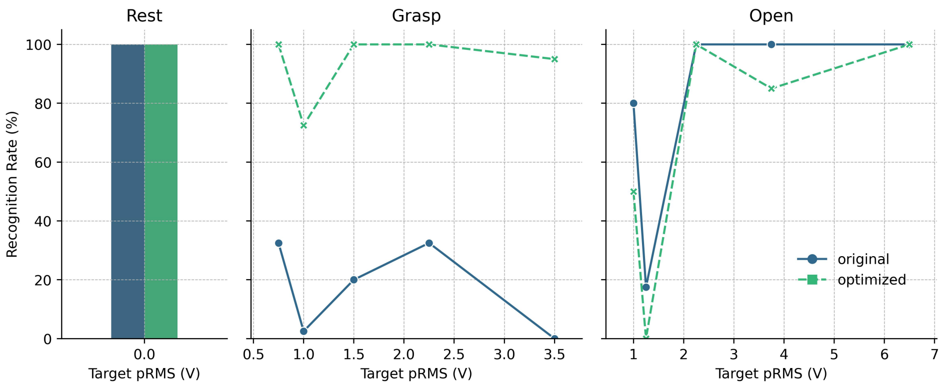

(c) Recognition rates after 10 min task.

Fig.4.18: Participant' s recognition rates. Notably, in "Open" of (b), the lines indicating "original" and "optimized" are almost the same value, hence they are shown as overlapping.

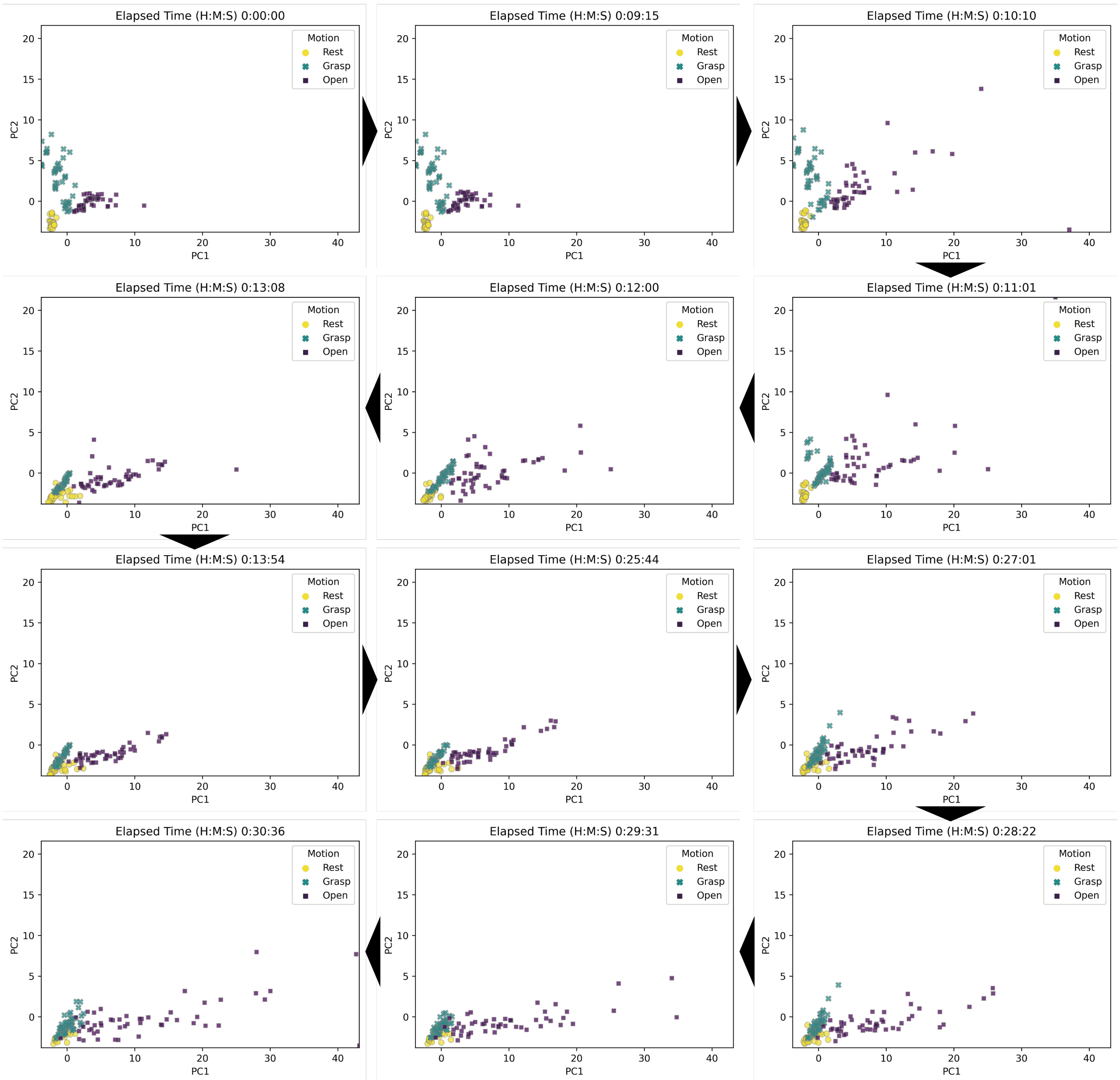

Fig.4.19: Changes in teacher data. The 24-dimensional space of the teacher data is dimensionally reduced to two dimensions through principal component analysis (PCA). The PCA is learned from the initial teacher data. The time elapsed since the first learning is indicated at the top of each figure. When the elapsed time is 0:09:15, the first measurement of the recognition rate is completed, and the first task is commenced while updating the teacher data. The teacher data at 0:13:54 are used for the second measurement of the recognition rate. When the elapsed time is 0:25:44, the second measurement of the recognition rate is complete, and the second task is commenced while updating the teacher data. The teacher data at 0:30:36 are used for the third measurement of the recognition rate.

4.6.3 Discussion

Teacher data

Fig.4.19 shows that the variance of the clusters for the grasping motion decreased, whereas the variance of the clusters for the opening motion increased. This suggests that the method does not necessarily increase the variance of the clusters, but possibly maintains an appropriate cluster size for the input myoelectric signals.

Adaptability of the proposed method

The clusters of the grasping motions before and after adaptation have a small overlap. Considering this and the fact that the initial recognition rate of the grasping motion was small, it can be assumed that this was a condition in which the teacher data was mismeasured. The fact that the recognition rate was improved by optimizing the teacher data even in such a case indicates the high adaptive capability of this method.

Limitations of the proposed method

As in Experiment 1-1, the clusters for the resting motion and grasping motion overlapped. This is attributed to the clusters moving toward an area near the resting motion, as the muscle contraction force naturally tends to be weaker for motions that are easier to perform. Although this did not affect the recognition rate, the effect on the usability of the system is unclear; hence, it is necessary to verify the results by actual task evaluations.

Optimal teacher data

As described in Section 2.10.2, mathematically ideal teacher data would have low within-class variance, high between-class variance, and boundary data eliminated (Yamanoi et al. 2021; Ryu Kato 2008). However, as the adaptive learning progressed in this study, the within-class variance increased and the between-class variance decreased, as shown in Fig.4.19. This is also the case in Experiment 1-1, which was conducted with non-disabled subjects, as observed in Fig.4.16. Experiment 1-1 was adapted with the weakest possible muscle contraction force, whereas Experiment 1-2 was adapted with the muscle contraction force that the participant could easily control on the MPH. Both experiments were the result of learning muscle contraction patterns that were easy for the user to control during actual use. These results support the hypothesis stated in Section 2.10.2 that ideal teacher data does not necessarily make it easier for the user to control.

4.7 Experiment2: Adaptation to narrow range time variation

To verify the effectiveness of the proposed method for a narrow range of time variations, experiments were conducted involving non-disabled participants. The target case is one of the early time variations described in Section 4.2, mismeasurement of the teacher data. This time variation was selected from a number of narrow time variations because, as explained in Section 2.10.2, manual labeling of the teacher data is necessary for practical use, and this has been a barrier to the application of the pattern recognition control method for MPHs. This is why it is important for the field to address this issue.

In this study, the effectiveness of this method is verified by comparing the recognition rate after adaptive learning with the recognition rate measured using the initially measured teacher data. The reason for limiting the validation of this experiment to experiments with non-disabled participants is that there are few participants with upper limb deficiencies who are able to use different muscle contraction patterns for multiple movements, and it is difficult to obtain their cooperation to participate in the experiment.

It should be noted that before these experiments, performance verification with artificial data was conducted. These results are presented in Appendix A.

4.7.1 Experimental conditions

Table.4.4: Experimental Conditions of Experiment2.

Measurement	
Sampling frequency (Hz)	2000
Quantization bit rate (bit)	12
Filter (Hardware)	· 50 Hz notch filter · Bandpass filter with a 1–1000 Hz bandwidth
Filter (Software)	50-Hz High pass filter
Potential range (V)	-2.5 to 2.5
Feature Extraction	
Period (ms)	10
Number of samples	256
Overlapping samples	236
Window function	Hann window
Extracted Frequency (Hz)	23.4375, 46.875, 70.3125, 93.75, 140.625, 187.5, 250.0, 312.5
Smoothing (points)	5
Bluetooth Communication	
Sending Period (ms)	20
Processing when sending accumulated feature vectors	Averaging
Motion Intention Estimation	
Method	Artificial Neural Networks (ANN)
Number of Neurons (input layer)	$D = 24$
Number of Neurons (hidden layer)	32
Number of Neurons (output layer)	8
Activate function	Sigmoid (hidden layer) Softmax (output layer)
Experiment	
Measurement motion	Rest, Grasp, Open, Three finger pinch, Wrist flexion, Wrist extension, Wrist pronation, Wrist supination (Fig.4.20)
Sampling points per measurement	20
Sampling times for recognition rate	9 (3 measurements per motion)
Devices	
Microcomputer	SH72546R, Renesas Electronics Corporation
EMG sensor	Dry Electrode (Togo, Yuta, et al. 2019)
Tablet	Xiaomi Pad 5, Xiaomi

The experimental conditions are described in this subsection. The parameters of the CCCL were as follows: $a_{max} = 8$, $e_{max} = (3000, 3000, 3000, 3000, 3000, 3000, 3000, 3000)$, $\boldsymbol{\rho}_{\min} = (0.9, 0.7, 0.7, 0.7, 0.7, 0.7, 0.7, 0.7)$, $\eta_1 = 0.0002$, $\eta_2 = 0.000002$, $\lambda = 5$, $\alpha = 0.5$, $\beta = 0.95$, $n_{\max} = 50$, $n_{\min} = 20$, $g_{\min} = 100$, $T_{\mathrm{UTO}} = 100$. This parameter was determined experimentally. The parameter determination is described in Appendix B. The other parameters used in the experiment are listed in Table 4.4. The experiment was conducted on a person with upper limb deficiencies with approval from the UEC ethics committee (permit No.10006(5)).

In the experiments in Section 4.5 and Section 4.6, experiments were conducted while confirming the recognition results by controlling the myoelectric prosthetic hand and observing its movements, as in the actual use of the prosthetic hand. However, as presented in Table.4.4, some of the movements in this study were different from those actually possible using the myoelectric prosthetic hand because the movements were selected to facilitate the separation of the muscle contraction patterns. Therefore, for simplicity, an illustration of the hand movements, which corresponds to the participant's hand movements are shown on the tablet as recognition results.

The detailed procedure of the experiment is as follows:

1. The teacher data are sampled for each operation.
2. The classifier is trained by the sampled teacher data.
3. The evaluation data of each motion are measured. The participants then observe the recognition results using a tablet, as they do during the actual operation.
4. Adaptive learning is conducted for 2 min. Participants repeat the motions so that their intended motions match the actual recognition results displayed on the tablet.
5. The evaluation data of each motion are measured. The participants then observe the recognition results using a tablet, as they do during the actual operation. This recognition is performed using the parameters updated by the adaptive learning.
6. Adaptive learning is conducted for another 2 min. Participants repeat the motions so that their intended motions match the actual recognition results displayed on the tablet.
7. The evaluation data of each motion are measured. Participants then observe the

recognition results using a tablet, as they do during the actual operation. This recognition is performed using the parameters updated by the adaptive learning.

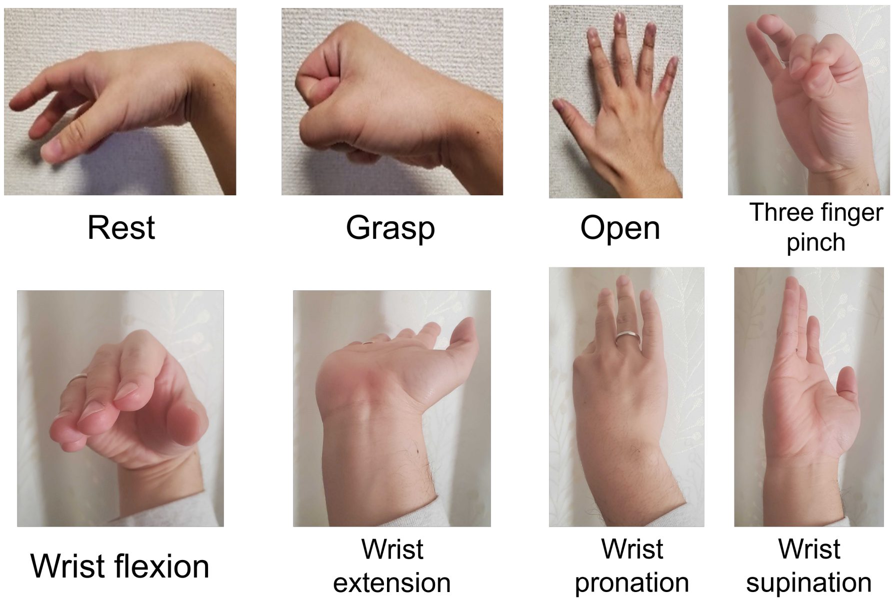

Fig.4.20: Motions evaluated in Experiment2.

4.7.2 Results

The average of the recognition rate of the six participants is shown in Fig.4.21. Fig.4.22 shows the number of stable movements of the six participants when the stable recognition rate was set above 80.0%. The changes in participant A's teacher data are shown in Fig. 4.23. In this experiment, the recognition rate was calculated by assuming that the unrecognizable action was the correct answer. The "original" is the result of recognizing the evaluation data using the initial teacher data, and "optimized" is the result of recognizing the evaluation data using the teacher data optimized by the proposed method. The significant difference of the recognition rate and the number of stable motions between before and after the adaptive learning was tested, as well as between the "original" and "optimized" for each process. The Wilcoxon signed-rank test was used.

The update interval τ_{L} was approximately 57.4 s on average.

The results showed that the recognition rate increased significantly by an average of 6.5 % after 2 min and by an average of 4.0 % after 4 min from before the adaptive learning. In addition, a comparison between the "original" and "optimized" showed that the recognition rate of "optimized" was significantly greater than that of "origin" by an average of 7.4 % both after 2 min and 4 min. The average recognition rate of "optimized" was 83.5 % after 2 min of adaptive learning and 81.0 % after 4 min of adaptive learning, which was higher than the stable recognition rate of 80.0 %.

There was no significant difference in the number of stable motions. The average number of stable motions increased by 1 after 2 min from before the adaptive learning, but decreased by 0.17 after 4 min. In the comparison between "origin" and "optimized", "optimized" had an average of 0.83 more motions than "origin" at 2 min, whereas "optimized" had an average of 0.5 more motions than "origin" at 4 min.

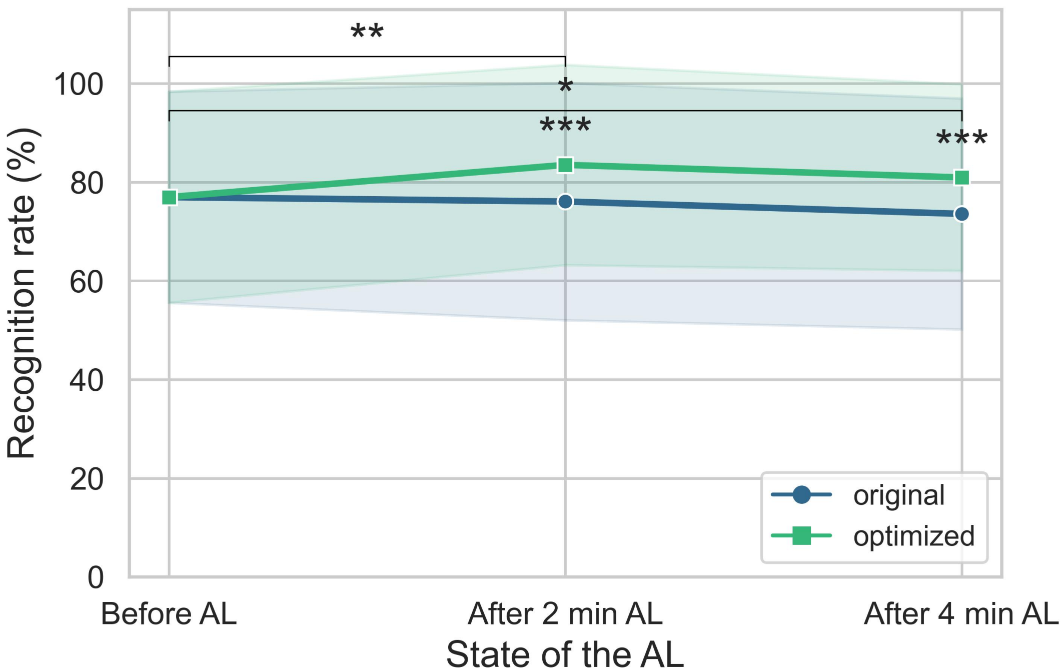

Fig.4.21: Trends in the average recognition rate for each motion for the six participants.

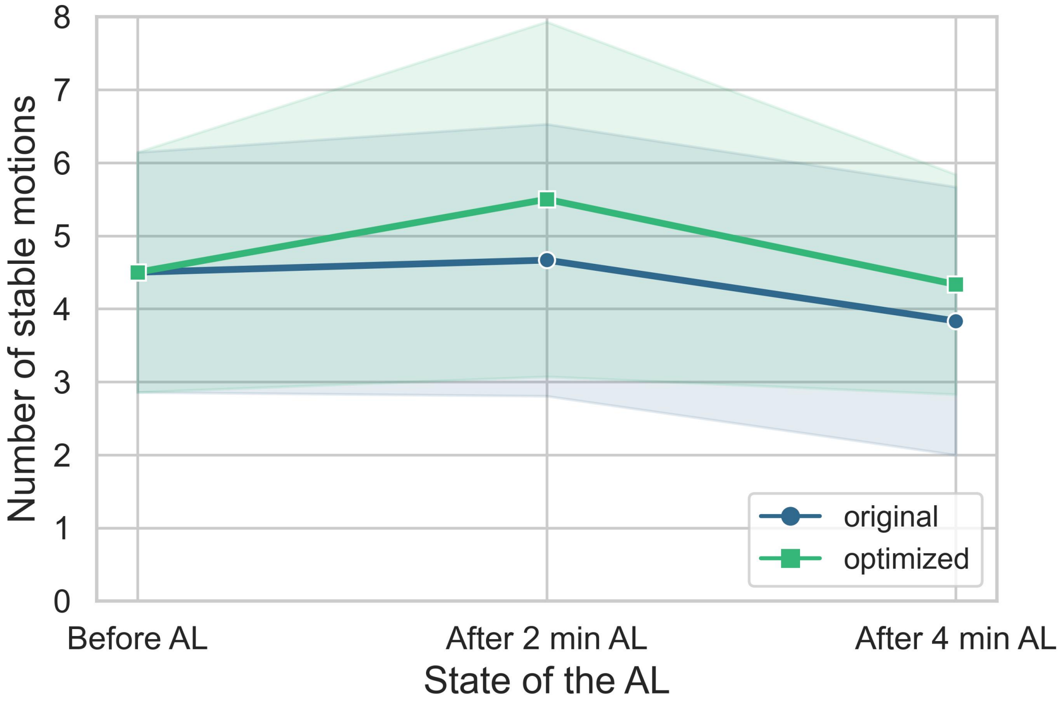

Fig.4.22: Trends in the number of stable motions of the six participants.

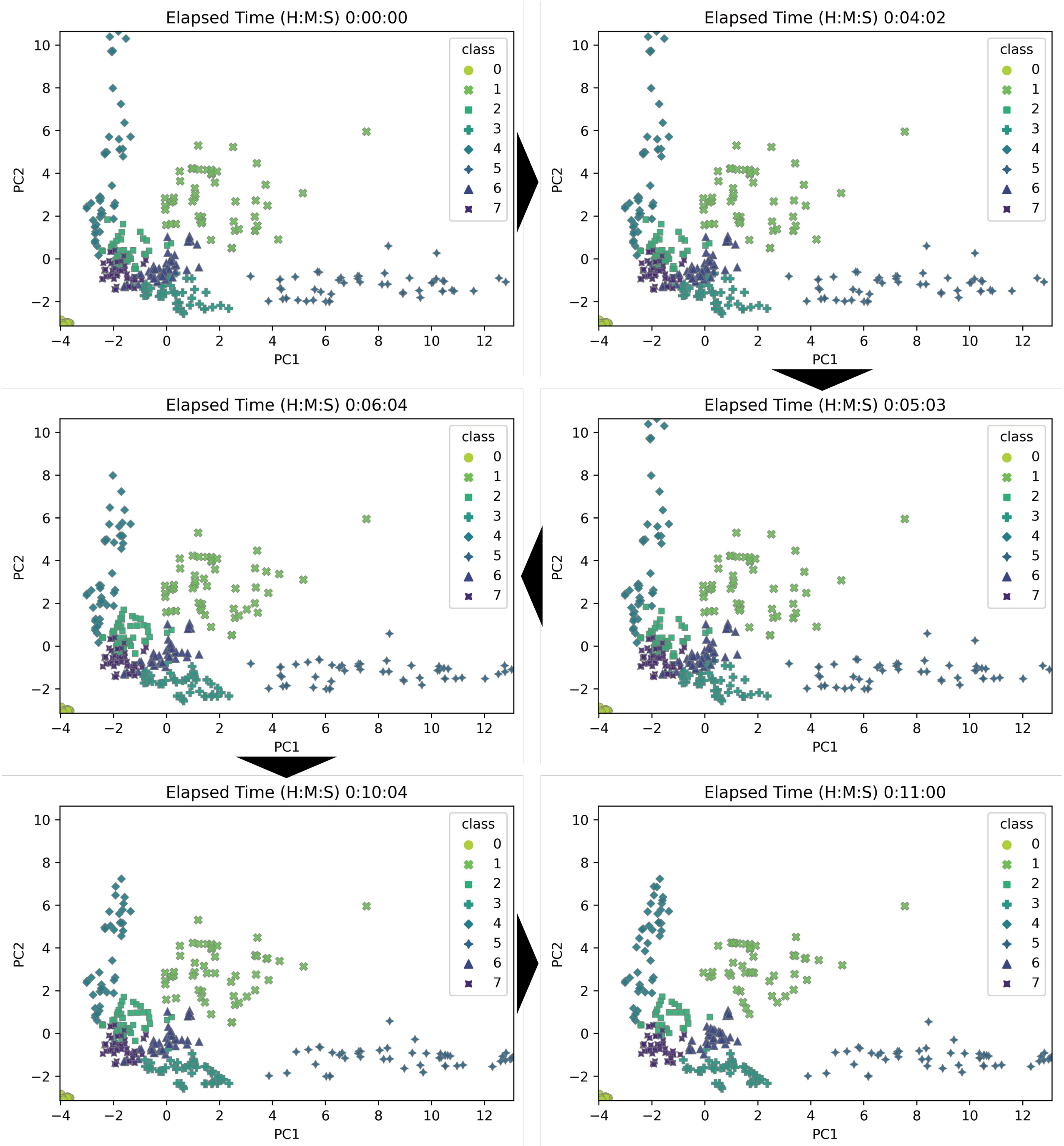

Fig.4.23: Changes in participant A's teacher data. The 24-dimensional space of the teacher data is dimensionally reduced to two dimensions through principal component analysis (PCA). The PCA is learned from the initial teacher data. The time elapsed since the first learning is indicated at the top of each figure. The teacher data at 0:06:04 are used for the second measurement of the recognition rate. The teacher data at 0:11:00 are used for the third measurement of the recognition rate. The motions of each class are rest, grasp, open, three finger pinch, wrist flexion, wrist extension, wrist pronation and wrist supination, starting from the number 0.

Because there were differences in the participants' proficiency rates in this experiment, which resulted in differences in the average recognition rates, the participants' proficiency rates were categorized into top, medium, and low categories based on their recognition rates before adaptive learning, and the results were compared. The recognition rates and categorization are listed in Table.4.5. Ryu Kato confirmed that there is a correlation between the proficiency level and motion recognition rate (Ryu Kato 2008).

Table.4.5: Average of the recognition rate for each participant before adaptive learning.

Participant	Recognition rate (%)	Category
A	85.1	Top
B	77.2	Middle
C	67.4	Lower
D	66.4	Lower
E	76.9	Middle
F	88.8	Top

Results of the top two participants

Fig.4.24 shows the average of the recognition rates of the top two participants. Fig.4.25 shows the number of stable motions of the top two participants when the recognition rate of the stable controllable motions was above 80.0 %.

The results showed that the recognition rate increased by an average of 5.6 % after 2 min from before adaptive learning, and decreased by an average of 0.21 % after 4 min. In the comparison between "origin" and "optimized," "optimized" was on average 8.3 % larger than "origin" at 2 min, whereas "optimized" was significantly larger than "origin" at 4 min by 5.6 % on average. The average recognition rate of "optimized" was 92.5 % after 2 min of adaptive learning and 86.7 % after 4 min of adaptive learning.

There was no significant difference in the number of stable motions. The number of stable motions increased by an average of 2 motions after 2 min of adaptive learning but decreased by 0.5 motions after 4 min of adaptive learning. In the comparison between "origin" and "optimized", "optimized" had an average of 1.5 more motions than "origin" at 2 min, whereas "optimized" had an average of 0.5 more motions than "origin" at 4 min.

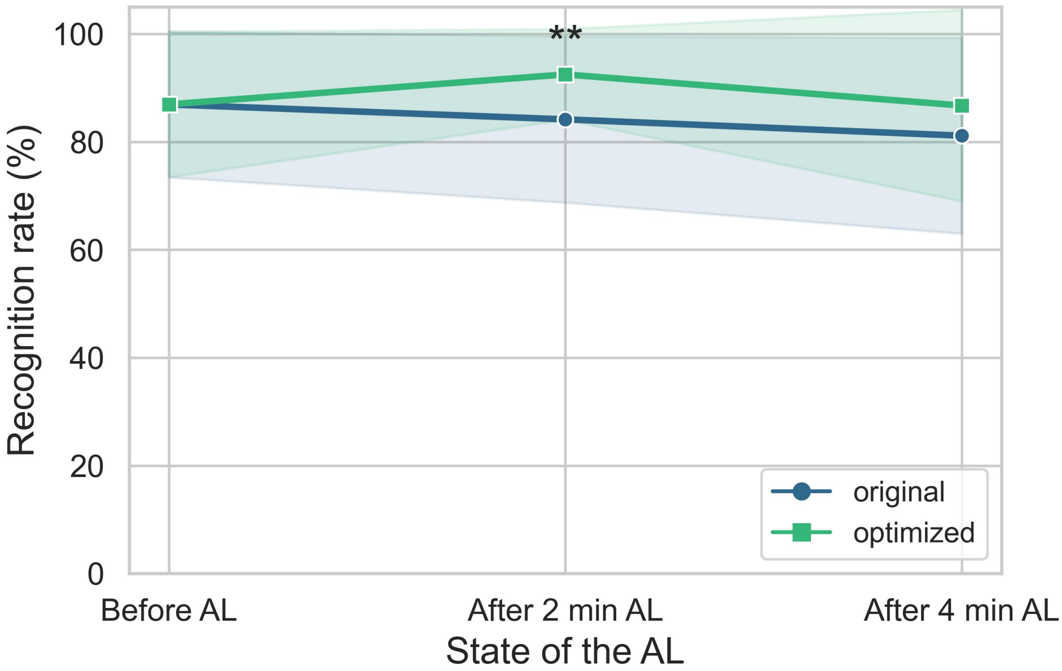

Fig.4.24: Trends in the average recognition rate for each motion for the top two participants.

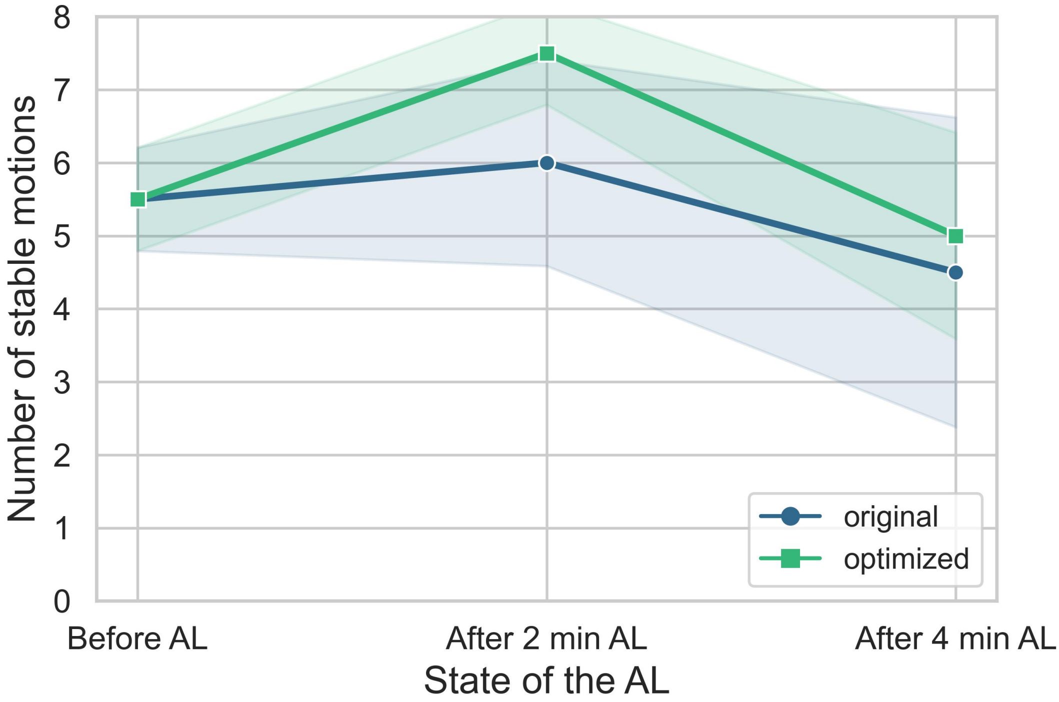

Fig.4.25: Trends in the number of stable motions of the top two participants.

Results of the middle two participants

The transition of the average of the recognition rate of the middle two participants is shown in Fig.4.26. Fig.4.27 shows the number of stable motions of the middle two participants when the recognition rate of the motion that could be controlled stably was over 80.0 %.

The results show that the recognition rate increased by an average of 7.0 % after 2 min from before adaptive learning. Four minutes later, the recognition rate increased significantly by an average of 4.7 %. In the comparison between "origin" and "optimized," "optimized" was significantly larger than "origin" by an average of 5.9 % after 2 min, whereas "optimized" was significantly larger than "origin" by an average of 5.6 % after 4 min. The average recognition rate of "optimized" was 84.0 % after 2 min of adaptive learning and 81.7 % after 4 min of adaptive learning.

There was no significant difference in the number of stable motions. The average number of motions increased by 1 after 2 min of adaptive learning, but decreased by an average of 0.5 after 4 min of adaptive learning. In the comparison between "origin" and "optimized", "optimized" had an average of 1 more motion than "origin" at 2 min, but there was no difference between "optimized" and "origin" at 4 min.

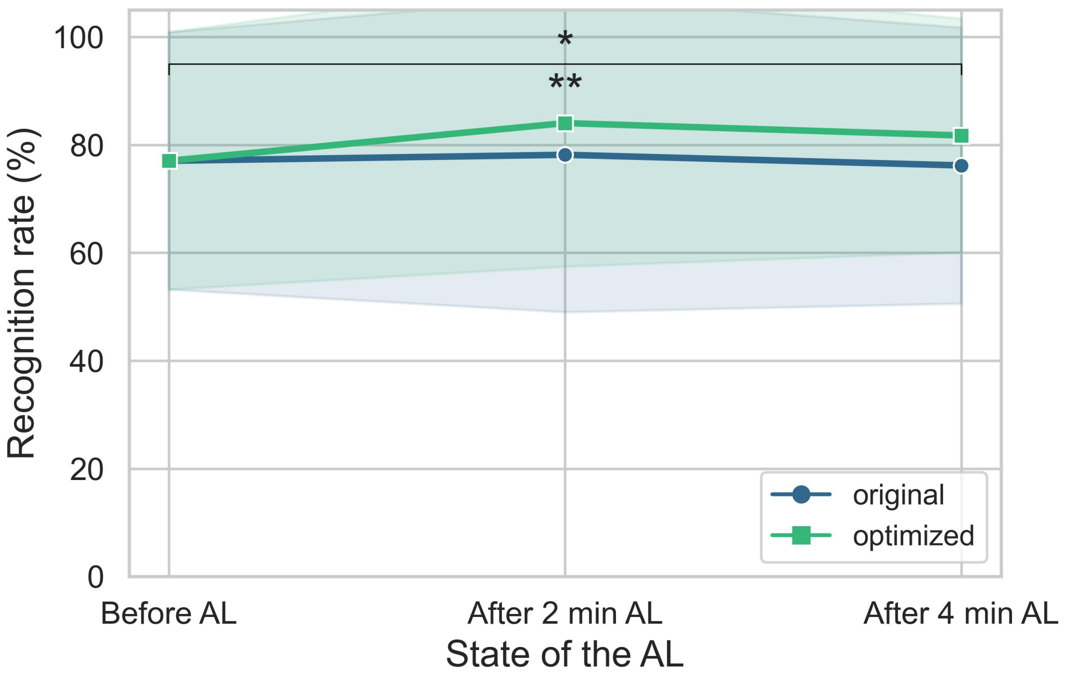

Fig.4.26: Trends in the average recognition rate for each motion for the middle two participants.

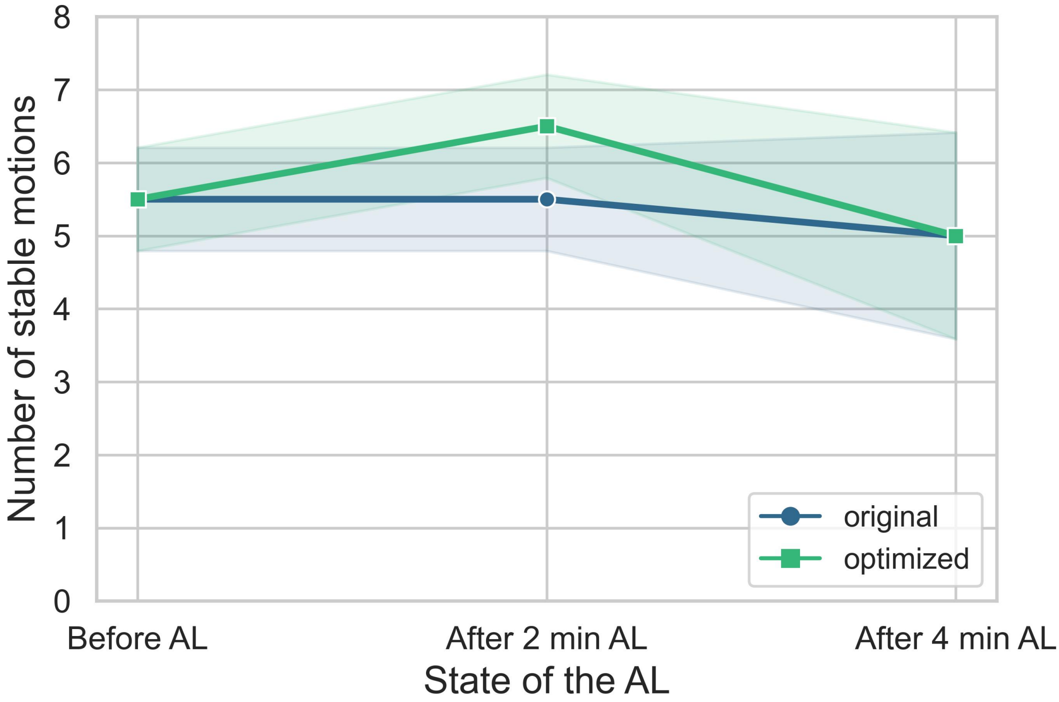

Fig.4.27: Trends in the number of stable motions of the middle two participants.

Results of the lower two participants

. The average of the recognition rate of the lower two participants is shown in Fig.4.28. Fig.4.29 shows the number of stable motions for the lower two participants when the recognition rate of the motion that could be controlled stably was above 80.0 %.

The results show that the recognition rate increased by an average of 7.1 % after 2 min from the pre-adaptive learning period, and by an average of 7.5 % after 4 min. In the comparison between "origin" and "optimized," "optimized" was on average 8.1 % larger than "origin" at 2 min, whereas it was significantly larger than "origin" at 4 min by an average of 11.0 %. The average recognition rate of "optimized" was 74.0 % after 2 min of adaptive learning and 74.4 % after 4 min of adaptive learning.

There was no significant difference in the number of stable motions. There was no change from before to after 2 min of adaptive learning, but there was an increase of 0.5 motion after 4 min of adaptive learning. There was no difference between "optimized" and "origin" at 2 min, but "optimized" had one more motion than "origin" at 4 min.

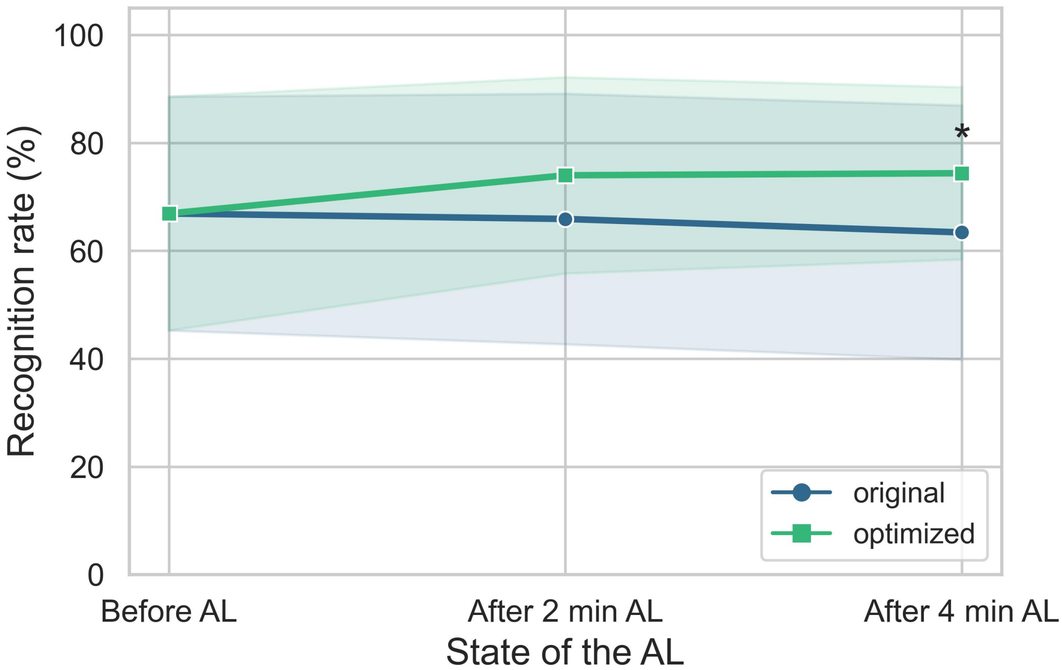

Fig.4.28: Trends in the average recognition rate for each motion for the lower two participants.

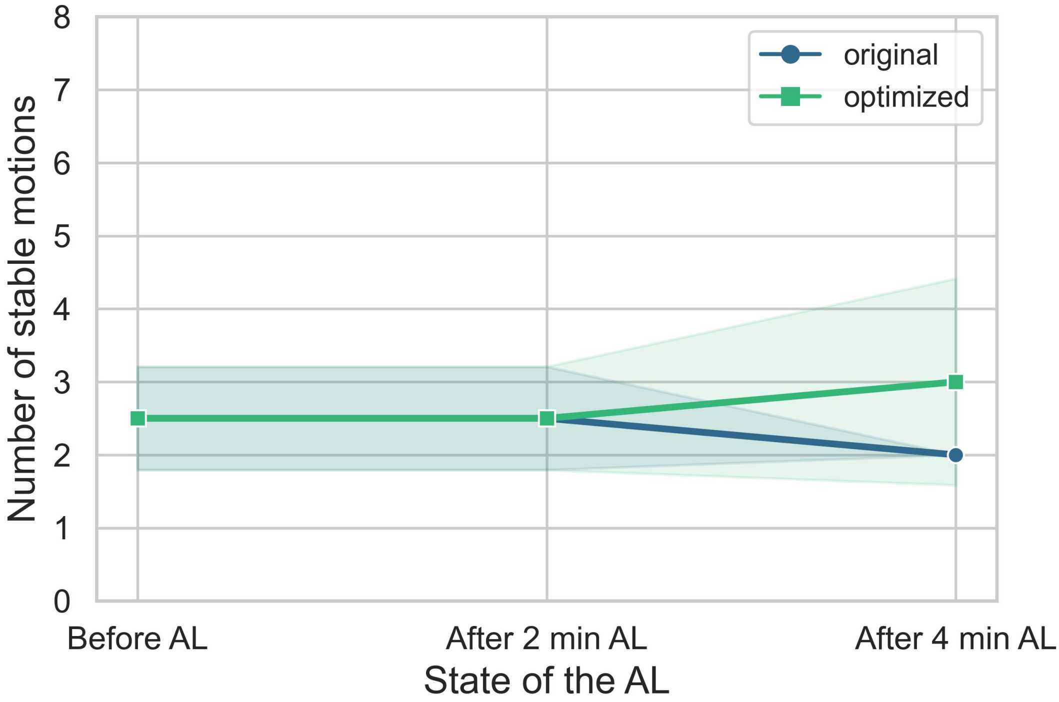

Fig.4.29: Trends in the number of stable motions of the lower two participants.

4.7.3 Discussion

Teacher data

Fig.4.23 shows that the overlapping teacher data that initially overlapped were gradually removed. In addition, the size of the clusters tended to decrease. Because participant A was a highly proficient participant, as presented in Table.1, the adaptation progressed in such a way that the ideal teacher data (low within-class variance, high between-class variance, and boundary data eliminated) was obtained.

To explore in more detail how differences in proficiency affect adaptation, the adaptation results of Participant A, who had high proficiency, and Participant C, who had low proficiency, were compared by examining the differences in their teacher data before and after adaptation. The comparison of the adaptation results for each participant is shown in Fig.4.30 and Fig.4.31. First, there is a significant difference in the teacher data before adaptation. While Participant A's teacher data show some overlap and noise, a certain degree of cluster separation is evident. In contrast, Participant C's teacher data has high separation in some clusters, but clusters 3, 2, and 7 show considerable overlap.

This leads to observable differences in the improvement trend of teacher data through adaptation. Participant A's teacher data, as shown in Fig.4.30, progresses with adaptation by removing teacher data between clusters, resulting in increased inter-class variance and reduced intra-class variance. However, Participant C's teacher data in Fig.4.31 shows some overlapping teacher data being removed or moving, with some progress towards ideal teacher data; however, the overlapping in clusters 3, 2, and 7 could not be completely resolved. This indicates that to effectively utilize the functionality of a time variation adaptive system, it is necessary to train for muscle contraction pattern separation to avoid overlap in the teacher data. Users with a higher proficiency level, who can separate muscle contraction patterns to some extent, are likely to utilize the functions of a time variation adaptive system more effectively in cases of narrow range time variation.

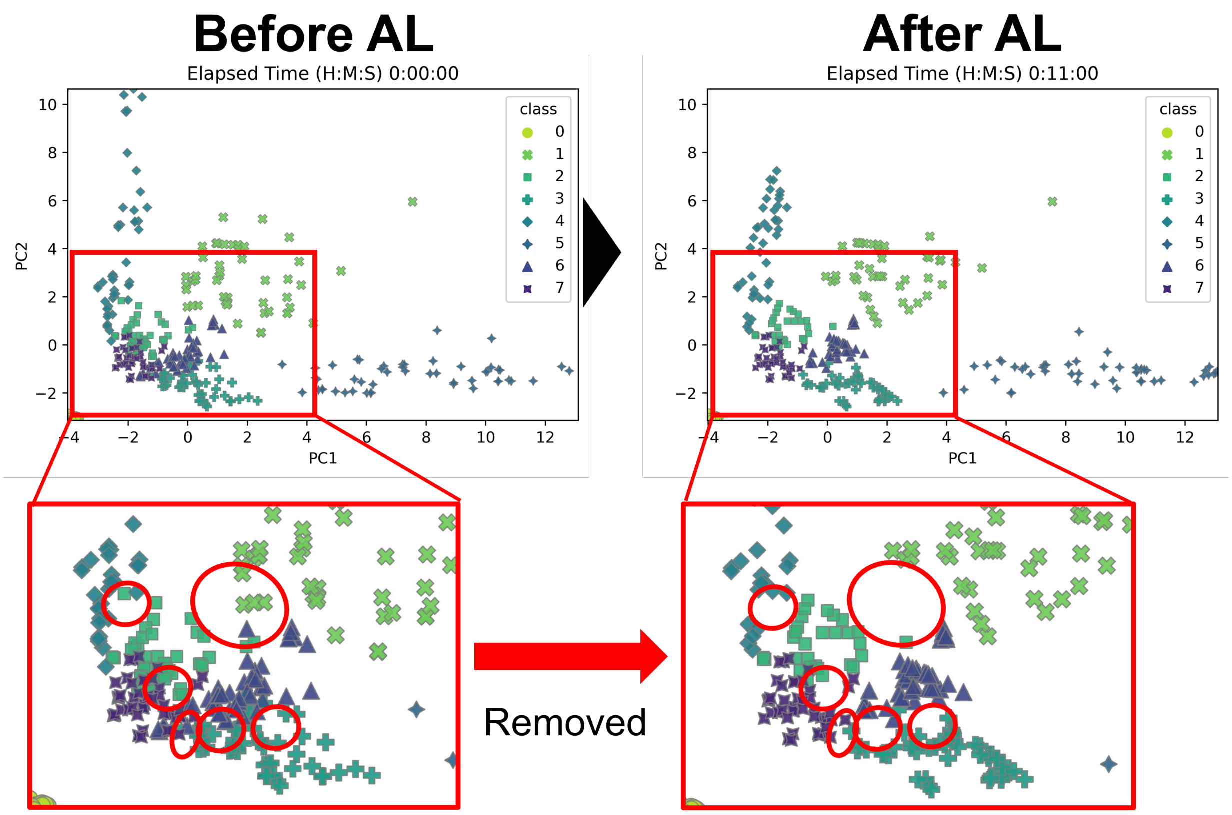

Fig.4.30: Differences in teacher data before and after adaptation for Participant A with high proficiency.

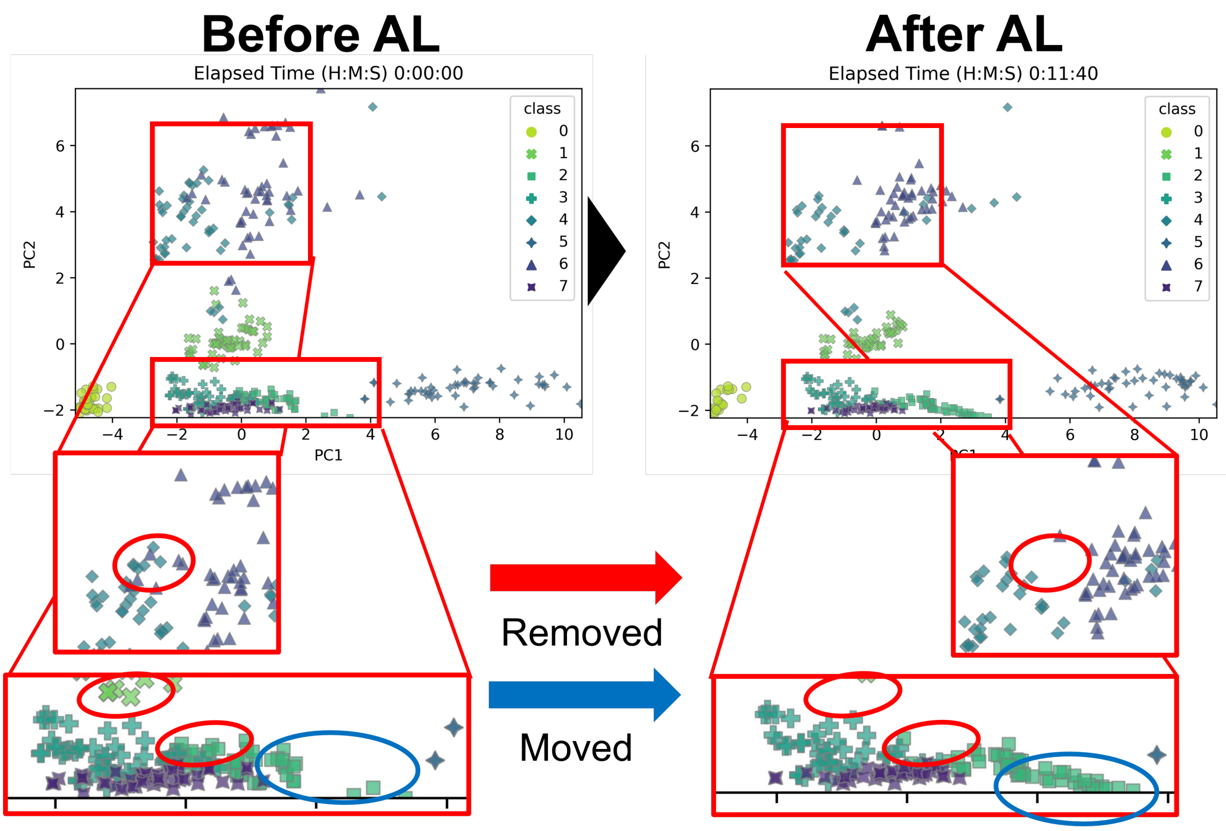

Fig.4.31: Differences in teacher data before and after adaptation for Participant C with low proficiency.

Parameters according to proficiency

As shown in Fig.4.29, the two participants with the lowest proficiency level improved only up to three stable motions. This is because of the low ability to separate muscle contraction patterns. To increase the number of stable motions, it is necessary to improve the ability to separate muscle contraction patterns through training. For such users with low proficiency, it is believed that operability can be further improved by adapting to changes in the muscle contraction force using the parameters used in Experiments 1-1 and 1-2.

Visual feedback of the feature space to the user

This study mainly provided visual feedback to the user of the motion of the MPH during adaptive learning to show how the current muscle contraction pattern is recognized by the control system. However, during adaptive learning, the user did not receive feedback on the state of competition in the feature space, making it difficult to present a new appropriate muscle contraction pattern to the user. If the user receives visual feedback of the contention state of the feature space, he or she can consciously explore muscle contraction patterns that are easy to recognize. For example, the wrist flexion and wrist extension clusters at the edge of Fig.4.23 can be moved to a position with lower competition by increasing the muscle contraction force and decreasing the competition in the center. Therefore, combining feature space feedback and adaptive learning is one of my future tasks.

4.8 Conclusion

In this chapter, a method to address the reduction in the control stability of MPHs caused by time variations in the EMG was developed and evaluated.

Section 4.2 described the time-variation in the EMG, which is the cause of the recognition instability. Referring to previous studies, the time variability in the EMG was classified into three types based on the speed of change.

Section 4.3 described conventional methods for managing time variation in EMG. Learning, self-organization, and adaptation were listed as the approaches to manage time variation, and the approach to apply to each conventional method was discussed.

Section 4.4 described the method that tracks the time variation in the EMG developed in this study, which was based on the frequency of the data input.

Section 4.4.4 described the myoelectric control system and application used in the experiments in this study.

In Section 4.5, the results and discussion of the experiment with non-disabled participants for a wide range of time variations were described.

In Section 4.6, the results and discussion of the experiment with a person with upper limb deficiencies for a wide range of time variations were described.

In Section 4.7, the results and discussion of the experiment with non-disabled participants for a narrow range of time variations were described.

Chapter 5 Feature direction: Realization and verification of adaptive grasping with multi-DOF MPHs equipped with touch sensors

5.1 Introduction

In this chapter, combining evolutionary robotics with MPH control has enabled adaptive object grasping according to myoelectric signals. The model introduced is capable of anticipating suitable joint movements, drawing insights from the data acquired through touch sensors that monitor the contact state between the hand and object grasped.

As mentioned in Section 2.9.2, even when using pattern recognition control, there is a limit to the number of movements available to the user. With our proposed method, as shown in Fig.5.1, by allocating specific movements to adaptive grasping within pattern recognition control, users can avoid having to differentiate grasping movements for different objects, thus reducing the control burden.

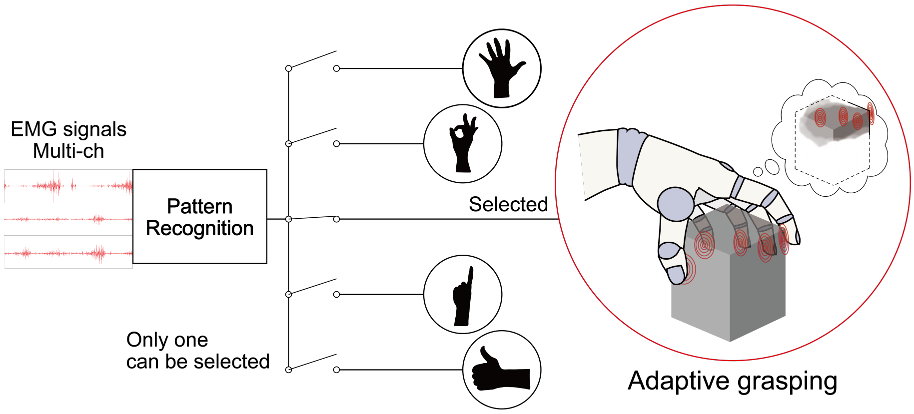

Fig.5.1: Illustration of application method of our proposed approach in pattern recognition control.

However, methods for achieving adaptive grasping based on the contact state of the hand and grasped objects have not been realized in the field of MPHs. Moreover, when learning a controller to achieve adaptive grasping based on hand–object contact interactions, the design of the hand becomes a crucial element. Yet, the effective design requirements for such a method have not been verified.

The aim of this chapter is to confirm the feasibility of achieving adaptive grasping to objects using an ideal multi-DOF prosthetic hand with this proposed method and to verify the hidden design requirements necessary for this method through physics simulation.

The reason for verifying with physics simulation is that developing a hand with similar DOFs as a human hand would involve significant time and financial costs. By verifying through physics simulation beforehand, the cost of developing the hand can be reduced.

Section 5.2, describes the research on the two grasping motion taxonomies that are often used as references for the design of electric prosthetic hands.

Section 5.3 describes the hardware and software approaches to research on complementing the human grasping function, respectively.

Section 5.4 describes the proposed method.

Section 5.5 describes the experiment to evaluate the efficacy and adaptability of the proposed approach and two comparative evaluations.

Section 5.6, describes the results of the experiments and comparisons.

Finally, Section 5.7 discusses the results of the verification.

5.2 Previous research: Grasping motion taxonomy

In the research of multi-DOF prosthetic and robotic hands, a comparison with grasping motion classification is one of the indices to design them and to evaluate their realizable motion patterns. Grasping motion classification is based on grasping motions under various environments and conditions, and most of them are extensions of the two major grasping motion classifications, power grasp and precision grasp, by Napier (Napier 1956). This paper presents the research on the two grasping motion taxonomies that are often used as references for the design of electric prosthetic hands.

5.2.1 Grasping motion taxonomy by Cutkosky

Cutkosky extended Napier's grasp classification (Napier 1956) and classified grasping motions in manufacturing (Cutkosky 1989). The grasping taxonomy was derived from Napier's classification of the grip strength and precision grasping and was classified into 16 types.

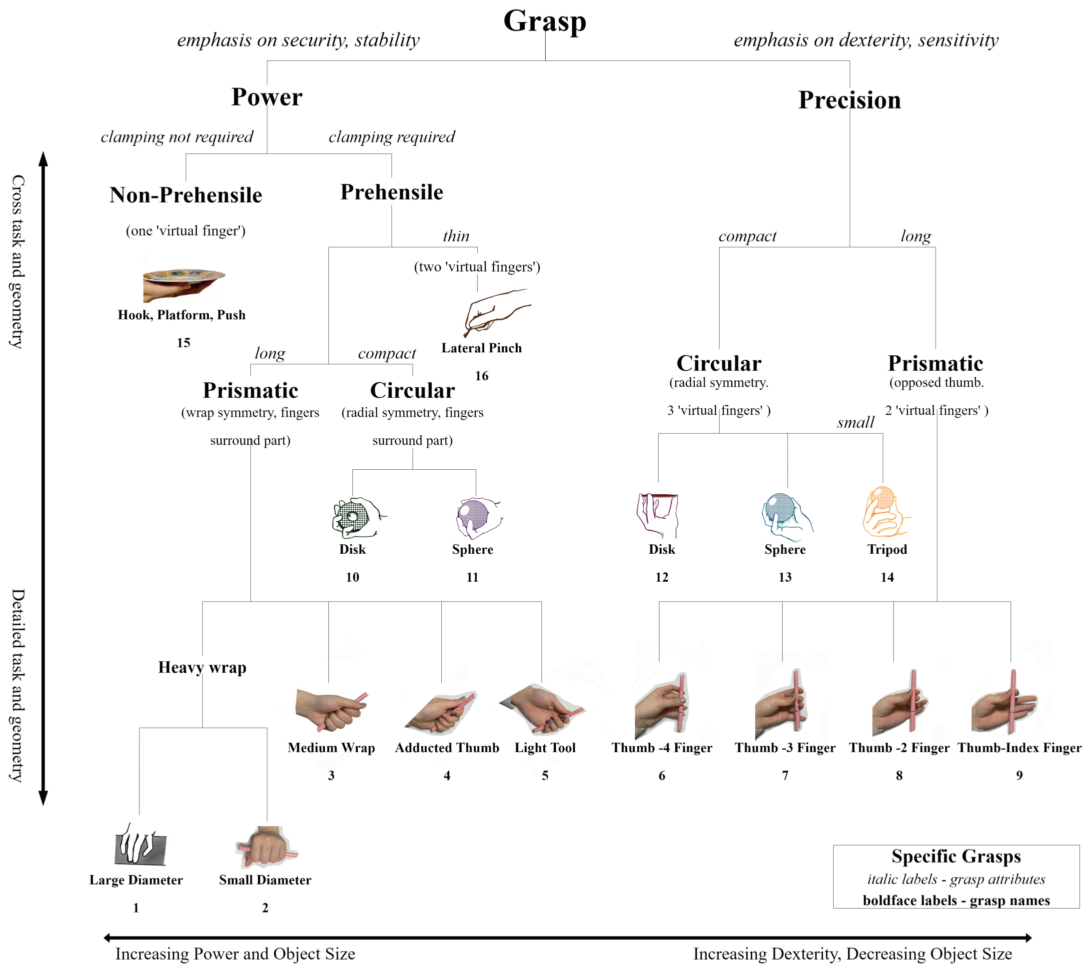

Fig.5.2: Grasping motion taxonomy by Cutkosky. Prepared with reference to (Cutkosky 1989).

5.2.2 Grasping motion taxonomy by KAMAKURA et al.

KAMAKURA et al. classified grasping motions into 14 types for practical purposes such as promoting the differentiation of hand movement patterns in therapeutic situations and training the use of tools (KAMAKURA et al. 1978).

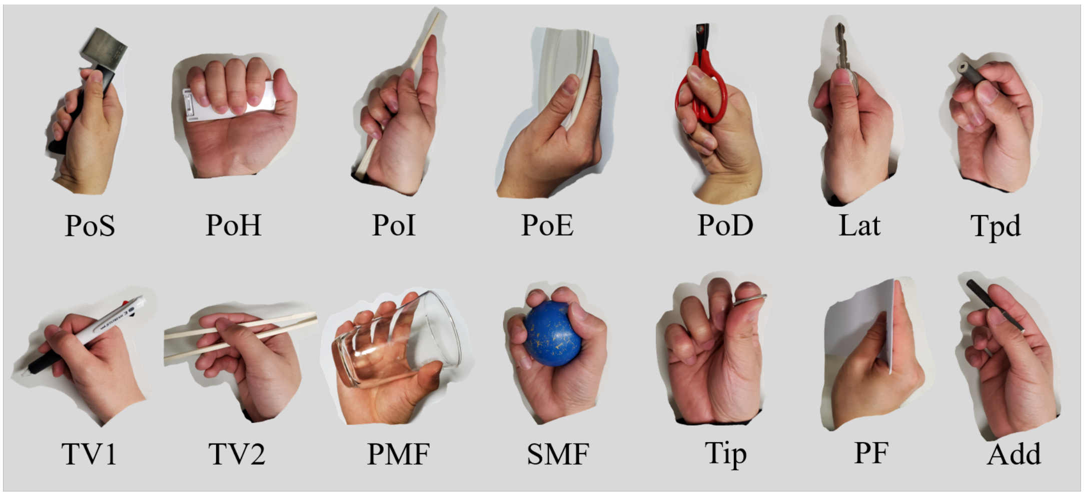

Fig.5.3: Grasping motion taxonomy by KAMAKURA et al. Prepared with reference to (KAMAKURA et al. 1978).

5.3 Previous research: Research on interpolation of the human adaptive grasping function

The control method based on pattern recognition necessitates the user to choose a grasping style that is tailored to the object, a process that is often subconscious for humans, leading to a decrease in the ease of use. Essentially, to achieve skilled manipulation (software) with the mechanical components of the fingers (hardware), an exploration into the integration of these two components is essential. Nonetheless, investigations into the incorporation of human adaptive grasping capabilities have been carried out separately for software and hardware.

However, studies using robots on human grasping functions have explored approaches integrating both software and hardware.

This study describes the hardware and software approaches to research on complementing the prosthetic hand's grasping function. Finally, we explain an approach that integrates software and hardware using robots.

5.3.1 Hardware-based approach

Here, we focus on hardware and describe related research on achieving adaptive grasping to object shapes using complex multi-DOF hands.

Adaptive grasp

Fukaya and Ogasawara used a robot hand with a cooperative link mechanism (Fukaya and Ogasawara 2017) to realize 11 out of 14 grasping types by (KAMAKURA et al. 1978). Each finger is connected by a link, and the power from one motor is branched and transmitted to five fingers. As a result, each finger automatically maintains a balance of contact forces. This cooperative link mechanism enables the hand to bend to fit the shape of the object to be grasped and perform adaptive grasping without controlling each joint.

When applied to a prosthetic hand, the above adaptive grasp is useful because it can adapt to the shape of the object with only simple control of the grasping and opening motions and a small number of motors. However, while the underactuated hand can adapt to the object and grasp it, it has the disadvantage that it cannot precisely manipulate the object, or gesture without interacting with the object, which limits the hardware. Chen and Xiong pointed out that adaptive grasping with an underdriven robotic hand tends to miss to grasp the object (Chen and Xiong 2016).

5.3.2 Software-based approach

Here, we focus on software and describe related research on achieving adaptive grasping to object shapes using complex multi-DOF hands.

Optimization of grasping motion by image recognition

Methods combining image recognition have been studied to interpolate human adaptive grasping functions (Došen et al. 2010; Ghazaei et al. 2017). Ghazaei et al. used a webcam attached to an MPH to pre-determine grasping motions from images captured before grasping, resulting in four different grasping motions depending on the object shape (Ghazaei et al. 2017). However, Ghazaei et al. pre-determined the correspondence between the grasping shape and grasping motion from the image data only. In reality, the same type of object has different sizes and orientations, hence the grasping motion cannot be adequately determined from the image data alone.

5.3.3 Integrated approach of hardware and software

Optimization of grasping motion by tactile sensors

Tada, Hosoda, and Asada constructed a robot hand system that combines a visual sensor and a human-like flexible finger with multiple tactile sensors. The robot hand was made to lift an object repeatedly, and the linear Neural Network (NN) acquired the grasping behavior for lifting the object based on the information from the visual and tactile sensors using Hebbian learning (Tada, Hosoda, and Asada 2005). The NN learns the relationship between the tactile and visual sensors, and using this NN, it is possible to control the grasping force only with the input from the tactile sensor after learning.

Gianluca Massera, Cangelosi, and Stefano Nolfi used a robot arm that imitated a human hand in a physics simulation to perform reaching and grasping motions (Gianluca Massera, Cangelosi, and Stefano Nolfi 2007). The robot arm was controlled by a Continuous Time Recurrent Non-linear Network (CTRNN) with 16 motors on the arm and 2 motors controlling the opening and closing of the hand, respectively. The robot controller was optimized by evolutionary computation to grasp a sphere and a cylinder.

Tuci, Massera, and Nolfi used a robot arm similar to the one used by Gianluca Massera, Cangelosi, and Stefano Nolfi to perform the task of classifying spheres and ellipsoids using active perception. Active perception is a perception method in which the robot acts on its own to gather information to compensate for missing information. In this method, the hand of the robot arm is used to roll an object in an enveloping manner, and the object is classified based on the position at which it is rolled (Tuci, Massera, and Nolfi 2009).

5.3.4 Summary of previous research

In Sections 5.3.3 and 5.3.2, methods for achieving adaptive grasping to object shapes using complex multi-DOF hands have been described, focusing on both hardware and software approaches. Regarding the hardware approach, owing to issues such as the ease of dropping grasped objects and constraints on hardware, it is difficult to operate it in the manner assumed in this study, hence it is not used in the present research. The software approach, which uses image recognition, has problems such as an insufficient response to differences in the object size or orientation. The integrated approach of software and hardware enables tasks such as reaching movements to objects, grasping, and object classification by learning the correlation between the object contact, sensor data, and motor control.

Based on the above, this study aims to apply the integrated approach of software and hardware to MPHs.

5.4 Proposed Method: Learning Myoelectric Control and Adaptive Object Grasping via Evolutionary Computation

In the pattern recognition control method, it was necessary to use different muscle contraction patterns for different hand movements. However, as described in Section 2.9.2, this is a burden for people with upper limb deficiencies. In particular, it is difficult to select a grasping posture that adapts to the object or a stable grasping method that does not drop the object. Existing approaches to object grasping by evolutionary robotics allow grasping and classification of various types of objects using a robotic hand (Floreano and Stefano Nolfi 2007; Gianluca Massera, Cangelosi, and Stefano Nolfi 2007; Tuci, Massera, and Nolfi 2009; Bongard 2010). In this framework, the robot hand interacts with the object to be grasped, and inputs from the robot hand's touch sensors are mapped to outputs from the motors that control the robot hand's joints. This mechanism is based on the embodiment concept proposed by Pfeifer and Bongard (Pfeifer and Bongard 2006). None of the existing research methods for object grasping based on evolutionary robotics can control the open/close state of the hand by myoelectricity.

If adaptive grasping can be realized by predicting an appropriate scheme for operating the joints based on the contact state information between the hand and grasped object obtained from the touch sensor, and if the voluntary opening and closing of the joints can be controlled by myoelectricity, appropriate grasping can be realized for various objects even with simple myoelectric input. Fig.5.4 is an illustrative diagram of the approach in this study. Referring to existing research, the parameters of the robot hand controller are optimized to improve task performance through evolutionary computation by predicting joint motion with the robot hand repeatedly performing object grasping tasks. In particular, an MPH control learning environment is added using teacher data from grasping and opening motions to the conventional pickup learning environment for autonomous robots. This enables the establishment of an MPH control method that enables adaptive grasping of objects while allowing the hand to open and grasp arbitrarily.

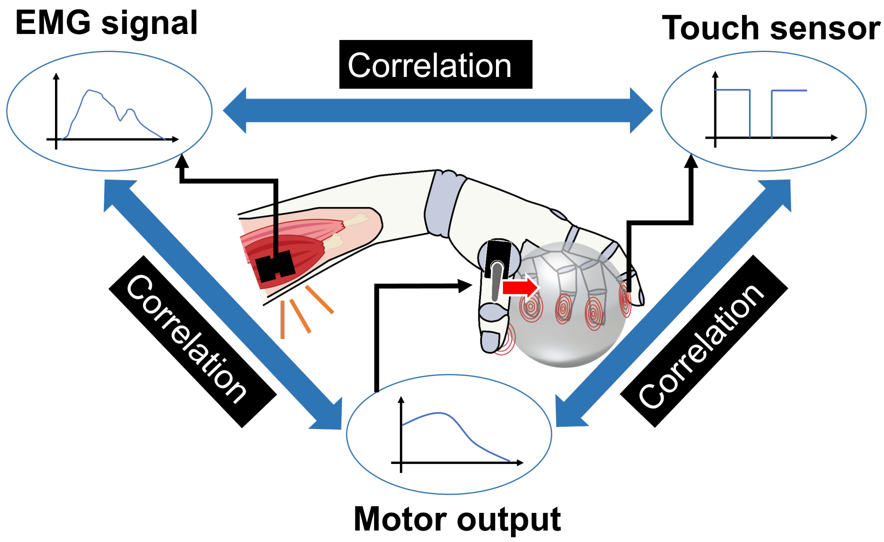

Fig.5.4: Illustrative diagram of the approach in this study.

An overview of the proposed method is shown in Fig.5.5. In the proposed method, evolutionary computation is used to optimize the parameters in parallel. Therefore, if the number of individuals in the population is P, the set of vectors and scalars are represented by bold and unbold capital letters (e.g., $\boldsymbol{W} = (\boldsymbol{w}_1, \boldsymbol{w}_2, ...\boldsymbol{w}_p, ..., \boldsymbol{w}_P))$. For the t-th variable, vector, or set of variables, the parameter is denoted by (t) (e.g. $\boldsymbol{x}(t)$). Every set represents a population.

A schematic representation of the methodology is shown in Figure 5.5. The parameters are optimized in parallel through evolutionary computation. Let P denote the total count of individuals in the population. The bold and non-bold uppercase letters indicate sets of vectors and scalars, respectively (e.g., $\boldsymbol{W} = (\boldsymbol{w}_1, \boldsymbol{w}_2, ...\boldsymbol{w}_p, ..., \boldsymbol{w}_P))$. For a parameter, a variable, a vector, or a set of variables in the t-th step, the notation (t) is used (e.g., $\boldsymbol{x}(t)$). All the considered sets represent the population.

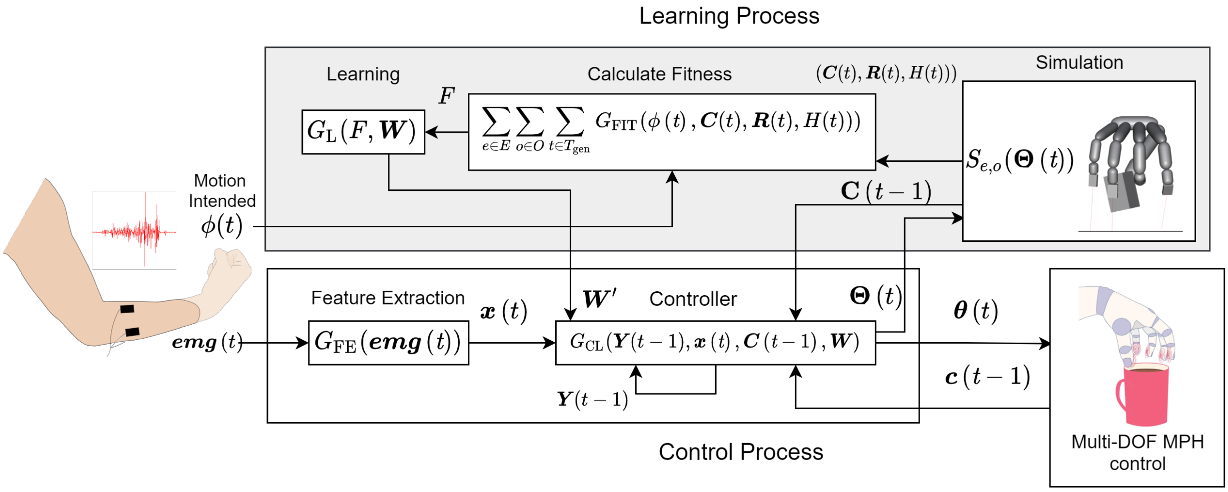

Fig.5.5: Overview of the proposed method. $\boldsymbol{x}(t)$ defines the feature vector at time t. The set of vectors of the distance sensor for each individual are represented by $\boldsymbol{R}(t)$, whereas $\boldsymbol{C}(t)$ denotes the set of the individual touch sensor input vectors $\boldsymbol{c}(t)$. The height sensor inputs for each individual are $H(t)$, and $\boldsymbol{\Theta}(t)$ represents the set of vectors indicating the target joint angles for MPH control. E is the set of environments e of the simulation. O is the set of objects o used in the simulation. T_{gen} is the number of steps for which the simulation is performed. The controllers' parameter vectors for each individual are grouped in the set $\boldsymbol{W}$, with fitness values calculated using G_{FIT} contained in set F. The updated parameter vectors derived from $\boldsymbol{W}$ are represented by $\boldsymbol{W}'$. This figure is cited from (Kuroda et al. 2022).

This method involves two processes: (a) learning process and (b) control process.

During the control process, the EMG vector at time t, denoted as $\boldsymbol{emg}(t)$, is measured and the feature vector $\boldsymbol{x}(t)$ is derived by applying the feature extraction function G_{FE} to $\boldsymbol{emg}(t)$. If the p-th individual achieves the highest fitness after the learning process, the controller generates the target joint angles vector $\boldsymbol{\theta}_p(t)$. This is achieved by calculating the neurons vector of the p-th controller $\boldsymbol{y}_p(t-1)$, $\boldsymbol{x}(t)$, touch sensors vector $\boldsymbol{c}(t-1)$, and the parameters of the p-th controller $\boldsymbol{w}_p$.

In the learning process, the controller G_{L} produces the set of target vectors for the individuals, calculated from the neurons vector set $\boldsymbol{Y}(t-1)$, $\boldsymbol{x}(t)$, the individual's touch sensors vector set $\boldsymbol{C}(t-1)$, and the controllers' parameter vector set $\boldsymbol{W}$. The function G_{FIT} for calculating fitness receives the motion intent $\phi(t)$, touch sensors vector set $\boldsymbol{C}(t)$, distance sensors vector set $\boldsymbol{R}(t)$, and height sensors set $H(t)$, each sourced from $S_{e,o}$ at every step.

When the T_{gen} step simulation concludes for all given environments E and objects O, the set of fitness values F is obtained. The learning function G_{L} updates $\boldsymbol{W}$ based on F.

5.4.1 Morphology

In this study, a 3D hand model on a physics simulation is used for training to validate the proposed method. The objective of this study is to confirm the feasibility of achieving adaptive grasping to objects using an ideal multi-DOF prosthetic hand with the proposed method and to pre-emptively verify the hidden design requirements necessary for this method through physics simulation. The reason for utilizing physics simulation for verification is that developing a hand with similar DOFs as a human hand would involve significant time and financial costs. By conducting preliminary verification through physics simulation, the cost of developing the hand can be reduced. The shapes of the 3D models are described in detail in Section 5.5.

This section describes the morphology of the hand required by the proposed method.

5.4.2 Sensory organs

EMG sensor

Let $\boldsymbol{emg}(t)$ be the vector of the myoelectric potentials measured from the EMG sensor of a user. Subsequently, the feature extraction function G_{FE} is applied to this vector and this vector is translated to the feature vector $\boldsymbol{x}(t)$, as shown in Eq. (5.4-1).

$$\boldsymbol{x}(t) = G_{\mathrm{FE}}(\boldsymbol{emg}(t)) \; . \tag{5.4-1}$$

Touch sensor

The hands need to have touch sensors to sense the objects to be grasped. The input of the i-th touch sensor to the controller $c_i(t)$ can be defined as follows:

$$c_i\left(t\right) = \begin{cases} 1. & \text{if the part touches the floor or the objects} \\ 0. & \text{otherwise} \end{cases} \tag{5.4-2}$$

Here, let $\boldsymbol{C}(t) = (\boldsymbol{c}_1(t), ..., \boldsymbol{c}_p(t), ..., \boldsymbol{c}_{|C(t)|}(t))$ be the set of individuals in $\boldsymbol{c}_p(t) \in \mathbb{R}^{N_c}$, which is the vector of the touch sensor inputs to the p-th controller. The number of and placement of sensors are described in Section 5.5.

Distance sensor

The hands are equipped with distance sensors in each fingertip to measure the distance to an object when the ray of light from the fingertip strikes it. The value of the i-th distance sensor at the t-th steps can be determined as

$$r_i\left(t\right) = 1 - \frac{d_i(t)}{d_{\max}}. \tag{5.4-3}$$

$d_i(t)$ represents the distance between the sensor and objects intercepting the light ray. $d_{\max}$ denotes the farthest distance that can be measured. This equation is employed to scale the distance sensor's reading to a 0 to 1 range. In addition, let $\boldsymbol{R}(t) = (\boldsymbol{r}_1(t), ..., \boldsymbol{r}_p(t), ..., \boldsymbol{r}_{|R(t)|}(t))$ be the set of individual vectors $\boldsymbol{r}_p(t) \in \mathbb{R}^{N_r}$, each representing the distance sensor inputs for the p-th controller. It should be noted that distance sensors are exclusively utilized for fitness computation and are not part of the controller input.

Object height sensor

Objects targeted for grasping are equipped with height sensors. $h_p(t)$ is the height between the height sensor placed at the center of the object to be grasped by the p-th hand and the floor. The compiled readings from the height sensors are represented by $H(t) = (h_1(t), ..., h_p(t), .., h_{|H(t)|}(t))$. These sensors play a role exclusively in fitness calculation, not in controller input.

5.4.3 Controller

An RNN was used as a controller. The RNN outputs target angles of the motor through a hidden layer. Each neuron in the hidden and output layers of the RNN is updated as follows:

$$y_i\left(t\right) = \tanh\left(y_i\left(t-1\right) + \tau \sum_{j \in J} w_{ij} y_i\left(t-1\right)\right) . \tag{5.4-4}$$

In this context, $y_i(t)$ signifies the output from the neuron i at step t., while τ represents the RNN's learning rate, preset to 1 for the sake of simplicity. The synaptic weight connecting neurons j and i is denoted by w_{ji}, and J signifies the neuron set providing input to neuron i. The weight vectors in the p-th controller are grouped in individual sets $\boldsymbol{w}_p$, collectively represented by $\boldsymbol{W}$. The RNN, comprising input, hidden, and output layers, is encapsulated by function G_{RNN}, delineated for each individual. The output layer neuron vectors $\boldsymbol{y}_p(t)$ for each individual at time t, denoted by $\boldsymbol{Y}(t) = (\boldsymbol{y}_1(t), ..., \boldsymbol{y}_p(t), ..., \boldsymbol{y}_{|Y(t)|}(t))$, is defined as follows:

$$\boldsymbol{Y}(t) = G_{\mathrm{RNN}}\left(\boldsymbol{Y}(t-1), \boldsymbol{x}(t), \boldsymbol{C}(t-1), \boldsymbol{W}\right) . \tag{5.4-5}$$

$\boldsymbol{Y}(t)$ is transformed into $\boldsymbol{\Theta}(t) = (\boldsymbol{\theta}_1(t), ..., \boldsymbol{\theta}_p(t), ..., \boldsymbol{\theta}_{|\boldsymbol{\Theta}(t)|}(t))$, which is the set of target angle vectors for the individuals, $\boldsymbol{\theta}_p(t) \in \mathbb{R}^{N_\theta}$, by applying the function G_{TA} to derive the target angles.

$$\boldsymbol{\Theta}(t) = G_{\mathrm{TA}}(\boldsymbol{Y}(t)) \tag{5.4-6}$$

The controller derives the target values of the joint angles from the input values from the sensors, as indicated in Eqs. 5.4-5 and 5.4-6, and it is represented by the function G_{CL}.

$$\boldsymbol{\Theta}(t) = G_{\mathrm{CL}}\left(\boldsymbol{Y}(t-1), \boldsymbol{x}(t), C_(t-1), \boldsymbol{W}\right) . \tag{5.4-7}$$

5.4.4 Fitness functions and tasks

Besides the autonomous robots' learning environment for mastering pickup tasks as highlighted in earlier works Gianluca Massera, Cangelosi, and Stefano Nolfi 2007Tuci, Massera, and Nolfi 2009Bongard 2010, an environment is added for MPH control learning using the teacher data of grasping and opening motions to enable the adaptive grasping of objects and the realization of opening and closing motions at arbitrary times. Essentially, environment 1 is introduced for the mastery of myoelectric control and environment 2 for object grasping skills acquisition. Each setting undergoes the T_{gen}-step procedure where, at every step, the controller's performance is assessed through a fitness function. A higher fitness corresponds to a higher performance of the controller.

Let $S_{e,o}$ be a function that represents the computation in the simulation for the e-th environment involving object o. When the joint angle's target value vector of the p-th individual is fed into the system, the touch and distance sensor vectors and the readings from the height sensor for that individual are output. When a set of joint angle target values is input, the corresponding sets of touch, distance, and height sensor readings for the individual are produced, as follows:

$$S_{e,o}(\boldsymbol{\theta}_p(t)) = (\boldsymbol{c}_p(t), \boldsymbol{r}_p(t), h_p(t)), \tag{5.4-8}$$

$$S_{e,o}(\boldsymbol{\Theta}(t)) = (\boldsymbol{C}(t), \boldsymbol{R}(t), H(t)). \tag{5.4-9}$$

In the context of environment 2, the learning of various types of grasping objects, individual simulations for each object are executed and their fitness scores are totaled. Here, O denotes the set of objects designated for learning, with o representing an element within set O. In environment 1, there is no object to be learned. Consequently, o is $\emptyset$, and the subscript o of $S_{1,o}$ is ignored to yield S_1. If o is not $\emptyset$ in environment 1, $S_{1,o}$ does not exist.

Environment 1

In this environment, learning is focused on the motions of grasping and opening, guided by myoelectric signals. The cumulative controllable joint angle serves as a metric for these actions. To elaborate, a zero total value indicates an opening motion where the joint angle is near zero; conversely, a grasping motion is inferred when the joint angle approaches its maximum value. The introduced method alternates between these two motions, enhancing the learning efficiency of opening and closing actions by increasing the transition speed between them. The fitness function is structured to yield higher scores when the hand's total joint angle aligns closely with the input myoelectric motion. In addition, a hyperbolic tangent is adopted to prevent the fitness from becoming sparse.

The expression for the fitness function for the p-th individual in the environment 1 at step t is given by

$$f_p^1\left(\phi(t), S_1(\boldsymbol{\theta}_p(t))\right) = \begin{cases} \dfrac{\tanh\left(\frac{\theta_{\text{sum}}-\theta_{\text{grasp}}}{\omega_\theta}\right) - \tanh\left(\frac{-\theta_{\text{grasp}}}{\omega_\theta}\right)}{\tanh\left(\frac{\theta_{\max}-\theta_{\text{grasp}}}{\omega_\theta}\right) - \tanh\left(-\frac{\theta_{\text{grasp}}}{\omega_\theta}\right)} & \text{if } \phi(t) \text{ is grasping.} \\ \dfrac{-\tanh\left(\frac{\theta_{\text{sum}}-\theta_{\text{grasp}}}{\omega_\theta}\right) + \tanh\left(\frac{\theta_{\max}-\theta_{\text{grasp}}}{\omega_\theta}\right)}{\tanh\left(\frac{\theta_{\max}-\theta_{\text{grasp}}}{\omega_\theta}\right) - \tanh\left(-\frac{\theta_{\text{grasp}}}{\omega_\theta}\right)}. & \text{if } \phi(t) \text{ is opening.} \end{cases} \tag{5.4-10}$$

In this context, $\phi(t)$ denotes the motion corresponding to the measured $\boldsymbol{emg}(t)$. Other parameters include $\theta_{\max}$, representing the sum of the hand's maximum joint angles, θ_{grasp} as the total of target angles for the grasping posture, θ_{sum} indicating the sum of the current joint angles, and ω_θ serving as a weight to modulate the function's gradient.

Environment 2

Both myoelectric control learning and object grasp learning are integrated, addressing the potential issue of myoelectric control being overlooked if only object grasp learning is emphasized. The fitness function for object grasp learning is conceived, drawing insights from previous research Bongard 2010. The values provided by the distance, touch, and height sensors are used to evaluate the ability of the hand to reach the object, contact the object after reaching the object, and pickup performance, respectively. The object pickup task is considered because the grasp stability can be evaluated by examining whether the hand can grasp the object, and this information can be easily obtained from the height sensor.

In cases where object o is the subject of learning, the fitness function for the p-th individual in the 2nd environment at step t is represented as

$$f_{p,o}^{2-1}\left(\phi(t), S_{2,o}(\boldsymbol{\theta}_p(t))\right) = \begin{cases} \dfrac{\tanh\left(\frac{\theta_{\text{sum}}-\theta_{\text{grasp}}}{\omega_\theta}\right) - \tanh\left(\frac{-\theta_{\text{grasp}}}{\omega_\theta}\right)}{\tanh\left(\frac{\theta_{\max}-\theta_{\text{grasp}}}{\omega_\theta}\right) - \tanh\left(-\frac{\theta_{\text{grasp}}}{\omega_\theta}\right)} & \text{if } \phi(t) \text{ is grasping.} \\ \dfrac{3.5\left(-\tanh\left(\frac{\theta_{\text{sum}}-\theta_{\text{grasp}}}{\omega_\theta}\right) + \tanh\left(\frac{\theta_{\max}-\theta_{\text{grasp}}}{\omega_\theta}\right)\right)}{\tanh\left(\frac{\theta_{\max}-\theta_{\text{grasp}}}{\omega_\theta}\right) - \tanh\left(-\frac{\theta_{\text{grasp}}}{\omega_\theta}\right)} & \text{if } \phi(t) \text{ is opening.} \end{cases} \tag{5.4-11}$$

$$f_{p,o}^{2-2}\left(\phi(t), S_{2,o}(\boldsymbol{\theta}_p(t))\right) = \begin{cases} 10h_p(t) + \sum_{i=1}^{N_c} c_i\left(t\right) + \sum_{i=1}^{N_r} r_i\left(t\right) & \text{if } \phi(t) \text{ is grasping.} \\ 10h_p(t) - \sum_{i=1}^{N_c} c_i\left(t\right) + \sum_{i=1}^{N_r} r_i\left(t\right) & \text{if } \phi(t) \text{ is opening.} \end{cases} \tag{5.4-12}$$

$$f_{p,o}^{2}(\phi(t), S_{2,o}(\boldsymbol{\theta}_p(t)))) = f_{p,o}^{2-1}(\phi(t), S_{2,o}(\boldsymbol{\theta}_p(t))) + f_{p,o}^{2-2}(\phi(t), S_{2,o}(\boldsymbol{\theta}_p(t))) \tag{5.4-13}$$

Subsequently, the fitness of the p-th individual in each generation $f_p(t)$ can be calculated as follows.

$$f_p(t) = \sum_{e\in E}\sum_{o\in O} G_{\mathrm{FIT}}\left(\phi(t), S_{e,o}(\boldsymbol{\theta}_p(t))\right) \tag{5.4-14}$$

$$= f_p^1\left(\phi(t), S_1(\boldsymbol{\theta}_p(t))\right) + \sum_{o\in O} f_{p,o}^{2-1}\left(\phi(t), S_{2,o}(\boldsymbol{\theta}_p(t))\right) \tag{5.4-15}$$

G_{FIT} symbolizes the function responsible for calculating fitness. The set can be used as input from Eqs. 5.4-10 to 5.4-15. Hence, F, representing the cumulative fitness values of individuals after a T_{gen} steps simulation, is described as:

$$F = \sum_{e\in E}\sum_{o\in O}\sum_{t\in T_{\mathrm{gen}}} G_{\mathrm{FIT}}\left(\phi(t), S_{e,o}(\Theta(t))\right) \tag{5.4-16}$$

$$= \sum_{e\in E}\sum_{o\in O}\sum_{t\in T_{\mathrm{gen}}} G_{\mathrm{FIT}}\left(\phi(t), \boldsymbol{C}(t), \boldsymbol{R}(t), H(t)\right) \tag{5.4-17}$$

5.4.5 Learning methods

The set of fitness values, F, is derived from simulating the controllers with the set of weight vectors $\boldsymbol{W}$ across T_{gen} steps in all tasks and environments, serving as an indicator of each controller's efficacy. Utilizing this set, a new set of weight vectors $\boldsymbol{W'}$ is produced from $\boldsymbol{W}$ through the learning function G_{L}, articulated as follows.

$$\boldsymbol{W'} = G_{\mathrm{L}}(F, \boldsymbol{W}) \tag{5.4-18}$$

$\boldsymbol{W'}$ represent the candidate solutions generated from $\boldsymbol{W}$ to increase the fitness. By repeating this process, the parameters that increase the fitness are identified. In this method, evolutionary computation, characterized as a population-based metaheuristic method, is employed for learning.

5.5 Experiments

A controller was created for a multi-DOF MPH in Unity which is a physical simulation framework using the EMG measured in advance and verified the effectiveness of the controller. Our experimental focus was to evaluate the efficacy and adaptability of our approach, ensuring its applicability across different individuals. This assessment is crucial to ascertain the controller' s ability to operate with untrained myoelectric signals. Additionally, two comparative evaluations were conducted. The first comparison contrasted our approach against traditional methods, assessing adaptability relative to various object forms and dimensions. The second involved an analysis of hand movements in grasp classification vis-a-vis our technique, verifying adaptability with object forms challenging to simulate on the physics engine and efficacy in tasks beyond object pickup. Detailed learning conditions are expounded in the following sections.

Table.5.1: Joint range of motion

	Thumb				Other Fingers		
	1st	2nd	3rd	4th	1st	2nd	3rd
Max [°]	80	60	90	90	90	100	90
Min [°]	-10	-10	0	0	-10	0	-45

Table.5.2: Dimensions of five-finger robotic hand model

Finger	Part	Height [mm]	ϕ [mm]	Mass [kg]
Thumb	Metacarpal	62.7	19.1	0.05
	Proximal phalanx	30.2	19.1	0.01
	Distal phalanx	23.2	16.6	0.01
Index finger	Metacarpal	89.7	17.2	0.07
	Proximal phalanx	40	17.2	0.02
	Middle phalanx	22.6	14.9	0.01
	Distal phalanx	17.4	13.3	0.01
Middle finger	Metacarpal	87.3	17.3	0.07
	Proximal phalanx	45.4	17.3	0.02
	Middle phalanx	25.6	15.2	0.01
	Distal phalanx	19.7	14.4	0.01
Ring finger	Metacarpal	82.5	16.2	0.07
	Proximal phalanx	43.2	16.2	0.02
	Middle phalanx	24.4	14.2	0.01
	Distal phalanx	18.8	13.8	0.01
Little finger	Metacarpal	75.5	14.3	0.06
	Proximal phalanx	33.4	14.3	0.01
	Middle phalanx	16.7	12.8	0.01
	Distal phalanx	16.7	11.4	0.01
Trapezium	19.1		19.1	0.01
Carpals	55.5		19.1	0.02
			sum	0.52

Table.5.3: Parameters for five-finger robotic hand

Part	Parameter	Value
Joint	number	16
Motor	ω_v	2
EMG sensor	number [ch]	3
	sampling points (T_{EMG})	5
Touch sensor	number	5
	placement	on each distal phalanx
Distance sensor	$d_{\max}$	0.08 (m)
Controller	Number of neurons in the input layer	8
	Number of neurons in the hidden layer	30
	Number of neurons in the output layer	16

(a) Measurement condition of the EMG

Sampling frequency (Hz)	2667.683
Quantization bit rate (bit)	14
Filter (Hardware)	· 50 Hz notch filter · Bandpass filter with a 1–1000 Hz bandwidth
Filter (Software)	50 Hz high pass filter
Potential range (V)	-2.5 to 2.5

5.5.1 Morphology and parameters

Anthropomorphic robotic hand model

A model of an anthropomorphic robotic hand, illustrated in Figure 5.6, was created utilizing Unity' s primitive objects and was designated as the agent for our simulations. The model' s DOF and dimensions were based on Miyata' s kinematics model (Miyata et al. 2011) and average Japanese hand measurements provided by AIST (National Institute of Advanced Industrial Science and Technology) (Kouchi 2012), respectively. Joint placements were determined according to Hamilton' s functional length of the phalanges (Hamilton and Dunsmuir 2002), and motion ranges for the fingers were established based on studies by Yonemoto (K. Yonemoto, Shigenobu, and Kondo 1995) and Schunke (Schünke, Schulte, and Schumacher 2014). The prosthetic hand' s weight was fixed at 520 g, referencing Vinet' s study (Vinet et al. 1995), which indicated an upper weight limit of approximately 500 g for prosthetic hands. Joint motion ranges and dimensions are elaborated in Tables 5.1 and 5.2, respectively, with the other parameters outlined in Table 5.3.

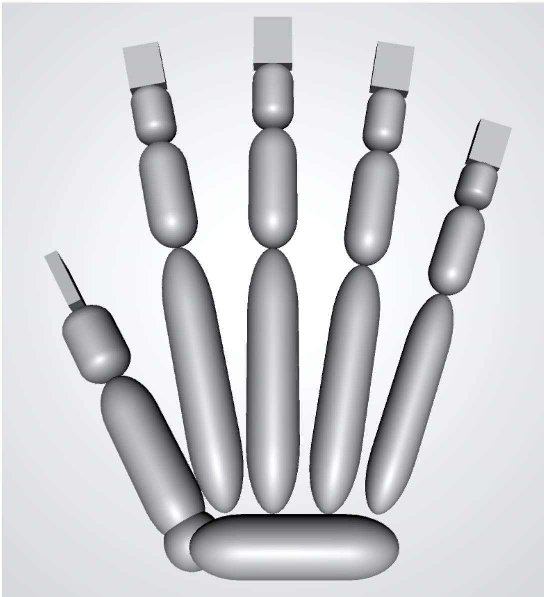

Fig.5.6: 16-DOF anthropomorphic robotic hand model. This figure is cited from (Kuroda et al. 2022).

Target angle derivation function

The joint target angles were calculated by applying the target angle derivation function to the controller outputs, illustrated below:

$$\begin{aligned}\boldsymbol{\Theta}(t) &= G_{\mathrm{TA}}(\boldsymbol{Y}(t)) \\ &= (0.5\boldsymbol{Y}(t) + 0.5)(\boldsymbol{\Theta}_{\max} - \boldsymbol{\Theta}_{\min}).\end{aligned} \tag{5.5-1}$$

$\boldsymbol{\Theta}_{\max}$ and $\boldsymbol{\Theta}_{\min}$ represent sets of the maximum and minimum angles of the joints, respectively.

Motor

The experimental setup assumed a scenario where the joints' angular velocities were controlled by proportional control. In this case, the angular velocity vector $v_p(t)$ of the joint angle of the p-th individual can be described using the weight ω_v:

$$\boldsymbol{v}_p(t) = \omega_v(\boldsymbol{\theta}_p(t) - \boldsymbol{\theta}_c). \tag{5.5-2}$$

$\boldsymbol{\theta}_c$ is the vector of the current joint angles.

Input from EMG Sensor

The integrated electromyogram (iEMG), derived from the EMG sensor, served as the input, computed using the function G_{iEMG} below:

$$G_{\text{iEMG}}(emg(t)) = \sum_{k=0}^{T_{\text{EMG}}} |emg(t-k)|, \tag{5.5-3}$$

$$iemg(t) = G_{\text{iEMG}}(emg(t)), \tag{5.5-4}$$

T_{EMG} is the number of samples. Subsequently, this study normalized $iemg(t)$ from -1 to 1 using the normalization function G_{NM}:

$$G_{\text{NM}}(iemg(t)) = \frac{2 \cdot iemg(t)}{emg_{\max} \cdot T_{\text{EMG}}} - 1, \tag{5.5-5}$$

$$iemg_{\text{nm}}(t) = G_{\text{NM}}(iemg(t)) \tag{5.5-6}$$

In general, the magnitude of the EMG signal varies from person to person. Therefore, the iEMG input signal was scaled from -1 to 1 using a scale transformation function G_{SC}, with $iemg_{\max}$ being the maximum value for each channel.

$$G_{\text{SC}}(iemg_{\text{nm}}(t)) = \begin{cases} 1, & \text{if } iemg_{\text{nm}}(t) > iemg_{\max} \\ (iemg_{\text{nm}}(t) + 1) \cdot \frac{2}{1 + iemg_{\max}} - 1, & \text{otherwise} \end{cases} \tag{5.5-7}$$

Using Eqs. 5.5-3 to 5.5-7, the following expression can be obtained:

$$G_{\text{FE}}(\boldsymbol{emg}(t)) = G_{\text{SC}}(G_{\text{NM}}(G_{\text{iEMG}}(\boldsymbol{emg}(t)))). \tag{5.5-8}$$

5.5.2 Learning conditions

The learning conditions employed in our experiments are outlined as follows:

A total of $P = 50$ agents were simulated for $T_{\text{gen}} = 1200$ steps. Each generation underwent one task in environment 1 and two tasks in environment 2 to compute the cumulative fitness function value. The weights of the RNN of the controller were updated based on this value. This process was iterated for $N_{\mathrm{gen}} = 250$ generations (participants A–E) or $N_{\mathrm{gen}} = 300$ generations (participant F). Subsequently, the optimized agents were evaluated by comparing the associated findings with those reported previously and those obtained using conventional methods. In this subsection, the EMG input conditions, tasks, and learning techniques are described.

EMG input conditions

EMG Measurement

EMG readings were obtained from non-disabled adult participants and a child participant with forearm deficiency, under the permission of the ethics committee of the University of Electro-Communication (permit No. 10006(5)). Three-channel electrodes (Togo, Yuta, et al. 2019) were utilized for adults (participants A-E) and a two-channel for the child (participant F), owing to the limited surface area available on the child' s residual limb. Consequently, the process was repeated for a greater number of generations for participant F in comparison with the other participants. The placement of sensors is illustrated in Figure 5.7.

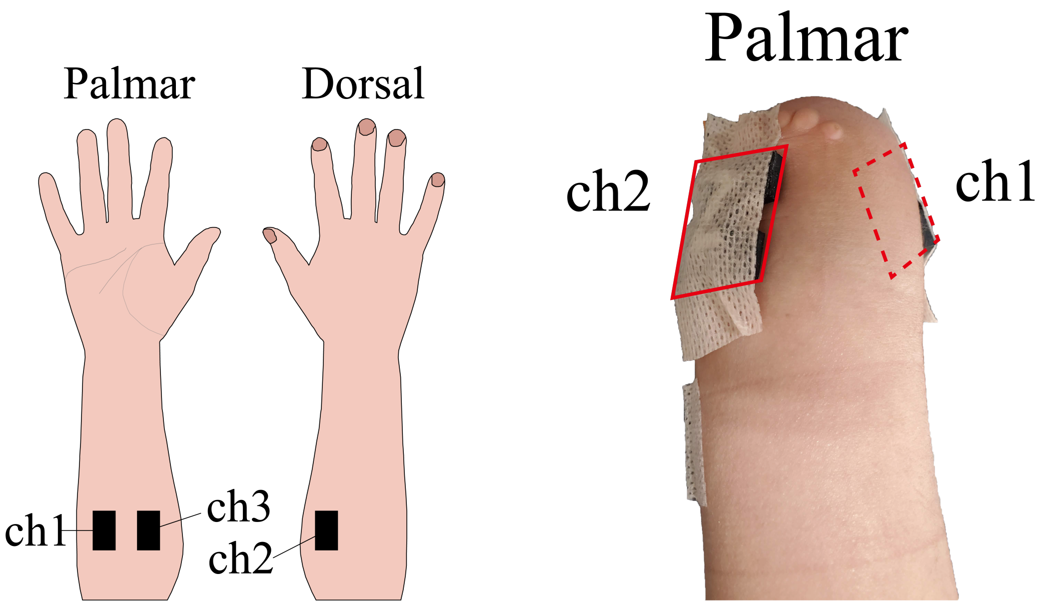

(a) (b)

Fig.5.7: (a) Sensor layout of Participant A-E. (b) Sensor layout of Participant F (congenital upper limb deficiency). ch1 is attached to the dorsal side, and the red dotted line indicates its position. These figures are cited from (Kuroda et al. 2022).

For adults, ch1 was positioned around the palmaris longus, flexor carpi ulnaris, and flexor digitorum superficialis; ch2 was attached around the extensor digitorum and extensor carpi radialis brevis; ch3 was placed around the flexor carpi radialis and pronator teres. For the child, ch1 was attached to the flexor, and ch2 to the extensor. The participants were instructed to alternate between grasping and opening their hands. The grasping here refers to a fist-clenching motion without holding any object. The measurer visually confirmed that each movement was performed as instructed before capturing the measurements. The EMG was then converted to iEMG as Eqs. 5.5-3 and 5.5-4. A series of 200 iEMG readings for both hand movements of grasping (flexion contraction) and opening (extensor contraction) were captured in ten alternating cycles starting with the grasping motion. Further details on the measurement parameters are detailed in Table 5.4a. To mitigate the 50 Hz electromagnetic noise generated by commercial power supplies in eastern Japan, both a 50 Hz high-pass filter and a notch filter were employed because the notch filter alone was not sufficient to remove this noise.

Input Sequence for the EMG Sensor

The input sequence of the iEMG signals was switched depending on the environment because different environments require different movements to accomplish the relevant tasks. The 3200 recorded iEMG signals were segregated into two separate datasets, each containing 1600 iEMG signals per channel, maintaining the original order. These datasets were utilized to train two distinct models for every participant. The organization of the data from each channel adhered to the sequence illustrated in Figure 5.8b, without changing the order of the data for each hand movement. Sequences 1 and 2 were used as the inputs for environments 1 and 2, respectively. The first and second halves of the dataset for each participant were referred to as datasets 1 and 2, respectively.

Tasks

The agents were tasked with completing three specific assignments within two distinct environments. The cumulative fitness score obtained was used for optimization. This subsection describes the tasks and environments.

Environment 1

In this setting, agents were tasked with executing hand opening and closing actions. They were specifically directed to accomplish the actions of grasping and opening the hand, guided by the EMG data corresponding to these specific motions. Notably, during this phase, the controller of the agent was not provided any information regarding the hand motion at the time of the EMG measurement.

Environment 2

In this second environment, the agents were challenged to lift both a cuboid and a sphere object, the dimensions of which are detailed as Cuboid0 and Sphere2 in Table 5.5. The EMG data, captured during the user' s grasping motion, was fed into the EMG sensor during the object pickup motion. After holding the object, the agents received the EMG data from the user's hand opening motion to initiate the object release process. It is essential to note that the lifting action was not executed by the agent's controller; instead, the hand model was pre-programmed to ascend automatically between the 451st and 750th steps before descending to its initial position. The hand' s movement trajectory is illustrated in Figure 5.8a. The choice of a cuboid over a cube as the target object was strategic to prevent the agent from falling into a local optimum when picking up a cube, which requires contacting the floor with the tip of the hand.

Table.5.5: Dimensions of the objects to be grasped

	Cuboid0	Cuboid1	Cuboid2	Cuboid3	Cuboid4	Cuboid5	Cuboid6	Cuboid7	Cuboid8	Cuboid9	Cube0	Cube1	Cube2
Width (cm)	3	4	5	3	3	2	3	2	7	7	3	4	5
Length (cm)	3	4	5	3	3	2	7	7	3	2	3	4	5
Height (cm)	5	6	7	6	7	7	3	2	3	2	3	4	5
	Sphere0	Sphere1	Sphere2										
Diameter (cm)	3	4	5										
	Capsule0	Capsule1	Capsule2	Capsule3	Capsule4	Capsule5	Capsule6	Capsule7					
Diameter (cm)	3	3.5	3	3	2.5	2.5	2	2					
Height (cm)	6	7	14	14	14	14	14	14					
Axis	y	y	x	z	x	z	x	z					

The parameters for the fitness functions for each environment were defined as follows: the sum of the hand's maximum joint angles was $\theta_{\max} = 1440$, the sum of the target angle for the grasping posture was $\theta_{\text{grasp}} = 720$, and the weight designated for modulating the function' s gradient was $\omega_\theta = 400$.

Learning

For the learning function G_{L}, the covariance matrix adaptation evolution strategy (CMA-ES) was incorporated (Hansen, Arnold, and Auger 2015). This is a sophisticated evolutionary computation technique characterized by its multipoint search functionality by considering a normal distribution. The constants were derived from the recommendations by Hansen and Auger (Hansen and Auger 2014).

5.5.3 Experimental Condition: Performance Evaluation of Optimized Agents

Figure 5.8c illustrates the relationships among the data sets, learning and evaluation schemes, and individuals. Each participant's data is split into two distinct datasets, further transformed into two separate sequences. Sequences 1 and 2 corresponded to environments 1 and 2, respectively. The evaluation process employs a dataset distinct from the one used during the training phase. The optimized controllers were selected from the population after training by extracting the ones with the highest fitness using the evaluation dataset presented in Table 5.8. An individual yielding the highest fitness from Dataset 1 for Participant X is denoted as Individual X-1, and from Dataset 2 as Individual X-2. The evaluation exclusively utilizes Sequence 2.

During the evaluation phase, an object was considered to be grasped successfully if it did not touch the floor between the 551st and 650th steps and when the hand was stagnant in space, as shown in Figure 5.8a, which corresponds to the trajectory of the hand in a 1200-step simulation. A successful opening motion is acknowledged if the object is released after 1200 steps. The evaluation phase employs Cuboid0 and Sphere2 objects, identical to those used in the training phase. The realization of the opening motion is confirmed by monitoring the joint angle's average value transition and alteration when the input EMG was switched.

5.5.4 Comparison 1: Comparison with the conventional method

The experiment detailed in Section 5.5.3 verified our methodology's effectiveness and applicability across diverse individuals. However, an additional layer of analysis is essential to gauge the method's adaptability across varying shapes and sizes of objects for grasping and to benchmark its performance against traditional methods. The adaptive grasping method described in Section 5.3 is too intricate to emulate on a physics engine, and the software-oriented approach demands an augmented volume of input signals, complicating a fair comparison. In this context, comparison between the proposed and conventional methods can be performed using the Hoshigawa et al.'s approach.

Conventional Method: Optimized hand shape

Hoshigawa et al. developed a simple prosthetic hand characterized by a 2-DOF, controlled by pattern recognition algorithms (Hoshigawa et al. 2015). This prosthetic hand supports the flexion and extension movements of the four fingers and thumb. The shape of the fingers has been optimized by pick-and-place experiments using actual devices so that the fingers can grasp tools that are expected to be frequently used in ADL. This approach aligns with the hardware-based methodologies elaborated in section 5.3, and as with adaptive grasping, the shape of the hardware is limited.

An artificial neural network was used as the pattern recognition method to distinguish between the grasping and opening motions in this comparison experiment. This control method is also used for the method of Hoshigawa et al. For training, dataset 2 (sequence 2 of participant) was used C). The other parameters were set as summarized in Table 5.6.

Table.5.6: Parameters of the conventional recognition method.

Recognition Method G_{PR}	Artificial Neural Network
Number of neurons (input layer)	3
Number of neurons (hidden Layer)	24
Number of neurons (output Layer)	2
Learning Method G_{L}	Adam Kingma and Ba 2015

Comparison Conditions

The comparative analysis was conducted under the framework outlined in Section 5.5.3, with the object pickup tasks serving as the benchmark for performance assessment. The individual C-1 model was employed in the evaluation. Both the proposed and traditional methodologies were evaluated using sequence 2, derived from dataset 2 of participant C. The object’ s characteristics underwent several modifications as outlined below:

- Object shape
- Orientation of the object relative to the hand

These object's features were altered in a sequential manner, and it was verified whether the agent could grasp the object under varying conditions. An object to be grasped was considered successfully grasped if it did not touch the floor between the 551st and 650th steps and when the hand was stagnant in space as in the Section 5.5.3.

The appearances of the shapes are shown in Figure 5.10.

In addition, when a user grasps an object using an MPH,

- the position of the object relative to the hand

is a factor controlled by the user. Therefore, it was considered that the user could grasp the object if the position of the object was changed sequentially and the pickup achievement condition was satisfied in any of the ranges. As illustrated in Figures 5.9a, 5.9c, and 5.9e, a total of 100 object positions were established during the evaluation phase.

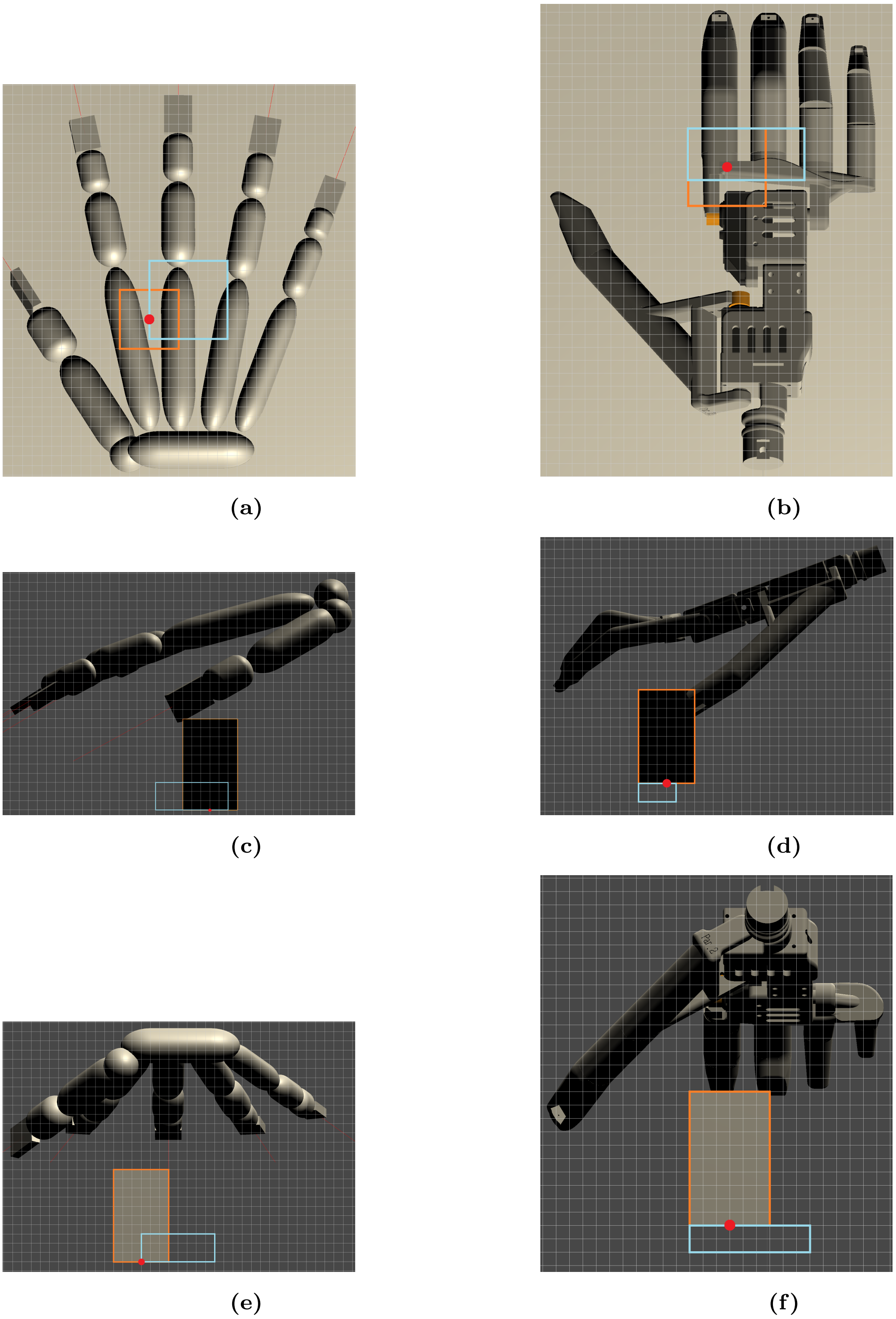

Fig.5.9: Range of object placement. Proposed method (a) top, (c) left, (e) back. Conventional method (b) top, (d) left, (f) back. The orange frame shows the outline of Cuboid0, the red dot represents the center of the bottom of the object, and the light blue frame indicates the area in which the center of the object moves. The square dimensions are 0.5×0.5. These figures are cited from (Kuroda et al. 2022).

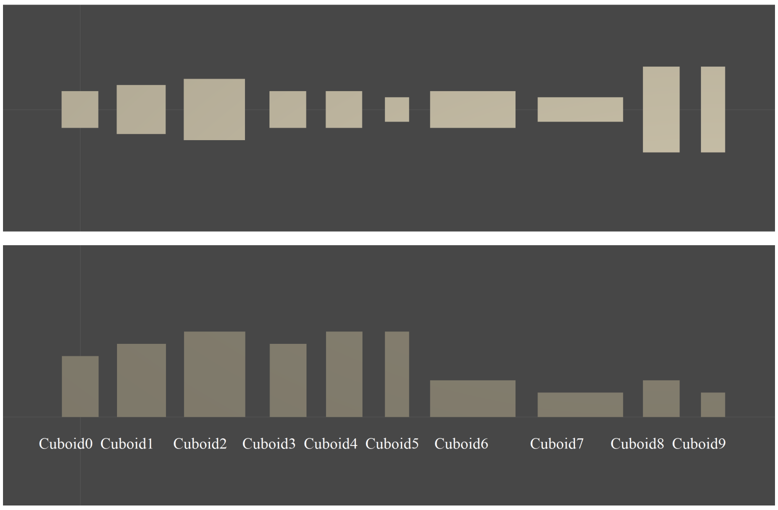

(a)

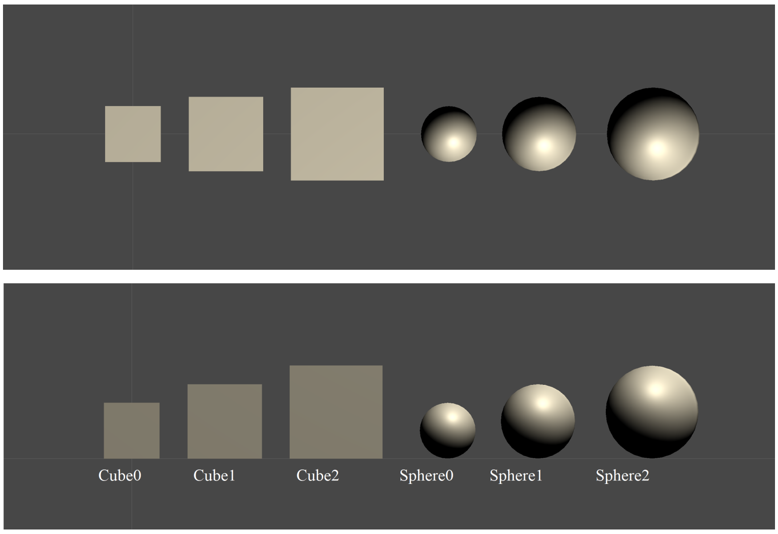

(b)

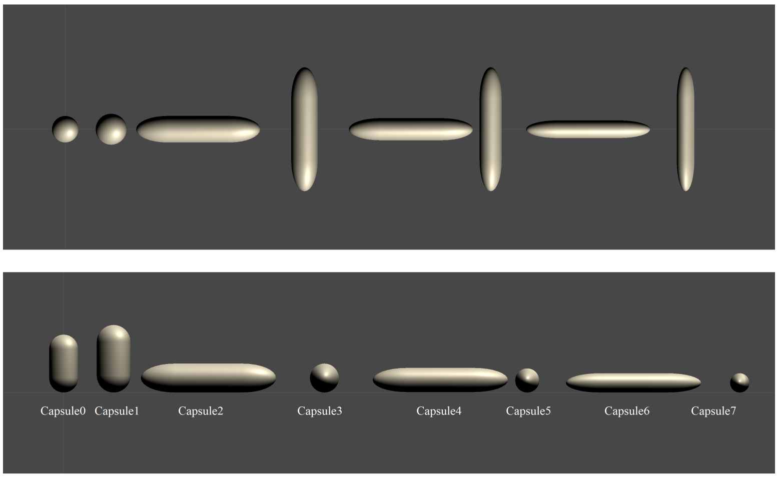

(c)

Fig.5.10: Object shapes. Top of each diagram: top view, bottom: front view. (a) Cuboids, (b) Cubes and spheres, (c) Capsules. These figures are cited from (Kuroda et al. 2022).

5.5.5 Comparison 2: Comparison with the grasping classification

The preceding subsection verified the agent' s generalizability to a variety of object shapes. However, the diversity of the object shapes that can be evaluated using the physics engine is limited. Therefore, the versatility of complex object shapes must be evaluated by grasping simple objects verified by the physics engine. The study of grasp taxonomy, which delves into the diversity of hand forms, offers a viable evaluation metric in this context.

The grasping classification pertains to the categorization of static hand movements and finds applications in rehabilitation training, robotic hand design, and prosthetic development. The ability to execute a diverse array of grasping motions is a key performance indicator in prosthetic hand research and serves as a versatility metric for object grasping. Notable examples include Kamakura's grasping taxonomy (KAMAKURA et al. 1978), which classifies hand motions observed in daily life, and Cutkosky's grasping taxonomy (Cutkosky 1989), which classifies hand motions observed by workers in machining factories.

In this study, the hand movements observed by our method were compared with these two classifications. These two taxonomies have different task domains: one caters to fundamental grasping tasks, whereas the other caters to grasping movements that are more complex and diverse. The proposed model is evaluated using these two taxonomies to verify its applicability to different grasping conditions and modalities.

The Individual C-1 model, which had the highest fitness, as tabulated in Table 5.8, was employed for this comparative analysis. Sequence 2, converted from dataset 2 of participant C, served as the evaluation dataset. The comparative methodology involved changing the shape of the primitive object in Unity (cube, sphere, capsule), having the agent grasp the object, and recording whether the grasping motion matched any of the grasping motion classifications.

5.6 Results

The results of the experiments and comparisons are presented in this section.

5.6.1 Performance Evaluation of Optimized Agents

This subsection presents the outcomes of evaluating agents that were trained employing the EMG readings from five able-bodied adult participants (A–E) and a child participant (F) with a forearm deficiency. Table 5.7 presents the results of examining whether the agent trained on each dataset could pick up and release the object. Figures 5.11a and 5.11b illustrate the mean joint angles when picking up Cuboid0 and Sphere2, respectively. The average joint angles across all participants during steps 551-651, a phase where the hand remains stagnant after grasping an object mid-air, are depicted in Figure 5.12. Table.5.8 lists the final fitness of the agent trained on each participant's myoelectricity.

The data reveals the capability of all participants to elevate Cuboid0 and Sphere2 and execute both grasping and opening motions according to the corresponding EMG readings. The average angle at the 750th step, when the myoelectricity during the grasping motion switched to that during the opening motion, was significantly larger than the average angle at the 1200th step (Wilcoxon's rank-sum test, Cuboid0: $p=0.0011$, Sphere2: $p=0.0011$). Figure 5.13a and 5.13b show how the Individual F-1 grasps Cuboid0 and Sphere2.

Table.5.7: Results of examining whether the agent can lift the object using the EMG data of each participant.

	Cuboid0	Sphere2
success rate (%)	100 (n=12)	100 (n=12)

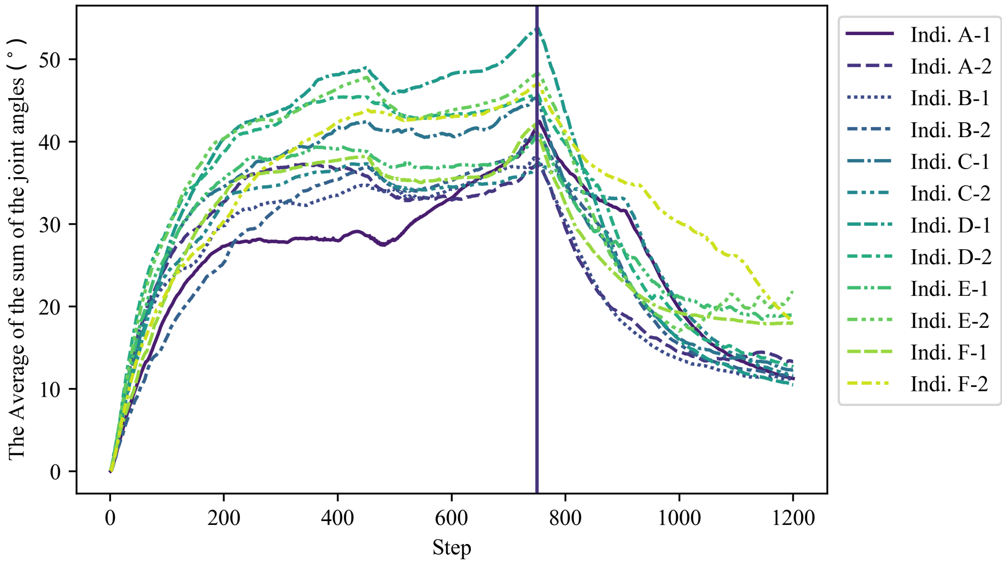

(a)

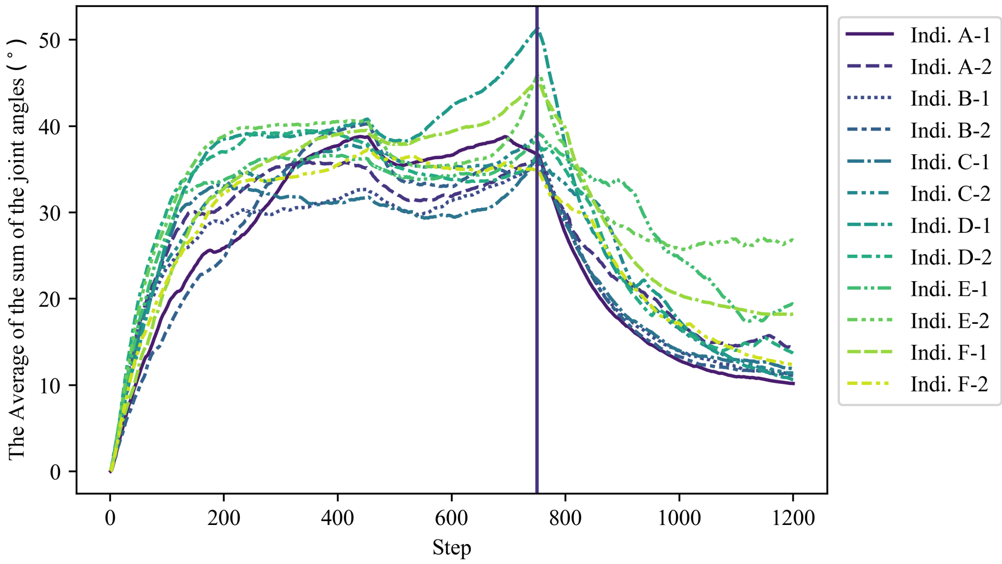

(b)

Fig.5.11: Changes in the mean values of the joint angles when the agent picks up (a) Cuboid0 and (b) sphere2. The vertical line signifies the transition where the EMG input shifts from grasping to opening. The term 'Indi.' is employed as an abbreviation for 'individual'. These figures are cited from (Kuroda et al. 2022).

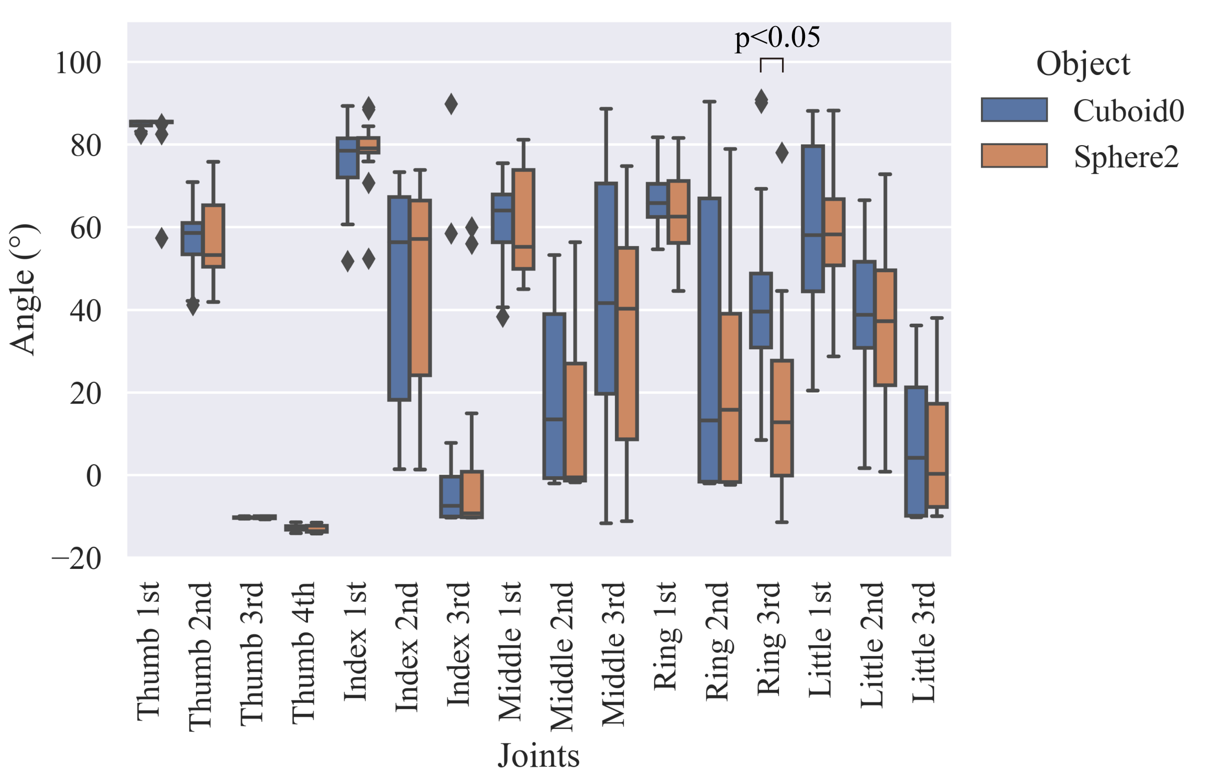

Fig.5.12: Average joint angles across all participants during steps 551-651 when the hand is stagnant after grasping an object in the air. Cuboid0 is represented in blue, while Sphere2 is in orange, with the rhombic shaped markers indicating the outliers. The joint angles are slightly out of the upper and lower limits because the body objects are pushed out by the objects when they come into contact with each other, and the relative values between the body objects shift slightly. This figure is cited from (Kuroda et al. 2022).

Table.5.8: Final fitness of the learned controllers

Participant	A		B		C		D		E		F	
Dataset	1	2	1	2	1	2	1	2	1	2	1	2
Fitness	53368.09	55648.21	56187.08	53971.32	65380.5	55256.67	60360.92	58035.37	54676.58	54697.28	60127.04	57501.81

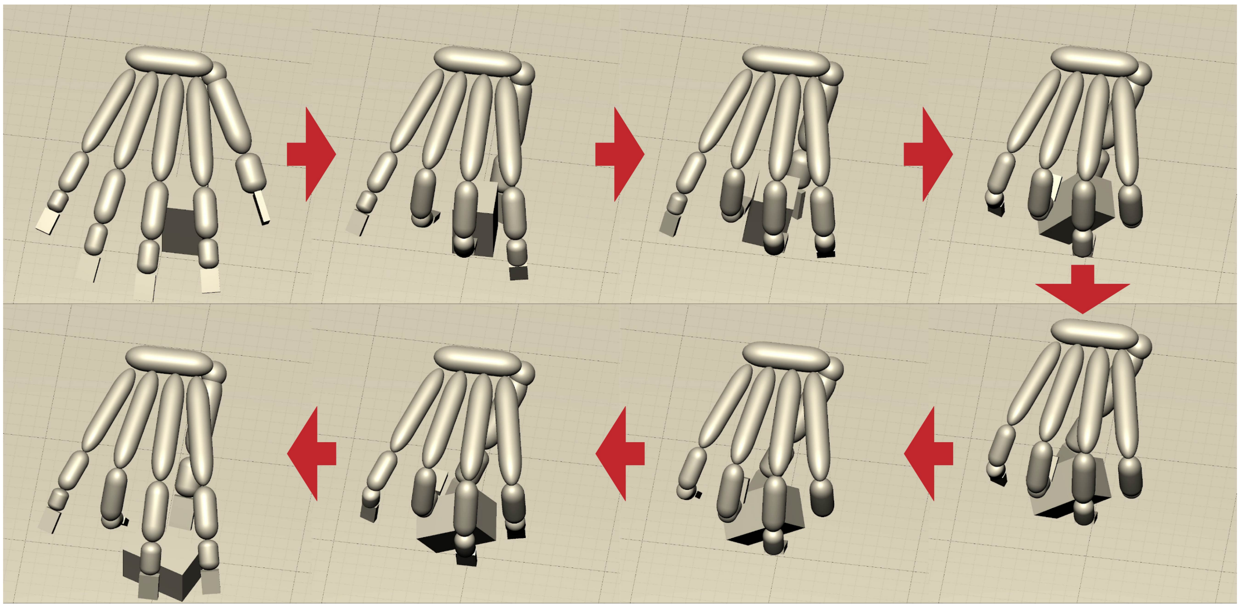

(a)

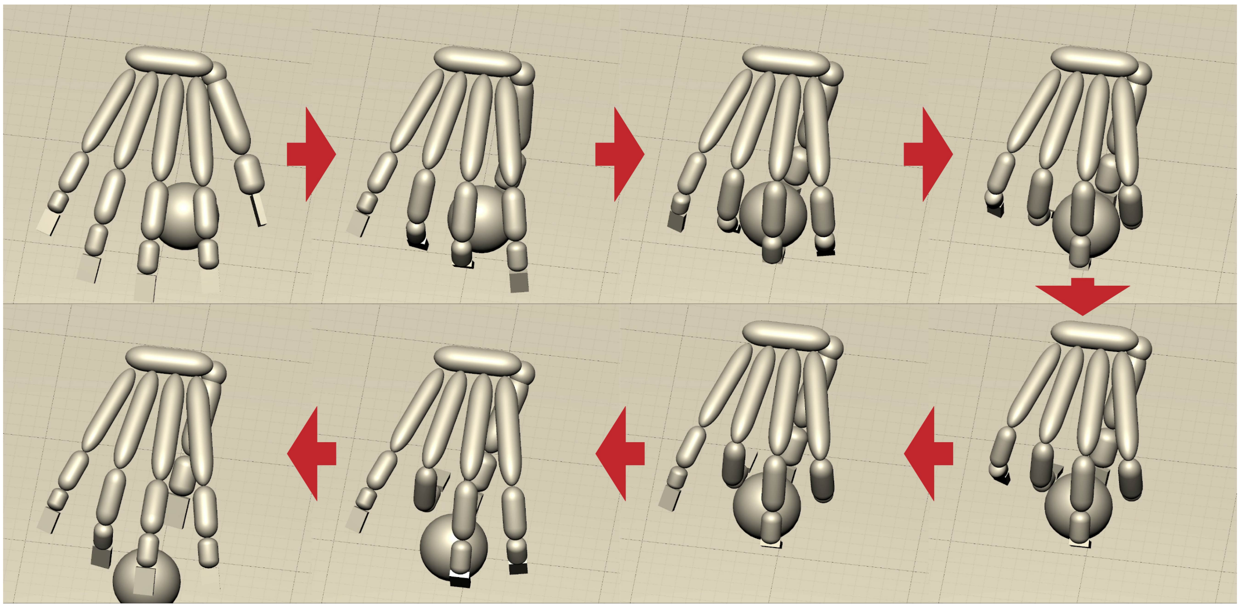

(b)

Fig.5.13: Individual F-1 grasping (a) Cuboid0 and (b) Sphere2, respectively. The red arrows indicate the passage of time. The following are the links to the videos. (a) `https://youtu.be/6oYrVZ_Bjis` (b) `https://youtu.be/XHXHHmOMrUQ` These figures are cited from (Kuroda et al. 2022).

5.6.2 Comparison with Conventional Method

The performance assessment contrasting the conventional and proposed methods in various object pickup scenarios is encapsulated in Table 5.9. The checkmarks (✓) denote the objects that were successfully grasped in the pickup task. All objects under consideration were successfully grasped using the proposed approach.

Table.5.9: Results of the object grasping experiment. Checkmarks (✓) indicate objects that were successfully grasped in the pickup task.

	Cuboid0	Cuboid1	Cuboid2	Cuboid3	Cuboid4	Cuboid5	Cuboid6	Cuboid7	Cuboid8	Cuboid9	Cube0	Cube1	Cube2
Proposed Method	✓	✓	✓	✓	✓	✓	✓	✓	✓	✓	✓	✓	✓
Conventional Method	✓	✓	✓	✓	✓	✓	✓	✓			✓	✓	✓

	Sphere0	Sphere1	Sphere2
Proposed Method	✓	✓	✓
Conventional Method			

	Capsule0	Capsule1	Capsule2	Capsule3	Capsule4	Capsule5	Capsule6	Capsule7
Proposed Method	✓	✓	✓	✓	✓	✓	✓	✓
Conventional Method			✓		✓			

5.6.3 Comparison with Taxonomy of Grasps

Comparison with Cutkosky's taxonomy of manufacturing grasps

Fig.5.14a shows the outcomes of the comparison with Cutkosky' s taxonomy of manufacturing grasps and the matched movements. Eight out of the 16 movements matched.

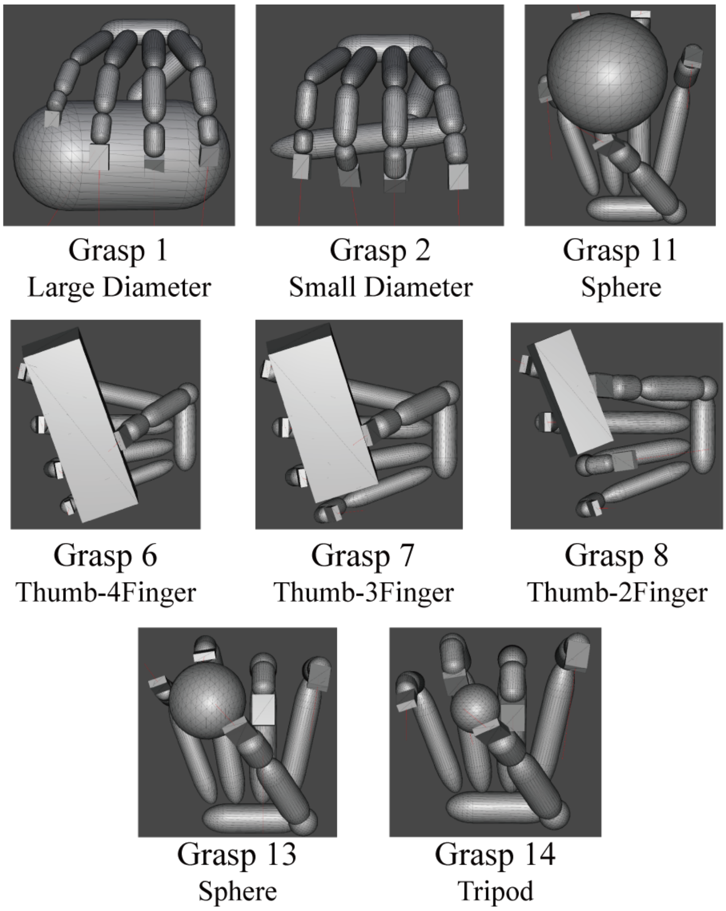

(a)

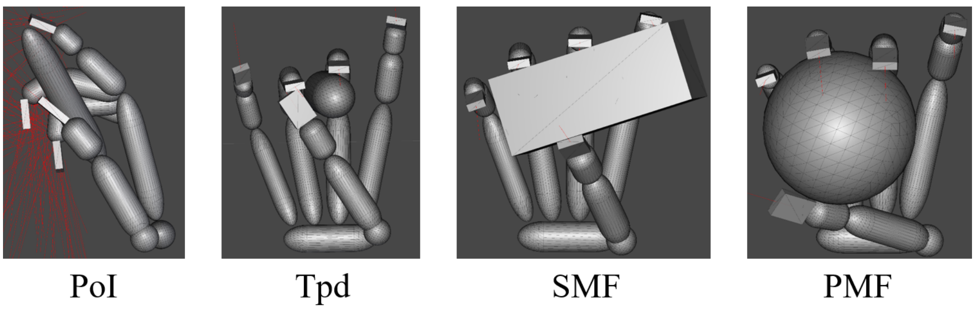

(b)

Fig.5.14: (a) Matching of the grasping motions with Cutkosky's categorized grasping motions, with numerical annotations denoting the specific grasp classification. (b) Matching of the grasping motions with the classification by Kamakura, with labels indicating the specific grasping categories. These figures are cited from (Kuroda et al. 2022).

Comparison with Kamakura et al.'s grasping motion classification

The results of the comparison with Kamakura et al.'s grasping motion classification and matched movements are shown in Figure 5.14b. Four out of the 14 movements matched.

5.7 Discussion

This section discusses the results of the verification.

5.7.1 Results of the Learning Process

The agents successfully performed opening and grasping motions according to the EMG. Furthermore, all six participants, including a child with a forearm deficiency, were able to lift both objects used for learning, Cuboid0 and Sphere2, utilizing their EMG data. These observations indicated the adaptability and applicability of the proposed method across a diverse users.

5.7.2 Comparison with Conventional Method

Compared with the existing method, the proposed method enables the robotic hand to successfully grasp all the considered objects (Table 5.9). The validation employed objects were characterized by planar (Cuboid0) and rounded (Sphere2) surfaces as learning models. Consequently, the acquired grasping strategies demonstrated efficacy even against untrained shapes (capsules, in this work) and varied dimensions in this study.

Massera et al. suggested that "certain behavioral strategies might be effective for a large variety of objects, and the limited differences in terms of shape and size of the objects to be grasped should not necessarily impact the rules that regulate the robot/environmental interactions." Gianluca Massera, Cangelosi, and Stefano Nolfi 2007

The results of this study support this suggestion.

5.7.3 Grasping posture observed in this study

Figure 5.11 illustrates that the thumb's first joint angle is the largest during object grasping, signifying that the thumb faces the middle and ring fingers in the grasp. This precision grasp is evident from Figure 5.13. Typically, precision grasps involve the thumb opposing the index or both the index and middle fingers, as highlighted in previous works Cutkosky 1989KAMAKURA et al. 1978. According to the study by Cotugno et al., the range of motion of the thumb has been reported to be biased towards forming a precision grasp (opposing the index finger or the index and middle fingers) in many robot hands Cotugno, Althoefer, and T. Nanayakkara 2017. This indicates that this grasping method is the standard posture adopted by robotic hands. However, such a pattern was not identified in this study.

This divergence in grasping postures stems from two primary reasons. In Kuo et al.'s research, they delineated the functional workspace for the precision thumb-finger grasp, characterizing it as the range of all possible positions in which the thumb-tip and each fingertip could simultaneously contact each other (Kuo et al. 2009). They found that the functional workspace of thumb-directed opposition is the largest among the four fingers (Kuo et al. 2009). In other words, generating a stable motion trajectory with the thumb facing the index finger is difficult. To prevent this complexity, human anatomical structures such as muscles, tendons, and ligaments related to the thumb contribute to stabilizing the thumb in humans (V. K. Nanayakkara et al. 2017). Given that our proposed approach replicates merely the joint architecture of the human hand, the proposed model may have adopted a strategy to stabilize the thumb by maintaining the first joint at the maximum angle instead of stabilizing the thumb with muscle tendons.

Additionally, the general precision grasp, characterized by the opposing orientation of the thumb and index finger, was not optimal for object pickup tasks owing to its specialized nature for object manipulation tasks, as indicated by the size of the functional workspace. Given our method' s exclusion of tasks pertaining to object manipulation, it may be that the thumb can perform the pickup task more stably when it is facing the middle or ring fingers than when it is facing the index finger. Supporting this notion, Kong et al. deduced that the sequence of contributions to the grasping force among fingers is as follows: middle, ring, index, and little finger (Kong et al. 2011). If this contribution directly correlates with the stability of an object' s grasp, it lends credence to the aforementioned hypothesis.

Therefore, it can be considered that the proposed method expresses a grasping motion that is appropriate for the hand form and task. While the conventional thumb-index opposition grasp is a staple in robotic applications. The proposed approach unveils the potential for unearthing novel grasping motions, infrequently observed in human grasping behaviors. From another perspective, it is clear that designing the morphology of the hand to induce dexterous control similar to that of humans is necessary. In particular, mechanically or software-wise replicating the anatomical structures such as muscles, tendons, and ligaments that stabilize the thumb could enable more natural grasping actions closer to human capabilities.

5.7.4 Comparison with the grasping motion classification: Results of matching conducted using two taxonomies

Figure 5.14 illustrates that eight of the 16 grasping motions aligned with Cutkosky's taxonomy, whereas four of the 14 motions corresponded with Kamakura et al.'s classification. These findings lead to a discussion on the constraints of our approach. There are three notable distinctions between Cutkosky' s and Kamakura et al.' s taxonomies, as elaborated below.

The initial distinction lies in the foundational elements of the taxonomies. Cutkosky' s classification is anchored in the hand' s skeletal structure, whereas Kamakura et al. base theirs on the distribution of contact on the palm. Consequently, to execute a grasp categorized by Kamakura et al., the palm predominantly needs to engage with the object. Given that our method prioritizes mimicking the hand' s kinematic model over the palm, achieving such grasping motions presents a challenge.

The second variance stems from the scope of tasks each taxonomy encompasses. Cutkosky' s classification is intended only for single-handed tasks, diverging from Kamakura et al.' s inclusion of dual-handed movements. Our study is centered around single-handed tasks, excluding cooperative actions, as reflected in the outcomes.

The third difference emerges from the complexity of the tools and objects each taxonomy considers. Cutkosky' s taxonomy is rooted in the industrial setting, encompassing basic shapes such as cylinders, spheres, and disks. Kamakura et al., however, extend their classification to intricate objects such as keys, scissors, and chopsticks, besides basic shapes. However, the behavior of the structural complexity of the objects used for training does not seem to affect the behavior.

One of the hypotheses of 3D object recognition is that 3D objects are recognized by an arrangement of simple geometric elements called "geons" (Biederman 1987). Studies measuring Japanese monkey brain cells also propose that hand shapes may be preconfigured, guided by primitive geometric attributes (such as flat, round, and elongated) shared with analogous objects (Bekey et al. 1993; Jeannerod et al. 1995; Murata et al. 2000). Consequently, training with objects embodying primitive geometric features could facilitate the grasp of more complex forms. The experimental results show that learning to grasp only primitive objects (Cuboid0 and Sphere2) enabled the grasping of unlearned shapes and objects. This supports the hypothesis that the structural complexity of the object used for learning does not affect the learned behavior of the model(Gianluca Massera, Cangelosi, and Stefano Nolfi 2007).

Conclusively, the comparison of the two grasping motion taxonomies uncovers areas warranting enhancement to broaden the variation of achievable hand movements. These include refining the replication of palm-involved grasping, integrating cooperative behaviors, and identifying the most effective and efficient primitive objects for training purposes.

5.8 Conclusion

In this chapter, combining evolutionary robotics with MPH control enabled adaptive object grasping according to myoelectric signals. The proposed mode was capable of anticipating the suitable joint movements, drawing insights from the data acquired through touch sensors that monitor the contact state between the hand and object grasped.

After training the 16-DOF robotic hand agents using the myoelectric signals from six participants, one of whom was a child with an upper limb deficiency, every agent was able to complete the pickup tasks. Furthermore, irrespective of the individual participants, the agents executed the pickup tasks adopting a consistent posture for specific objects, suggesting that through evolutionary computation, the hand was fine-tuned to a posture that minimizes the risk of dropping the object.

These findings underscored the efficacy of the proposed approach in facilitating adaptive object grasping. This result indicates that the proposed method can adaptively grasp objects with simple myoelectric control using a multi-DOF myoelectric prosthetic hand, regardless of the participants.

Furthermore, the requirements for ideal hardware necessary to apply this method were also verified. It was suggested that replicating the anatomical structures of the human hand, such as muscles, tendons, and ligaments that stabilize the thumb, is crucial. Additionally, challenges crucial for enhancing the functionality of the proposed method, such as learning to grasp using the palm of the hand, realizing and learning cooperative movements, and identifying objects that are efficient for learning, were identified.

Section 5.2 described the research on the two grasping motion taxonomies that are often used as references for the design of electric prosthetic hands.

Section 5.3 described the hardware and software approaches to research on complementing the human grasping function, respectively.

Section 5.4 described the proposed method.

In Section 5.5, the experiment to evaluate the efficacy and adaptability of my approach and two comparative evaluations were presented.

Section 5.6 described the results of the experiments and comparisons in this section.

Finally, Section 5.7 discussed the results of the verification.

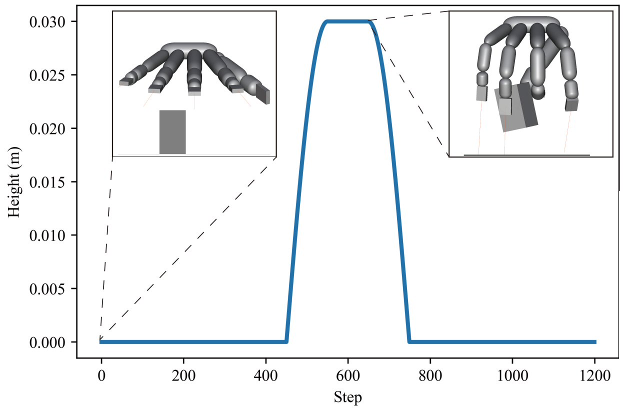

(a)

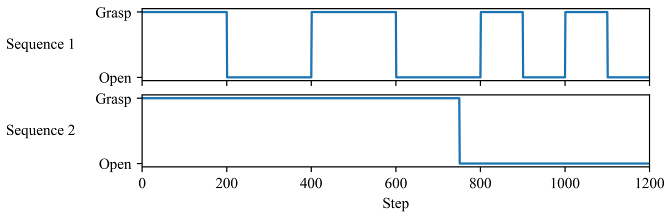

(b)

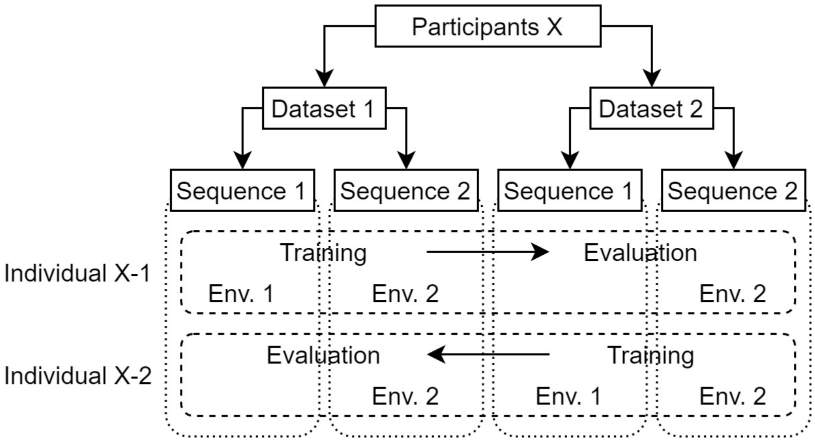

(c)

Fig.5.8: (a): Trajectory of the hand and screenshots of the hand at the 0-th step and highest position. The scale of the screenshots is the same. (b): Input sequence of EMG signals. (c): Relationships among the data sets, learning and evaluation schemes, and individuals in the experiments. Two datasets are created for each participant. Each dataset is transformed into two sequences. Sequences 1 and 2 refer to environments 1 and 2, respectively. The individuals with the highest fitness among the controllers learned from datasets 1 and 2 for participant X are known as individual X-1 and X-2, respectively. Sequence 2 is used for the evaluation. These figures are cited from (Kuroda et al. 2022).

Chapter 6 Registration of ready-made parts of multi-degree-of-freedom myoelectric prosthetic hand and application of the system to diverse participants

6.1 Introduction

This chapter explains the requirements for the registration of the developed BIT-UEC-Hand as a ready-made part and discusses the current issues based on the sales situation after registration as well as the AMD provision process. As explained in Section 1.3.2, the only MPHs that can be purchased through the AMD payment system are those registered as ready-made parts. Therefore, this study aimed to register the MPH developed in this study as a ready-made part to improve the accessibility of inexpensive and highly functional MPHs for the users.

This chapter also summarizes the application results of the system developed in this study to diverse participants.

Section 6.2 describes the requirements for registering an MPH as a ready-made part.

Section 6.3 describes the attempt to modularize the BIT-UEC-Hand components, which is one of the requirements for registration as ready-made parts.

Section 6.4 details the application for the BIT-UEC-Hand.

Section 6.5 describes the results of applying the ready-made parts, the details of the applied parts, and the pricing of the parts.

Section 6.6 describes the current sales status of the ready-made parts.

Section 6.7 discusses the results of applying the control system to various participants.

Section 6.8 discusses the issues faced during the registration process for the ready-made parts and the widespread use of registered MPHs.

6.2 Requirements for registration as ready-made parts

The following three criteria must be met to register an MPH as a ready-made part (Togo, Hiroshi Yokoi, et al. 2020):

1. The MPH system must be modularized depending on the component category of the ready-made parts.
2. The components must be made so that they can be connected and assembled into sockets by non-developers, such as prosthetists.
3. The developed MPH must have been evaluated for at least 90 days, in at least three participants, and at least two evaluation facilities.

Points 1 and 2 are the practical requirements for prosthetists to assemble the parts and sockets when the MPH is supplied. An electric hand must be attached to the end of the socket support, switches and batteries must be attached to the side, a controller must be placed inside, and an EMG sensor must be attached to the inner socket. In other words, each part must be removable using connectors or other means; if not, assembling will be challenging. This is because the support component of the socket is tubular, and, once the parts are attached to the support component, it is difficult to access the inside of the socket. Therefore, detaching parts, such as switches, by pulling out the connector’s connection from the mounting holes drilled in the support is necessary.

Regarding point 3, evaluating the performance of an MPH in three participants with upper limb defects is essential. Although the specific details of the evaluation have not yet been decided, the opinions of the participants, those of the person in charge of manufacturing, and those of the person in charge of field testing must be entered into the application form.

6.3 Modularization of BIT-UEC-Hand parts and creation of sockets

6.3.1 Modularization of BIT-UEC-Hand parts

To register the BIT-UEC-Hand as a ready-made part, each part was modularized. Fig.6.1 shows all the parts connected to the MPH. Each part can be disassembled and connected via connectors, as shown in Fig.6.2. The sensors can also be disassembled and connected as shown in Fig.6.3.

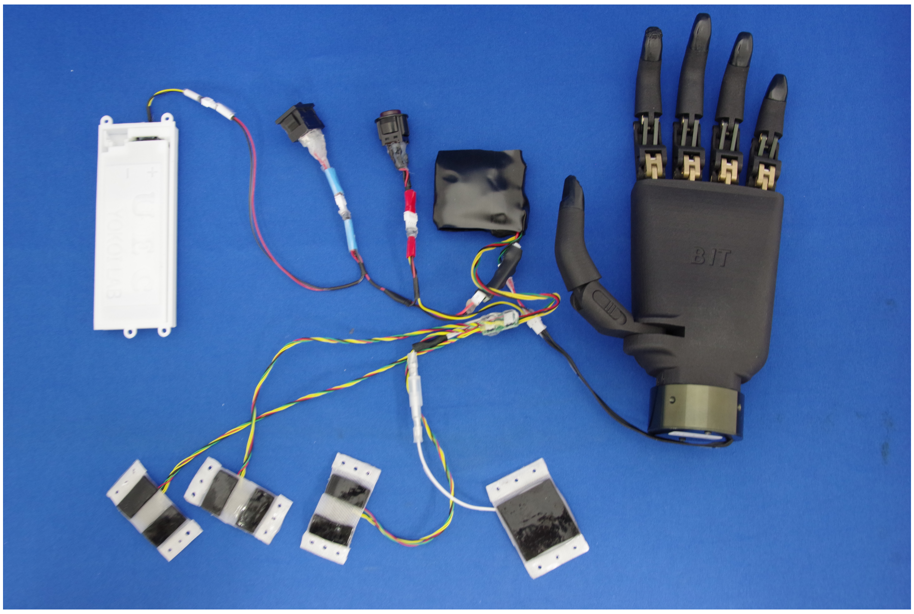

Fig.6.1: Illustration of BIT-UEC-Hand with each part connected

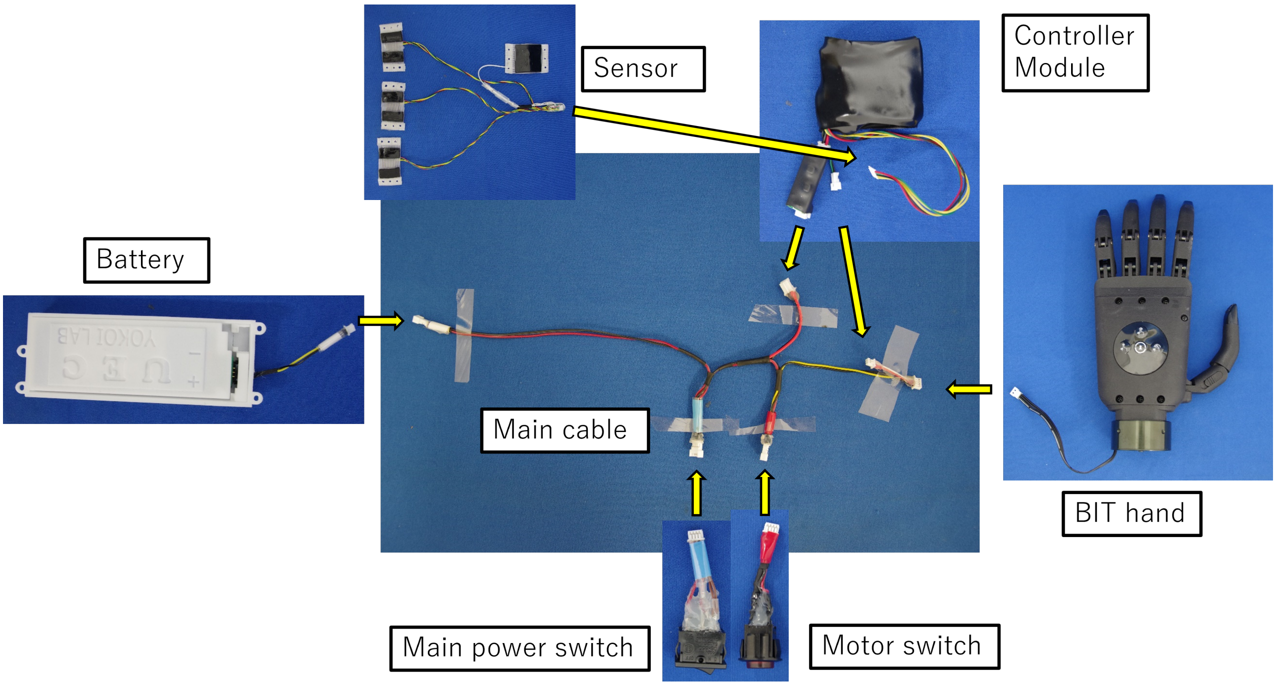

Fig.6.2: Schematic showing the connection of each connector of the BIT-UEC-Hand

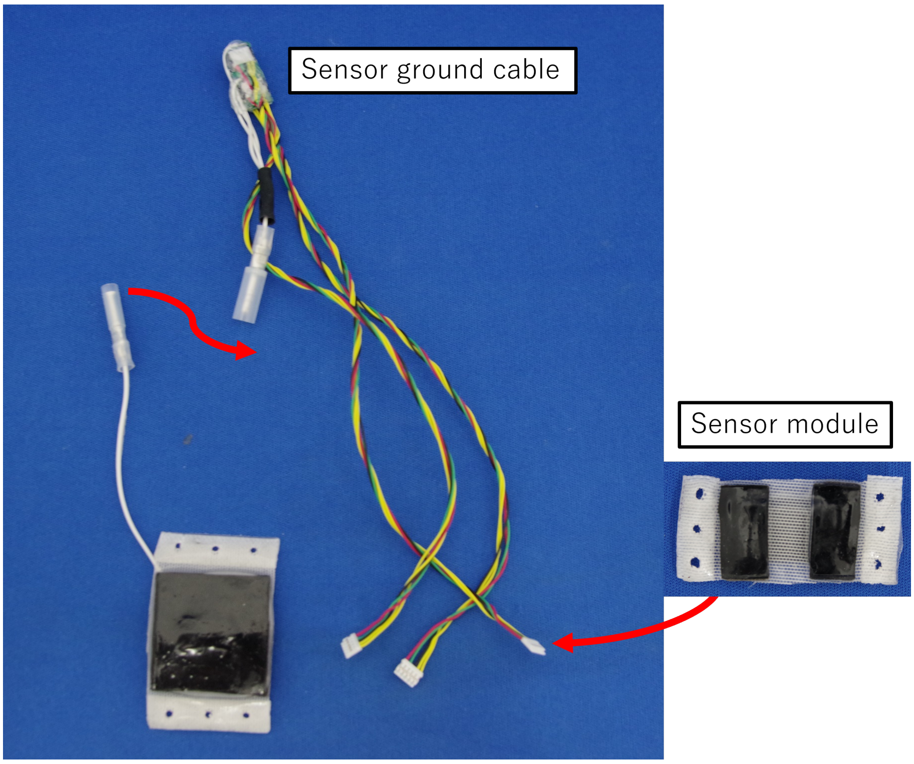

Fig.6.3: Schematic showing the connection of each sensor connector

6.3.2 Creation of Socket

The mold making, creation, and fitting of the socket to the human body must be conducted by a certified prosthetist according to the Artificial Limb Fitters Act (Act No. 61 of 1987). Therefore, the specifications of the socket were determined in consultation with a prosthetist.

An issue was encountered during the creation of the socket for the BIT-UEC-Hand related to the EMG sensors. The EMG sensors of the BIT-UEC-Hand are made of conductive silicone, and in a standard socket, the electrodes could become distorted when the residual limb is inserted, resulting in noise in the EMG signals.

Therefore, as a solution, we decided to use a two-layered cloth as shown in Fig.6.4 during the insertion of the residual limb into the socket, to prevent sensor distortion. A hole for pulling out the cloth, as illustrated in Fig.6.5, was made to remove the cloth after insertion. The cloth, made of the same material as parachutes with low friction resistance, reduces resistance due to skin friction, thus facilitating the insertion of the residual limb. Additionally, being double-layered, it enables the cloth to be pulled out without causing any relative movement of the skin to the socket.

The cloth is used as shown in Fig.6.6.

Fig.6.4: Cloth used during insertion of the residual limb into the socket.

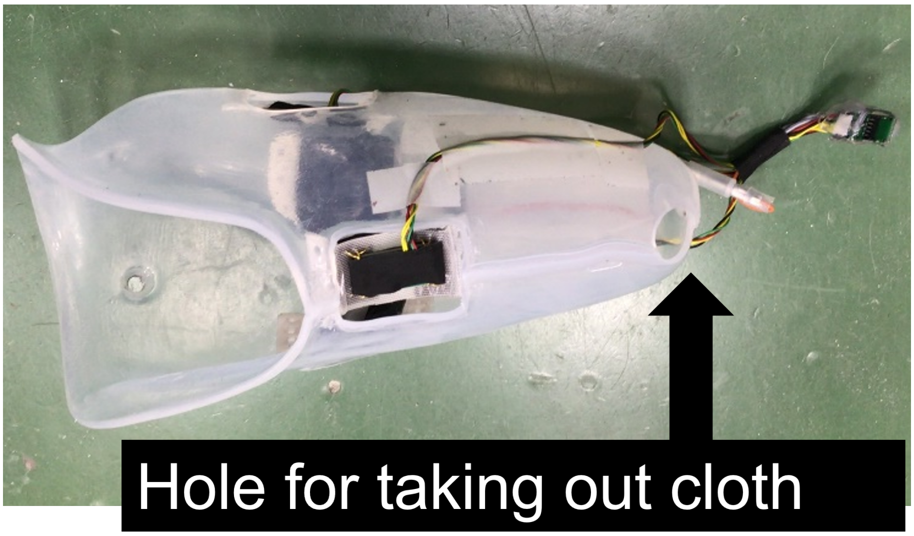

Fig.6.5: Position of the hole for pulling out the cloth after the residual limb is inserted into the socket.

Fig.6.6: Inserting the residual limb into the socket using the cloth.

6.4 Application for the registration of ready-made parts of the BIT-UEC-Hand

The sockets were fabricated in cooperation with Kowagishi Laboratory Co. Ltd., Tetsudou Kousaikai Prosthesis Support Center (public interest incorporated foundation), and Brace On R. Nagoya Corp. An evaluation was performed in cooperation with Toho-Kamagaya Hospital, Tokai University Hospital, and Brace On R-Nagoya Corp. The sockets produced by each prosthetic manufacturer and the evaluation of the BIT-UEC-Hand are summarized in Fig.6.7.

Mu-B ORG, Inc., a venture company from the Yokoi Laboratory of the University of Electro-Communications, applied the ready-made-parts.

	Participant A	Participant B	Participant C
Socket fabrication	Kowagishi Laboratory Co. Ltd. 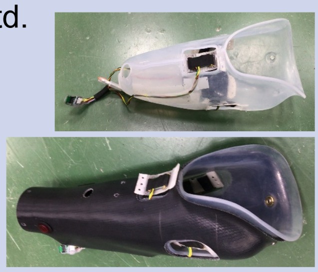	Tetsudou Kousaikai Prosthesis Support Center 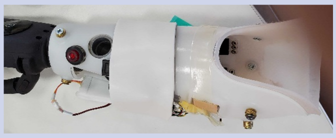	Brace On R. Nagoya Corp. 
Evaluation	Toho-Kamagaya Hospital 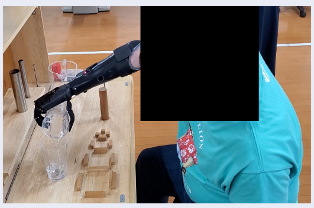	Tokai University Hospital 	Brace On R. Nagoya Corp. 

Fig.6.7: Sockets produced by each prosthetic manufacturer and the evaluation of the BIT-UEC-Hand.

6.5 Application results for ready-made parts

As a result of the application, BIT-UEC-Hand and its parts were registered as ready-made parts on March 31, 2022. The list of the registered parts is presented in Table.6.1. This has made it possible to purchase the BIT-UEC-Hand at public expense.

Table.6.1: List of registered parts

Part No.	Part Name	Price (yen)
MU001-HD-A-001	BIT ハンド (BIT hand)	1,130,000
MU002-SH-A-001	コントローラモジュール (Controller module)	259,560
MU003-EM-N-001	センサモジュール (Sensor module)	45,675
MU004-MT-N-001	モータスイッチ (Motor switch)	7,192
MU004-PS-N-001	主電源スイッチ (Main power switch)	7,088
MU004-PW-N-001	メインケーブル (Main cable)	12,050
MU004-SG-A-001	センサグランドケーブル (Sensor ground cable)	17,450
MU005-MB-N-001	バッテリーボックス (Battery box)	10,700
MU005-MB-N-002	バッテリー (Battery)	63,000
MU005-MB-N-003	バッテリーチャージャー (Battery charger)	15,000

6.6 Status of sales of ready-made parts

Only one BIT-UEC-Hand (excluding sales for research purposes) was purchased through the industrial accident compensation insurance as of March 5, 2023.

6.7 Application of the control system to a variety of participants

The control system developed in this study can be applied to various participants, not limited to multi-DOF prosthetic hands, by simply replacing the hand. Here, the application of the proposed system to various participants is summarized.

6.7.1 Application to the child's forearm MPH

We applied our developed control system to a child's MPH (Nakao et al. 2022) (Fig.6.8).

Figures 6.9-6.14 show the use of this MPH in performing ADL.

Fig.6.15 shows an elementary school boy using the MPH we developed naturally while reading a comic book.

Fig.6.8: MPH for children developed by our research group.

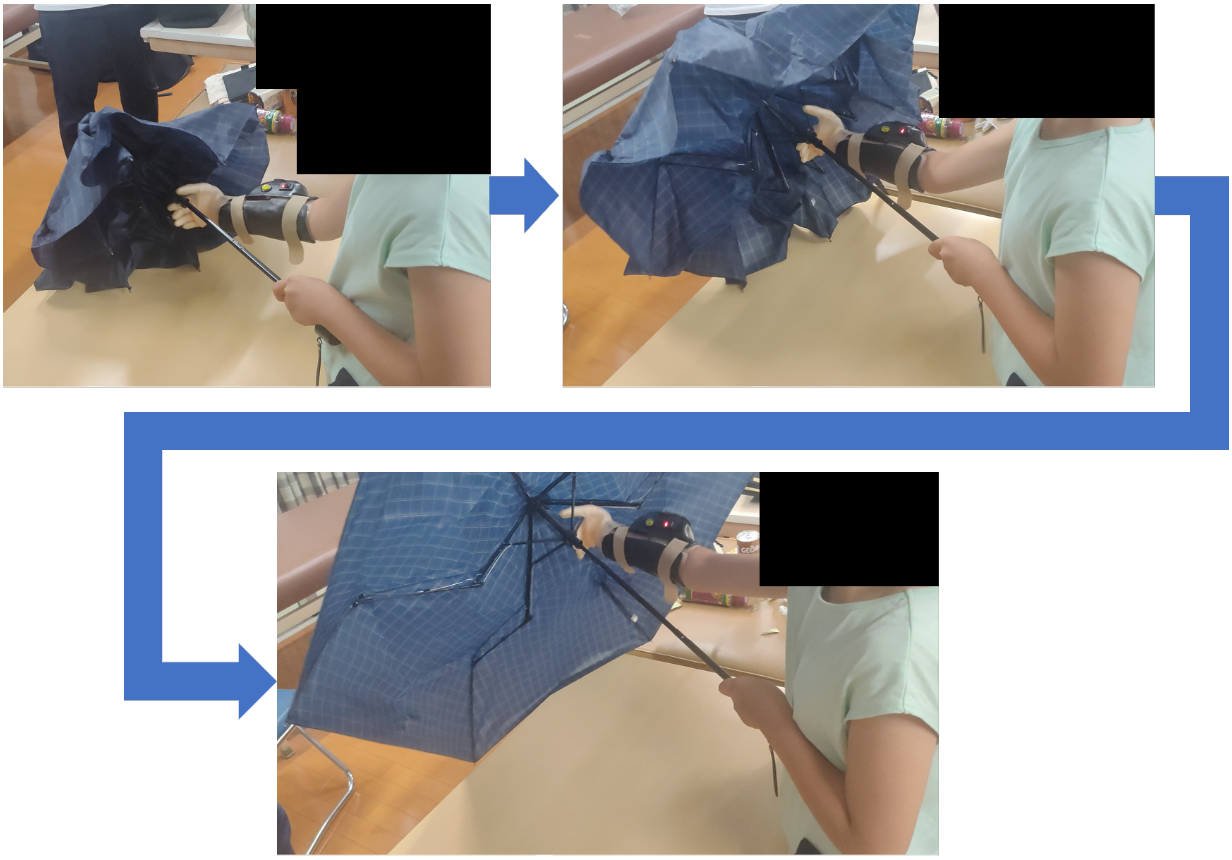

Fig.6.9: Use of the MPH to open an umbrella. The non-disabled hand held the umbrella handle while the MPH pushed up the runner to open the umbrella.

Fig.6.10: Using the MPH to sew fabric. The fabric was held with the MPH, and the non-disabled hand threaded the needle through the fabric.

Fig.6.11: Opening a can. The can was held with the MPH, and the stay-on-tab was opened using the fingers of the non-disabled hand.

Fig.6.12: Use of the MPH to hang laundry (towel). The towel was held with the MPH, and the non-disabled hand used a clothespin to fix it.

Fig.6.13: Use of the MPH to handle a toy frying pan. The handle of the frying pan was held with the prosthetic hand, and the non-disabled hand used a spatula.

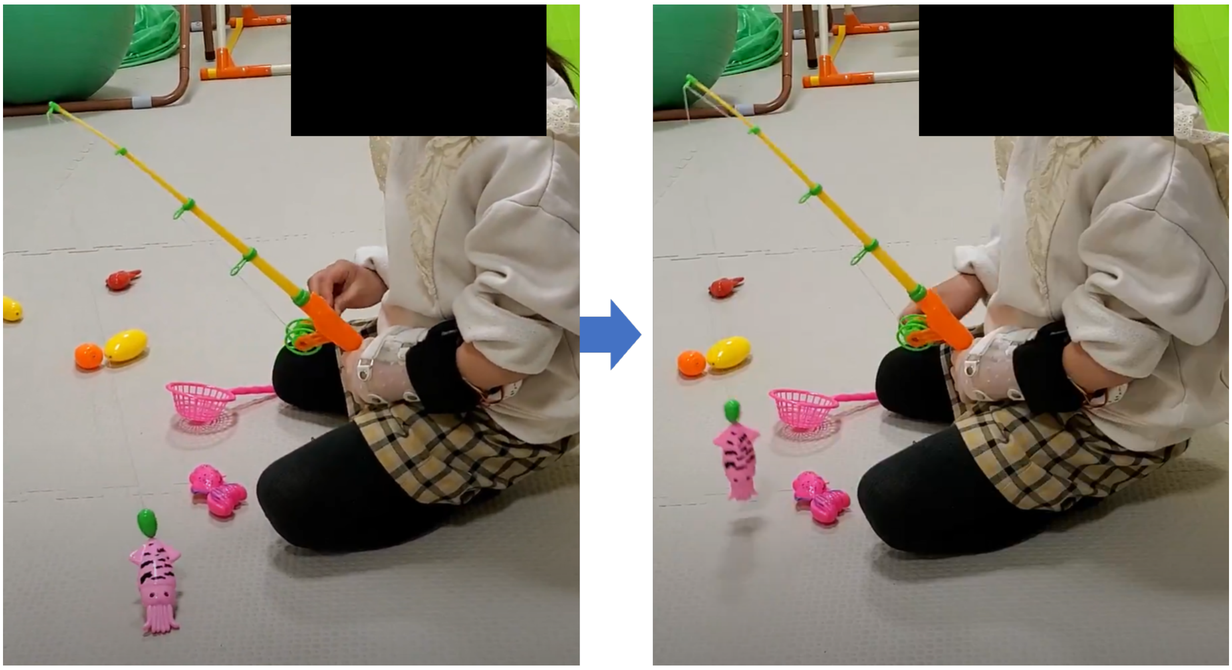

Fig.6.14: Use of the MPH to handle a fishing rod. The handle of the rod was held with the MPH, and the non-disabled hand turned the reel.

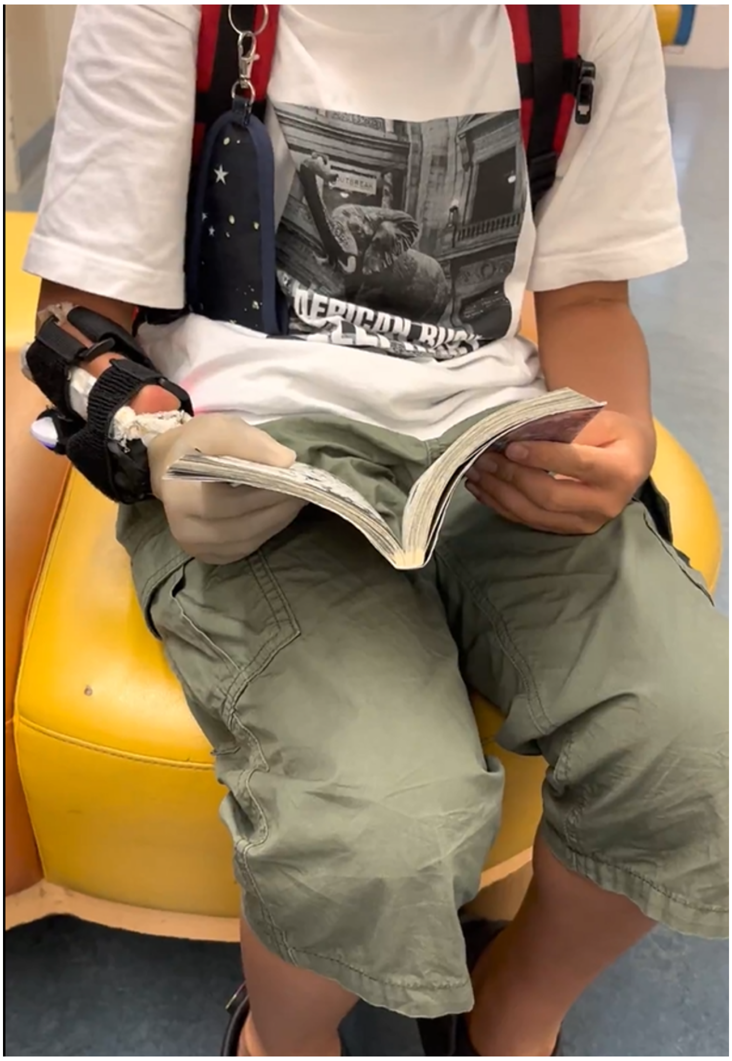

Fig.6.15: Use of the MPH to read a comic book. The primary school boy, a regular user of our developed MPH, naturally used it to read a comic book.

6.7.2 Application to the wrist-separated MPH for children

We applied our developed control system to a wrist-separated MPH for children (Inoue et al. 2023) (Fig.6.16).

Fig.6.17 shows the application of the developed MPH to move blocks placed at a high position.

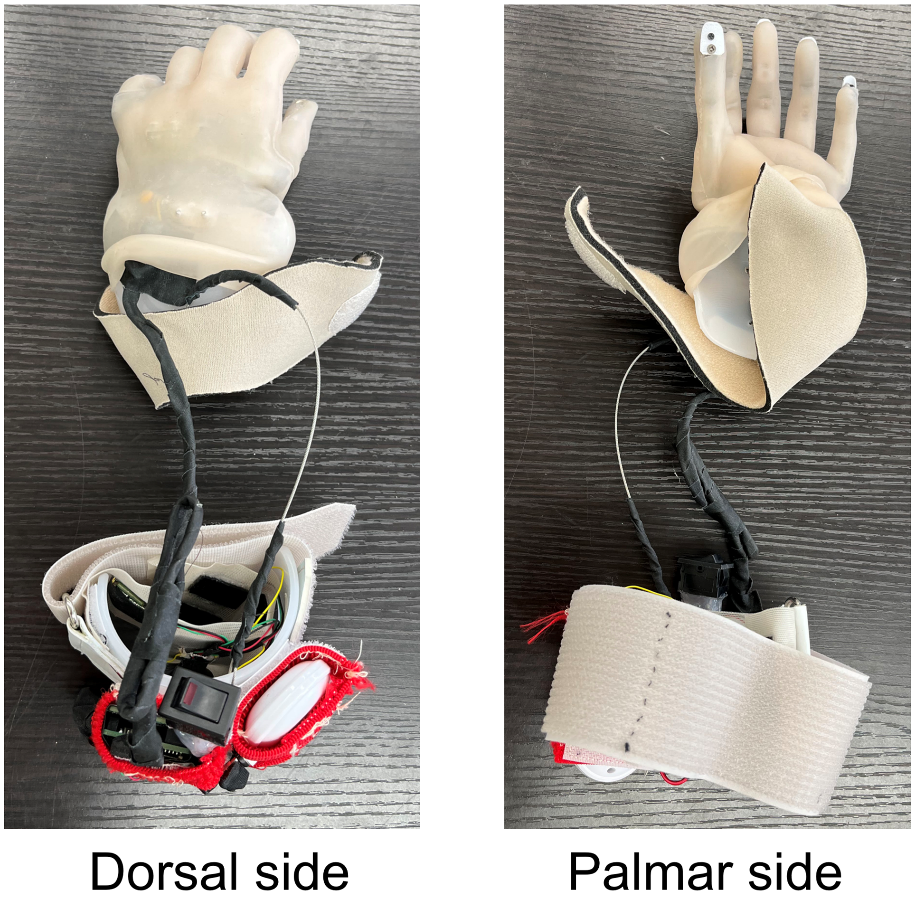

Fig.6.16: Wrist-separated MPH for children developed by our research group.

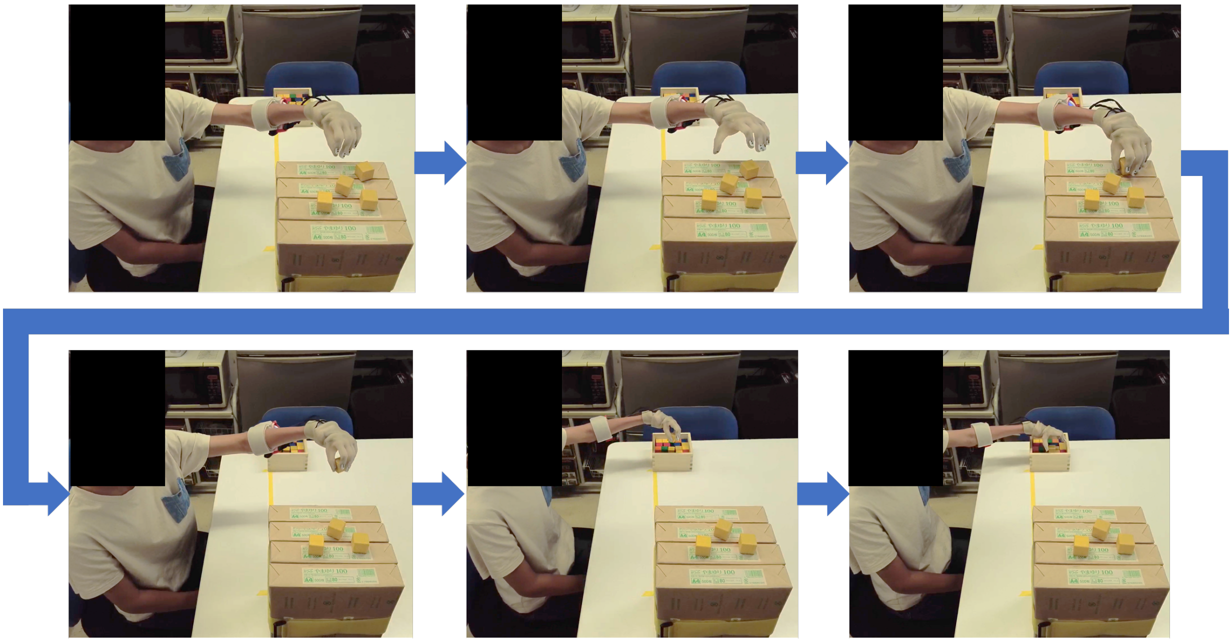

Fig.6.17: Grasping and moving a block in a high place with the MPH. The developed control system enables grasping and opening while utilizing the residual DOF of the wrist.

6.7.3 Application to the 2-DOF Forearm MPH for children

We applied our developed control system to the 2-DOF Forearm MPH for children (6.18) developed by our research group. This MPH had one DOF in the hand and another in the wrist, controlling hand grasping and opening movements, and wrist pronation and supination, respectively. To control this MPH, the proposed system must manage five motions, including rest.

Fig.6.18: Two-DOF forearm MPH for children developed by our research group.

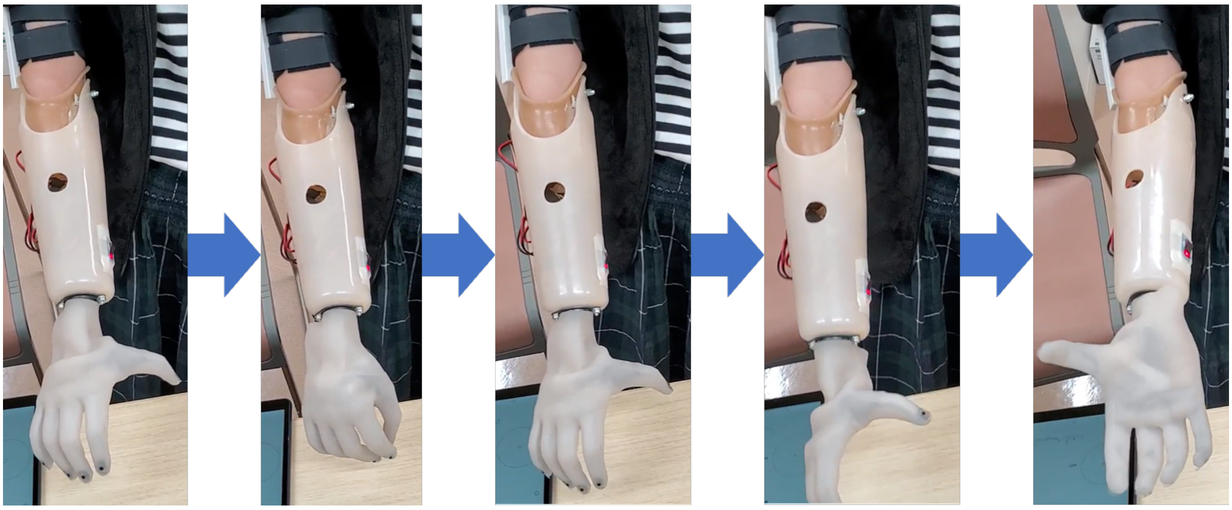

Fig.6.19: Use of the MPH to perform wrist pronation, supination, and opening/closing movements.

6.7.4 Application of the time variation adaptive system to various participants

We applied the time variation adaptive system developed in Chapter 4 to participants in various clinical situations of MPH use. The common measurement conditions for each verification are summarized in Table.6.2.

Table.6.2: Common Application Conditions

Measurement	
Sampling frequency (Hz)	2000
Quantization bit rate (bit)	12
Filter (Hardware)	· 50 Hz notch filter · Bandpass filter with a 1–1000 Hz bandwidth
Filter (Software)	50-Hz High pass filter
Potential range (V)	-2.5 to 2.5
Feature Extraction	
Period (ms)	10
Number of samples	256
Overlapping samples	236
Window function	Hann window
Extracted Frequency (Hz)	23.4375, 46.875, 70.3125, 93.75, 140.625, 187.5, 250.0, 312.5
Smoothing (points)	5
Bluetooth Communication	
Sending Period (ms)	20
Processing when sending accumulated feature vectors	Averaging
Motion Intention Estimation	
Method	Artificial Neural Networks (ANN)
Number of Neurons (input layer)	$D = 24$
Number of Neurons (hidden layer)	40
Number of Neurons (output layer)	3
Activate function	Sigmoid (hidden layer) Softmax (output layer)
Experiment	
Sampling points per measurement	20
Devices	
Microcomputer	SH72544R, Renesas Electronics Corporation
EMG sensor	Dry Electrode (Togo, Yuta, et al. 2019)
Smartphone	ROG Phone 3, ASUS

Time variation in cases of unstable control of certain movements

We applied the time variation adaptive system to an adult male with an upper limb amputation experiencing unstable recognition of the three-finger pinch during rest, grasp, open and three-finger pinch movements. After a period of adaptive learning, we conducted the first recognition rate measurement. After resuming and completing another phase of adaptive learning, we performed the second recognition rate measurement. The measurement omitted the open movement, and the conditions are summarized in Table.6.3. It should be noted that the number of data samples collected for the recognition rate measurement differed in each session.

The results are shown in Fig.6.20.

Table.6.3: Conditions of application for an adult male

Experiment	
Measurement motion	Rest, Grasp, 3 finger pinch
Sampling points for recognition rate	
Rest (1st)	40
Grasp (1st)	40
3 finger pinch (1st)	60
Rest (2nd)	120
Grasp (2nd)	120
3 finger pinch (2nd)	120

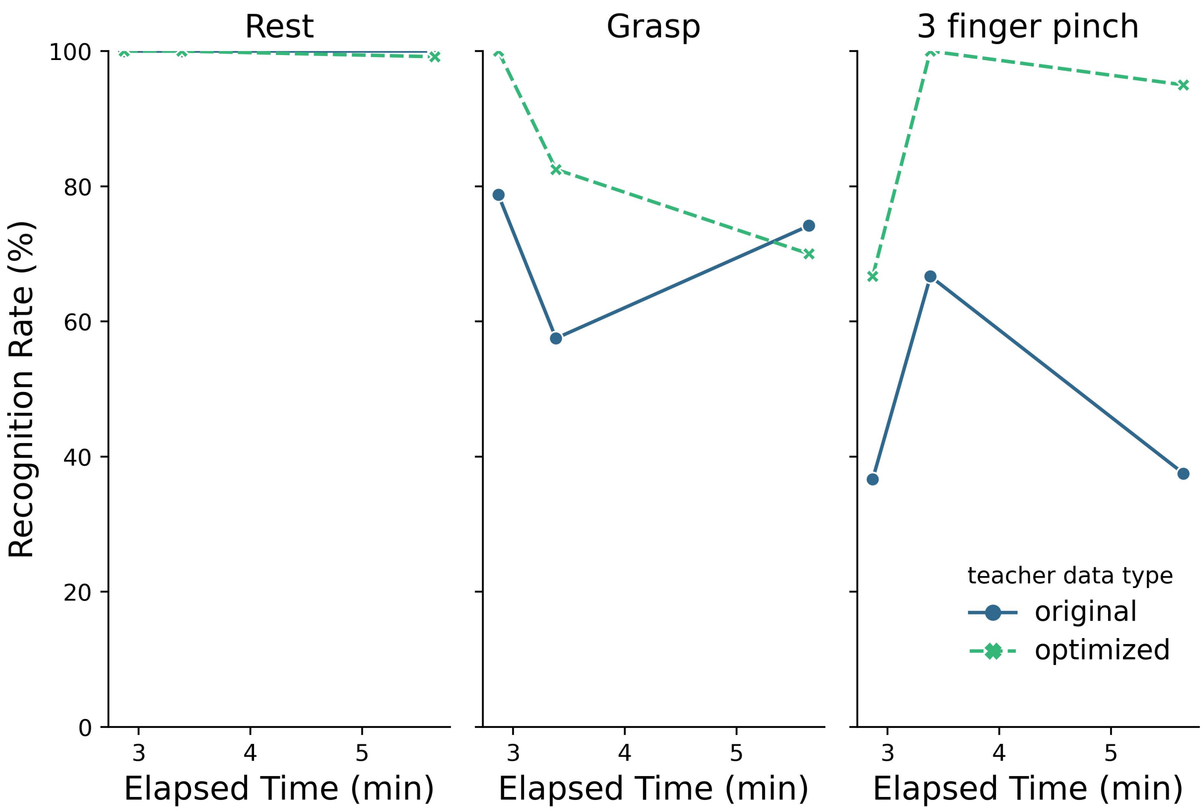

Fig.6.20: Changes in recognition rate when using the time variation adaptive system during unstable control. 'Original' represents the results measured using the classifier learned from the initial teacher data. 'Optimized' shows the results measured using the classifier learned from the teacher data updated by the time variation adaptive system. Notably, the 'optimized' classifier was always used for measuring the recognition rate.

Application of time variation adaptive system to a child

We applied the time variation adaptive system to a boy with palm hypoplasia and examined the changes in the recognition rate. The movements recognized were rest, grasp, and open. After measuring and learning from the teacher data (before adaptive learning), the first recognition rate measurement was conducted. After a period of adaptive learning, the second recognition rate measurement was performed. The conditions are summarized in Table.6.4. It should be noted that the number of data samples collected for the recognition rate measurement differed in each session.

The results are shown in Fig.6.21.

Table.6.4: Conditions of application for a male child

Experiment	
Measurement motion	Rest, Grasp, Open
Sampling points for recognition rate	
Rest (1st)	80
Grasp (1st)	80
Open (1st)	80
Rest (2nd)	160
Grasp (2nd)	120
Open (2nd)	140

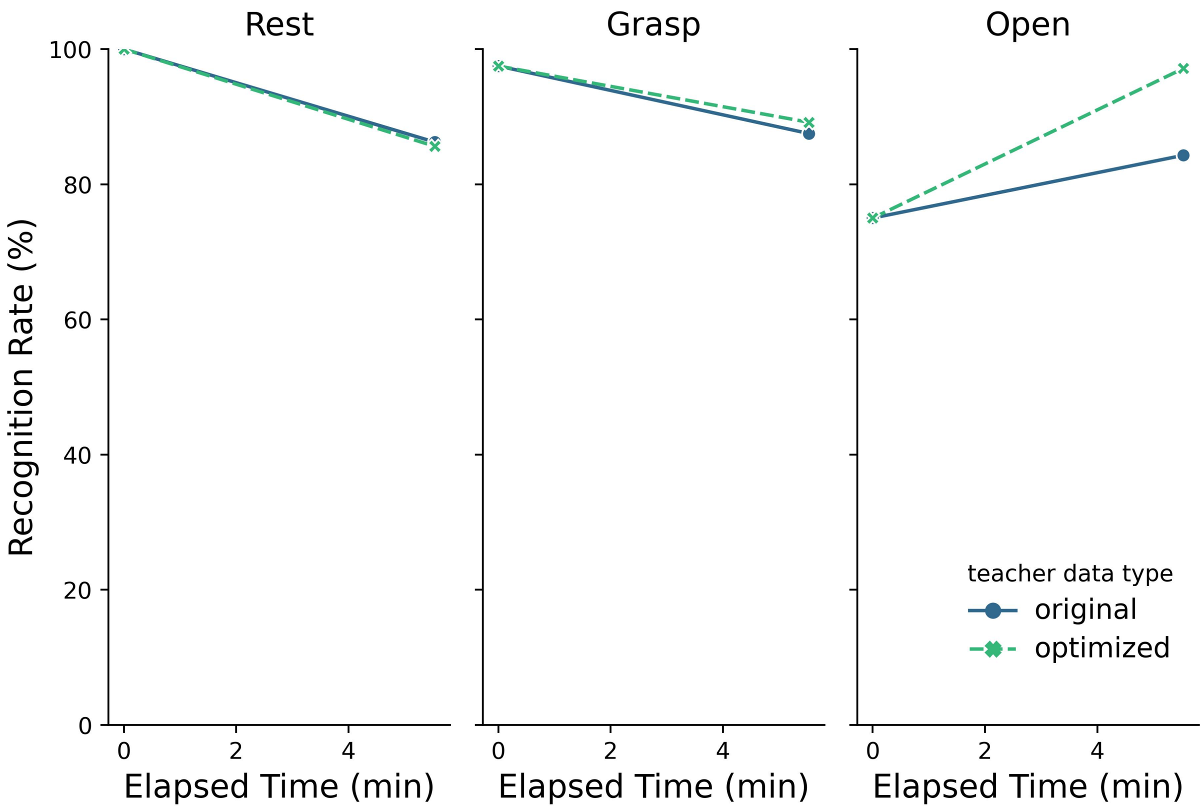

Fig.6.21: Changes in recognition rate when applying the time variation adaptive system to a child. 'Original' represents the results measured using the classifier learned from the initial teacher data. 'Optimized' shows the results measured using the classifier learned from the teacher data updated by the time variation adaptive system. Notably the 'optimized' classifier was always used for measuring the recognition rate.

6.8 Discussion

6.8.1 Regarding registration as ready-made parts

Only one BIT-UEC-Hand was purchased after approximately a year of registration as ready-made parts. There are only a few studies or reports on the sales of other commercially available multi-DOF MPHs in Japan, and prior studies have reported only a few cases of the purchase at one's own expense (Tanaka 2018). Therefore, the number of sales is not small. However, the purchaser was one of the participants in the clinical study of this MPH , and no purchases from third parties have been reported.

There are two reasons for this situation. The first reason is the lack of awareness among physicians. In the case of public expense and industrial accident compensation insurance, MPHs are selected by the physicians (Tanaka 2018). Therefore, it is difficult to be chosen as the MPH to be prescribed if it is not well-known to physicians. Therefore, making physicians aware of the related technology is essential. Ottobock and Ossur are the only two other companies selling a multi-DOF MPH. Both companies have been selling prosthetics for several years. Ottobock, in particular, has a large share of MPHs that are currently available (Tanaka 2018). This difference is significant, and for a start-up company to gain similar visibility, it would need to be well-known by exhibiting and presenting at a large number of related conferences, which is highly expensive and time-consuming .

The second reason is that the condition for receiving payment through industrial accident compensation insurance is that the MPH must be "well used" (Chin 2018). For this purpose, the patient must be trained to wear the MPH for 4 weeks in principle and for a maximum of 10 weeks. After a trial-wearing period of up to 6 months, the MPH is issued after a physician determines its suitability. In addition, the institutions that provide this training must also meet the prescribed conditions and are limited (Ministry of Health and Welfare n.d.[a]). Furthermore, prosthetic hands are necessary for training and are usually rented from the manufacturer or provided by the hospital. There are only a few applications of multi-DOF MPHs and pattern recognition-controlled MPHs, and training methods have not been established, as is the case with the long-established Myobock.

In particular, the only pattern recognition-controlled MPHs are the UEC-e hand (Togo, Hiroshi Yokoi, et al. 2020) and Ottobock's Myoplus, registered as ready-made parts in 2018 and 2022, respectively; therefore, it is expected that most rehabilitation physicians have never used them. Hence, the provision of prosthetic hands for training and the establishment of training programs will be necessary to disseminate the developed MPHs.

The field tests required for registering ready-made parts are a heavy burden, and it has become challenging to improve the hardware and register it as ready-made parts at a high frequency. Among these, the software is one element that can be improved relatively easily in MPHs. Ready-made parts are registered for hardware, and there is no registration for the software installed in them. Therefore, software improvement is considered an essential element for improving usability.

6.8.2 Application of proposed system to various participants

From the results of applying the control system in Sections 6.7.1, 6.7.2, and 6.7.3, it is evident that the proposed system can be applied to various types of participants.

Especially, as shown in Fig.6.9-6.14, the proposed system was applied to multiple elementary school girls and boys, enabling them to perform daily living tasks. This fact demonstrates that, in addition to the adult participants tested in Chapter 3, the proposed system is applicable to children, a group with fewer instances of MPH use.

The scenario depicted in Fig.6.15, where a boy who had been using our developed MPH at home naturally began using the MPH to read a comic book, also underscores the applicability of the proposed system.

Moreover, in Fig.6.17, the task of moving blocks was completed using a wrist-separated MPH. This demonstrated that stable operation of the MPH was possible even with wrist movement, using the proposed control system.

In Fig.6.19, control of the 2-DOF prosthetic hand for children, which requires five movements including rest, grasp, open, pronation, and supination, was achieved. This indicated that the proposed system could identify a variety of patterns even in the case of children.

Thus, the applicability of the control system developed in Chapter 3 to various participants has been confirmed.

In Section 6.7.4, the applicability of the developed time variation adaptive system to various participants was also confirmed.

Particularly, as shown in Fig.6.20, the application of the control system in a clinical setting, where issues such as time variation in a participant's myoelectric signals could lead to unstable control, confirmed an increase in the recognition rate of previously unstable movements, thereby emphasizing the effectiveness of the proposed time variation adaptive system.

Similarly, the increase in the recognition rate for children who find it difficult to label teacher data, as shown in Fig.6.4, suggests the system' s wide applicability to various participants and its high usability.

Therefore, the applicability of the time variation adaptive system developed in Chapter 4 to various participants was confirmed.

6.9 Conclusion

This chapter explained the requirements for the registration of the developed BIT-UEC-Hand as a ready-made part and discussed the current issues based on the sales situation after registration as well as the AMD provision process.

This chapter also summarized the application results of the system developed in this study to diverse subjects.

Section 6.2 described the requirements for registering an MPH as ready-made parts.

Section 6.3 described the attempt to modularize the BIT-UEC-Hand components, which is one of the requirements for their registration as ready-made parts.

Section 6.4 described the details regarding the application of the BIT-UEC-Hand.

Section 6.5 described the results of the ready-made-parts application, the details of the applied parts, and the pricing of the parts.

Section 6.6 described the current sales status of the parts.

Section 6.7 discussed the results of applying the control system to various participants.

Finally, Section 6.8 discussed the issues with the registration process for the ready-made parts and the widespread use of registered MPHs.

Chapter 7 Conclusion and Future Prospects

7.1 Conclusion

The objective of this study was as follows:

To clarify the problems of assistive technologies and systems for persons with disabilities through the actual development of a myoelectric prosthetic hand and to investigate methods for developing assistive technologies that can sustainably improve their QOL.

The following four approaches were used to achieve the objectives of this study:

- Development of a practical multi-degree-of-freedom (DOF) MPH system.
- Elucidation of the requirements of people with disabilities through functional and subjective evaluation in clinical application.
- Development of control methods to solve the issues related to pattern recognition obtained from clinical application.
- Improving user accessibility by registering inexpensive and highly functional MPHs as components for ready-made parts (完成用部品).

Here, we assessed whether the objective of improving the quality of life for upper limb amputees was achieved by comparing the research requirements outlined in Chapter 2 of this study with the research results.

7.1.1 Achievement of the engineering requirements

Here, we discuss the degree of fulfillment of the engineering requirements summarized in Table.2.10. The achievements are further compiled in Table.7.1.

Table.7.1: Achievement of engineering requirements

<table>
<tr><td colspan="2">Condition</td><td>Result</td></tr>
<tr><td colspan="2">Development of a practical MPH</td><td>• Five-finger independently driven MPH
• Lightweight (330 g)
• All peripheral devices inside the socket
• Users could four motions</td></tr>
<tr><td rowspan="2">Addressing the challenges of pattern recognition control</td><td>Control stability</td><td>• Unsupervised adaptation to narrow and wide time variations
• 2 min adaptation for narrow
• Improved the number of stable motions by average 1 motion
• 5 min adaptation for wide
• Stable MPH control with unlearned muscle contraction force</td></tr>
<tr><td>Limitation in number of actions</td><td>• Grasping 24 different objects
• Eight out of the 16 movements realized in Cutkosky's taxonomy.</td></tr>
</table>

Development of a practical MPH

A lightweight (330 g) five-finger independently driven MPH (BIT-UEC-Hand) was developed. All peripheral devices such as controllers were installed inside the socket. From Fig.3.13, it was shown that the user was able to use four motions (resting, grasping, opening, and three-finger pinching) to perform task evaluation.

The performance and wide applicability of this system were confirmed through application to diverse participants and various tasks. Particularly, as shown in Fig.7.1 (reproduced from Fig.3.17), the actual use of the BIT-UEC-Hand at work highlighted the effectiveness of the proposed system.

Additionally, children were able to perform complex tasks such as sewing fabric with a needle as shown in Fig.7.2 (reproduced from Fig.6.10). The system was also successfully applied to other child prosthetic hands, such as the wrist-separated type (Fig.7.3, reproduced from Fig.6.17) and the 2-DOF type (Fig.7.4, reproduced from Fig.6.19), demonstrating its broad applicability and practicality.

(a) Participant A harvesting a shiitake mushroom on the unaffected side by holding down the mushroom bed using the BIT-UEC-Hand

(b) Participant A holding and carrying a case containing shiitake mushrooms with both hands

(c) Participant A grabs dried mushrooms using the BIT-UEC-Hand and places them in a bag

Fig.7.1: Participant A working with the BIT-UEC-Hand (Reprinted).

Fig.7.2: Use of the MPH to sew fabric. The fabric was held by the MPH, and the non-disabled hand threaded the needle through the fabric (Reprinted).

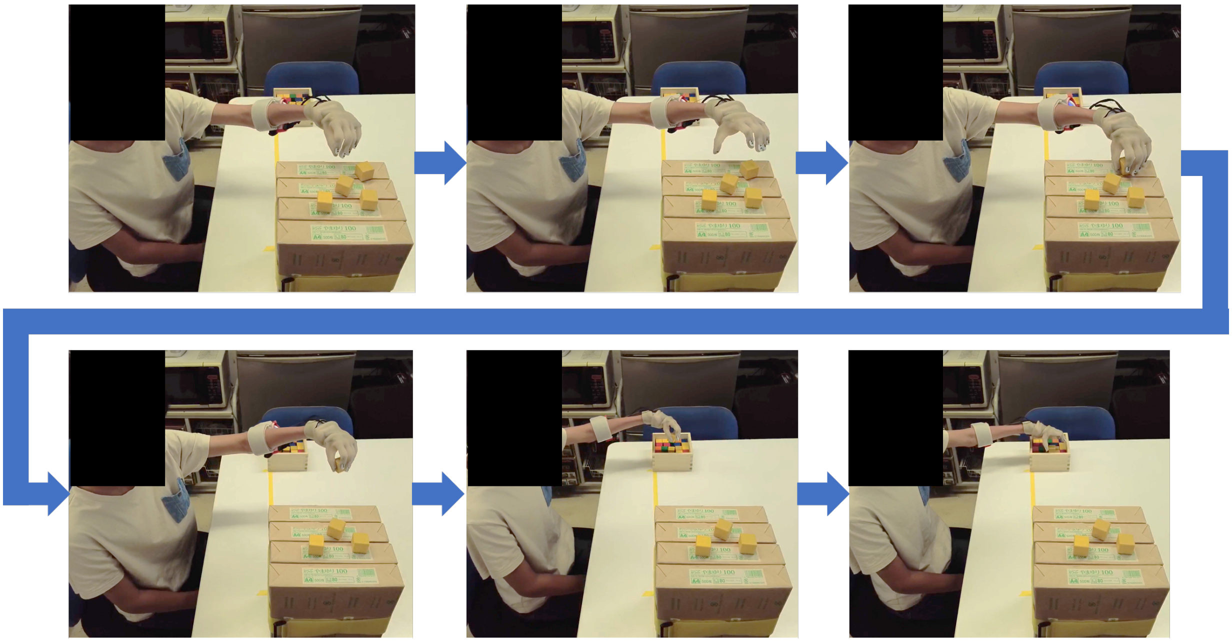

Fig.7.3: Grasping and moving a block in a high place using the MPH. The developed control system enables grasping and opening while utilizing the residual DOF of the wrist (Reprinted).

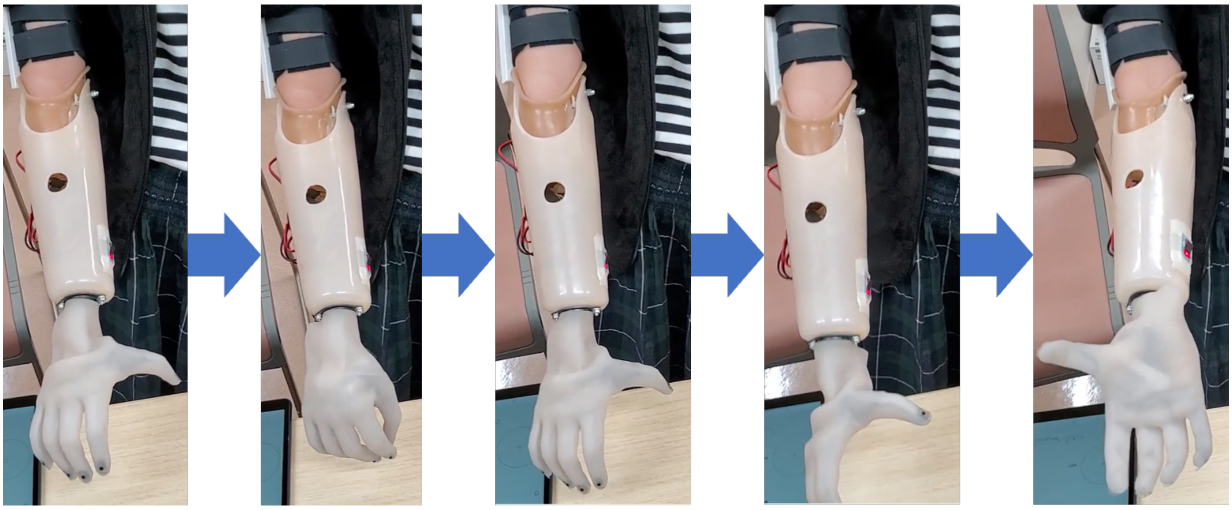

Fig.7.4: Use of the MPH to perform wrist pronation, supination, and opening/closing movements (Reprinted).

Addressing the challenges of pattern recognition control

Adaptation to narrow and wide time variations of myoelectricity was achieved by changing only the parameters and improving the recognition rate. For a wide range of time variations, 5 min of unsupervised adaptation resulted in stable MPH control with unlearned muscle contraction force. For the narrow range of time variation, only 2 min of unsupervised adaptation improved the number of stable motions by an average of one motion compared to the number of stable motions before adaptive learning (Fig.4.22).

Importantly, systems for time variation adaptation, previously limited to non-portable environments such as PCs, were made usable in real environments through the implementation of a parameter transfer system called the shadow system using portable devices such as tablets and smartphones. The performance of the time-variation adaptation function was confirmed not only in the basic performance evaluation in Chapter 4 but also in clinical settings dealing with control instabilities and applications to children, as discussed in Section 6.7.4. These findings suggest the potential of the proposed time variation adaptive system to expand the applicability of MPHs, even to users who previously found pattern recognition control challenging.

Furthermore, a controller capable of adaptively grasping 24 types of objects was developed and proven effective. By combining this controller with pattern recognition control, users no longer need to differentiate grasp movements for objects, freeing up muscle contraction patterns for other movements and reducing control load. The hidden design requirements of multi-DOF prosthetic hands for effective utilization of this controller were also validated through simulation. The results suggested the importance of replicating anatomical structures such as muscles, tendons, and ligaments of the human hand to stabilize the thumb control. Additional challenges, such as learning palm-based grasping and coordinating movements, were also suggested as important to enhance the functionality of the proposed method. The adaptive grasping based on the contact state information between the hand and object, proposed in this study, emphasizes the importance of the hand design, thus providing a stepping stone toward the practical application of the proposed method.

As a result of this study's development, the technologies in the roadmap in Fig.2.6 from Chapter 2.5 has progressed as shown in the following Fig.7.5. It should be noted that Fig.7.5 is an excerpt of the key parts of the roadmap. The technologies, previously represented by dashed lines, have progressed to the level indicated by the thick solid lines.

As described in this section, the implementation of adaptive learning methods in real environments was achieved, and adaptive grasping based on the tactile interaction between the hand and objects, previously unrealized in the field of MPHs, was proposed and validated. Particularly, the proposal of this adaptive grasping functionality signifies a shift in the design concept of multi-DOF prosthetic hands, from merely imitating the skeletal structure of the human hand to emulating its flexible structure.

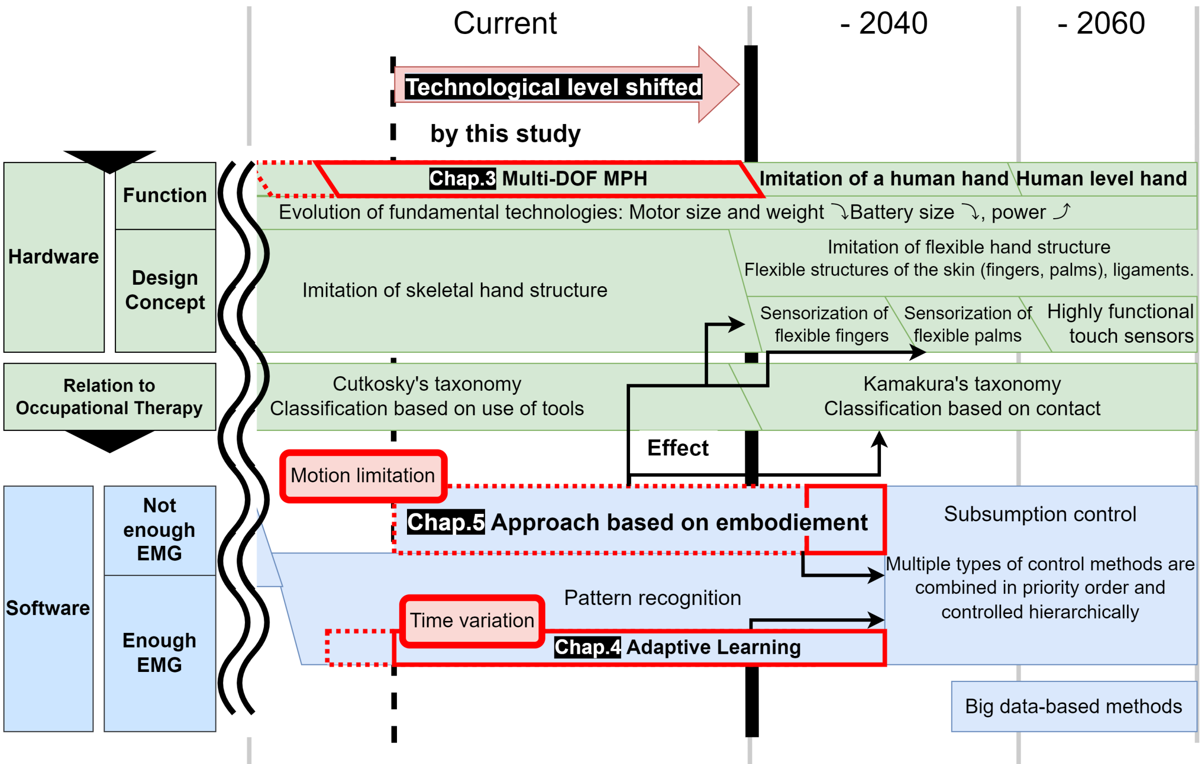

Fig.7.5: Illustration of how the technology level in the roadmap has progressed because of this study. Notably, this figure is an excerpt from the roadmap in Fig.2.6.

7.1.2 Achievement of the requirements related to rehabilitation and social implementation

Here, we discuss the extent to which the rehabilitation and social implementation requirements, summarized in Table.2.11, have been met. The achievements are further compiled in Table.7.2.

Table.7.2: Achievement of the requirements related to rehabilitation and social implementation

Condition	Result
Evaluation through Long-term clinical application	• Applied the MPH for approximately 3 months • Two participants • Periodic task and questionnaire evaluations • Revealed effectiveness in the workplace • Revealed burden of the training for pattern recognition • Revealed limitations of pattern recognition control
Improving user accessibility	• Registered as ready-made-parts • 1,130,000 yen • Same price range with Myobock

Evaluation through long-term clinical application

Two participants underwent long-term clinical application of the BIT-UEC-Hand for approximately 3 months. Periodic task and questionnaire evaluations were conducted. These revealed the possibility that the multi-DOF MPH was effective in the workplace and that pattern recognition control did not require as extensive training as indicated in previous studies; moreover, it revealed the limitations of pattern recognition control.

To conduct clinical research, we considered systems that could be implemented in real-world environments. This enabled us to identify and address challenges related to introducing the latest systems. Particularly, issues related to integrating EMG sensors into MPH sockets, as discussed in Section 6.3, were challenging points that could have been overlooked without clinical research. Although the performance of conductive silicone EMG sensors has been documented in studies such as (Togo, Yuta, et al. 2019), their practical integration with conventional prosthetic hand sockets had not been validated. This issue and its resolution, which were identified through clinical research-based development, underscore the effectiveness of this research approach in the field.

Improving user accessibility

The BIT-UEC-Hand was registered as ready-made-parts at 1,130,000 yen. The price of Myobock, a single-DOF MPH from Ottobock, which is commonly used in Japan, is 517,500 to 1,212,500 yen. A multi-DOF MPH was successfully registered as a ready-made-part at the same price range.

In addition, the fact that users who previously used low-DOF MPHs have purchased and are now using the BIT-UEC-Hand indicates that we have successfully enhanced the accessibility of multi-DOF MPHs for users.

7.1.3 Summary

After comparing the requirements of this study with the research results, it can be concluded that the development methodology of assistive technology for the disabled, based on clinical research, was effective. The technological issues of MPHs, such as the time variation of EMG signals and the limitation in the number of movements, were identified. Practical solutions for these issues have been implemented and validated. This has contributed to improving the accessibility of MPHs by expanding the range of application of MPHs. In addition, guidelines were clarified as a basis for research to further expand the range of application of MPHs. Furthermore, it was revealed that the accessibility to high-functioning MPHs was low due to issues in the distribution system. To address this, we improved accessibility by socially implementing cost-effective multi-DOF MPHs. Thus, approaches from both the individual and social models of disability were achieved, demonstrating the effectiveness of the proposed development methodology based on clinical research.

7.2 Future Prospects

The following is a list of problems that remain unsolved in this study.

7.2.1 Development of MPHs led by people with disabilities

In this study, as a research and developmental method that incorporates the needs of people with disabilities in a manner that does not deviate significantly from the current research and development process, a method to improve MPHs by obtaining feedback from long-term clinical application was developed. However, several needs could not be met without incorporating conditions from the initial stage of development, such as the need for actual fine movements (e.g., pressing a seal, pressing a camera shutter, etc.), among the demands expressed by the participants during the experimental process.

Of course, each user has unique needs, and these needs do not apply to all users. However, it is possible to develop a more versatile MPH by proactively incorporating users into the development process from the early stages of research and by integrating researchers' knowledge with the knowledge gained from the users' experiences.

7.2.2 Comparison with the existing multi-DOF MPHs

This study could not compare our proposed MPH system with the existing multi-DOF MPHs owing to availability issues. However, this comparison is essential to identify the areas of improvement.

7.2.3 Improvement of electric hand after long-term clinical application

In this study, improvements were focused on the software as re-registration of the ready-made parts was unnecessary. However, there are several problems with the electric hand, and it is essential to improve it. Specifically, the contact area during grasping should be increased, side grasping should be enabled, and the grasping shape should be more similar to that of a natural hand.

7.2.4 Development of benchmarks for the time variation tracking methods

A major problem in the research on time-variation tracking methods is the lack of effective benchmarks. This is because previous studies have focused on specific time variations, and no studies have classified and evaluated the time variation based on the speed of change. Therefore, it is difficult to compare each time-variation adaptation method and determine the superiority or inferiority of the methods. Thus, developing benchmarks and evaluation methods that enable comparisons between methods would be essential to further the research in this field.

謝辞

本研究の遂行にあたり，ご指導，ご協力を賜りました多くの方々に心から感謝申し上げます．

はじめに，著者の指導教員であり，多大なるご指導を賜りました

電気通信大学 情報理工学研究科 共同サステイナビリティ研究専攻 教授 横井浩史 先生

に心から感謝申し上げます．研究においては独創的なアイデア，適切な助言をいただき，また本研究の関連分野のみならず広い範囲の知識，知見についておしえていただきました．

また，共同サステイナビリティ研究専攻の先生方，学生の皆様にも授業や研究発表を通して，異なる視点から様々な意見をいただき，非常に励みになりました．

横井・姜・東郷研究室の先生方，先輩方，同期の皆様にも資料の添削や発表練習，研究室生活において大変お世話になりました．心より御礼申し上げます．

東京理科大学の助教である山野井 佑介先生の研究への助言や資料作成・発表方法などの丁寧な指導はとても励みになりました．厚く御礼申し上げます．

横井研究室の秘書兼研究員である矢吹佳子様にも非常にお世話になりました．困ったことがあるたびに相談に乗っていただき励みになりました．

パートナーである掛川智紘さんには本論文に掲載した一部の画像の作成を手伝っていただきました．また，彼女自身，障害を持ちながらも陰ながら必死に私をサポートしていただきました．深く感謝します．

そして，いつも私を支えてくれた家族，友人達に心からの感謝の意を表します．

This work was supported by JSPS KAKENHI (Grant Numbers: JP23H00166, JP23H03785, JP21K14125), JST SPRING (Grant Number JPMJSP2131), JKA through its Promotion funds from Keirin RACE, and the New Energy and Industrial Technology Development Organization (NEDO).

2024 年 3 月 25 日

Bibliography

Acemoglu, Daron and Joshua D. Angrist (Oct. 2001). "Consequences of Employment Protection? The Case of the Americans with Disabilities Act". In: *Journal of Political Economy* 109 (5), pp. 915–957. ISSN: 0022-3808. DOI: 10.1086/322836.

Atzori, Manfredo et al. (Jan. 2015). "Characterization of a Benchmark Database for Myoelectric Movement Classification". In: *IEEE Transactions on Neural Systems and Rehabilitation Engineering* 23 (1), pp. 73–83. ISSN: 1534-4320. DOI: 10.1109/TNSRE.2014.2328495.

Aultman, Julie M (2006). "Eugenomics: Eugenics and Ethics in the 21 st Century". In: *Genomics, Society and Policy* 2 (2), pp. 28–49. ISSN: 1746-5354.

Bekey, George A et al. (1993). "Knowledge-based control of grasping in robot hands using heuristics from human motor skills". In: *IEEE Transactions on Robotics and Automation* 9 (6), pp. 709–722. ISSN: 1042296X. DOI: 10.1109/70.265915.

Belter, Joseph T. et al. (2013). "Mechanical design and performance specifications of anthropomorphic prosthetic hands: A review". In: *Journal of Rehabilitation Research and Development* 50 (5), pp. 599–618. ISSN: 07487711. DOI: 10.1682/JRRD.2011.10.0188.

Bhaskaranand, Kumar, Anil K. Bhat, and K. Narayama Acharya (Sept. 2003). "Prosthetic rehabilitation in traumatic upper limb amputees (an Indian perspective)". In: *Archives of Orthopaedic and Trauma Surgery* 123 (7), pp. 363–366. ISSN: 09368051. DOI: 10.1007/s00402-003-0546-4.

Biddiss, Elaine and Tom Chau (2007). "Upper limb prosthesis use and abandonment: A survey of the last 25 years". In: *Prosthetics and Orthotics International* 31 (3), pp. 236–257. ISSN: 03093646. DOI: 10.1080/03093640600994581.

Biederman, Irving (1987). "Recognition-by-Components: A Theory of Human Image Understanding". In: *Psychological Review* 94 (2), pp. 115–147. ISSN: 0033295X. DOI: 10.1037/0033-295X.94.2.115.

Bongard, Josh (2010). "The utility of evolving simulated robot morphology increases with task complexity for object manipulation". In: *Artificial Life* 16 (3), pp. 201–223. ISSN: 10645462. DOI: 10.1162/artl.2010.Bongard.024.

Bottomley, A, A. B.Kinnier Wilson, and A. Nightingale (1963). "Muscle Substitutes and Myo-Electric Control". In: *Radio and Electronic Engineer* 26 (6), pp. 439–448. ISSN: 00337722. DOI: 10.1049/ree.1963.0169.

Bouffard, Jason et al. (2012). *Interactions Between the Phantom Limb Sensations, Prosthesis Use, and Rehabilitation as Seen by Amputees and Health Professionals.*

Brooks, R. (1986). "A robust layered control system for a mobile robot". In: *IEEE Journal on Robotics and Automation* 2 (1), pp. 14–23. ISSN: 0882-4967. DOI: 10.1109/JRA.1986.1087032.

Brosius, Jürgen and Martin Kreitman (July 2000). "Eugenics—evolutionary nonsense?" In: *Nature Genetics* 25 (3), pp. 253–253. ISSN: 1061-4036. DOI: 10.1038/76994.

Buchanan, Allen et al. (2001). *From chance to choice: Genetics and justice.* Cambridge University Press. ISBN: 1316583937.

Cabinet Office Japan (2012). *Annual Report on Government Measures for Persons with Disabilities (Summary) 2012.*

– (2022). *Annual Report on Government Measures for Persons with Disabilities (Summary) 2022.*

Carroll, Douglas (May 1965). "A quantitative test of upper extremity function". In: *Journal of Chronic Diseases* 18 (5), pp. 479–491. ISSN: 00219681. DOI: 10.1016/0021-9681(65)90030-5.

Chen, Wenrui and Caihua Xiong (Jan. 2016). "On Adaptive Grasp with Underactuated Anthropomorphic Hands". In: *Journal of Bionic Engineering* 13 (1), pp. 59–72. ISSN: 16726529. DOI: 10.1016/S1672-6529(14)60160-8.

Chin, Takaaki (2018). "Current Status and Views on the Future of Myoelectric Prosthesis (published in Japanese)". In: *The Japanese Journal of Rehabilitation Medicine* 55 (5), pp. 394–399.

Choi, Young Mi (2015). "Utilizing end User Input in Early Product Development". In: *Procedia Manufacturing* 3, pp. 2244–2250. ISSN: 23519789. DOI: 10.1016/j.promfg.2015.07.368.

Cifrek, Mario et al. (May 2009). "Surface EMG based muscle fatigue evaluation in biomechanics". In: *Clinical Biomechanics* 24 (4), pp. 327–340. ISSN: 02680033. DOI: 10.1016/j.clinbiomech.2009.01.010.

Cipriani, Christian, Marco Controzzi, and Maria Chiara Carrozza (2010). "Objectives, criteria and methods for the design of the SmartHand transradial prosthesis". In: *Robotica* 28 (6), pp. 919–927. ISSN: 02635747. DOI: 10.1017/S0263574709990750.

Cordella, Francesca et al. (2016). *Literature review on needs of upper limb prosthesis users*. DOI: 10.3389/fnins.2016.00209.

Cotugno, Giuseppe, Kaspar Althoefer, and Thrishantha Nanayakkara (2017). "The Role of the Thumb: Study of Finger Motion in Grasping and Reachability Space in Human and Robotic Hands". In: *IEEE Transactions on Systems, Man, and Cybernetics: Systems* 47 (7), pp. 1061–1070. ISSN: 21682232. DOI: 10.1109/TSMC.2016.2531679.

Cutkosky, Mark R (1989). "On Grasp Choice, Grasp Models, and the Design of Hands for Manufacturing Tasks". In: *IEEE Transactions on Robotics and Automation* 5 (3), pp. 269–279. DOI: 10.1109/70.34763.

Došen, Strahinja et al. (Aug. 2010). "Cognitive vision system for control of dexterous prosthetic hands: Experimental evaluation". In: *Journal of NeuroEngineering and Rehabilitation* 7 (1), pp. 1–14. ISSN: 17430003. DOI: 10.1186/1743-0003-7-42/FIGURES/10.

Egermann, Marcus, Philip Kasten, and Marc Thomsen (Aug. 2009). "Myoelectric hand prostheses in very young children". In: *International Orthopaedics* 33 (4), pp. 1101–1105. ISSN: 03412695. DOI: 10.1007/s00264-008-0615-y.

Engdahl, Susannah M. et al. (June 2015). "Surveying the interest of individuals with upper limb loss in novel prosthetic control techniques". In: *Journal of NeuroEngineering and Rehabilitation* 12 (1), pp. 1–11. ISSN: 17430003. DOI: 10.1186/s12984-015-0044-2.

Feder, J.N. et al. (Aug. 1996). "A novel MHC class I–like gene is mutated in patients with hereditary haemochromatosis". In: *Nature Genetics* 13 (4), pp. 399–408. ISSN: 1061-4036. DOI: 10.1038/ng0896-399.

Floreano, Dario and Stefano Nolfi (2007). "Handbook of Robotics Chapter 61 : Evolutionary Robotics". In.

Franzke, Andreas W. et al. (Aug. 2019). "Users' and therapists' perceptions of myoelectric multi-function upper limb prostheses with conventional and pattern recognition control". In: *PLoS ONE* 14 (8). ISSN: 19326203. DOI: 10.1371/journal.pone.0220899.

Fritsch, Kelly, Clare O'connor, and A K Thompson (2016). *Keywords for Radicals: The Contested Vocabulary of Late-Capitalist Struggle*. AK Press.

Fritzke, B (1995). "A growing neural gas network learns topologies". In: *Advances in Neural Information Processing Systems 7*, pp. 625–632.

Fukaya, Naoki and Yuki Ogasawara (2017). "Development of humanoid hand with cover integrated link mechanism for daily life work". In: *2017 IEEE 6th Global Conference on Consumer Electronics, GCCE 2017* 2017-Janua (Gcce), pp. 1–4. DOI: 10.1109/GCCE.2017.8229384.

Furui, Akira et al. (June 2019). "A myoelectric prosthetic hand with muscle synergy–based motion determination and impedance model–based biomimetic control". In: *Science Robotics* 4 (31). ISSN: 2470-9476. DOI: 10.1126/scirobotics.aaw6339.

Gama, João et al. (2014). *A survey on concept drift adaptation*. DOI: 10.1145/2523813.

Geethanjali, Purushothaman (July 2016). "Myoelectric control of prosthetic hands: state-of-the-art review". In: *Medical Devices: Evidence and Research* Volume 9, pp. 247–255. ISSN: 1179-1470. DOI: 10.2147/MDER.S91102.

Ghazaei, Ghazal et al. (2017). "Deep learning-based artificial vision for grasp classification in myoelectric hands". In: *Journal of Neural Engineering* 14 (3). ISSN: 17412552. DOI: 10.1088/1741-2552/aa6802.

Glynn, M K et al. (Aug. 1986). "Management of the upper-limb-deficient child with a powered prosthetic device." In: *Clinical orthopaedics and related research* (209), pp. 202–5. ISSN: 0009-921X.

Gu, Guoying et al. (Aug. 2021). "A soft neuroprosthetic hand providing simultaneous myoelectric control and tactile feedback". In: *Nature Biomedical Engineering 2021*, pp. 1–10. ISSN: 2157-846X. DOI: 10.1038/s41551-021-00767-0.

Gu, Yikun et al. (Apr. 2018). "Robust EMG pattern recognition in the presence of confounding factors: features, classifiers and adaptive learning". In: *Expert Systems with Applications* 96, pp. 208–217. ISSN: 09574174. DOI: 10.1016/j.eswa.2017.11.049.

Hamilton, R. and R. A. Dunsmuir (Dec. 2002). "Radiographic assessment of the relative lengths of the bones of the fingers of the human hand". In: *Journal of Hand Surgery* 27 B (6), pp. 546–548. ISSN: 02667681. DOI: 10.1054/jhsb.2002.0822.

Hamraie, Aimi and Kelly Fritsch (Apr. 2019). "Crip Technoscience Manifesto". In: *Catalyst: Feminism, Theory, Technoscience* 5 (1), pp. 1–33. ISSN: 2380-3312. DOI: 10.28968/cftt.v5i1.29607.

Hansen, Nikolaus, Dirk V. Arnold, and Anne Auger (Jan. 2015). "Evolution strategies". In: Springer Berlin Heidelberg, pp. 871–898. ISBN: 9783662435052. DOI: 10.1007/978-3-662-43505-2_44.

Hansen, Nikolaus and Anne Auger (2014). "Principled design of continuous stochastic search: From theory to practice". In: vol. 45. Springer, pp. 145–180. DOI: 10.1007/978-3-642-33206-7__8. URL: https://hal.inria.fr/hal-00808450v1.

Hargrove, L. et al. (Aug. 2007). "A Real-Time Pattern Recognition Based Myoelectric Control Usability Study Implemented in a Virtual Environment". In: IEEE, pp. 4842–4845. ISBN: 978-1-4244-0787-3. DOI: 10.1109/IEMBS.2007.4353424.

Hargrove, Levi J. et al. (Dec. 2017). "Myoelectric Pattern Recognition Outperforms Direct Control for Transhumeral Amputees with Targeted Muscle Reinnervation: A Randomized Clinical Trial". In: *Scientific Reports* 7 (1). ISSN: 20452322. DOI: 10.1038/s41598-017-14386-w.

Heller, Morton A., Gail J. Rogers, and Carl L. Perry (Jan. 1990). "Tactile pattern recognition with the optacon: Superior performance with active touch and the left hand". In: *Neuropsychologia* 28 (9), pp. 1003–1006. ISSN: 00283932. DOI: 10.1016/0028-3932(90)90114-4.

Hermansson, Liselotte M., Lennart Bodin, and Ann Christin Eliasson (Mar. 2006). "Intra- and inter-rater reliability of the assesment of capacity for myoelectric control". In: *Journal of Rehabilitation Medicine* 38 (2), pp. 118–123. ISSN: 00365505. DOI: 10.1080/16501970500312222.

Hermansson, Liselotte M., Anne G. Fisher, et al. (May 2005). "Assessmet of Capacity for Myoelectric Control: A new Rasch-built measure of prosthetic hand control". In: *Journal of Rehabilitation Medicine* 37 (3), pp. 166–171. ISSN: 16501977. DOI: 10.1080/16501970410024280.

Hioki, Masaaki et al. (2011). “Design and control of electromyogram prosthetic hand with high grasping force”. In: pp. 1128–1133. ISBN: 9781457721373. DOI: 10.1109/ROBIO.2011.6181439.

Hiraoka, Koichi et al. (2011). *Social welfare studies : social policy and social work [Shakai Fukushigaku] (published in Japanese))*. Yuhikaku Publishing.

Hiyoshi, Yutaro et al. (Aug. 2018). “Development of a parent wireless assistive interface for myoelectric prosthetic hands for children”. In: *Frontiers in Neurorobotics* 12 (AUG). ISSN: 16625218. DOI: 10.3389/fnbot.2018.00048.

Hori, Masatsugu (2021). *[Can Disability Studies Create a Symbiotic Society?] Shogaigaku wa kyosei shakai wo tsuukureruka (in Japanese)*. Akashi Shoten.

Hoshigawa, Suguru et al. (2015). “Structure design for a Two-DoF myoelectric prosthetic hand to realize basic hand functions in ADLs”. In: vol. 2015-Novem. IEEE, pp. 4781–4784. ISBN: 9781424492718. DOI: 10.1109/EMBC.2015.7319463.

Huang, Han-Pang et al. (n.d.). “EMG classification for prehensile postures using cascaded architecture of neural networks with self-organizing maps”. In: vol. 1. IEEE, pp. 1497–1502. ISBN: 0-7803-7736-2. DOI: 10.1109/ROBOT.2003.1241803.

Huang, Qi et al. (June 2017). “A novel unsupervised adaptive learning method for long-term electromyography (EMG) pattern recognition”. In: *Sensors (Switzerland)* 17 (6). ISSN: 14248220. DOI: 10.3390/s17061370.

Hudak, Pamela L. et al. (June 1996). “Development of an upper extremity outcome measure: The DASH (disabilities of the arm, shoulder, and head)”. In: *American Journal of Industrial Medicine* 29 (6), pp. 602–608. ISSN: 0271-3586. DOI: 10.1002/(SICI)1097-0274(199606)29:6<602::AID-AJIM4>3.0.CO;2-L.

Imaeda, Toshihiko et al. (July 2005). “Validation of the Japanese Society for Surgery of the Hand version of the Disability of the Arm, Shoulder, and Hand questionnaire”. In: *Journal of Orthopaedic Science* 10 (4), pp. 353–359. ISSN: 09492658. DOI: 10.1007/s00776-005-0917-5.

Inoue, Y. et al. (Mar. 2023). “Development of Separate Exoskeleton Socket of Wrist Joint on Myoelectric Prosthetic Hand for Congenital Defects with Symbrachydactyly”. In: IEEE, pp. 164–169. ISBN: 978-1-6654-9028-3. DOI: 10.1109/CBS55922.2023.10115392.

Ito, Asa (2019). *The Remembering Body [Kiokusuru Karada] (published in Japanese)*. Shunjusha.

Jang, Chul Ho et al. (2011). “A Survey on Activities of Daily Living and Occupations of Upper Extremity Amputees”. In: *Annals of Rehabilitation Medicine* 35 (6), p. 907. ISSN: 2234-0645. DOI: 10.5535/arm.2011.35.6.907.

Jeannerod, M et al. (July 1995). “Grasping objects: the cortical mechanisms of visuomotor transformation”. In: *Trends in Neurosciences* 18 (7), pp. 314–320. ISSN: 01662236. DOI: 10.1016/0166-2236(95)93921-J.

Jiang, Yinlai et al. (2014). “Development and evaluation of simplified EMG prosthetic hands”. In: pp. 1368–1373. ISBN: 9781479973965. DOI: 10.1109/ROBIO.2014.7090524.

Kafer, Alison (2013). *Feminist, queer, crip.* Indiana University Press. ISBN: 0253009413.

Kajimoto, Shu (Sept. 2013). “Issues through Financial Support for the Myoelectric Upper Limb Prosthesis under the Services and Supports for Persons with Disabilities Act”. In: *Japanese journal of occupational medicine and traumatology* 61 (5), pp. 305–308.

KAMAKURA, Noriko et al. (1978). “POSITIONAL PATTERNS FOR PREHENSION IN NORMAL HANDS”. In: *The Japanese Journal of Rehabilitation Medicine* 15 (2), pp. 65–82. ISSN: 0034-351X. DOI: 10.2490/jjrm1963.15.65.

Kasuya, Masahiro, Ryu Kato, and Hiroshi Yokoi (Aug. 2015). “Development of a Novel Post-Processing Algorithm for Myoelectric Pattern Classification”. In: *Transactions of Japanese Society for Medical and Biological Engineering* 53 (4), pp. 217–224. ISSN: 1347443X. DOI: 10.11239/ajsmbe.53.217.

Kato, R, H Yokoi, and T Arai (2006). “Real-time Learning Method for Adaptable Motion-Discrimination using Surface EMG Signal”. In: pp. 2127–2132. DOI: 10.1109/IROS.2006.282492.

Kato, Ryu (2008). “Study on rehabilitation of motor function using an EMG prosthetic hand that adapts to individual differences and temporal variations of EMG signals”. In.

Kato, Ryu and Hiroshi Yokoi (2009). “Evaluation of Motor Recovery by Using Adaptive Myoelectric Hand”. In: 27 (8), pp. 926–932.

KAWAMURA, Jiro et al. (1999). “The Upper-limb Amputees. A Survey and Trends in Kinki Area of Japan.” In: *The Japanese Journal of Rehabilitation Medicine* 36 (6), pp. 384–389. ISSN: 1880-778X. DOI: 10.2490/jjrm1963.36.384.

Kawamura, Jiro et al. (2001). “Financial Support System for Myoelectric Hands in Other Countries -Results of Questionnaire Using e-mail- (published in Japanese)”. In: *Japanese journal of occupational medicine and traumatology* 49, pp. 501–508.

Kaye, Richard and Stephan Konz (Sept. 1986). “Volume and Surface Area of the Hand”. In: *Proceedings of the Human Factors Society Annual Meeting* 30 (4), pp. 382–384. ISSN: 0163-5182. DOI: 10.1177/154193128603000417.

Kim, ChoYeop and WonYoung Kim (2021). *Becoming a Cyborg [Cyborg ni naru] (published in Japanese)*. Iwanami Shoten.

Kingma, Diederik P. and Jimmy Lei Ba (2015). “Adam: A method for stochastic optimization”. In: *3rd International Conference on Learning Representations, ICLR 2015 - Conference Track Proceedings*, pp. 1–15.

Kitagawa, Yuya (2018). *Policy Studies in Disability Welfare [Shogaisha Fukushi no Seisakugaku] (published in Japanese))*. Koyoshobo.

Kong, Yong-Ku et al. (Nov. 2011). “Individual finger contribution in submaximal voluntary contraction of gripping”. In: *Ergonomics* 54 (11), pp. 1072–1080. ISSN: 0014-0139. DOI: 10.1080/00140139.2011.620176.

Kouchi, Makiko (2012). *AIST Nihonjin no Te no Sunpo Data (AIST Dimension Data of Japanese Hand)*. URL: https://www.airc.aist.go.jp/dhrt/hand/index.html.

Krawczyk, Bartosz and Alberto Cano (July 2018). “Online ensemble learning with abstaining classifiers for drifting and noisy data streams”. In: *Applied Soft Computing Journal* 68, pp. 677–692. ISSN: 15684946. DOI: 10.1016/j.asoc.2017.12.008.

Kuiken, Todd A et al. (Feb. 2007). “Targeted reinnervation for enhanced prosthetic arm function in a woman with a proximal amputation: a case study”. In: *The Lancet* 369 (9559), pp. 371–380. ISSN: 01406736. DOI: 10.1016/S0140-6736(07)60193-7.

Kuiken, Todd A. et al. (2016). “A Comparison of Pattern Recognition Control and Direct Control of a Multiple Degree-of-Freedom Transradial Prosthesis”. In: *IEEE Journal of Translational Engineering in Health and Medicine* 4. ISSN: 21682372. DOI: 10.1109/JTEHM.2016.2616123.

Kuo, Li-Chieh et al. (Oct. 2009). “Functional workspace for precision manipulation between thumb and fingers in normal hands”. In: *Journal of Electromyography and Kinesiology* 19 (5), pp. 829–839. ISSN: 10506411. DOI: 10.1016/j.jelekin.2008.07.008.

Kuroda, Yuki et al. (2022). “Coevolution of Myoelectric Hand Control under the Tactile Interaction among Fingers and Objects”. In: *Cyborg and Bionic Systems* 2022. DOI: 10.34133/2022/9861875. eprint: https://spj.science.org/doi/pdf/10.34133/2022/9861875. URL: https://spj.science.org/doi/abs/10.34133/2022/9861875.

Kyberd, Peter J. and Wendy Hill (June 2011). “Survey of upper limb prosthesis users in Sweden, the United Kingdom and Canada”. In: *Prosthetics and Orthotics International* 35 (2), pp. 234–241. ISSN: 03093646. DOI: 10.1177/0309364611409099.

Kyberd, Peter J., Constanze Wartenberg, et al. (Apr. 2007). “Survey of Upper-Extremity Prosthesis Users in Sweden and the United Kingdom”. In: *JPO Journal of Prosthetics and Orthotics* 19 (2), pp. 55–62. ISSN: 1040-8800. DOI: 10.1097/JPO.0b013e3180459df6.

Ladd-Taylor, Molly (2017). *Fixing the poor: Eugenic sterilization and child welfare in the twentieth century.* JHU Press. ISBN: 1421423731.

Laming, D R J (1968). *Information theory of choice-reaction times.* Academic Press.

Lessard, Steven et al. (Nov. 2016). “A bio-inspired tensegrity manipulator with multi-DOF, structurally compliant joints”. In: vol. 2016-November. Institute of Electrical and Electronics Engineers Inc., pp. 5515–5520. ISBN: 9781509037629. DOI: 10.1109/IROS.2016.7759811.

Light, Colin M., Paul H. Chappell, and Peter J. Kyberd (2002). “Establishing a standardized clinical assessment tool of pathologic and prosthetic hand function: Normative data, reliability, and validity”. In: *Archives of Physical Medicine and Rehabilitation* 83 (6), pp. 776–783. ISSN: 00039993. DOI: 10.1053/apmr.2002.32737.

Liu, Yixiang et al. (Feb. 2022). “A review on tensegrity structures-based robots”. In: *Mechanism and Machine Theory* 168, p. 104571. ISSN: 0094114X. DOI: 10.1016/j.mechmachtheory.2021.104571.

Lock, Blair, Kevin Englehart, and Bernard Hudgins (Jan. 2005). “Real-time myoelectric control in a virtual environment to relate usability vs. accuracy”. In: *MyoElectric Controls/Powered Prosthetics Symposium, Fredericton.*

Lombardo, Paul A. (Nov. 2018). *The power of heredity and the relevance of eugenic history.* DOI: 10.1038/s41436-018-0123-4.

Luchetti, Martina et al. (2015). "Impact of Michelangelo prosthetic hand: Findings from a crossover longitudinal study". In: *Journal of Rehabilitation Research and Development* 52 (5), pp. 605–618. ISSN: 19381352. DOI: 10.1682/JRRD.2014.11.0283.

MacLachlan, Malcolm et al. (July 2018). "Assistive technology policy: a position paper from the first global research, innovation, and education on assistive technology (GREAT) summit". In: *Disability and Rehabilitation: Assistive Technology* 13 (5), pp. 454–466. ISSN: 17483115. DOI: 10.1080/17483107.2018.1468496.

Mao, Yuyi et al. (Jan. 2017). "A Survey on Mobile Edge Computing: The Communication Perspective". In: *IEEE Communications Surveys & Tutorials* 19 (4), pp. 2322–2358. ISSN: 1553-877X. DOI: 10.1109/COMST.2017.2745201.

Massera, Gianluca, Angelo Cangelosi, and Stefano Nolfi (2007). "Evolution of prehension ability in an anthropomorphic neurorobotic arm". In: *Frontiers in Neurorobotics* 1 (NOV), pp. 1–9. ISSN: 16625218. DOI: 10.3389/neuro.12.004.2007.

Mathiowetz, V. et al. (1985). "Adult norms for the Box and Block Test of manual dexterity." In: *The American journal of occupational therapy. : official publication of the American Occupational Therapy Association* 39 (6), pp. 386–391. ISSN: 02729490. DOI: 10.5014/ajot.39.6.386.

Ministry of Foreign Affairs of Japan (Feb. 2023). *Convention on the Rights of Persons with Disabilities*. URL: https://www.mofa.go.jp/mofaj/gaiko/jinken/index_shogaisha.html.

Ministry of Health, Labour and Welfare (2010). *Basic agreement document between the plaintiffs and defense lawyers of the lawsuit for unconstitutionality of the Services and Supports for Persons with Disabilities Act and the national government (Ministry of Health, Labor and Welfare) (published in Japanese)*.

– (n.d.[a]). *Information on the reimbursement system for prosthetic limbs and other prosthetic devices [Gishi tou Hosouguhi Shikyuseido no Goannai] (published in Japanese)*. URL: https://www.mhlw.go.jp/content/11400000/001029333.pdf.

– (n.d.[b]). *Overview of the prosthetic device provision system [Hosoguhi shikyusedo no gaiyo] (published in Japanese)*. URL: https://www.mhlw.go.jp/stf/seisakunitsuite/bunya/hukushi_kaigo/shougaishahukushi/yogu/aiyo.html.

Miyata, Natsuki et al. (2011). "Individual hand model to reconstruct behavior from motion capture data". In: IEEE, pp. 1951–1956. ISBN: 9781612843865. DOI: 10.1109/ICRA.2011.5979768.

Mont, Daniel (2007). *Measuring disability prevalence*. Vol. 706. Citeseer.

Morton, John and Mark H. Johnson (1991). "CONSPEC and CONLERN: A two-process theory of infant face recognition." In: *Psychological Review* 98 (2), pp. 164–181. ISSN: 1939-1471. DOI: 10.1037/0033-295X.98.2.164.

Murata, Akira et al. (2000). "Selectivity for the shape, size, and orientation of objects for grasping in neurons of monkey parietal area AIP". In: *Journal of Neurophysiology* 83 (5), pp. 2580–2601. ISSN: 00223077. DOI: 10.1152/jn.2000.83.5.2580.

Nakagawa, Jun and Hideki Nitta (2015). *Japanese Disability Laws [Nihon no Shogaiho] (published in Japanese)*. Seibundoh.

Nakao, Soichiro et al. (2022). "Development of Robotic Hand for Prosthetic Limb using a Gear Mechanism for Infants with Congenital Upper Limb Defects". In: *Journal of the Robotics Society of Japan* 40 (10), pp. 40–903. ISSN: 0289-1824. DOI: 10.7210/jrsj.40.903.

Nanayakkara, Visakha K. et al. (June 2017). "The Role of Morphology of the Thumb in Anthropomorphic Grasping: A Review". In: *Frontiers in Mechanical Engineering* 3. ISSN: 2297-3079. DOI: 10.3389/fmech.2017.00005.

Napier, JR (1956). "The prehensile movements of the human hand. (British Volume)". In: pp. 902–913. DOI: 13376678.

National Council on Disability (2007). *The Impact of the Americans with Disabilities Act: Assessing the Progress Toward Achieving the Goals of the ADA*. URL: www.ncd.gov.

Natsuki, Oka and Seiji Yamada (2006). "Interaction Design for Adaptation [published in Japanese]". In: *Journal of the Japanese Society for Artificial Intelligence* 21 (6), pp. 642–647. DOI: 10.11517/jjsai.21.6_642.

Nielsen, Johnny L.G. et al. (2009). "Enhanced EMG signal processing for simultaneous and proportional myoelectric control". In: pp. 4335–4338. ISBN: 9781424432967. DOI: 10.1109/IEMBS.2009.5332745.

NISHIKAWA, Daisuke et al. (Dec. 2001). "On-Line Supervising Mechanism for Learning Data in Surface Electromyogram Motion Classifiers". In: *The Transactions of the Insti-*

tute of Electronics, Information and Communication Engineers J84-D-2 (12), pp. 2634–2643.

Nishikawa, Daisuke et al. (2000). “On-line learning based electromyogram to forearm motion classifier with motor skill evaluation”. In: *JSME International Journal, Series C: Mechanical Systems, Machine Elements and Manufacturing* 43 (4), pp. 906–915. ISSN: 13447653. DOI: 10.1299/jsmec.43.906.

Notake, Yukimasa (2005). “Why Are Babies with Malformations Born? - The Strategies of Life and the Genetic Pool [published in Japanese]”. In: *Journal of the Showa Medical Association* 65 (4), pp. 307–317. DOI: 10.14930/jsma1939.65.307.

Ogawa, Yoshimichi and Akihiro Sugino (2014). *[Understanding Disability Studies] Yokuwakaru Shogaigaku (in Japanese).* Minerva Shobo.

Okamura, Mihoko (2015). “Japan’s Policy for Supporting People with Disabilities : Focusing on Legislation to Ratify the Convention on the Rights of Persons with Disabilities (published in Japanese)”. In: *The Reference.*

Össur (Sept. 2018). *GRIP CHIPS.* URL: https://training.touchbionics.com/pdfs/gripchips_sale-sheet_a4_US_HR_FINAL.pdf.

Ostlie, Kristin et al. (Nov. 2012). “Prosthesis use in adult acquired major upper-limb amputees: Patterns of wear, prosthetic skills and the actual use of prostheses in activities of daily life”. In: *Disability and Rehabilitation: Assistive Technology* 7 (6), pp. 479–493. ISSN: 17483107. DOI: 10.3109/17483107.2011.653296.

Ottobock (n.d.[a]). *8E38 Quick change hand (published in Japanese).* URL: https://www.ottobock.com/ja-jp/prosthetic_ue/myoelectric/myobock/8e38.

– (2022). *bebionic Reimbursement Guide.*

– (2018). *Michelangelo.* URL: https://www.ottobockus.com/media/local-media/prosthetics/upper-limb/michelangelo/files/embrace-the-everyday-with-michelangelo.pdf.

– (n.d.[b]). *Prosthetics 2022 Upper limb.* URL: https://downloads.ctfassets.net/8ks1shyq5m87/1Qp3nC2VkzncIdh48M78zf/de1e991c84cbe1f6f57c6498ea061c02/Prosthetics_UL_2022_catalogus.pdf.

Ottobock US (n.d.). *bebionic.* URL: https://www.ottobockus.com/prosthetics/upper-limb-prosthetics/solution-overview/bebionic-hand/%5C#video-2.

Ottoobock Japan (n.d.). *Ottobock Myoelectric Electric Prosthetic Hand System (published in Japanese).* URL: https://assets.ctfassets.net/8ks1shyq5m87/1L39xfgiJZEDpC3f6R6k30/9511c7f8c85b1617df88745a50b7cf1f/cat_myoelectric_2021.pdf.

Pacific Supply Co., Ltd (n.d.). *i-limb (published in Japanese).* URL: https://www.p-supply.co.jp/ossur/catalog/touch-bionics.

Parajuli, Nawadita et al. (Oct. 2019). "Real-time EMG based pattern recognition control for hand prostheses: A review on existing methods, challenges and future implementation". In: *Sensors (Switzerland)* 19 (20). ISSN: 14248220. DOI: 10.3390/s19204596.

Pfeifer, Rolf and Josh Bongard (2006). *How the body shapes the way we think: a new view of intelligence.* DOI: 10.7551/mitpress/3585.003.0018.

Platz, Thomas et al. (2005). "Reliability and validity of arm function assessment with standardized guidelines for the FugI-Meyer Test, Action Research Arm Test and Box and Block Test: a multicentre study". In: *Clinical Rehabilitation* 19, pp. 404–411. DOI: 10.1191/0269215505cr832oa.

Pylatiuk, Christian, Stefan Schulz, and Leonhard Döderlein (Dec. 2007). "Results of an internet survey of myoelectric prosthetic hand users". In: *Prosthetics and Orthotics International* 31 (4), pp. 362–370. ISSN: 03093646. DOI: 10.1080/03093640601061265.

Resnik, Linda et al. (Mar. 2018). "Evaluation of EMG pattern recognition for upper limb prosthesis control: A case study in comparison with direct myoelectric control". In: *Journal of NeuroEngineering and Rehabilitation* 15 (1). ISSN: 17430003. DOI: 10.1186/s12984-018-0361-3.

Robeyns, Ingrid (2021). "The capability approach". In: Routledge, pp. 72–80.

– (Mar. 2005). "The Capability Approach: a theoretical survey". In: *Journal of Human Development* 6 (1), pp. 93–117. ISSN: 14699516. DOI: 10.1080/146498805200034266.

Rumelhart, David E and David Zipser (1985). "Feature discovery by competitive learning". In: *Cognitive Science* 9 (1), pp. 75–112. ISSN: 03640213. DOI: 10.1016/S0364-0213(85)80010-0.

Sadoyama, T, H Miyano, and Yatabemachi Higashi (1981). "Applied Physiology Frequency Analysis of Surface EMG to Evaluation of Muscle Fatigue". In: *Eur J Appl Physiol* 47, pp. 239–246.

Sato, Hisao and Atsushi Ozawa (2013). *An Introduction to Social Welfare Policy and Program for Persons with Disabilities [Shogaisha fukushi no sekai] (published in Japanese).* 5th ed. Yuhikaku Publishing.

Schünke, Michael, Erik Schulte, and Udo Schumacher (2014). *PROMETHEUS LernAtlas der Anatomie: Allgemeine Anatomie und Bewegungssystem.* 2nd ed. Igakushoin [published in Japanese], p. 289.

Sears, H. H. and J. Shaperman (1991). *Proportional myoelectric hand control: An evaluation.* DOI: 10.1097/00002060-199102000-00005. URL: https://europepmc.org/article/med/1994966.

Seki, Tatsuya et al. (2014). "Development of Five-Finger Multi-DoF Myoelectric Hands with a Power Allocation Mechanism". In: *Journal of Mechanics Engineering and Automation* 4, pp. 97–105.

– (2013). "Development of five-finger multi-DoF myoelectric hands with a power allocation mechanism". In: *Proceedings - IEEE International Conference on Robotics and Automation* 4, pp. 2054–2059. ISSN: 10504729. DOI: 10.1109/ICRA.2013.6630852.

Sen, Amartya (1999). "Commodities and capabilities". In: *OUP Catalogue.*

Sensinger, Jonathon W., Blair A. Lock, and Todd A. Kuiken (2009). "Adaptive pattern recognition of myoelectric signals: Exploration of conceptual framework and practical algorithms". In: *IEEE Transactions on Neural Systems and Rehabilitation Engineering* 17 (3), pp. 270–278. ISSN: 15344320. DOI: 10.1109/TNSRE.2009.2023282.

Shew, Ashley (Mar. 2020). "Ableism, Technoableism, and Future AI". In: *IEEE Technology and Society Magazine* 39 (1), pp. 40–50+85. ISSN: 1937416X. DOI: 10.1109/MTS.2020.2967492.

Simon, Ann M., Blair A. Lock, and Kathy A. Stubblefield (Apr. 2012). "Patient Training for Functional Use of Pattern Recognition–Controlled Prostheses". In: *JPO Journal of Prosthetics and Orthotics* 24 (2), pp. 56–64. ISSN: 1040-8800. DOI: 10.1097/JPO.0b013e3182515437.

Simon, Ann M., Kristi L. Turner, et al. (June 2019). "Pattern recognition and direct control home use of a multi-articulating hand prosthesis". In: IEEE, pp. 386–391. ISBN: 978-1-7281-2755-2. DOI: 10.1109/ICORR.2019.8779539.

Smith, Roger O. et al. (July 2018). "Assistive technology products: a position paper from the first global research, innovation, and education on assistive technology (GREAT) summit". In: *Disability and Rehabilitation: Assistive Technology* 13 (5), pp. 473–485. ISSN: 17483115. DOI: 10.1080/17483107.2018.1473895.

Snyder, Sharon L and David T Mitchell (2006). *Cultural Locations of Disability*. University of Chicago Press. ISBN: 0226767310.

Steeper (2017). *Owners of Steeper Group*. URL: https://www.steepergroup.com/about-steeper/steeper-group/our-story/owners-at-steeper-group/.

Sugimoto, Akira (2008). *How people with disabilities have lived [Shogaisha wa do ikite kitaka] (published in Japanese)*. Gendaishokan.

Sun, Jianwei, Xuemin Cao, and Guangsheng Song (June 2020). "Design method for a bionic wrist based on tensegrity structures". In: *Biosurface and Biotribology* 6 (2), pp. 31–36. ISSN: 24054518. DOI: 10.1049/bsbt.2019.0022.

Tada, Yasunori, Koh Hosoda, and Minoru Asada (2005). "Learn to grasp utilizing anthropomorphic fingertips together with a vision sensor". In: pp. 3323–3328. ISBN: 0780389123. DOI: 10.1109/IROS.2005.1545028.

Takahashi, Koji (2011). "Historical Changes and Future Prospects of Prosthetic Hands [Gi-shu no rekishiteki hensen to kongo no tenbo (published in Japanese)]". In: *Bulletin of the Japanese Society of Prosthetics and Orthotics* 27 (1), pp. 18–20.

Tanaka, Yohei (2018). "Current status and future prospects of myoelectric prostheses [Kindengishu Dendogishu no genjo to kadai] (published in Japanese)". In: *Bulletin of the Japanese Society of Prosthetics and Orthotics* 34 (2), pp. 110–114.

Tebbutt, Emma et al. (Nov. 2016). *Assistive products and the Sustainable Development Goals (SDGs)*. DOI: 10.1186/s12992-016-0220-6.

The Association for Technical Aids (n.d.[a]). *bebionic hand (published in Japanese)*. URL: https://www1.techno-aids.or.jp/search/trader_detail.php?id=14615472.

– (n.d.[b]). *i-Limb Quantum Hand (published in Japanese)*. URL: https://www1.techno-aids.or.jp/search/trader_detail.php?id=14615963.

– (n.d.[c]). *i-Limb Ultra Hand (published in Japanese)*. URL: https://www1.techno-aids.or.jp/search/trader_detail.php?id=14615964.

Tiffin, Joseph and E. J. Asher (1948). "The Purdue Pegboard: norms and studies of reliability and validity." In: *Journal of Applied Psychology* 32 (3), pp. 234–247. ISSN: 1939-1854. DOI: 10.1037/h0061266.

Al-Timemy, Ali H. et al. (June 2016). "Improving the Performance Against Force Variation of EMG Controlled Multifunctional Upper-Limb Prostheses for Transradial Amputees". In: *IEEE Transactions on Neural Systems and Rehabilitation Engineering* 24 (6), pp. 650–661. ISSN: 15344320. DOI: 10.1109/TNSRE.2015.2445634.

Toboso, Mario (June 2011). *Rethinking disability in Amartya Sen's approach: ICT and equality of opportunity*. DOI: 10.1007/s10676-010-9254-2.

Togo, Shunta, Hiroshi Yokoi, et al. (Mar. 2020). "Social Implementation of EMG Prosthetic Hand (published in Japanese)". In: *Journal of the Robotics Society of Japan* 38 (2), pp. 127–130.

Togo, Shunta, Murai Yuta, et al. (2019). "Development of an sEMG sensor composed of two-layered conductive silicone with different carbon concentrations". In: *Scientific Reports*. DOI: 10.1038/s41598-019-50112-4.

Tokoro, Hiroyo (2010). "Reasonable accommodation under ADA and employment for persons with disabilities (published in Japanese)". In: *The review of comparative social security research* 171, pp. 62–71.

Tomorrow, Unlimited (n.d.). *Unlimited Tomorrow*. URL: https://www.unlimitedtomorrow.com/process/.

TSUJI, Toshio et al. (1993). "Discrimination of Forearm Motions from EMG Signals by Error Back Propagation Typed Neural Network Using Entropy". In: *Transactions of the Society of Instrument and Control Engineers* 29 (10), pp. 1213–1220. ISSN: 0453-4654. DOI: 10.9746/sicetr1965.29.1213.

Tsuji, Toshio et al. (Mar. 2003). "A recurrent log-linearized Gaussian mixture network". In: *IEEE Transactions on Neural Networks* 14 (2), pp. 304–316. ISSN: 10459227. DOI: 10.1109/TNN.2003.809403.

Tuci, E, G Massera, and S Nolfi (2009). "Active categorical perception in an evolved anthropomorphic robotic arm". In: pp. 31–38. ISBN: 9781424429592. DOI: 10.1109/CEC.2009.4982927.

Union of the Physically Impaired Against Segregation (1976). *Fundamental Principles of Disability: Being a Summary of the Discussion Held on 22nd November, 1975 and Containing Commentaries from Each Organisation*. UPIAS/Disability Alliance.

Vinet, Robert et al. (1995). “Design methodology for a multifunctional hand prosthesis”. In: *Department Veterans Affairs Journal of Rehabilitation Research and Development* 32 (4), pp. 316–324. ISSN: 0748-7711.

Voisin, Julien, Geneviève Benoit, and C. Elaine Chapman (July 2002). “Haptic discrimination of object shape in humans: two-dimensional angle discrimination”. In: *Experimental Brain Research* 145 (2), pp. 239–250. ISSN: 0014-4819. DOI: 10.1007/s00221-002-1117-6.

Wiesenfeld, Stephen L. (Sept. 1967). “Sickle-Cell Trait in Human Biological and Cultural Evolution”. In: *Science* 157 (3793), pp. 1134–1140. ISSN: 0036-8075. DOI: 10.1126/science.157.3793.1134.

Wikler, D (Apr. 1999). “Can we learn from eugenics?” In: *Journal of Medical Ethics* 25 (2), pp. 183–194. ISSN: 0306-6800. DOI: 10.1136/jme.25.2.183.

World Health Organization (May 2022). *Global Report on Assistive Technology.* Ed. by World Health Organization & United Nations Children’s Fund. ISBN: 9789240049451.

– (2001). *ICF : International classification of functioning, disability and health.* World Health Organization. ISBN: 9241545429.

World Health Organization. and World Bank. (2011). *World report on disability.* World Health Organization, p. 325. ISBN: 9789241564182.

Yamanoi, Yusuke (2019). “Hand motion estimation using big data considering time variant characteristics of signal features for myoelectric hand control (published in Japanese))”. In.

Yamanoi, Yusuke et al. (Jan. 2021). “Learning Data Correction for Myoelectric Hand Based on “Survival of the Fittest” ”. In: *Cyborg and Bionic Systems* 2021. ISSN: 26927632. DOI: 10.34133/2021/9875814.

Yang, Dapeng et al. (Feb. 2019). “Improving the functionality, robustness, and adaptability of myoelectric control for dexterous motion restoration”. In: *Experimental Brain Research* 237 (2), pp. 291–311. ISSN: 0014-4819. DOI: 10.1007/s00221-018-5441-x.

Yokoi, Hiroshi et al. (2009). “Mutually Adaptable EMG Devices for Prosthetic Hand”. In: *The International Journal of Factory Automation, Robotics andSoft Computing* (1), pp. 74–83.

Yonemoto, Kyozo, Ishigami Shigenobu, and Toru Kondo (1995). "Kansetsukadoiki narabini Sokuteiho (Joint Range of Motion Display and Methods of Measurement)". In: *The Japanese Journal of Rehabilitation Medicine* 32, pp. 207–217.

Yonemoto, Shohei et al. (2000). *Eugenics and Human Society: Where is the Century of Life Sciences Heading? [Yūseigaku to Ningen Shakai - Seimeikagaku no Seiki wa Doko e Mukau no ka].* 1st ed. Kodansha [publidhed in Japanese], p. 286. ISBN: 4061495119.

Yozbatiran, Nuray, Lucy Der-Yeghiaian, and Steven C. Cramer (Jan. 2008). "A standardized approach to performing the action research arm test". In: *Neurorehabilitation and Neural Repair* 22 (1), pp. 78–90. ISSN: 15459683. DOI: 10.1177/1545968307305353.

Research achievements

Journal

Peer reviewed publications

International

[1] Yuki Kuroda, Yusuke Yamanoi, Shunta Togo, Yinlai Jiang, Hiroshi Yokoi, ”Co-Evolution of Myoelectric Hand Control Under the Tactile Interaction Among Fingers and Objects”, Cyborg and Bionic Systems, vol.2022, 2022

国内

[1] 中尾聡一郎，平井太智，小野祐真，山野井佑介，黒田勇幹，矢吹佳子，東郷俊太，姜銀来，加藤龍，高木岳彦，石原正博，横井浩史, ”先天性上肢欠損のための歯車機構を用いた幼児用義手の手先具の開発”, 日本ロボット学会誌

International conferences

Peer reviewed publications

Oral presentation

[1] Yuki Kuroda, Tatsuki Tsujimoto, Takayoshi Shimada , Yoshiko Yabuki , Dianchun Bai , Yusuke Yamanoi , Yinlai Jiang , Jinying Zhu and Hiroshi Yokoi , ”Development and Clinical Evaluation of a Five-Fingered Myoelectric Prosthetic Hand with Pattern Recognition,” 2022 IEEE 4th Global Conference on Life Sciences and Technologies (LifeTech), 2022, pp. 235-236, Osaka, Japan, March 7-9, 2022. (IEEE LifeTech 2022 Outstanding Student Paper Awards for Oral Presentation).

[2] Yuki Kuroda, Taichi Hirai, Yoshiko Yabuki, Yusuke Yamanoi, Yinlai Jiang and Hiroshi Yokoi , ”Development and Evaluation of a Lightweight Two-Degree-of-Freedom Electric Prosthetic Hand for Toddlers,” 2022 IEEE 4th Global Conference

on Life Sciences and Technologies (LifeTech), 2022, pp. 237-238, March 7-9, 2022.

[3] Yuki Kuroda, Shunta Togo, Yinlai Jiang, "EMG Classification by Using Swarm Intelligence for Myoelectric Prosthetic Hand", 2018 IEEE International Conference on Intelligence and Safety for Robotics (ISR 2018), No.112, pp.452-457, Shenyang, China, Aug.24-27, 2018.

[4] Yuki Inoue, Yuki Kuroda, Yusuke Yamanoi, Yoshiko Yabuki and Hiroshi Yokoi, "Development of Separate Exoskeleton Socket of Wrist Joint on Myoelectric Prosthetic Hand for Congenital Defects with Symbrachydactyly", 2022 IEEE International Conference on Cyborg and Bionic Systems (CBS), Wuhan and Online, China, Mar.24-26, 2023.

[5] Hai Jiang, Yusuke Yamanoi, Yuki Kuroda, Peiji Chen, Shunta Togo and Hiroshi Yokoi, "Conditional Generative Adversarial Network-based Finger Position Estimation for Controlling Multi-Degrees-of-Freedom Myoelectric Prosthetic Hands", 2022 IEEE International Conference on Cyborg and Bionic Systems (CBS), Wuhan and Online, China, Mar.24-26, 2023.

国内学会

査読なし

口頭発表

[1] 黒田 勇幹，山野井 佑介，東郷 俊太，姜 銀来，加藤 龍，横井 浩史，“筋電信号の時変性に適応する教師データ更新手法に関する研究”，第 38 回日本ロボット学会学術講演会，1H3–01，オンライン，2020 年 10 月 9-11 日.

[2] 高橋明丈, 矢吹佳子, 山野井佑介, 黒田勇幹, 小野祐真, 中尾聡一郎, 平井太智, 横井浩史, “ADL における機能向上のための対立回転機構を用いた幼児用義手の開発”，第 36 回日本義肢装具学会 (The Japanese Society of Prosthetics and Orthotics) , SIA-5, ハイブリッド開催, 2020.（優秀学生演題賞).

[3] 矢吹 佳子，黒田 勇幹，山野井 佑介，平井 太智，小野 祐真，中尾 聡一郎，横井 浩史，”個性適応システムを有するユニバーサルソケットの有用性評価”，第 36 回日本義肢装具学会学術大会，H-2-5，東京大学/WEB ハイブリッド開催，10.31-11.1,2020

[4] 矢吹佳子，山野井佑介，黒田勇幹，島田岳佳，大谷俊介，千田知広，溝口恒雄，高木岳彦，高山真一郎，横井浩史,”超小型対立回転機構を用いた手掌筋電義手，能動指義手の開発”,O7-1，第 37 回日本義肢装具学会学術大会,2021 年 10 月 16 日-17 日

[5] 中尾 聡一郎，平井 太智，小野 祐真，山野井 佑介，黒田勇幹，矢吹 佳子，東郷 俊太，姜 銀来，加藤 龍，高木 岳彦，石原 正博，横井 浩史，“回内・回外機能を有し個性に適応する幼児用筋電義手の開発と評価”，第 38 回日本ロボット学会学術講演会，3H1–02，オンライン，2020 年 10 月 9-11 日.

[6] 平井 太智，中尾 聡一郎，小野 祐真，黒田勇幹，矢吹 佳子，山野井 佑介，東郷 俊太，姜 銀来，加藤 龍，横井 浩史，“先天性前腕欠損者のための幼児用 2 自由度電動義手の開発”，第 38 回日本ロボット学会学術講演会，3H1–01，オンライン，2020 年 10 月 9-11 日.

[7] 矢吹 佳子，黒田 勇幹，村井 雄太，日吉 祐太郎，叶 鶴松，雍 旭，景 暁バイ，東郷 俊太，姜 銀来，横井 浩史，”個性に適応する幼児用筋電義手の開発と評価”，第 36 回日本ロボット学会学術講演会，3P2-10，中部大学春日井キャンパス，2018 年 9 月 7 日.

[8] 鎌田 舞花，矢吹 佳子，黒田 勇幹，山野井 佑介，東郷 俊太，姜 銀来，横井 浩史，”筋電義手の熟達度に関する研究”，第 40 回バイオメカニズム学術講演会，2B2-2，中京大学春日井キャンパス，2019 年 12 月 1 日.

ポスター発表

[1] 黒田 勇幹，東郷 俊太，姜 銀来，横井 浩史，筋電義手への応用を目的とした筋電を含む感覚情報を得る自律エージェントの開発と検討，第 12 回進化計算シンポジウム 2018，P4-12，休暇村志賀島（福岡県福岡市），2018 年 12 月 9 日.

[2] 黒田 勇幹，山野井佑介，島田岳佳，Hai Jiang, 矢吹佳子，Dianchun Bai, 高木岳彦，Yinlai Jiang，横井浩史，”個性適応型学習機能を有した他自由度筋電義手の臨床適応と性能評価”，STP-10, 第 37 回日本義肢装具学会学術大会,2021 年 10 月 16 日-17 日.

[3] 黒田 勇幹，矢吹 佳子，山野井 佑介，東郷 俊太，姜 銀来，横井 浩史，”子供用筋電義手ソケットの開発”，第 36 回日本義肢装具学会，SG-12, ハイブリッド開催,10.31-11.1, 2020.

[4] 大谷俊介，平井太智，黒田勇幹，矢吹佳子，山野井佑介，東郷俊太，姜銀来，横井浩史,”可動指を変えた幼児用 2 自由度電動義手の開発”，STP-6, 第 37 回日本義肢装具学会学術大会,2021 年 10 月 16 日-17 日.

[5] 井上祐希，島田岳佳，高橋明丈，千田知広，大谷俊介，黒田勇幹，山野井佑介，矢吹佳子，高木岳彦，横井浩史，”小児手掌欠損者に対する筋電義手の開発”，STP-7, 第 37 回日本義肢装具学会学術大会,2021 年 10 月 16 日-17 日.

[6] 千田知広，島田岳佳，黒田勇幹，矢吹佳子，山野井佑介，横井浩史，高木岳彦，”回内外と掌背屈運動を活かす分離型ソケットの開発”，STP-9, 第 37 回日本義肢装具学会学術大会,2021 年 10 月 16 日-17 日.

[7] 矢吹 佳子，小野 祐真，平井 太智，黒田 勇幹，山野井 佑介，横井 浩史，”サイズ変更に適応可能なソケットを用いた子供用筋電義手の開発”，日本機械学会ロボティクス・メカトロニクス講演会 2020（ROBOMECH2020 in KANAZAWA），2A1-F06, オンライン開催，5.27-29，2020

Appendix A Validation of the time variation adaptation system using artificial data

A.1 Introduction

To evaluate the performance of the developed time-variation adaptation system, verification was conducted using two-dimensional artificial data. Additionally, parameter optimization was performed using Bayesian optimization. The results obtained with the highest and lowest objective value parameters were compared to examine how each parameter contributes to adaptation.

Among the parameters, those optimized were $\boldsymbol{\rho}\mathrm{min}$, η_1, η_2, $amax$, and e_{max}. It should be noted that $\boldsymbol{\rho}\mathrm{min}$ was fixed at 0.9 for the first class, simulating rest, while the parameters for other classes were optimized. The other parameters of the CCCL were as follows: $\lambda = 5$, $\alpha = 0.5$, $\beta = 0.95$, $n\mathrm{max} = 50$, $n_{\mathrm{min}} = 20$, $g_{\mathrm{min}} = 20$, $T_{\mathrm{UTO}} = 100$.

The number of teacher data was 20 for each class, whereas the number of evaluation data was 120 for each class. The recognition rate (accuracy) is calculated for every 120 pieces of evaluation data input for each class.

A.2 Validation with artificial data simulating wide-range time variation

A.2.1 Dataset

The dataset was created (Fig.A.1) to mimic a wide range of time variations, with Class 2 and Class 3 approaching Class 1, which mimics rest, over time. Artificial data were generated from normal distributions with standard deviations of 0.5, 1.7, and 2.0, respectively, and shifted over time. The total number of artificial data, including the training data, was 6000.

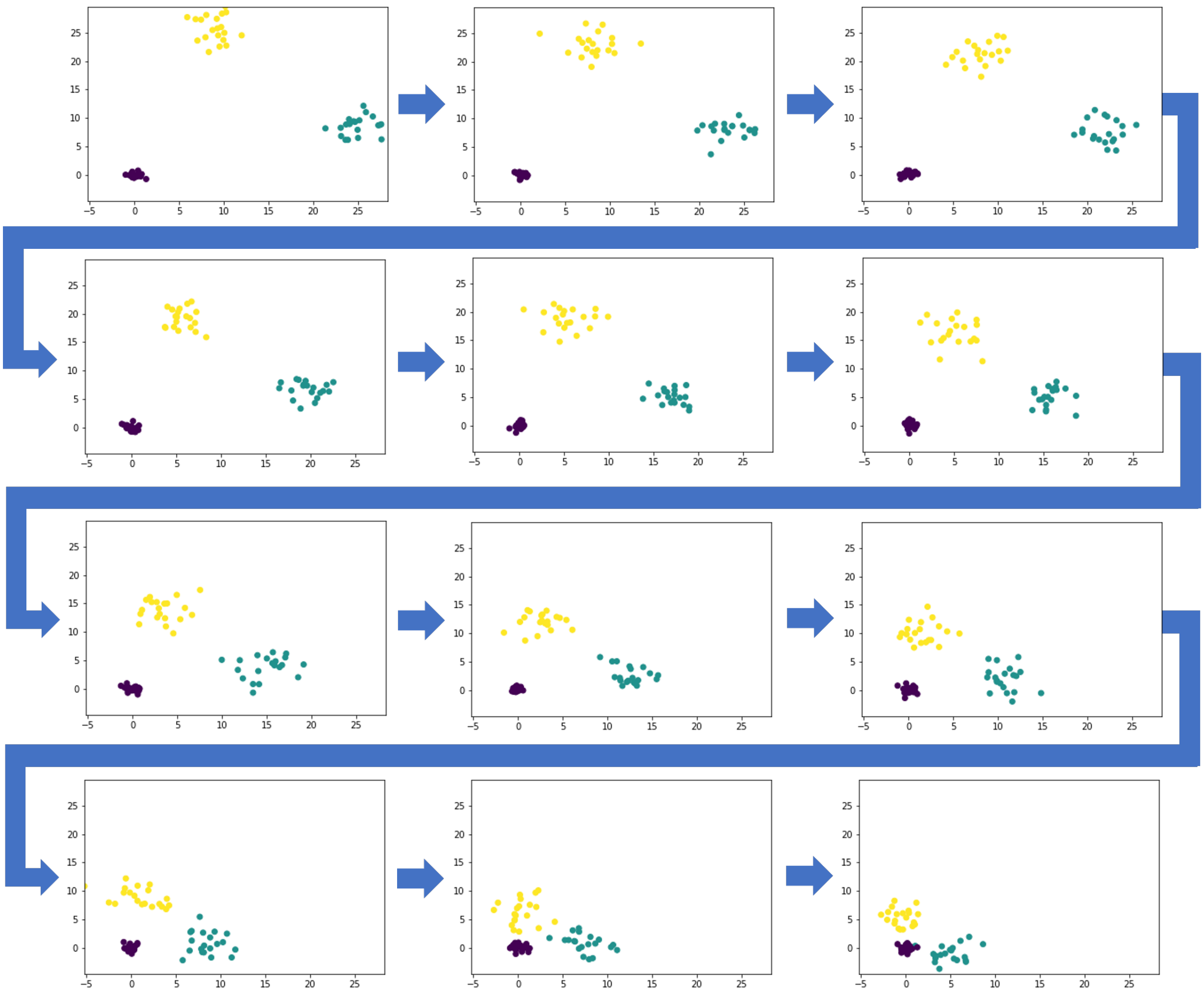

Fig.A.1: Artificial data simulated a wide range of time variations.

A.2.2 Parameter Optimization

The optimal parameters were computed through 10 trials of Bayesian optimization. The parameters were optimized with $\boldsymbol{\rho}_{\min}$ ranging from 0.6 to 0.8, η_1 from 0.006 to 0.6, η_2 from 0.00006 to 0.006, a_{max} from 8 to 20 and e_{max} from 1000 to 6000.

The objective value for optimization was set as the average recognition rate (accuracy).

A.2.3 Validation results and discussion

The optimization results indicated that the optimal parameters were $\boldsymbol{\rho}\text{min} = (0.9, 0.75, 0.75)$, $\eta_1 = 0.23$, $\eta_2 = 0.00087$, $amax = 8$, and $e_{max} = (1907, 1907, 1907)$. The results were rounded to two significant figures.

Conversely, the parameters with the lowest objective value were $\boldsymbol{\rho}\text{min} = (0.9, 0.66, 0.66)$, $\eta_1 = 0.011$, $\eta_2 = 0.0014$, $amax = 8$, and $e_{max} = (5777, 5777, 5777)$.

The objective values for each trial are shown in Fig.A.2.

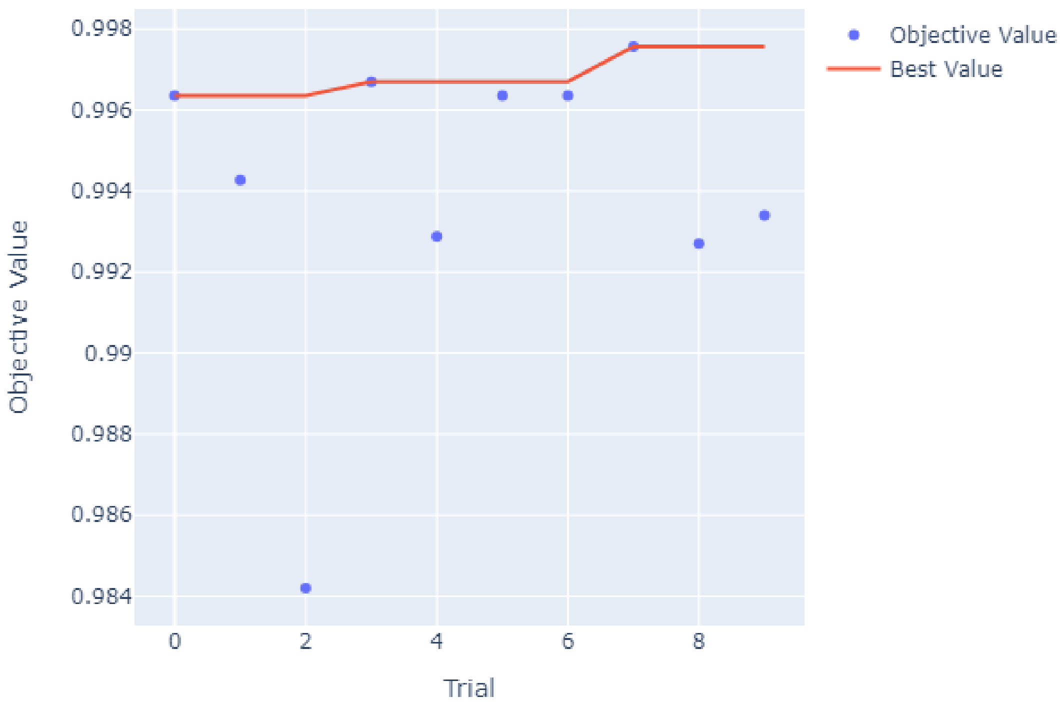

Fig.A.2: Changes in objective values for each trial.

The changes in the recognition rate (accuracy) for each set of parameters are shown in Fig.A.3 and Fig.A.4. It is observed that even with non-optimal parameters, the system maintained a higher accuracy than without adaptation. With optimal parameters, the accuracy remained close to 100 % despite time variability, demonstrating the high performance of the proposed method.

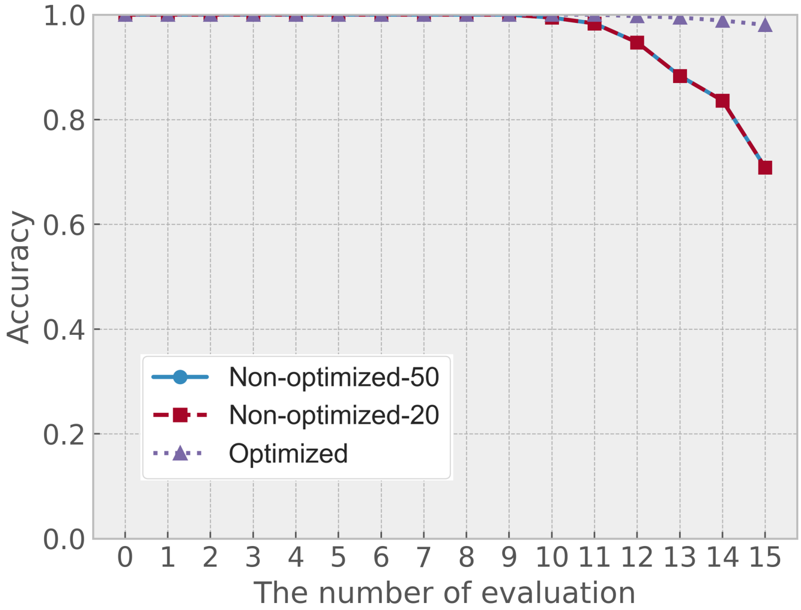

Fig.A.3: Changes in recognition rate (accuracy) with a system using optimal parameters. "Non-optimized-50" refers to the classifier trained with 50 training data for each class without adaptation, and "Non-optimized-20" refers to the classifier trained with 20 training data for each class without adaptation. "Optimized" represents results using the time variation adaptation system.

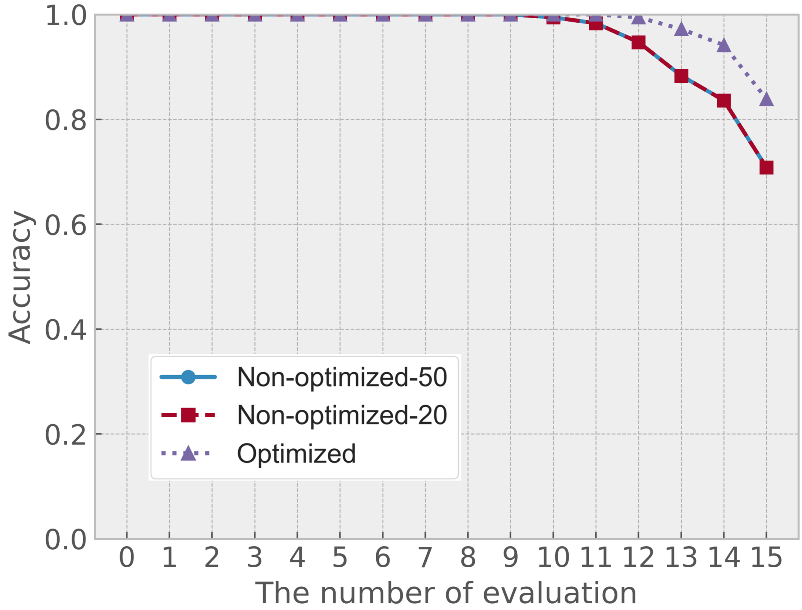

Fig.A.4: Changes in recognition rate (accuracy) with a system using parameters that had the lowest objective values. "Non-optimized-50" refers to the classifier trained with 50 training data for each class without adaptation, whereas "Non-optimized-20" refers to the classifier trained with 20 training data for each class without adaptation. "Optimized" represents results using the time variation adaptation system.

To intuitively understand the relationship between the objective value and the parameters, a parallel coordinate plot of the optimization results is presented in Fig.A.5.

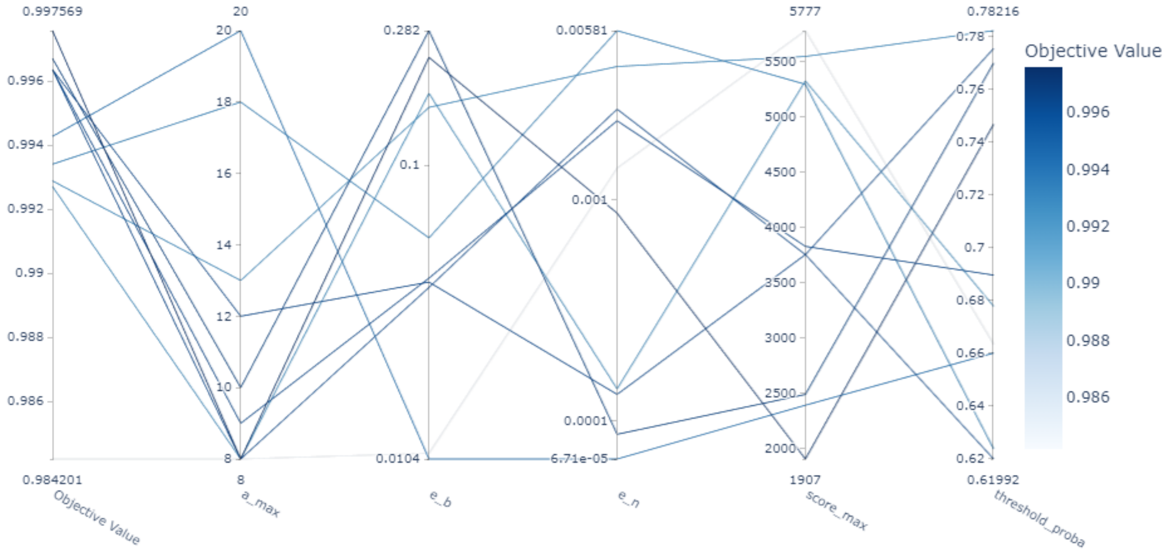

Fig.A.5: Parallel coordinate plot of optimization results. "threshold_proba" represents $\boldsymbol{\rho}$min, "e_b" represents η_1, "e_n" represents η_2, "a_max" represents $amax$, and "score_max" represents e_{max}.

The plot in Fig.A.5 indicates that higher values of e_{max} correspond to smaller objective values, suggesting that e_{max} significantly impacts performance. The edge's evaluation value e increases over time and resets when new input is received in the vicinity. Therefore, a higher e_{max} means that training data are less likely to be deleted owing to time variation.

To confirm the impact of e_{max}, the adaptation behavior with optimal parameters is compared to that with the worst-performing parameters. The adaptation behavior for each case is shown in Fig.A.6 and Fig.A.7.

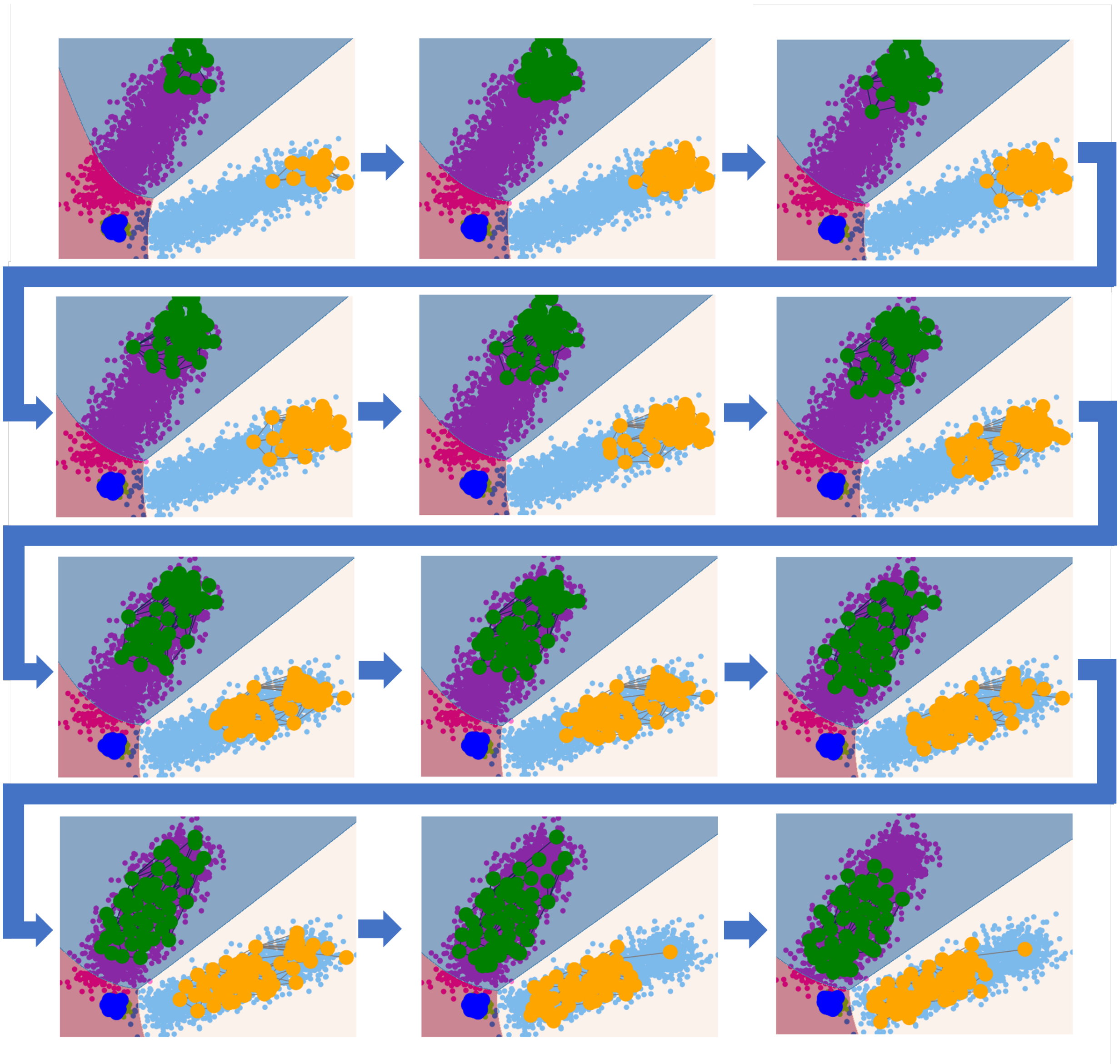

Fig.A.6: Adaptation behavior with a system using optimal parameters. Small circular markers in the background represent all input data, while larger circular markers represent teacher data. The three colored areas in the figure represent decision regions, where data falling within these regions are classified into the corresponding classes.

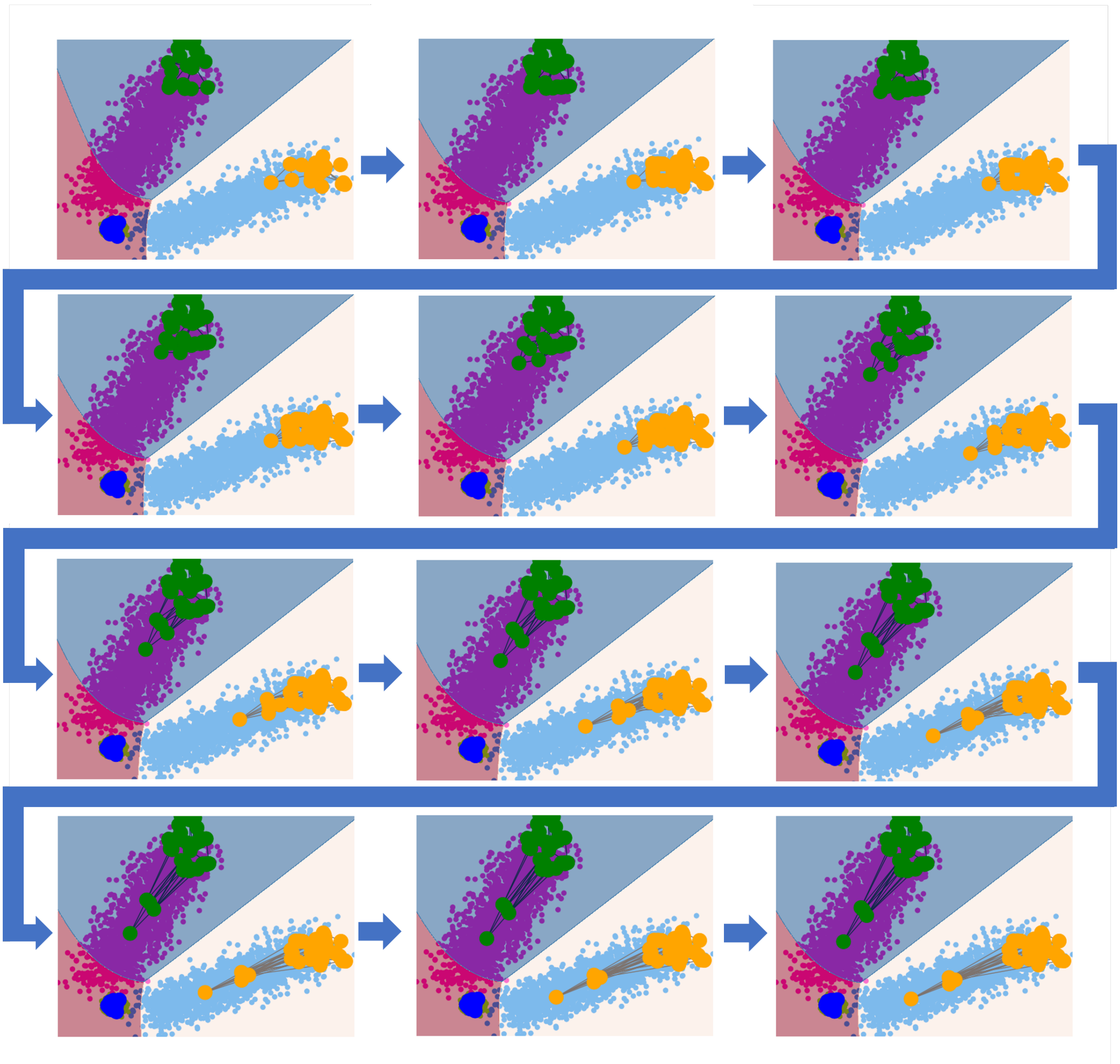

Fig.A.7: Adaptation behavior with a system using the worst-performing parameters. Small circular markers in the background represent all input data, while larger circular markers represent teacher data. The colored areas in the figure represent decision regions, where data falling within these regions are classified into the corresponding classes.

In Fig.A.7, self-organization causes the teacher data to move closer to the input data. However, owing to the high e_{max}, the teacher data remain even after the input data position has changed. Because the limit of the number of teacher data has been reached, no new teacher data are generated in areas of high input frequency, and only a few teacher data are adapted to the time variation of the input data.

In contrast, the results using the optimal parameters, as shown in Fig.A.6, demonstrate that the appropriate setting of e_{max} allowed for a dynamic adjustment of the teacher data. When the input data diverged from the initial position of the teacher data, the teacher data moved correspondingly. Additionally, some of the teacher data far from the initial teacher data were deleted, and new teacher data were generated near the input data. This process resulted in the proper relocation of the cluster's central position.

The above shows that the appropriate setting of e_{max} is important for data with a large amount of movement.

A.3 Validation with artificial data simulating narrow-range time variation

A.3.1 Dataset

The dataset was created to simulate narrow-range time variations, consisting of eight competing classes that move within a narrow range over time (Fig.A.1). The artificial data were generated from normal distributions with standard deviations of 0.5, 1.0, 1.2, 1.7, 0.6, 0.8, 1.0, and 2.0, respectively, and evolved over time. There were a total of 4800 artificial data points including the teacher data.

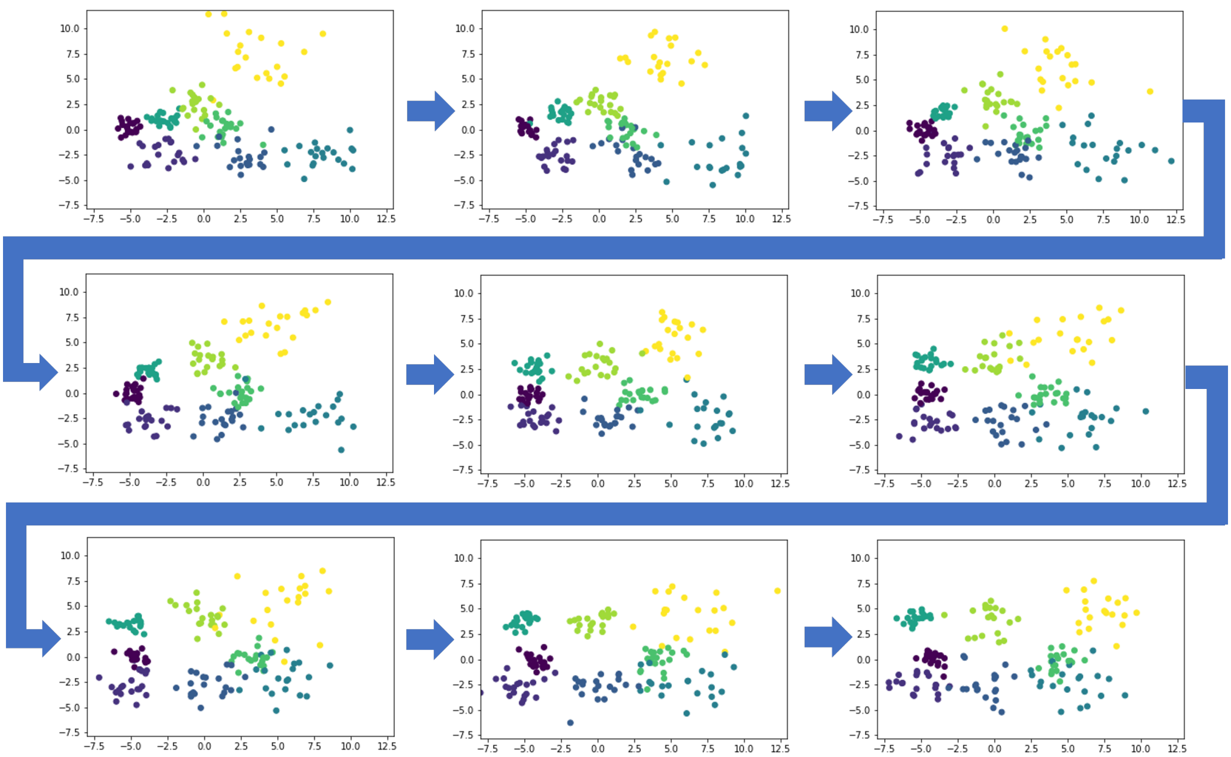

Fig.A.8: Artificial data simulating narrow-range time variation.

A.3.2 Parameter Optimization

Parameter optimization was performed using Bayesian optimization over 30 trials. The parameters $\boldsymbol{\rho}$min were optimized within a range of 0.3 to 0.8, η_1 from 0.006 to 0.6, η_2 from 0.00006 to 0.006, $amax$ from 8 to 20, and e_{max} from 1000 to 8000.

The objective value for optimization was the average value of the recognition rate (accuracy).

A.3.3 Validation results and discussion

The optimization results indicated that the optimal parameters were $\boldsymbol{\rho}$min $= (0.9, 0.31, 0.31, 0.31, 0.31, 0.31, 0.31, 0.31)$, $\eta_1 = 0.31$, $\eta_2 = 0.0016$, $amax = 11$, and $e_{max} = (2740, 2740, 2740, 2740, 2740, 2740, 2740, 2740)$. These results were rounded to two significant figures.

The parameters with the lowest objective value were $\boldsymbol{\rho}$min $= (0.9, 0.36, 0.36, 0.36, 0.36, 0.36, 0.36, 0.36)$, $\eta_1 = 0.0063$, $\eta_2 = 0.0028$, $amax = 9$, and $e_{max} = (3941, 3941, 3941, 3941, 3941, 3941, 3$

The objective values for each trial are shown in Fig.A.9.

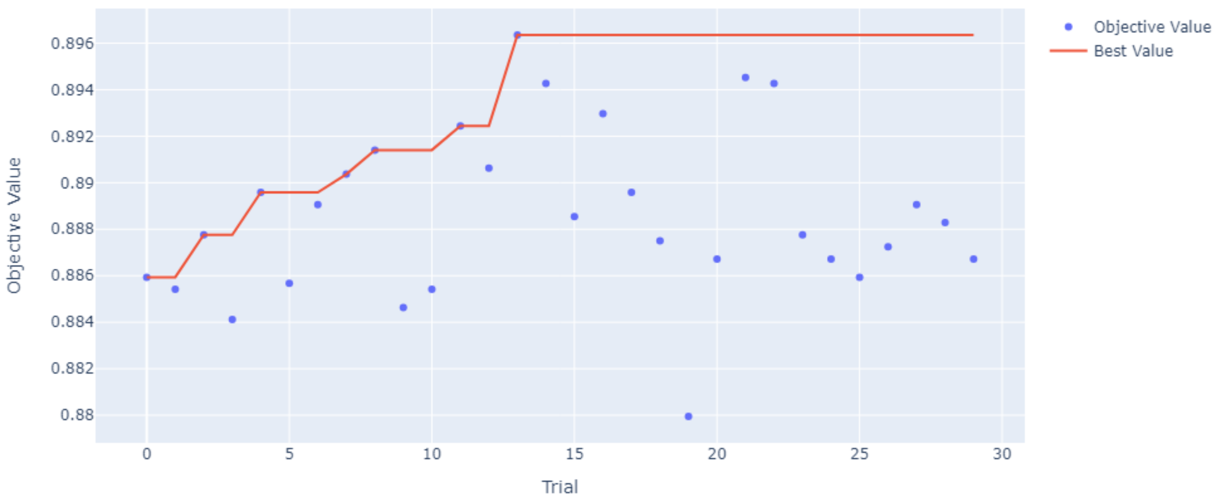

Fig.A.9: Changes in objective values for each trial.

The changes in the recognition rates (accuracy) for each parameter set are depicted in Fig.A.10 and Fig.A.11. Even with inappropriate parameters, the system maintained similar recognition rates to the non-adaptive case. The optimal parameters resulted in higher recognition rates in the second and third evaluations compared to the non-adaptive case. Given the minor changes in the dataset, the ability to improve the recognition rates amidst slight time variations highlights the effectiveness of the proposed method.

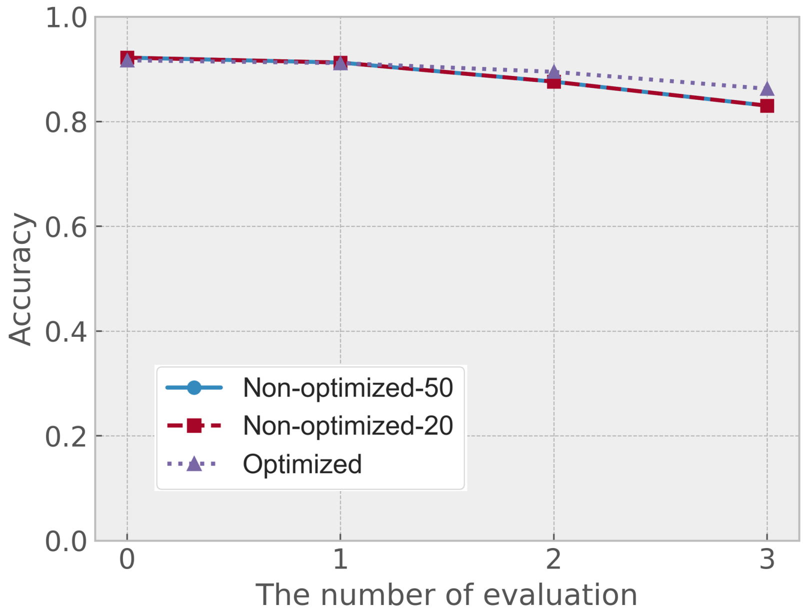

Fig.A.10: Changes in recognition rate (accuracy) using the system with optimal parameters. "Non-optimized-50" represents the recognition rate using a classifier trained with 50 teacher data for each class without adaptation, "Non-optimized-20" with 20 teacher data for each class, and "Optimized" using the time-variation adaptation system.

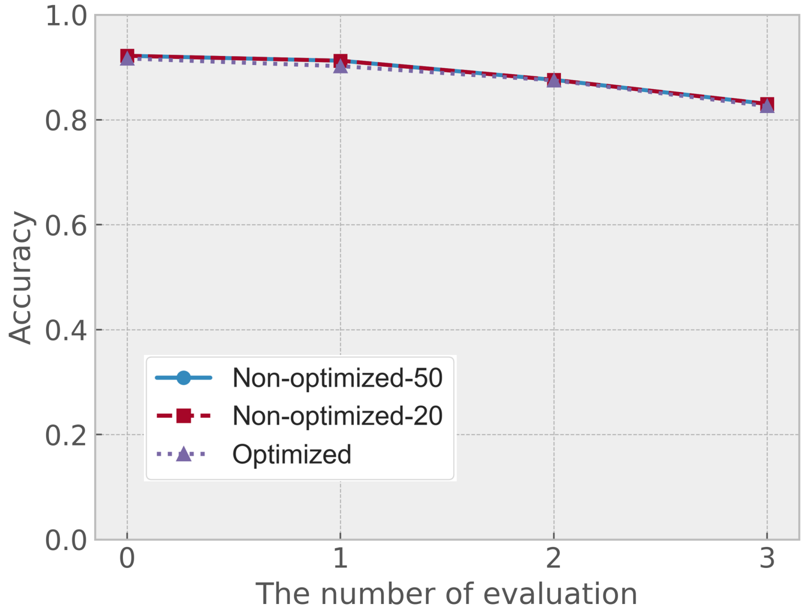

Fig.A.11: Changes in recognition rate (accuracy) using the system with the lowest objective value parameters. "Non-optimized-50" represents the recognition rate using a classifier trained with 50 teacher data for each class without adaptation, "Non-optimized-20" with 20 teacher data for each class, and "Optimized" using the time-variation adaptation system.

To intuitively understand the relationship between the objective value and parameters, a parallel coordinate plot summarizing the optimization results is presented in Fig.A.12.

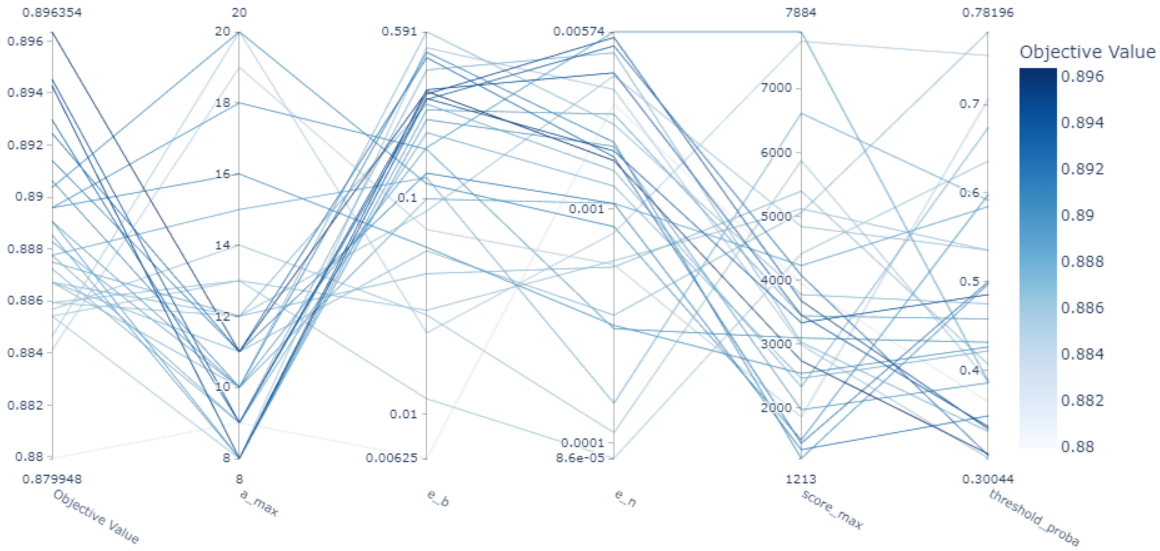

Fig.A.12: Parallel coordinate plot of optimization results. "threshold_proba" represents $\boldsymbol{\rho}$min, "e_b" represents η_1, "e_n" represents η_2, "a_max" represents $amax$, and "score_max" represents e_{max}.

The results in Fig.A.12 indicate that smaller values of $\boldsymbol{\rho}$min, $emax$, and a_{max}, and larger values of η_1 and η_2, tend to yield higher objective values. This trend suggests that all parameters are set to enhance plasticity, indicating that sufficient plasticity is necessary for adaptation in datasets with high levels of competition, such as the one used here. However, it should be noted that the optimal parameters, while directed toward increasing plasticity, do not simply take the maximum or minimum values in their respective ranges, implying that a certain degree of moderate plasticity is necessary.

To understand the differences in plasticity, a comparison was made between adaptations using the optimal parameters and those using the parameters with the poorest objective value. The adaptation processes for each are shown in Fig.A.13 and Fig.A.14.

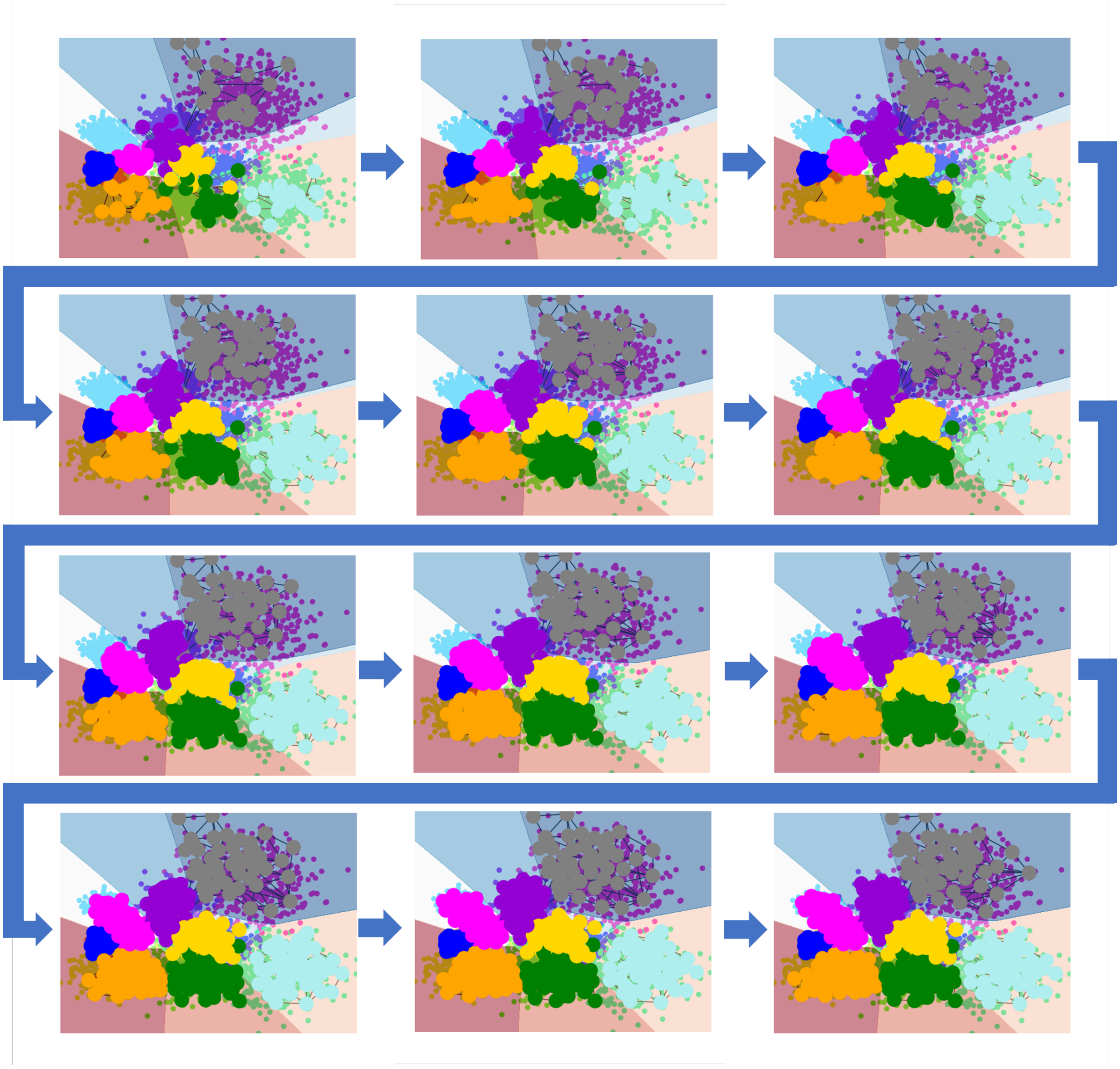

Fig.A.13: Adaptation process with the system using optimal parameters. Small round markers in the background represent all input data. The teacher data are represented by larger round markers. The colored areas in the diagram represent the decision regions, where data entering these regions are classified into corresponding classes.

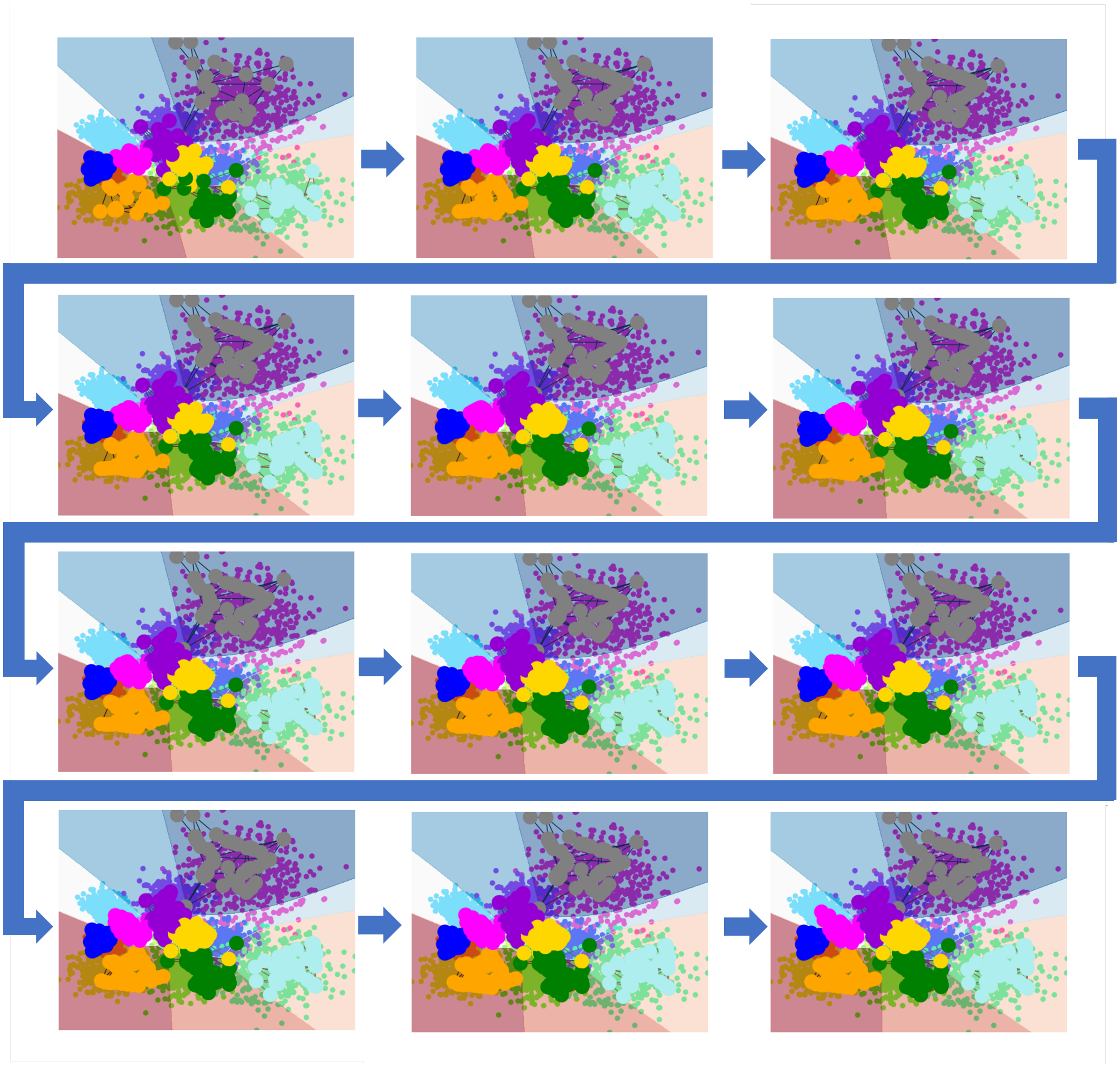

Fig.A.14: Adaptation process with the system using parameters with the worst objective value. Small round markers in the background represent all input data. The teacher data are represented by larger round markers. The colored areas in the diagram represent the decision regions, where data entering these regions are classified into corresponding classes.

The adaptation process with the system using the parameters with the poorest objective values shows a slight change in the clusters. There is minimal adaptation to the input data, with only minor movements of the teacher data.

In contrast, the results using optimal parameters (Fig.A.13) show that the range of the teacher data expands in response to the input data, indicating adaptation to changes in the input data.

These findings underscore the importance of setting parameters with appropriate plasticity. However, it should be noted that the input data used here do not contain noise. In real-world scenarios, data typically include noise, and high plasticity could be susceptible to the effects of this noise. Therefore, stricter limitations on plasticity are anticipated for actual data applications.

Appendix B Optimization of parameters for time variation adaptation system

B.1 Introduction

Parameter optimization was performed for adaptation to a narrow range of time variations (Experiment 2) in Chapter 4.The optimization was performed using experiments with a single participant. The CCCL parameters optimized were $\boldsymbol{\rho}_{\min}$, η_1, and η_2.

The other parameters of the CCCL were as follows: $a_{max} = 8$, $e_{max} = (3000, 3000, 3000, 3000, 3000, 3000, 3000, 3000)$, $\lambda = 5$, $\alpha = 0.5$, $\beta = 0.95$, $n_{\max} = 50$, $n_{\min} = 20$, $g_{\min} = 100$, $T_{\mathrm{UTO}} = 100$. The experiment was conducted with the permission of the ethics committee of the University of Electro-Communication (permit No.10006(5)).

Initially, optimization was performed for $\boldsymbol{\rho}_{\min}$, followed by η_1 and η_2.

B.2 Optimization of $\boldsymbol{\rho}_{\min}$

This section discusses the results of optimizing $\boldsymbol{\rho}$min. $\boldsymbol{\rho}$min is a parameter used to filter noise in G_{UTO}, and when the posterior probability $\boldsymbol{pt}$ output by the Pattern Recognition Function GPR is lower than $\boldsymbol{\rho}_{\min}$, it is discarded as noise. A higher value results in a stricter criterion for noise determination.

With $\eta_1 = 0.0002$ and $\eta_2 = 0.000002$, the values of $\boldsymbol{\rho}_{\min}$ were varied among $(0.9, 0.6, 0.6, 0.6, 0.6, 0.6, 0.6, 0.6)$, $(0.9, 0.7, 0.7, 0.7, 0.7, 0.7, 0.7, 0.7)$, and $(0.9, 0.8, 0.8, 0.8, 0.8, 0.8, 0.8, 0.8)$ to observe differences in recognition rates. The experimental method and calculation of recognition rates were similar to Experiment2 in Section 4.7.

The recognition rates for each setting are shown in Fig.B.1, Fig.B.2, and Fig.B.3, averaging the rates for the eight movements. A comparison showed that the highest recognition rate, both after 2 and 4 minutes of adaptive learning, was achieved with $\boldsymbol{\rho}_{\min} = (0.9, 0.7, 0.7, 0.7, 0.7, 0.7, 0.7, 0.7)$.

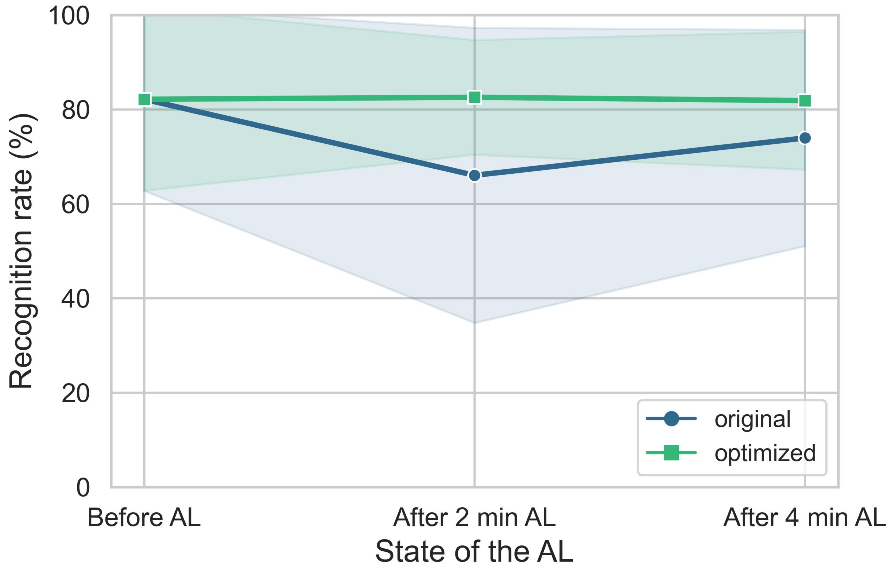

Fig.B.1: Change in recognition rate at $\boldsymbol{\rho}_{\min} = (0.9, 0.6, 0.6, 0.6, 0.6, 0.6, 0.6, 0.6)$.

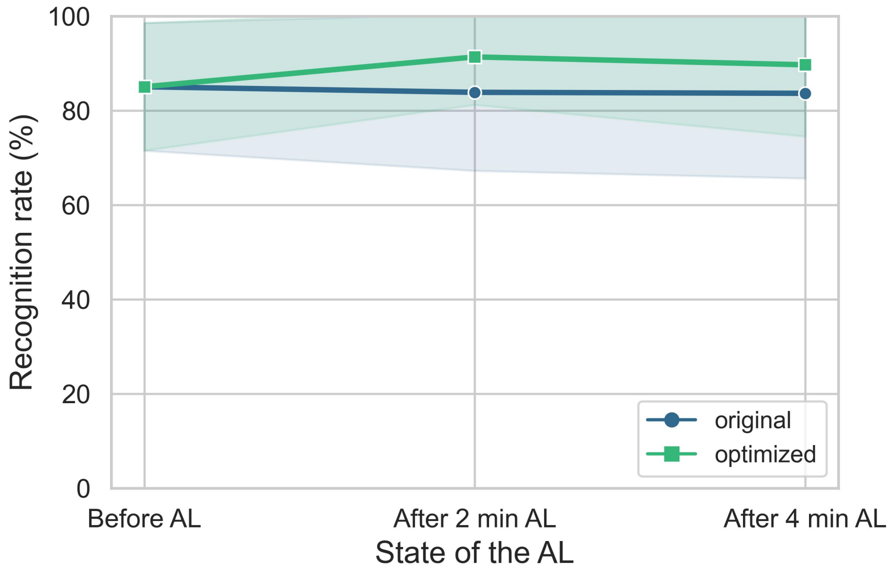

Fig.B.2: Change in recognition rate at $\boldsymbol{\rho}_{\min} = (0.9, 0.7, 0.7, 0.7, 0.7, 0.7, 0.7, 0.7)$.

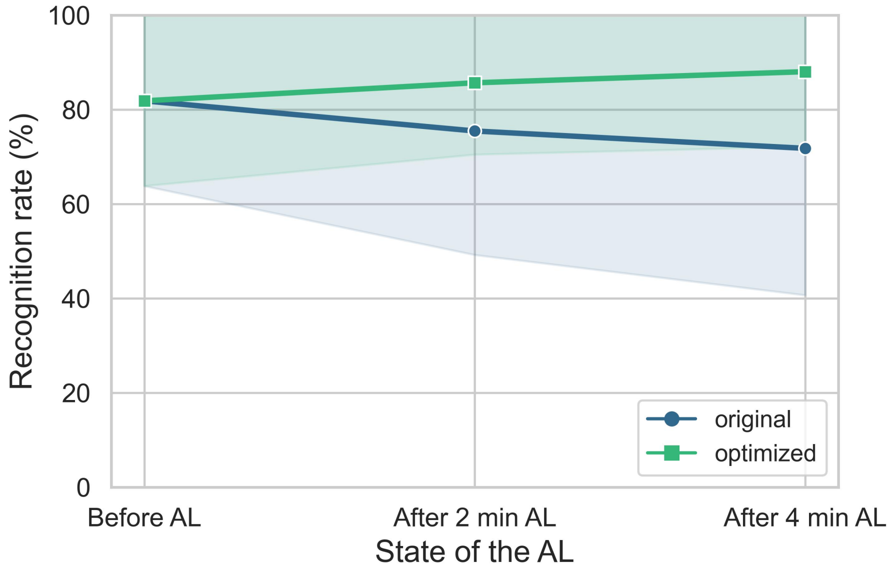

Fig.B.3: Change in recognition rate at $\boldsymbol{\rho}_{\mathrm{min}} = (0.9, 0.8, 0.8, 0.8, 0.8, 0.8, 0.8, 0.8)$.

B.3 Optimization of η_1 and η_2

This section discusses the optimization of η_1 and η_2. These parameters determine the magnitude of movement of the teacher data towards the input data during the self-organization process; larger values result in more significant movement toward the input data.

The value of $\boldsymbol{\rho}_{\mathrm{min}}$, determined in Section B.2 as $(0.9, 0.7, 0.7, 0.7, 0.7, 0.7, 0.7, 0.7)$, was fixed, and η_1 and η_2 were tested with the following settings: $(\eta_1 = 0.002, \eta_2 = 0.00002)$, $(\eta_1 = 0.0002, \eta_2 = 0.000002)$, $(\eta_1 = 0.00001, \eta_2 = 0.0000001)$, and $(\eta_1 = 0.00002, \eta_2 = 0.0000002)$. The experimental method and calculation of recognition rates were the same as in Experiment2, Section 4.7.

The recognition rates are shown in Fig.B.4-B.7. The recognition rates are the average of the eight motions. As a result of the comparison, the recognition rates of Fig.B.5, Fig.B.6, and Fig.B.7 are almost the same.

Here, if η_1 and η_2 are made smaller, the plasticity for the adaptation is reduced. Therefore, $(\eta_1 = 0.0002, \eta_2 = 0.000002)$, which has the largest value of η_1 and η_2 among

Fig.B.5, Fig.B.6, and Fig.B.7, which showed the best performance, was selected as the optimal value.

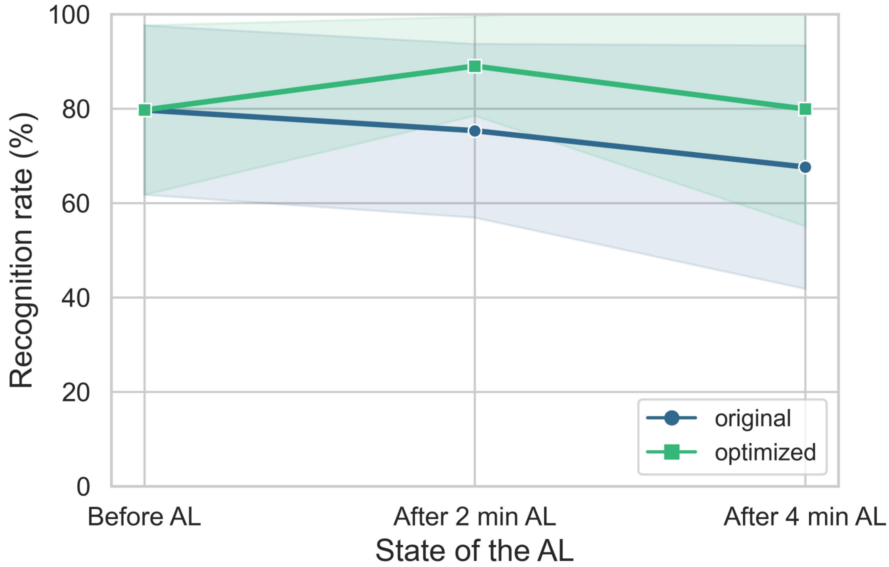

Fig.B.4: Change in recognition rate at ($\eta_1 = 0.002, \eta_2 = 0.00002$).

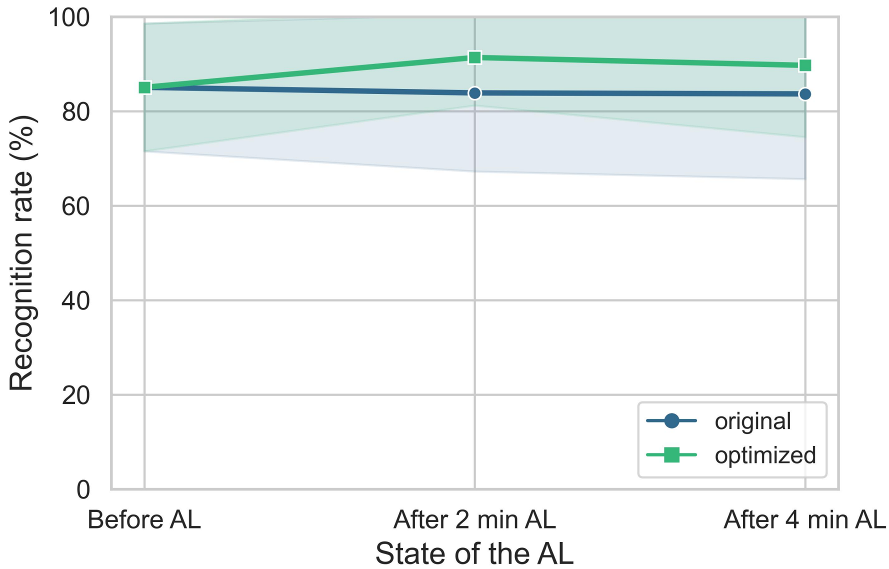

Fig.B.5: Change in recognition rate at ($\eta_1 = 0.0002, \eta_2 = 0.000002$) (Fig.B.2 reprinted).

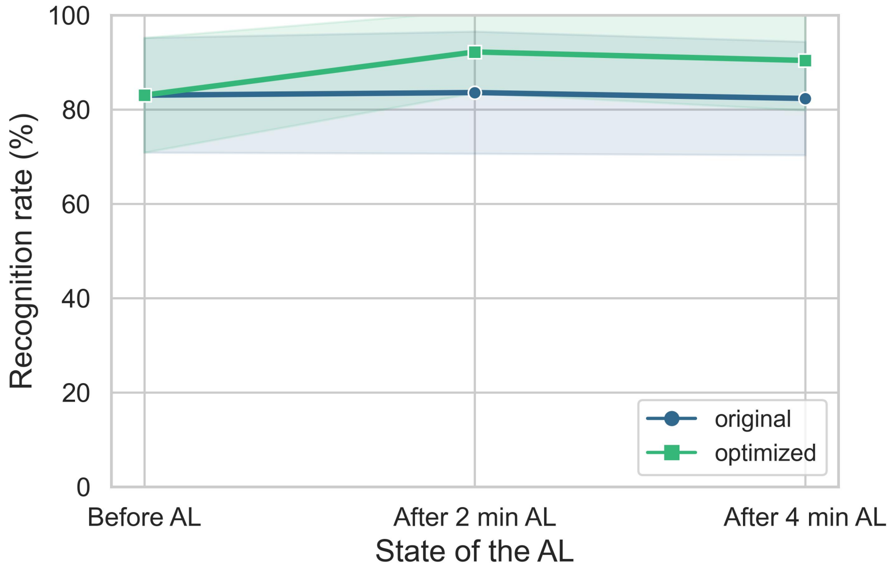

Fig.B.6: Change in recognition rate at ($\eta_1 = 0.00001, \eta_2 = 0.0000001$).

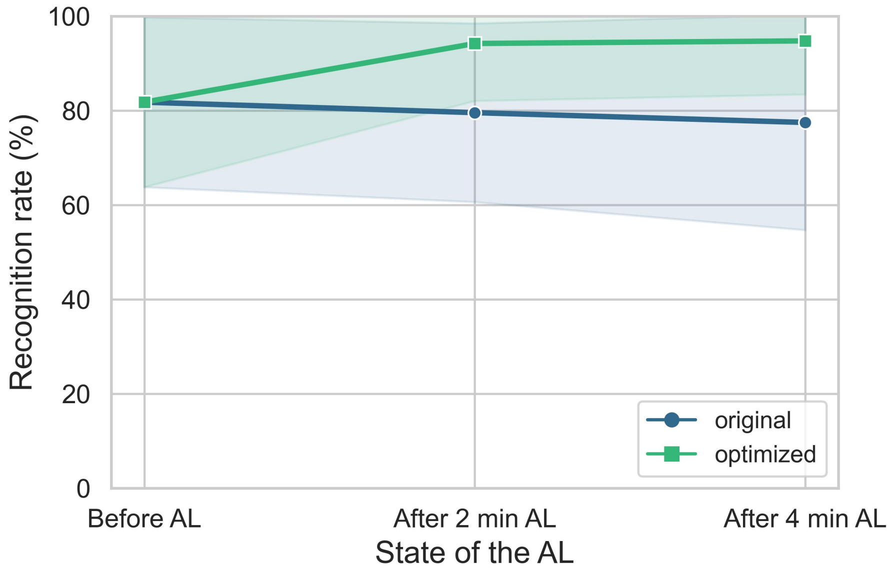

Fig.B.7: Change in recognition rate at ($\eta_1 = 0.00002, \eta_2 = 0.0000002$).